INFORMATION TO USERS

University of Alberta

Extended End Plate Moment Connections Under Cyclic Loading

by

Bryan Tyrone Adey   ©

A thesis submitted to the Faculty of Graduate Studies and Research in partial fulfillment of the requirements for the degree of Master of Science

in

Structural Engineering

Department of Civil and Environmental Engineering

Edmonton, Alberta

Fall 1997

Canadä

University of Alberta

Library Release Form

Name of Author: Bryan T. Adey

Title of Thesis: Extended End Plate Moment Connections Under Cyclic Loading
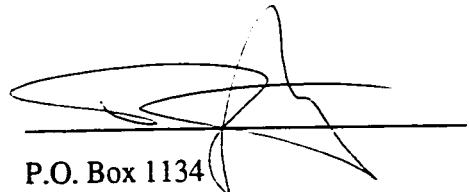
Degree: Master of Science

Year This Degree Granted: 1997

Permission is hereby granted to the University of Alberta Library to reproduce single copies of this thesis and to lend or sell such copies for private, scholarly, or scientific research purposes only.

The author reserves all other publication and other rights in association with the copyright in the thesis, and except as hereinbefore provided, neither the thesis nor any substantial portion thereof may be printed or otherwise reproduced in any material form whatever without the author's prior written permission.

P.O. Box 1134
128 School Street
Middleton, Nova Scotia
Canada
B0S 1P0
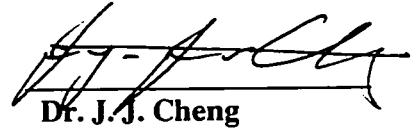
University of Alberta

Faculty of Graduate Studies and Research

The undersigned certify that they have read, and recommended to the Faculty of Graduate Studies and Research for acceptance, a thesis entitled Extended End Plate Connections Under Cyclic Loading by Bryan Tyrone Adey in partial fulfillment of the requirements for the degree of Master of Science in Structural Engineering.

Dr. G. Y. Grondin

Dr. J. J. Cheng

Dr. B. M. Patchett

Prof. A. E. Peterson

Abstract

An experimental investigation of 15 cyclically loaded extended end plate connections was undertaken to determine the important design parameters. The parameters investigated were beam size, bolt layout, use of extension stiffeners, end plate thickness, and welding technique. Of the 15 test specimens, 12 were designed to confine failure to the end plate and three were designed to develop the plastic moment capacity of the beam. In addition to the experimental program, a literature survey was conducted and ten models, developed to predict the capacity of extended end plate moment connections, were evaluated.

Of the beam sizes tested (W360x51, W460x97 and W610x125) the W460x97 beam connections provided the most ductility. The relaxed bolt configurations increased energy dissipation capacity and maximum connection rotation. The use of extension stiffeners increased energy dissipation capacity and raised connection yield rotation. Increased end plate thickness increased connection moment capacity. The variation of welding techniques did not greatly affect connection performance. Bolt bending and loss of preload was common. Extended end plate connections showed potential for use in seismic zones.

Acknowledgments

Table of Contents

.

List of Tables

List of Figures

List of Symbols

a = distance between centerline of bolts and edge of flange fillet weld (Figure 2.13)

a_i = distance between centerline of exterior bolts and edge of exterior flange fillet weld (Figure 2.13)

a_o = distance between centerline of interior bolts and edge of interior flange fillet weld (Figure 2.13)

a' = distance between edge of bolt head and toe of fillet weld (Figure 2.13)

a'_i = distance between edge of bolt head and toe of fillet weld (Figure 2.13)

a'_o = distance between edge of bolt head and toe of fillet weld (Figure 2.13)

A_f = area of beam tension flange

A_s = cross sectional area of bolt shaft

A_w = area of beam web

b = distance between centerline of exterior bolts and edge of end plate (Figure 2.13)

B = bolt force

B_{ep} = width of end plate (Figure 2.13)

B_f = bolt design strength

B_o = initial bolt pretension

B_o' = bolt tension where separation occurs at the bolt line

B_u = ultimate bolt tensile stress

B_y = bolt yield stress

c = distance between centerline of exterior bolts and centerline of interior bolts (Figure 2.13)

$$C = B_o(\frac{B_o' - B}{B_o' - B_o})$$

d = depth of beam

d_b = nominal bolt diameter

d_f = depth of beam - flange thickness (Figure 2.13)

d_h = sum of bolt hole diameters across width of end plate

di = distance between centerline of interior bolts and interior face of flange (Figure 2.13)

do =   distance between centerline of exterior bolts and exterior face of flange (Figure 2.13)

f_b =   width of beam flange

F =   flange force

F_x =   axial force in the beam

F_{yep} =   end plate yield stress

g =   bolt pitch

h =   length of end plate from one edge of end plate to the opposite beam flange

k_1 = $l_s + 1.43 l_t + 0.71 l_n$

k_2 = $k_1 + 0.2 l_n + 0.4 l_w$

k_3 = $0.4 T_{ep}$

k_4 = $0.1 l_n + 0.2 l_w$

l =   effective length of end plate

l_t =   length of bolt threads between full bolt shaft and nut

l_s =   length of bolt shank

l_w =   thickness of washers

n =   number of bolt holes across the width of the end plate

M_b =   beam moment

M_p =   plastic moment capacity

M_{pe} =   plastic moment capacity per unit length of end plate

p =   length of yield line that extends along the web

p_{b13} =   distance between centerline of first interior bolts and third interior bolts

p_e =   distance between toe of flange fillet weld and centerline of adjacent bolts minus one quarter bolt diameter

p_{ei} = p_e for interior of connection

p_{eo} = p_e for exterior of connection

p_{fi} =   distance between centerline of first interior bolts and interior face of adjacent flange

p_{fo} =   distance between exterior face of flange and centerline of exterior bolts

p_t	=	distance between exterior face of flange and centerline of first interior bolts
p_{t3}	=	distance between exterior face of flange and centerline of third interior bolts
P_t	=	largest tensile force in connection
t_f	=	flange thickness (Figure 2.13)
t_w	=	web thickness (Figure 2.13)
t_s	=	stiffener thickness
T_a	=	experimental end plate thickness
T_{ep}	=	predicted end plate thickness
T_{ep1}	=	predicted end plate thickness using yield line mechanism #1
T_{ep2}	=	predicted end plate thickness using yield line mechanism #2
w	=	length of end plate tributary to each bolt
w_b	=	width of bolt head
w_f	=	flange weld splay
w_s	=	stiffener weld splay
w_w	=	web weld splay
X	=	distance from end of end plate to face of flange
Z	=	beam plastic section modulus
Z_f	=	beam flange plastic section modulus
σ_y	=	average of beam and end plate yield stress
α	=	di/l
α	=	$3/2 \cdot \alpha - 2\alpha^3$
α	=	$6\alpha^2 - 8\alpha^3$

1. Introduction

Strength, stiffness, and ductility are essential for connections in moment resisting frames in earthquake resistant steel construction. In an attempt to provide these three essential attributes, current Canadian and American design codes (CSA/CAN-S16.1-94, 1994; AISC, 1994) specify that beam-to-column connections shall be designed for the least of: 1) the plastic moment capacity of the beam; or, 2) the moment corresponding to the shear capacity of the column joint panel zone. This is intended to assure that the inelastic hinging that may occur in the connection during high seismic activity will not take place at the joinery but in the beam or panel zone. In addition, AISC (1994) specifies that: 1) the beam flanges must be welded to the column using full penetration groove welds; and, 2) the type of beam web connection must be designed as a function of the ratio of the plastic moment capacity of the flanges to the plastic moment capacity of the entire cross-section.

1.1 Statement of Problem

Over the past three decades moment connections have been used extensively in areas of high seismic activity. Until recently, the bolted web - welded flange (BWWF) moment connection was one of the most common moment connections in use. Relatively poor performance of the BWWF moment connection was observed during the Northridge Earthquake (AISC Special Task Committee on the Northridge Earthquake, 1994; Anon., 1994a, 1994b; Tremblay et al., 1995). The most common type of connection failure observed in steel structures subjected to the Northridge earthquake was cracking of the welds at the bottom flange.

General public concerns about the problem have prompted the engineering community to develop alternatives to replace the traditional BWWF connection with connections capable of resisting joint cracking (Rosenbaum, 1995; Rosta, 1995). Chapter 2 will review some of these alternatives.

One alternative to the BWWF connection is the extended end plate moment connection. This type of moment connection is particularly suitable in situations where

field welding is not desirable. One of the advantages of extended end plate connections is that the full penetration welds can be conducted under controlled shop conditions and in the most favorable welding position. The extended end plate also offers enhanced ductility at the beam to flange connection.

1.2 Objectives

A literature review on the behaviour of extended end plate moment connections has revealed that more research is needed to investigate the cyclic behaviour of this type of connection. Only a limited number of cyclically loaded tests have been conducted on end plate connections for small beams and an even smaller number of tests have been conducted on connections for medium and large beams. The main objective of the investigation presented in the following chapters is to extend the current experimental database to better understand the behaviour of extended end plate moment connections under cyclic loading. The literature indicates that the effect of beam size, bolt configuration and end plate thickness are parameters that should be specifically investigated.

A series of tests on full-size extended end plate connections was carried out to investigate the effect of various geometry and fabrication parameters on the cyclic behaviour of extended end plate moment connections for beams of small, medium and large capacity. The main objectives of the testing program were to:

- investigate the effect of beam size;
- investigate the effect of various bolt configurations;
- investigate the effect of extension stiffeners;
- investigate the effect of plate thickness;
- evaluate two different welding procedures; shielded metal-arc welding using E48018 electrode without access holes and flux-cored arc welding using E4802T-9-CH wire with access holes;

- evaluate the ability of extended end plate moment connections to force inelastic hinging in the beam; and

- identify the parameters that are most influential on the cyclic behaviour of extended end plate moment connections.

1.3 Scope

The behaviour of the extended end plate is the main focus of the study presented in the following. Therefore, in order to observe the behaviour of end plates up to failure, 12 of the 15 test specimens were designed with end plates significantly weaker than the beam and column. Three test specimens were designed to develop the full plastic moment capacity of the beam.

The test program consisted of a total of 15 test specimens. Three beam sizes (W360x51, W460x97, and W610x125) were investigated. The W360x51, S series, included three plate thicknesses (13 mm, 13.3 mm and 19 mm) and two bolt layouts. The W460x97, M series, included two plate thicknesses (15.9 mm and 19 mm) and three bolt patterns. The connections in the M series were tested both with and without extension stiffeners and test specimens were prepared using two welding procedures. The W610x125, B series, included two end plate thicknesses (15.9 mm and 19 mm) and three bolt patterns. Connections in the B series were tested both with and without extension stiffeners.

1.4 Organization of Thesis

A literature review is presented in Chapter 2. This review presents an overview of the problems experienced in steel frame connections in the Northridge earthquake and an overview of past research on BWWF and end plate moment connections. Chapter 3 presents a description of the experimental program conducted to investigate the behaviour of extended end plate moment connections under quasi-static cyclic loading. The results of 15 full-scale tests are presented in Chapter 4. An evaluation of strength prediction models and a comparison of the test results are presented in Chapter 5. Conclusions and recommendations for design and future research follow in Chapter 6. Material test results,

bolt elongation data and the values of the parameters used in the prediction models are presented in appendices A, B and C, respectively.

.

2. Literature Review

2.1 Preamble

Lateral forces on buildings essentially come from two sources, wind loads, occurring daily, and seismic loads occurring less frequently. Buildings are generally designed to perform elastically under daily wind loads. However, economics dictate that during earthquakes, selected portions of structures be designed to perform inelastically.

There are two basic methods for resisting lateral forces in steel structures; framing systems and shear wall systems. Framing systems use different geometric arrangements of steel members to resist lateral forces. Shear wall systems rely on either specifically designed concrete, masonry or steel plate walls to resist lateral forces. Concentration here will be on framing systems.

Three framing systems have traditionally been used to resist lateral forces in steel structures: concentrically braced frames, eccentrically braced frames and moment resisting frames (Figure 2.1).

The bracing members in concentrically braced frames (CBFs) extend diagonally across the bays of a structure, from one corner connection to the other (Figure 2.1a). One advantage of concentrically braced frames is their remarkable stiffness in the elastic range. During seismic activity, however, the braces of CBFs are required to dissipate energy inelastically. There are a number of reasons for the ineffectiveness of CBFs in seismic zones. They have limited potential for load redistribution once inelastic action has occurred in the brace (Redwood and Jain, 1992), their limited redundancy leads to high risk, and their energy dissipation capacity is decreased with brace slenderness (Redwood and Channagiri, 1991). In seismic zones CBFs are the least resilient of the three conventional steel frames.

Eccentrically braced frames (EBFs) are a modified version of concentrically braced frames. A slight change in geometry (Figure 2.1b) allows EBFs to combine the best attributes of both the CBFs and moment resisting frames (MRFs): stiffness and ductility. The diagonal bracing in EBFs is offset from the corner of the bays by shear links. The shear link is expected to deform inelastically and dissipate energy during an earthquake

allowing the remainder of the structure to remain elastic. The shear link must be adequately stiffened to prevent buckling, as it is better able to dissipate energy in shear than in bending (Hjelmstead and Popov, 1983; Kasai and Popov, 1986). Approximately 75 to 80 percent of the frame stiffness in EBFs comes from the braces and the remainder comes from the shear link connection to the column (Roeder and Popov, 1978). End plate connections are frequently used in both CBFs and EBFs to connect the beam and column. One disadvantage of braced frames, not exclusive to seismic zones, is that bracing severely restricts open spaces in a structure.

Moment resisting frames (MRFs), the third traditional framing system, have in recent years become a dominant type of steel framing in seismic zones. Inelastic action in a MRF can occur in the column, beam, connection or any combination of these three components, depending upon the design philosophy. The lateral forces imposed on MRFs are resisted through the bending of their members and connections. An attractive feature of MRFs is their large unobstructed open spaces which increase the usage of a structure. As well, MRFs usually attract smaller seismic forces than braced or shear wall systems (steel plate shear walls excluded) because of their flexibility and relatively long period of vibration (Astaneh-Asl, 1995). Until recently MRFs have been thought to have the ability to dissipate large amounts of energy through inelastic action during earthquake events, without permanent damage. This misconception was brought to the forefront by the 1994 Northridge earthquake. Fractures developed in many of the connections of the MRFs that weathered the Northridge earthquake (Popov, 1995)

The following presents a brief historical overview of moment connections, starting with problems observed after the Northridge earthquake. The bolted web – welded flange (BWWF) moment connection is given particular attention since it was the most common type of moment connection used in the Los Angeles area prior to the Northridge earthquake. Some of the research that is underway to improve the behaviour of moment connections is then reviewed. One of the methods discussed for improving the moment connection is the extended end plate connection. A history of end plate moment connections over the past three decades is presented. The review is divided into five

categories: moment capacity prediction, overall connection behaviour, prying action, bolt behaviour and weld behaviour.

2.2 Moment Resisting Frames

Moment resisting frames were used extensively in structures built to resist earthquakes prior to the Northridge earthquake on January 17, 1994. Northridge questioned the ability of MRFs by causing connection failures in more than 100 buildings (Malley, 1995).

The most common MRF connection in the Northridge region were the bolted web – welded flange moment connection (Figure 2.2). The Northridge earthquake brought to light a number of areas of concern in the BWWF connection. The problem areas reported by Sabol (1994) in the BWWF connection were:

1. failure of the frame girder bottom flange welds (Figure 2.3a);
2. failure of the frame girder top flange welds (Figure 2.3b);
3. cracks in the shear tab or shearing of the web bolts (Figure 2.3c);
4. cracks in the frame column (Figure 2.3d); and
5. divots of steel removed from the face of the column flange (Figure 2.3e).

The predominant mode of failure was the failure of the frame girder bottom flange weld.

There are many suggestions for possible causes of failure of BWWF connections. Malley (1995) cites a number of examples such as:

1. lack of toughness and through thickness ductility in base metals;
2. welding back up bars being left in place;
3. lack of fusion between initial weld pass and subsequent passes;
4. inadequate preheat;
5. the use of large diameter welding electrodes;
6. poor weld toughness;
7. poor ability of the bolted web to develop moment; and
8. the ever increasing trend of the engineering community towards the use of fewer fully restrained moment connections leading to larger moment connections and fewer load paths.

Other possible causes of BWWF connection failure have been proposed by the AISC Special Task Commitee on the Northridge Earthquake (STCNE) (1994), Popov (1995) and Krawinkler (1996).

1. poor welding workmanship;
2. restraint of the top flange from floor slabs;
3. height of the neutral axis in composite floor decks;
4. improper design requirements for panel zones;
5. large variance in ductility of steel depending on rolling direction;
6. large and inconsistent gaps between the yield and ultimate strengths of steel; and
7. large discrepancies between the anticipated and actual steel strengths.

Popov (1995) also points out that the connection damage observed in the Northridge earthquake shows a lack of ductility in the BWWF connection and that possibly a change in design philosophy is required; a change from rigid to semi-rigid connections.

Numerous ideas have been proposed for the repair of BWWF connections damaged in the Northridge earthquake, and how to improve moment connection design for new structures. Some repair ideas are listed below.

1. Gouging out the existing weld and rewelding (Malley, 1995);
2. Beam reduction either via flame cutting, shown in Figure 2.4a, 2.4b and 2.4c, or via drilling holes (Popov, 1995);
3. Addition of cover plates, shown in Figure 2.4d (Popov, 1995);
4. Addition of side plates, shown in Figure 2.4e (Nelson, 1996, Rosenbaum, 1995);
5. Cutting horizontal slits in the column web (Rosenbaum, 1995);
6. Replacing cracked steel and rewelding (STCNE, 1994);
7. Welding of beam web directly to the column (STCNE, 1994);
8. Addition of reinforcing plates and haunches, shown in Figure 2.4f and 2.4g (Malley, 1995; STCNE, 1994);
9. Welding of shear plates directly to the beam web (STCNE, 1994); and,
10. Use of vertical ribs (stiffeners), shown in Figure 2.4h (Krawinkler, 1996).

(The authors referenced may or may not be the origin of the idea but have reported that the repair method was possible.) Research is currently progressing to find experimental results backing the concepts for proposed repair techniques. As well as backing these concepts this research is indicating that the answer to the BWWF problem may be a switch to an alternate moment connection design altogether.

2.3 Bolted Web Welded Flange Moment Connections

Substantial research has been done on the bolted web welded flange moment connection over the past three decades. The material on BWWF connections is reviewed because of their similarity to the end plate moment connection, a possible alternative to BWWF connections. In the end plate connection the end plate in some respects acts as a column flange. Similar modes of failure are apparent for both connections. The following summarizes some of the re search in the BWWF moment connection area. Load versus displacement curves for two BWWF connections from two test programs have been included (Figures 2.6 - 2.9) to allow the reader to make their own comparisons between some of the extended end plate connections tested in the University of Alberta test program described in the following chapters.

2.3.1 Popov and Stephen (1970)

Popov and Stephen (1970) tested eight specimens to compare fully welded connections to BWWF connections under cyclic loading. Five specimens were constructed with W460x74 beams and three with W610x113 beams; all specimens used a W310x158 column and ASTM A325 bolts. Failure was at least partially due to cracking in the heat affected zones in three of the medium size BWWF connections and one of the large size BWWF connections (Figure 2.5). No cracks were observed in the two all welded connections.

Some doubt was cast into the theory that shear is carried solely by the web at the connection by testing a connection without web - column attachment. The connection without web-column attachment developed cracks at the toes of the copings, and although

it did not perform as well as those with web attachments it performed better than anticipated. Slip was apparent in the bolted connections.

2.3.2 Krawinkler and Popov (1982)

Krawinkler and Popov (1982) tested various moment connections with W200x31, W460x74 and W610x113 beams under cyclic loading. They investigated the performance of BWWF connections (varying the bolt diameter in the web connection), connections with bolted flanges and welded webs, connections with welded flange splices (cover plates welded to the flanges), and fully welded connections. Their investigation of bolt sizes showed that small bolts lead to more ductile connections than large bolts. The connections with bolted flanges and welded webs showed that bolt slip may reduce the energy dissipation per cycle. Failure of the BWWF connections occurred by fractures in the heat affected zones at the beam flange welds after reaching large rotations. Failure of the fully welded connections occurred due to local buckling of the beam flanges without the formation of cracks. Connections with welded flange splices were determined to be inferior to both the BWWF and fully welded connections. Overall Krawinkler and Popov found that connections could be good energy dissipaters and that, if detailed properly, could perform without loss in strength under seismic loading.

2.3.3 Popov, Amin, Louie and Stephen (1986)

Popov, Amin, Louie and Stephen (1986) reported on eight tests using W460x60 beams and either ASTM A325 or A490 bolts. The use of stiffeners and doubler plates in the column shear panel zone was examined. Popov et al. found that doubler plates increase the connection capacity and that stiffeners are essential in the column panel zone. It was also determined that small increases in the panel zone thickness, over that specified by the current code, greatly improved the ductility of the joints by forcing a plastic hinge to form in the beam. All connections developed cracks in the welds or the heat affected zone immediately adjacent the welds. The load versus beam tip displacement for one specimen, with doubler plates in the column panel zone and the abscence of column stiffeners, that failed by fracture of a flange weld, is shown in Figure 2.6. Popov et al.,

10

(1986) reported the load applied to the end of the cantilevered specimens (the beam tip) and the beam tip displacement. The load was applied 1645 mm from the column centerline. The load versus beam tip displacement for one specimen, with doubler plates and column stiffeners, that failed by fracture of a flange weld following fracture of the stiffener weld, is shown in Figure 2.7.

2.3.4 Engelhardt and Husain (1992)

Engelhardt and Husain (1992) tested eight connections using W460x89, W530x85 and W610x82 beams, and a W310x202 column. Their test program was designed to examine the relationship between the beam flange to entire section modulus (Z_f/Z) ratio, the web detail and the rotation capacity of the connection. The tests showed no correlation between the Z_f/Z ratio, the web detail, and the rotation capacity of the connection. All connections failed by fracture in flange heat affected zones. The load versus beam tip displacement curves of specimens 1 and 3, in the Engelhardt and Husain (1992) test program are shown in Figures 2.8 and 2.9, respectively. The distance from column face to load application was 2439 mm. Specimen 1 was a BWWF connection with a W610x82 beam and failed by sudden fracture at the bottom flange weld. Specimen 3 was a BWWF connection with a W610x82 beam and supplemental web welds and failed by sudden fracture of the bottom flange welds. Although some of the variability in connection performance was attributed to the Z_f/Z ratio and the changes in web details, most of the variability was attributed to the beam flange groove welds. Further information on the changes in web detail are given elsewhere (Engelhardt and Husain, 1992).

2.3.5 Tsai, Wu and Popov (1995)

Ten tests were performed by Tsai, Wu and Popov (1995) on BWWF connections subjected to cyclic loading. They investigated the Z_f/Z ratio, the use of supplemental web welds and the column panel zone strength. The beam sizes tested were W530x74, W530x92, W530x123 and W530x150. Cracks occurred in the flange heat affected zones. Maximum observed rotation capacities were between 0.5 and 1.0 degree and all

11

connections reached the plastic moment capacity of the beam. It was concluded that there was no correlation between the plastic section modulus ratio and connection performance and that supplemental web welds improved rotation capacity. Tsai, Wu and Popov (1995) also claimed that column panel zones when properly proportioned can enhance the deformation capacity of the connection.

2.3.6 Kaufman, Xue, Lu and Fisher (1996)

Kaufman, Xue, Lu and Fisher (1996) examined the crack surfaces of a number of connections damaged during the Northridge earthquake and performed dynamic tension tests of simulated beam flange to column connections. The fracture surfaces examined by Kaufman, Xue, Lu and Fisher (1996) all showed the origin to be associated with inadequate weld root penetration either from entrapped slag or porosity at the backup bar. (A connection detail with backup bars is shown in Figure 2.2.) Fifteen preliminary and five full-scale dynamic cyclic tests of large size beam to column connections were performed. The full-scale beam and column were W920x223 and W360x463, respectively. It was concluded that:

1. low toughness weld metal and geometric conditions contribute to brittle fracture;

2. removing backup bars and adding higher toughness weld reinforcement is not the best rehabilitation method;

3. connection behaviour varies greatly between static and dynamic loading;

4. self shielded flux cored electrode E480TG-K2 (a weld metal made from a silicon killed steel with a minimum impact strength of 27J @ -20 degrees Celsius) improved connection ductility and energy dissipation compared to connections welded with filler metal without notch toughness requirements;

5. connections can be repaired by removing welds and rewelding using tougher electrodes;

6. bolted web connections reinforced with fillet welds around the shear tabs perform as well as fully welded webs;

7. continuity plates (column stiffeners) significantly improve the behaviour of fully welded moment connections.

2.3.7 Roeder and Foutch (1996)

Roeder and Foutch compared 91 tests performed from 1960 to 1996. They found that the flexural ductility (flexural ductility = maximum beam tip displacement/beam tip displacement at yield) of a connection was dependent upon many factors. Some of their specific findings are that the flexural ductility of a BWWF connection is:

1. reduced by yielding of the panel zone;
2. reduced with increasing beam depth;
3. increased by increasing the length of the plastic hinge in the beam;
4. increased with columns oriented for weak axis bending;
5. increased (inconsistently) by reinforcing the connection; and
6. affected by the thickness of beam flanges.

Roeder and Foutch (1996) noted that column stiffeners are often required to prevent local damage in the column and doubler plates are usually needed to limit the amount of panel zone yielding. The panel zone yielding was found to be a reliable source of energy dissipation. Roeder and Foutch observed that connections with medium size beams (W310 and W460 sections) exhibit the most ductile behaviour.

The large amount of research on BWWF moment connections and especially the research that followed the Northridge earthquake has lead to improvements in the BWWF connection. This research however has also allowed engineers to devise potential solutions to the moment connection problem which depart from traditional thinking.

2.4 Reduced Flange Moment Connections

One popular concept originating from recent research is the reduced flange moment connection. In this type of connection, the beam cross-section is intentionally reduced to ensure hinging occurs at some distance away from the connection. The connections themselves are no different than the BWWF connections.

2.4.1 Iwankiw and Carter (1996)

Four tests were performed by Iwankiw and Carter (1996): two using W760x147 beams and W360x262 columns and two using W920x223 beams and W360x381 columns. E480TG-K2 welding electrode (with toughness requirement) was used for the flanges and E480T-7 electrode (without toughness requirement) was used for the shear tabs and column stiffeners. All four connections experienced column panel zone yielding, beam flange yielding, plastic hinge formation in the beam, and finally, beam flange buckling adjacent the connection. Cracks, however, did develop in two of the connections. One connection specimen experienced cracks in the beam flange heat affected zone beginning at a flange tip and propagating across the width. Another connection experienced column divot rupture beginning in the column flange heat affected zone and propagating through the base metal. Although cracks developed in two of the four tests, failure did not occur until well past the rotations which occurred in the structures exposed to the Northridge earthquake. The rotations observed in the Iwankiw et al. (1996) specimens were between 1.4 and 2.3 degrees. The rotations occuring in the Northridge earthquake, reported by Iwankiw et al. (1996), were less than 0.6 degrees.

2.4.2 Engelhardt, Winneberger, Zekany and Potyraj (1996)

Engelhardt, Winneberger, Zekany and Potyraj (1996) tested five reduced flange connections. The first four tests used W360x634 columns and various beam sizes. The four beam sizes tested were, W920x223, W920x238, W920x253, and W920x289. The fifth test had a W360x382 column and a W760x220 beam. All connections achieved rotations in excess of 1.15 degrees and four tests were in excess of 1.72 degrees. The only observed fracture occurred in the reduced flange area and started after the connections had undergone large rotations. Self shielded flux cored arc welding with an electrode possessing a Charpy V-Notch toughness of 27.1 J at -29 degrees Celsius was used for all welding and the backing bar was removed.

2.4.3 Chen, Yeh and Chu (1996)

Chen, Yeh and Chu also investigated the performance of the reduced flange connection. Their research shows that the ultimate strength and stiffness of a reduced flange connection is virtually the same as that of a connection without flange reduction but that it significantly increases the amount of plastic rotation prior to failure. Chen et al. state that the problem in BWWF connections is not the strength of the weld metal but the unreliability of the plastic deformation. Five specimens were tested using H600x300x12x20 beams and a box column 500x500x20x20 mm. Chen et al. found that by reducing the beam flange and forcing the yielding of the beam to occur over a larger area than would normally occur, leads to substantial increases in the rotation ductility. The use of reduced beam flange connections takes the focus away from the welding imperfections because it reduces the role the welding plays in energy dissipation.

Chen et al. also tested two simple frames on a shake table comparing the difference between the traditional BWWF connection and the BWWF connection with reduced beam flanges. The frames were identical except for the reduction in beam flange. The traditional BWWF connection failed with cracks that originated in the heat affected zone near the weld toe and propagated into the web. No cracks occurred in the connection with reduced flange area.

Research to date, although limited, has shown that the reduced flange moment connection is an effective way to force most of the inelastic deformation to occur in the beam away from the welded connection. Tests indicate that the reduced flange moment connection may be a superior connection in seismic zones compared to the traditional BWWF.

2.5 End Plate Connections

Another option to BWWF connections is end plate moment connections. The end plate moment connection involves welding plates to the ends of the beam in a fabrication shop and bolting the beam to the column flange on the construction site. The search for a solution to the moment connection problem has brought new focus on end plate connections.

End plate connections have the obvious benefits of reducing the cost of welding and eliminating poor quality welds which may arise from poor field conditions. Substantial research has been done on end plate connections under monotonic loading and recently research has begun on end plate connections under cyclic loading. Previous research on end plate connections, can be divided into five categories: moment capacity prediction; overall connection behaviour; prying forces; bolt behaviour; and weld behaviour. Although these categories are closely linked, an effort is made to separate them for better comprehension.

2.5.1 Prediction of End Plate Connection Moment Capacity

End plates behave in one of the three ways defined by Kennedy, Vinnakota and Sherbourne (1981). The categories of end plate behaviour relate closely to the degree of prying force involved in the connection. In end plate connections there is a tendency for the end plate to lose contact with the column flange at the bolt line (Figure 2.10). When contact is lost at the bolt line, the bolts in the end plate experience additional force. The bolts must now offset the flange force and the prying force. Figure 2.15 illustrates the additional force incurred by plate separation. End plates behave as either,

1. thick end plates - where no prying forces are present;
2. intermediate end plates - where plastic hinges begin to form; or
3. thin end plates - where plastic hinges have formed and maximum prying forces are present.

Classification of an end plate, and the degree of prying force, is dependent on applied force, bolt size and strength, end plate thickness and geometry, column flange properties and panel zone behaviour. The many parameters that affect end plate behaviour give indication of the complexity of the end plate connection and of the inherent difficulty in predicting their behaviour.

Many design equations for end plate connections have been developed. Basically, the equations can be classified into three categories. The categories and authors who have used the methods to predict end plate behaviour are listed as follows:

2. Yield Line Theory (Packer and Morris, 1977; Mann and Morris, 1979; Grundy et al., 1980; Whittaker and Walpole, 1982; Murray and Borgsmiller, 1995); and

3. Finite Element Method (Krishnamurthy, 1978; Kukreti, Ghassemieh and Murray, 1990; Tsai and Popov, 1990).

2.5.1.1 T-Stub Analogy

The T-stub analogy for the analysis of extended end plate connections assumes that end plate connections can be modelled as T-stubs and that simple equilibrium equations may be used to solve for the capacity of the end plate.

2.5.1.1.1 Agerskov (1976)

Agerskov (1976) developed two approximate equations to predict the moment capacity of end plate connections. The first equation is based on the assumption that full plastification through the cross-section of the end plate occurs prior to end plate separation at the bolt lines. The bolt line is the section of the end plate passing through the bolts parallel to the beam flange and the load line is the section of the end plate adjacent to the beam flange (Figure 2.10). The second equation is based on the assumption that end plate separation at the bolt lines occurs prior to yielding of the end plate. Essentially the equations reflect thick and thin end plate behaviour, respectively. Agerskov's end plate connections were made between two beam segments as opposed to between a beam and a column (Figure 2.12). Agerskov used 15 tests to validate his predictions. It is noted in his research that there is a limit to the extent of prying forces.

In Agerskov's research the moment distribution in the end plates was determined based on the experimental bolt forces. From these moment distributions it was clear that the yield moment of the end plate connection first occurred at the toe of the fillet welds (fillet welds were used instead of complete penetration welds). It was also demonstrated that as the load was increased beyond this yield load, the moment at the bolt line remained unchanged while plastification occurred at the toe of the fillet welds. This happened

because as the end plate yields at the toe of the fillet welds the end plate losses stiffness. The loss in stiffness keeps the moment at the bolt line at approximately the same level as that corresponding to first yield until strain hardening occurs. Because increase in load at the bolt line is not possible until strain hardening occurs at the toe of the fillet weld Agerskov rejected the concept that a mechanism forms in the end plate prior to strain hardening at the toe of the fillet weld. Agerskov's equations are presented below. Common geometric dimensions of end plate connections are shown in Figure 2.13.

Separation before yielding of the end plate

The force in the beam flange is given as

$$F(b+di) - B \cdot b = \frac{1}{4} w \cdot T_{ep}^2 \sqrt{F_{yep}^2 - 3(\frac{F}{w \cdot T_{ep}})^2} \tag{2.1}$$

and the force in the bolts is given as

$$\frac{1}{10} \frac{B_o T_{ep}}{A_s} + \frac{B - B_o}{A_s} \cdot (\frac{1}{2} \cdot k_1 + k_4) = \frac{l^3}{w \cdot T_{ep}^3} (F \cdot \alpha_1 - B \cdot \alpha_2) \tag{2.2}$$

Yielding of the end plate before separation

The force in the beam flange is given as

$$F(di+b) - B \cdot b + C \cdot b = \frac{1}{4} w \cdot T_{ep}^2 \sqrt{F_{yep}^2 - 3(\frac{F}{w \cdot T_{ep}})^2} \tag{2.3}$$

and the force in the bolts is given as

$$\frac{1}{10} \frac{B_o - C}{A_s} T_{ep} = \frac{l^3}{w \cdot T_{ep}^3} (F \cdot \alpha_1 - (B - C)\alpha_2) \tag{2.4}$$

where;

$\alpha \quad = \quad di/l$

$\alpha_1 \quad = \quad \frac{3}{2} \cdot \alpha - 2\alpha^3$

$\alpha_2 \quad = \quad 6\alpha^2 - 8\alpha^3$

$A_s \quad = \quad$ cross sectional area of bolt shaft

b = distance between centerline of exterior bolts and edge of end plate (Figure 2.13)

B = bolt force

B_o = initial bolt pretension

B_o' = bolt tension where separation occurs at the bolt line = $B_o(1 + \dfrac{k_3}{k_2})$

$$C = B_o(\frac{B'_o - B}{B'_o - B_o})$$

di = distance between center of interior bolts and interior flange face (Figure 2.13)

F = flange force

F_{yep} = end plate yield stress

k_1 = $l_s + 1.43l_t + 0.71l_n$

k_2 = $k_1 + 0.2l_n + 0.4l_w$

k_3 = $0.4T_{ep}$

k_4 = $0.1l_n + 0.2l_w$

l = $2(di - b)$

l_t = length of bolt threads between full bolt shaft and nut

l_s = length of bolt shank

l_w = thickness of washers

T_{ep} = predicted end plate thickness

w = length of end plate tributary to each bolt

Agerskov's equations were developed for end plate connections with equal bolt spacing on either side of the beam flange. This value will be referred to as *di* when the bolt spacing is equal. When the bolt spacing is different on the interior and exterior portions of the connection *di* will be used to denote the interior bolt spacing from the beam flange and *do* will be used to denote the exterior bolt spacing from the beam flange. This is illustrated in Figure 2.13.

Some of the assumptions Agerskov used to derive the above equations are:

1. end plate connections can be modelled as T stub connections;

2. the beam web has a negligible effect on the stiffness of the connection (the experimental data in Agerskov's research showed that the web does make the interior portion of the connection stiffer than the exterior portion.);

3. no end plate bending occurs under the beam flange welded area (Figure 2.14); and

4. the beam flange welded area is equal to 1.4 times the flange thickness.

Agerskov's experimental program showed that these assumptions were reasonable.

2.5.1.1.2 Witteveen, Stark, Bijlaard, Zoetemeijer (1982)

Witteveen et al. (1982) investigated unstiffened moment connections. The end plate connections tested were designed to confine the connection failure to the end plate and bolts. Witteveen et al. acknowledged three types of end plate connection failure: connection failure due to bolt fracture; connection failure where the bolts yield and yield lines develop in the end plate adjacent the flange welds; and connection failure where yield lines develop in the end plate near the bolts and welds.

Three prediction equations for the maximum flange force were developed to account for these modes of failure and are shown in the same order as presented above.

$$F = B_f \tag{2.5}$$

$$F = \frac{2l \cdot M_{pe} + B_f b}{a' + b} \tag{2.6}$$

$$F = \frac{4l \cdot M_{pe}}{a'} \tag{2.7}$$

$$b < 1.25a', \ b < di$$

where;

a' = distance between the edge of bolt head and toe of fillet weld (Figure 2.13)

B_{ep} = width of end plate (Figure 2.13)

B_f = bolt design strength

F = maximum flange force

20

l = effective length of end plate

l = $g + 4a' + 1.25b,$ if $g < 4a' + 1.25b$

l = $8a' + 2.5b,$ if $g > 4a' + 1.25b$

l < B_{ep}

M_{pe}= plastic moment capacity per unit length of end plate

g = bolt pitch

Other variables have been previously defined.

The equation that Witteveen et al. proposed for the calculation of the end plate thickness is as follows:

$$T_{ep} = \sqrt{\frac{F \cdot a'}{l \cdot F_{yep}}} \tag{2.8}$$

where F, a', l, and F_{yep} are as defined above.

Like many other proposed equations (Agerskov, 1976; Surtees and Mann, 1970; Mann and Morris, 1979; Grundy et al., 1980), the design equations presented by Witteveen et al. do not account for the highly nonlinear behaviour of end plates.

2.5.1.2 Yield Line Theory

Yield line theory involves approximation of end plate yield lines and calculation of the theoretical moment capacity using the virtual work method. The yield line theory was used to predict the end plate capacities in the U of A test program, presented in the following chapters.

2.5.1.2.1 Mann and Morris (1979), Surtees and Mann (1970), Packer and Morris (1977)

Mann and Morris (1979) used the yield line theory to predict the performance of end plate connections. A 33 percent increase in the bolt capacity was suggested by Mann and Morris to compensate for the additional bolt forces induced by prying action. It was noted that thick end plates cannot easily be modelled using the yield line theory because of the development of yield zones rather than yield lines. It was also observed that modest changes in the end plate thickness greatly affect end plate performance. The equations

21

derived by Mann and Morris were a combination of those derived by Surtees (1970) and Packer and Morris (1977).

Surtees and Mann (1970) proposed the following equation for the calculation of the required end plate thickness:

$$T_{ep} = \sqrt{\frac{M_b}{F_{yep} \cdot d_f \cdot (2 \cdot B_{ep} / c + d_f / g)}}$$

(2.9)

where;

c = distance between centerline of exterior bolts and centerline of interior bolts (Figure 2.13)

M_b = beam moment

Other variables have been previously defined.

The yield line pattern used by Surtees and Mann is presented in Figure 2.15. This equation was believed to be a limiting strength design criterion. The equation proposed by Packer and Morris (1977) is:

$$T_{ep} = \sqrt{\frac{M_b \cdot a}{F_{yep} \cdot d_f \cdot (B_{ep} - d_h)}}$$

(2.10)

where;

a = distance between centerline of bolts and edge of flange fillet weld (Figure 2.13)

d_b = nominal bolt diameter

d_h = sum of bolt hole diameters across width of end plate

n = number of bolt holes across width of end plate

Other variables have been previously defined.

Mann and Morris presented a similar equation:

$$T_{ep} = \sqrt{\frac{M_b \cdot a}{d_f \cdot F_{yep} \cdot B_{ep}}}$$

(2.11)

The diameter of the bolts was dropped from the equation because it was thought that the work done deforming the bolts compensated for the loss of plate strength due to the holes.

22

2.5.1.1.2 Grundy, Thomas and Bennetts (1980)

Grundy et al. (1980) advocate a design procedure based on an equilibrium approach. Assuming the angle between the beam and the column is 90 degrees, the equations proposed by Grundy et al. (1980) take the following form:

$$T_{ep} = \sqrt{\frac{2P_t \cdot di}{B_{ep} \cdot F_{yep}}} \qquad (2.12)$$

where;

d_f = depth of beam - flange thickness (Figure 2.13)

F_x = axial force in beam

P_t = largest tensile force in the connection = $\dfrac{M_b}{d_f} - \dfrac{F_x}{2}$ $\qquad$ (2.13)

Other variables have been previously defined.

Grundy et al. also developed a complete set of design equations for the design of the end plate moment connections including the bolt forces and spacing, column panel zone strength and the design of stiffeners. The complete design procedure is described elsewhere (Grundy et al., 1980).

2.5.1.2.3 Whittaker and Walpole (1982)

Whittaker and Walpole (1982) also used the yield line theory to predict the behaviour of end plate connections and, like Mann and Morris (1979), used a modified version of the equation derived by Surtees and Mann (1970) (Eq. (2.9)). Whittaker and Walpole, however, accounted for weld thickness and believed that the yield line along the beam web extended 0.6 times the beam depth. yield line pattern, Surtees and Mann's and yield line patterns Whittaker and Walpole's are shown in Figure 2.15. The following expression for the end plate thickness was derived from this assumed yield line pattern.

$$T_{ep} = \sqrt{\frac{M_b}{F_{yep} \cdot d_f \cdot \left[(\dfrac{2 \cdot B_{ep}}{c - t_f - w_f}) + (\dfrac{2 \cdot p}{g - t_w - 2 \cdot w_w}) \right]}} \qquad (2.14)$$

where,

p = the length the yield line extends along the web

t_f = flange thickness (Figure 2.13)

t_w = web thickness (Figure 2.13)

w_f = flange weld splay (Figure 2.13)

w_w = web weld splay (Figure 2.13)

Other variables have been previously defined.

2.5.1.2.4 Murray and Borgsmiller (1995)

Murray and Borgsmiller (1995) recently used the yield line theory to develop equations to predict the required end plate thickness for connections using multiple rows of bolts. Two equations were developed to account for the possibility of differing yield line patterns depending on the end plate geometry. The various proposed yield line patterns are presented in Figure 2.16.

The predicted plate thickness using yield line pattern 1 is:

$$T_{ep1} = \sqrt{\frac{M_b / F_{yep}}{\frac{B_{ep}}{2} \cdot \left[\frac{1}{2} + \frac{h}{p_{fo}} + \frac{h - p_t}{p_{fi}} + \frac{h - p_{t3}}{u} \right] + 2 \cdot \left[(p_{fi} + p_{b13} + u)(\frac{h - p_t}{g}) \right]}} \qquad (2.15)$$

$$u = \frac{1}{2} \sqrt{b_f \cdot g \cdot \frac{(h - p_{t3})}{(h - p_t)}}$$

h = length of end plate from one edge of end plate to the opposite beam flange

p_{b13} = distance between centerline of first interior bolts and third interior bolts

p_{fi} = distance between centerline of first interior bolts and interior face of adjacent flange

p_{fo} = distance between exterior face of flange and centerline of exterior bolts

p_t = distance between exterior face of flange and centerline of first interior bolts

p_{t3} = distance between exterior face of flange and centerline of third interior bolts

All above defined variables are shown in Figure 2.16. Other variables have been previously defined.

<u>The required plate thickness predicted using yield line pattern 2 is:</u>

$$T_{ep2} = \sqrt{\frac{M_b / F_{yep}}{\frac{B_{ep}}{2}\left[\frac{1}{2} + \frac{h}{p_{fo}} + \frac{(h - p_t)}{u}\right] + \frac{2}{g} \cdot (p_{fi} + p_{bi3}) \cdot (h - t_f) + \frac{2u}{g} \cdot (h - p_{i3}) + g / 2}} \quad (2.16)$$

where;

$$u = \frac{1}{2}\sqrt{b_f \cdot g}$$

The Murray and Borgsmiller model was able to predict their test results to within 13 percent for nine out of ten tests. The test falling outside this 13 percent range failed prematurely due to bolt failure. In the calculation of M_b they assumed either thick, intermediate or thin end plate behaviour as discussed previously (Kennedy et al., 1981).

2.5.1.3. Finite Element Analysis

2.5.1.3.1 Krishnamurthy (1978)

Krishnamurthy (1978) pointed out that one flaw with the T-stub analogy is assuming the bending moment at the bolt line is equal to the bending moment at the load line. Biaxial bending around the bolt holes ensures a larger moment at the load line. Krishnamurthy (1978) and Agerskov (1976) suggested that the bending in an end plate occurs largely between the toe of the flange weld and the edge of the bolt head. This is in contrast to the conventional T-stub method which uses the distance between the face of the flange and the centerline of the adjacent bolts as the distance over which bending in the end plate occurs.

Krishnamurthy (1978) notes that the end plate is stiffer on the interior of the connection due to the presence of the beam web and that the end plate inflection point may or may not be centered between the edge of the bolt head and the toe of the flange weld when the applied force overcomes the clamping force of the bolts. Based on the above considerations, Krishnamurthy used a finite element analysis to develop a modified

T-stub approach. The actual design equation proposed by Krishnamurthy was determined by a regression analysis of the results of numerous finite element studies. The design equation proposed for the prediction of the end plate moment is:

$$M = 1.29(\frac{\sigma_y}{B_u})^{0.4} (\frac{B_y}{F_{yep}})^{0.5} (\frac{f_b}{B_{ep}})^{0.5} (\frac{A_f}{A_w})^{0.32} (\frac{p_e}{d_b})^{0.25} M_t \qquad (2.17)$$

where;

M_t = 0.25 $F·p_e$

A_f = area of beam tension flange

A_w = area of beam web

B_y = bolt yield stress

B_u = ultimate bolt tensile stress

F = $\dfrac{M_b}{d_f}$

f_b = width of beam flange

p_e = distance between toe of flange fillet weld and centerline of adjacent bolts minus one quarter bolt diameter

σ_y = average of beam and end plate yield strength

The end plate thickness is calculated using

$$T_{ep} = \sqrt{\frac{6M}{B_{ep} \cdot F_{yep}}} \qquad (2.18)$$

where M is given by equation 2.17. B_{ep} and F_{yep} are previously defined.

Nine tests on end plate moment connections were conducted using W310x45, W410x39 and W410x60 beams to successfully verify Krishnamurthy's design equations. The proposed modified T-stub method resulted in a reduction in end plate thickness over that suggested by the current code leading to more flexible connections. Krishnamurthy's tests used ASTM A325 bolts and were conducted monotonically.

2.5.1.3.2 Kukreti, Ghassemieh and Murray (1990)

Kukreti, Ghassemieh and Murray (1990) studied the behaviour of large capacity end plate connections with and without extension stiffeners. The connections were designed using the finite element method (FEM). Design equations were established for stiffened end plate connections to limit plate separation between the column flange and the end plate and to limit the strain in the end plate.

The end plate thickness required to limit plate separation is given as:

$$T_{ep1} = \frac{0.00553 \cdot a^{0.873} \cdot g^{0.577} \cdot F^{0.917}}{d_b^{0.924} \cdot t_s^{0.112} \cdot B_{ep}^{0.682}} \tag{2.19}$$

where;

t_s = stiffener thickness

Other variables have been previously defined.

The end plate thickness required to limit end plate strain is given as

$$T_{ep2} = \frac{0.00371 \cdot a^{0.257} \cdot g^{0.148} \cdot F^{1.017}}{d_b^{0.719} \cdot t_s^{0.162} \cdot B_{ep}^{0.319}} \tag{2.20}$$

All units in equations 2.20 and 2.21 are imperial (inch, kip).

Kukreti et al. (1990) verified their equation with experiments although no experimental data was presented in the cited reference.

Derivations of equations using finite element modelling may not be easily understandable by the practicing engineer. Therefore, there is still a need for the equations derived from simpler methods such as the yield line theory. The yield line theory and the equilibrium approach offer the benefit of knowing, from first principles, how all parameters have been obtained.

2.5.1.3.3 Recent Work

More recent work on finite element modelling of extended end plate connections has been performed by Shi, Chan and Wong (1996) and Choi and Chung (1996). Shi, Chan and Wong (1996) proposed an analytical procedure based on yield line and beam theory to represent the nonlinear moment-rotation relationship of end plate connections. They compared their procedure (presented in the referenced paper) with available experimental

27

results and determined their method could predict yield moment and connection stiffness. It was noted that their procedure repeatedly underestimated the maximum connection moment.

Choi and Chung (1996) used the finite element method to investigate end plate connections. Choi and Chung noted that large column flange deformations greatly influence connection behaviour and that unstiffened columns should not be used in end plate connection design. With more work the model developed by Choi and Chung may be used to characterize the behavioral characteristics of end plate connections. Detailed information is given in the referenced paper.

There are many prediction equations, some more detailed and more accurate than others and some easier to use but less accurate. It is difficult to arrive at simple but consistently accurate end plate moment capacity predictions due to the inherent complexity and high nonlinearity of end plate connection performance. Chapter 5 presents a comparison between ten different prediction equations with the results of 15 tests performed at the University of Alberta.

2.5.2 End Plate Behaviour

As previously mentioned end plates behave in fundamentally different ways depending on their thickness. Thickness, however, is not the only parameter affecting their behaviour. End plate behaviour is dependent on the degree of prying force on the end plate, the elastic or inelastic elongation of the bolts, the general quality of the weld metal and heat affected zone, the flexibility of the column panel zone, the beam depth, the bolt configuration and the magnitude of the applied forces. Obviously there are many parameters to be investigated in the study of end plate connections. Section 2.5.1 gave some indication of the amount of research that has been undertaken to arrive at equations for predicting the moment capacity of end plate connections. Some research programs, however, have been focused on the behaviour of the end plate connections themselves in an effort to determine the parameters that benefit the performance of the end plate connection. This research has been conducted using both monotonic and cyclic loading. (The research presented in Section 2.5.1 considers monotonic loading only.) It should be

kept in mind that the prediction of end plate capacity and experimental observations concerning the parameters affecting end plate performance can never be completely separated. The review of the research programs presented in the following is focused mainly on experimental observations and not on the prediction of moment capacities. The research programs have been grouped into two sections, namely, research programs dealing with monotonic loading and research programs dealing with cyclic loading.

2.5.2.1 Extended End Plate Connections Under Monotonic Loading

2.5.2.1.1 Grundy, Thomas and Bennetts (1980)

Grundy, Thomas and Bennetts (1980) studied various parameters that affected the performance of end plate connections. Grundy et al. studied end plates tested under monotonic loading to understand the performance of thin end plates. The three parameters specifically investigated were bolt size, end plate thickness and column stiffening.

Two tests were performed using W610x113 beams and W310x240 columns. One test was conducted with a 1 inch (25.4 mm) thick end plate and one with a 1.25 inch (31.8 mm) thick end plate. All end plates were designed to fail before yielding of the beam. A number of factors affecting end plate performance emerged from the research program. Grundy et al. found that prying forces were between 10 and 15 percent of the bolt force. This is substantially lower than the 33 percent suggested by Mann and Morris (1979). It was observed that, when placed at equal distance from the flange, the interior bolts attract more load than the exterior bolts and that thin end plates increase this unequal load distribution. This was also observed in the experimental program conducted by Mann and Morris (1979) and ignored in their design equations. It is also noted that all end plate connections are susceptible to brittle fracture and that this risk is reduced with thin end plates because their added flexibility allows for moment redistribution. Grundy et al. proposed a design procedure for the complete end plate moment connection. The design equation for end plate thickness was presented in Section 2.5.1.1.2.

2.5.2.1.2 Bose and Hughes (1995)

Bose and Hughes (1995) suggest that if semi-rigid connection design is used, rather than rigid connection design, end plate moment connections can be less elaborate and less costly. Semi-rigid design may be used because end plate connections possess the capability to act as plastic hinges and behave as ductile connections. It is noted that one downfall of ductile connections is their inefficiency in terms of strength due to large prying forces. Bose and Hughes (1995) propose that any connection with the ability to achieve a rotation of 1.7 degrees may be labeled a ductile connection and any connection unable to reach 1.1 degrees may be considered as a non-ductile connection.

The monotonically loaded tests conducted by Bose and Hughes consisted of the following beam sizes; W406x178, W457x191, W686x254 and W762x267. End plate failures were due to cracks developing in the heat affected zones adjacent to the flanges. Bose and Hughes noted the importance of beam span on connection classification. Rotational stiffness or rigidity is sometimes defined in terms of beam stiffness (i.e. Eurocode 3 for unbraced frames requires connection rigidity of 25 B/L, where B is the bending stiffness and L is the length of the connected beam). With this definition, a connection which may be considered rigid for a short span may not be considered rigid for a long span. Bose and Hughes also found a clear correlation between beam depth and ductility, and that achieving good ductility is possible in end plate connections for beams less than 700 mm deep. In fact Bose and Hughes claim that the depth of the beam is the most significant factor influencing the rigidity of the connection. Increasing the bolt spacing also resulted in increased connection ductility.

All research presented in Sections 2.5.1 and 2.5.2.1 was conducted under monotonic loading. Under monotonic loading end plates were shown to display excellent ductility and energy dissipation characteristics which further encourages their use in seismic zones.

2.5.2.2 Extended End Plate Moment Connection Under Cyclic Loading

2.5.2.2.1 Ghobarah, Osman and Korol (1990)

Much of the work on cyclic loading of extended end plate connections has been done by Ghobarah, Osman and Korol. Ghobarah et al. (1990) tested five specimens with

W360x45 beams and either a W360x64 or W360x79 column. They concluded that properly designed end plate connections provide excellent ductility and energy dissipation capacity; the same conclusion arrived at by many of the authors testing end plate connections under monotonic loading. The five specimens tested compared the performance of unstiffened end plate connections, stiffened end plate connections, and looked at the individual behaviour of the beam, column flange, stiffeners, bolts, and end plates. One inch (25.4 mm) A490 bolts were used in all tests, and all specimens were designed using the equations proposed by Mann and Morris (1979), and Packer and Morris (1977) and presented in Section 2.5.1. These equations were found by Ghobarah et al. to be satisfactory. The end plate connections tested showed excellent ductility.

It was concluded that bolts and unstiffened end plates should be designed for 1.3 times the plastic moment capacity (M_p) in order to limit bolt degradation and compensate for forces induced by prying action. It was also concluded that stiffened end plates can be designed for M_p and unstiffened columns should not be used in seismic zones. The overall end plate connection performance was found to be satisfactory for use in seismic zones.

2.5.2.2.2 Korol, Ghobarah and Osman (1990)

As an extension of the testing program presented in the previous section, Korol et al. (1990) tested end plates on slightly heavier beams, W360x57. The use of beams with stockier webs lead to improved behaviour because of the greater amount of energy required to force local buckling of the beam. Korol et al. (1990) found that the failure of the end plate and bolts required substantial amounts of energy but that this energy was not to be relied upon during an earthquake because of the brittle failure mode associated with failure of the bolts and end plate. Other observations included the loss of pretension in the bolts and a general loss of connection stiffness as the connections were cyclically loaded. It was also suggested that the reduction in connection stiffness would invariably lead to problems involving interstorey drift.

31

Ghobarah, Korol and Osman (1992) furthered their end plate connection research by testing four connections with W410x60 beams. For this testing program, all specimens were prepared with one inch (25.4 mm) A490 bolts, and both continuity and doubler plates were added to the column. All columns were subjected to an axial load during testing. It was found that panel zone yielding can dissipate large amounts of energy, doubler plates are effective in increasing the shear capacity of the column and that the end plate helps to control the inelastic deformation of the panel zone. Ghobarah et al. (1992) recommended that both the beam and panel zone be designed to participate in the energy dissipation in order to improve the overall energy dissipation capacity of the connection. Again, end plates demonstrated their suitability for use in seismic zones.

2.5.2.2.4 Tsai and Popov (1989)

Tsai and Popov (1989) tested three end plate connections under cyclic loading and modelled the local plate rigidities at the inner and outer bolts using finite element analysis. Two connections were constructed, one with a W460x60 beam and the other with a W530x66 beam. The third test specimen consisted of the repaired medium size beam connection (W460x60). Popov and Tsai looked at end plate connections with and without end plate stiffeners and varied the end plate thickness. Observations included the inelastic action of the connections due to bolt elongation and improved performance in end plate connections with the addition of end plate stiffeners. It was also found that local plate rigidity has a greater effect on end plate connection performance than prying action, for thick end plates (Popov and Tsai used 1-1/4" (31.8 mm) and 1-3/8 " (35 mm) thick end plates). Tsai and Popov analytically showed that unstiffened end plates are more than twice as rigid at the inner bolt holes than at the outer bolt holes. Tsai and Popov determined that end plate connections were excellent energy dissipaters and would perform satisfactorily in seismic zones.

2.5.3 Prying Action in End Plate Design

Many different factors have been suggested to account for the prying force in end plate connections. It is possible that the reason these factors are different is because the prying force in an end plate is affected by many parameters. Varying parameters such as the degree of bolt elongation, the thickness of end plate, end plate geometry, and end plate strength and flexibility may alter the degree of prying action occurring in the connection. It is therefore not surprising that different testing programs, with different end plates show different degrees of prying action.

2.5.3.1 Chasten, Lu and Driscoll (1992)

Chasten, Lu and Driscoll (1992) investigated the effect of prying action on the performance of end plates. They tested seven large end plate connections designed to achieve failure through excessive end plate deformation. The excessive deformation emphasized the prying action. Finite element models were used to model the connections. Past research has suggested that prying forces may be as low as 10 to 15 percent (Grundy et al., 1980) or as high as 33 percent (Packer and Morris, 1977; Mann and Morris, 1979).

The tests conducted by Chasten et al. (1992), used 1 inch (25.4 mm) ASTM A325 bolts, end plate thicknesses ranging from 19 mm to 25.4 mm, a W690x140 beam and a W360x287 column. It was found that prying forces do not start to develop until plastic hinging begins in the end plate. This is in agreement with the end plate classification system proposed by Kennedy et al. (1981) and outlined in Section 2.5.1. Chasten et al. (1992) observed failures including end plate shear, cracks in the heat affected zones originating at the toe of the welds and extending into the base metal, and bolt failure. The conclusion of their research was that prying action accounts for 30 to 40 percent of the bolt force.

2.5.3.2 Murray and Meng (1995)

Murray and Meng (1995) investigated the possibility of using shims to eliminate the prying forces induced by the bending of the end plate. The three connections tested, designed using the yield line theory, used W460x52 beams, W360x216 columns and

ASTM A325 bolts. Two of three tests performed were without shims, one using the turn of the nut method for tightening the bolts and one using instrumented bolts. There were no signs of distress in the end plate, bolts or column flange in any specimen, and failure occurred because of local buckling of the beam. The third test specimen was prepared with shims placed between the end plate and the column flange at points of load application (Figure 2.16). The third test experienced an unusual drop in bolt forces which may be attributed to yielding of the shims. The drop in bolt forces was not explained.

2.5.4 Bolt Behaviour in End Plate Design

The factors affecting bolt behaviour in end plate connections are bolt preload, direct load application and prying action. As prying action has already been mentioned and the direct loading of bolts is obvious, this section will focus on bolt preload, the load induced in the bolt during the construction of the connection.

2.5.4.1 Fleishman, Chasten, Lu and Driscoll (1991)

Fleishman, Chasten, Lu and Driscoll (1991) studied the effect of pretensioning bolts versus snug tightening bolts (initial bolt load). They found that snug tightened connections were basically as stiff as pretensioned connections and were actually stiffer when load reversal was applied. Pretensioned bolts are preloaded to 70 percent of their tensile strength whereas snug tightened bolts are stressed to only about 35 percent of their tensile strength.

Pretensioning bolts has a number of benefits such as lowering of the applied stress range which the bolt endures, reducing bolt fatigue, and helping to eliminate slip within the connection. Fleishman et al. (1991) found that bolt pretension did not affect the magnitude of the prying forces at ultimate load. Fleishman et al. also noted that at the beginning stages of loading there is unequal load sharing between bolts in end plate connections. This unequal load sharing is because the bolts on the interior of the connection have the load transferred to them via a stiffer mechanism, the beam web and flange, whereas the exterior bolts receive load via the beam flange alone. This observation was made earlier in the research performed by Agerskov (1976) and Krishnamurthy

(1978). It was also found by Fleishman et al. that snug tight bolts are better able to equally redistribute this initial load than pretensioned bolts.

The basic difference, in regards to connection performance, between snug tight bolts and pretensioned bolts is that snug tight bolts let plate separation and prying action begin at lower load levels. Pretensioned bolts force the end plate to yield earlier than snug tight bolts.

All tests performed by Fleishman et al. used ASTM A325 bolts of either 1 inch (25.4 mm) or 1-1/8 inch (28 mm) end plates, and W690x140 beam sections. It is interesting to note that they found that end plate connections with snug tight bolts under monotonic loading are more flexible than end plate connections using pretensioned bolts up until yielding of the end plate and then, it is possible for the end plate with snug tight bolts to become stiffer than the plate with pretensioned bolts. Their tests also indicated that under cyclic loading snug tight bolts lead to a stiffer connection. Under cyclic loading snug tight bolts lead to a stiffer connection because by the time of load reversal more deformation as occurred in the end plate of the connection with pretensioned bolts than in the one with snug tightened bolts. This excess deformation gives the snug tightened connection an apparent lower stiffness.

2.5.5 Weld Metal in End Plate Design

The performance of the weld metal and the heat affected zone is another very important parameter when investigating the behaviour of end plate connections. There has been little research done to investigate the effect of weld metals on the performance of end plate connections. In fact in much of the research done the weld metal and welding procedure used are not even reported. As mentioned in Section 2.2 the toughness or lack of toughness has been cited as a factor contributing to the damage of the BWWF connections during the Northridge earthquake. Kaufman, Xue and Lu (1996) determined that self shielded flux cored electrode E480TG-K2 with a toughness of 27J at -27 degrees Celsius improved connection ductility and energy dissipation, over gas shielded flux cored E480T-4 electrode with a toughness of 13.4 J at -21 degrees Celsius. There is a great

(1978). It was also found by Fleishman et al. that snug tight bolts are better able to equally redistribute this initial load than pretensioned bolts.

The basic difference, in regards to connection performance, between snug tight bolts and pretensioned bolts is that snug tight bolts let plate separation and prying action begin at lower load levels. Pretensioned bolts force the end plate to yield earlier than snug tight bolts.

All tests performed by Fleishman et al. used ASTM A325 bolts of either 1 inch (25.4 mm) or 1-1/8 inch (28 mm), and W690x140 beam sections. It is interesting to note that they found that end plate connections with snug tight bolts under monotonic loading are more flexible than end plate connections using pretensioned bolts up until yielding of the end plate and then, it is possible for the end plate with snug tight bolts to become stiffer than the plate with pretensioned bolts. Their tests also indicated that under cyclic loading snug tight bolts lead to a stiffer connection. Under cyclic loading snug tight bolts lead to a stiffer connection because by the time of load reversal more plastic deformation as occurred in the end plate of the connection with pretensioned bolts than in the one with snug tightened bolts. This larger deformation gives the snug tightened connection an apparent lower stiffness.

2.5.5 Weld Metal in End Plate Design

The performance of the weld metal and the heat affected zone is another very important parameter when investigating the behaviour of end plate connections. There has been little research done to investigate the effect of weld metals on the performance of end plate connections. In fact in much of the research done the weld metal and welding procedure used are not even reported. As mentioned in Section 2.2 the toughness or lack of toughness has been cited as a factor contributing to the damage of the BWWF connections during the Northridge earthquake. Kaufman, Xue and Lu (1996) determined that self shielded flux cored electrode E480TG-K2 with a toughness of 27J at -27 degrees Celsius improved connection ductility and energy dissipation, over gas shielded flux cored E480T-4 electrode with a toughness of 13.4 J at -21 degrees Celsius. There is a great

need for research in this area and for structural engineers to improve their understanding of the effect of weld metals and welding procedures on the behaviour of the connections.

2.6 Design Codes
2.6.1 CAN/CSA S16.1-94

CAN/CSA S16.1-94 says that beam-column moment connections should be designed to force yielding in the beam or the column and that failure of the connection is unacceptable (clause 27.2.5.1). No guidance, however is provided to achieve this. CAN/CSA S16.1-94 also recognizes that many of the earlier prescribed beam-column connections did not perform as well as anticipated in the Northridge earthquake and that designers should be aware of the most recent developments. It recommends that yielding should occur over as much material as possible (clause 27.2.5.1) and that partial penetration groove welds should not be used in seismic zones (clause 27.2.5.4). In the moment connection design portion of the Handbook of Steel Construction (1996) (page 3-80) it is again noted that the BWWF connections did not perform as well as anticipated in the Northridge earthquake. Here the only comment on end plate connections is that prying action must be considered and that the end plate helps to distribute flange forces over a greater depth of the column web than a fully welded joint. CAN/CSA S16.1-94 offers little guidance or information on end plate moment connections.

2.6.2. AISC 1994

The AISC (1994) Load and Resistance Factor Design Volume 2 elaborates more on the design of extended end plate moment connections than CAN/CSA S16.1-94. AISC, after making a number of design assumptions and restrictions, offers a design procedure for both stiffened and unstiffened extended end plate connections. The assumptions and restrictions particularly relevant to this research are listed below.

1. Fully tensioned high strength bolts (ASTM A325 or A490) of no greater than 1-1/2 inches in diameter must be used, except that ASTM A490 bolts should not be used in the stiffened eight bolt configuration;

2. Only static loading is permitted;

3. The recommended minimum distance from the face of the beam flange to the nearest bolt centerline is the bolt diameter plus 1/2 inch.

The design equation proposed in AISC 1994, based on the work of Krishnamurthy (1978), is shown here.

$$T_{ep} = \sqrt{\frac{1.2 \cdot [1.29 \cdot (\frac{\sigma_y}{B_u})^{2/5} \cdot (\frac{B_y}{F_{yep}})^{1/2}] \cdot (\frac{f_b}{B_{ep}})^{1/2} \cdot (\frac{A_f}{A_w})^{1/3} \cdot (\frac{p_e}{d_b})^{1/4} \cdot F \cdot (p_e)}{\phi \cdot F_{yep} \cdot B_{ep}}}$$

(2.21)

where;

$\phi = 0.9$

Other variables are defined in Section 2.5.1.

2.7 Summary of Research

Substantial research has been done to date on end plate connections. Many models have been developed to predict the behaviour of these connections, reflecting all or a combination of end plate thickness, weld size, beam size, bolt size, bolt tightening methods, end plate geometry and prying forces. There is, however, still much research to be done on end plate moment connections to fully understand what is happening and which end plate design should be used in seismic zones.

So far research supports the use of extended end plate connections in seismic zones. It shows that the end plate connection is capable of dissipating energy, behaving in a ductile manner, and developing the plastic moment capacity of the beam. However, before end plate moment connections can be used extensively in seismic areas more research is required. Further research is required to determine the end plate connection optimum geometry, the importance of weld metal and welding procedure, the importance of bolt sizing and loading, to refine and standardize the prediction equations used in design, and to evaluate the energy dissipation characteristics of end plate connections in comparison with other types of moment connections.
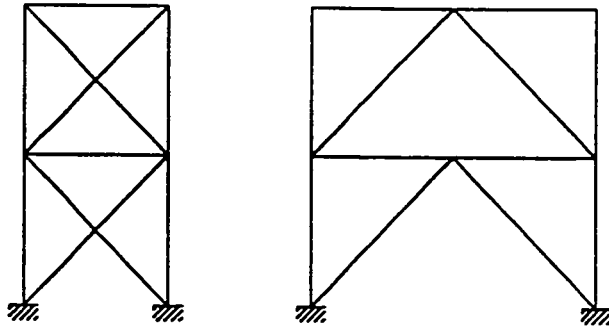
(a) Concentrically Braced Frame
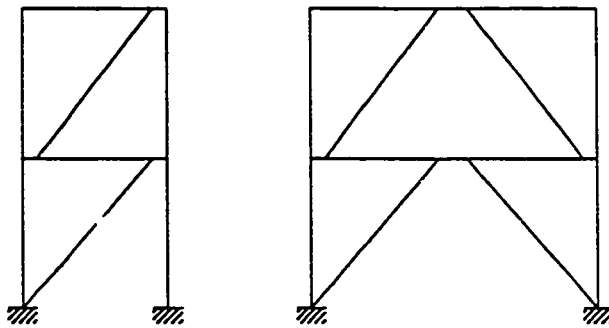
(b) Eccentrically Braced Frame
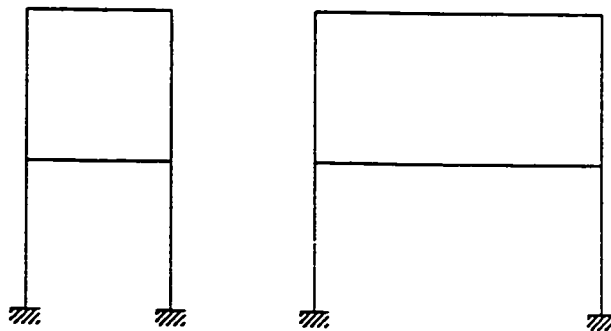
(c) Moment Resisting Frame

Figure 2.1 Typical Lateral Load Resisting Framing Systems

frame column flange

frame girder top flange weld

shear tab

frame girder bottom flange weld

back up bars
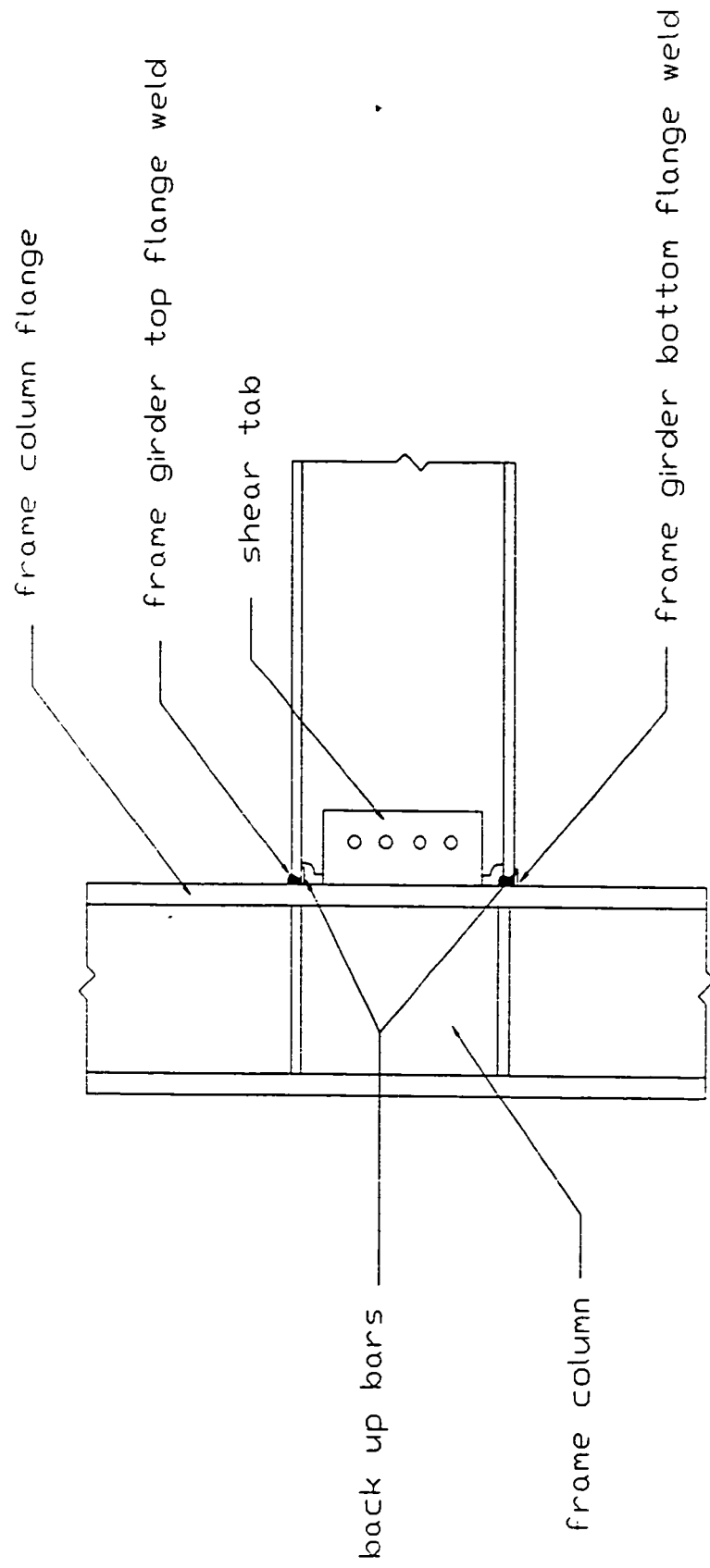
frame column

Figure 2.2 Typical Bolted Web Welded Flange Moment Connection
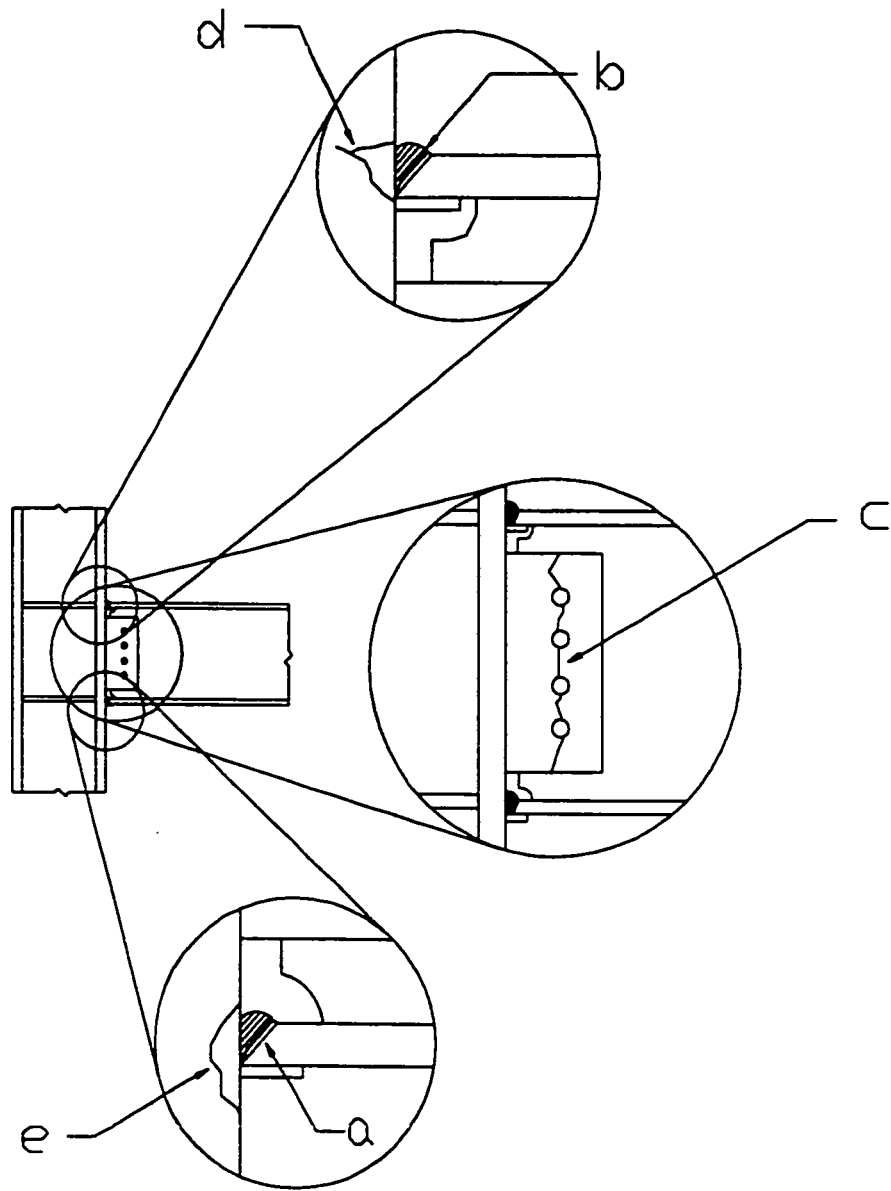
Figure 2.3 Common BWWF connection failures: (a) frame girder bottom flange weld, (b) frame girder top flange weld, (c) cracks in shear tab, (d) cracks in frame column, and (e) divots of steel removed from column flange.

40
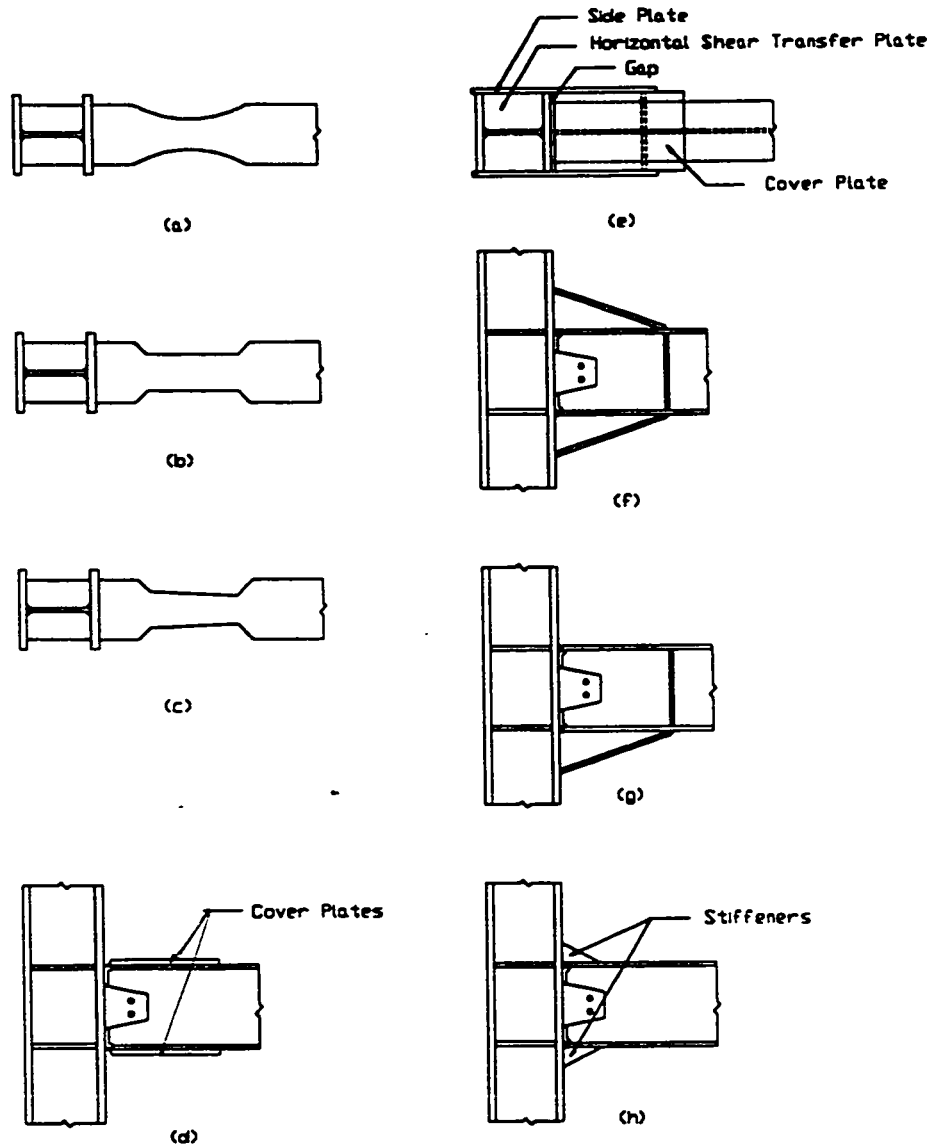
Figure 2.4 Possible alternatives to the traditional BWWF connection: (a) radius cut reduced flange, (b) constant cut reduced flange, (c) tapered cut reduced flange, (d) cover plates, (e) proprietary side plates, (f) top and bottom haunches, (g) bottom haunch, (h) stiffeners

41
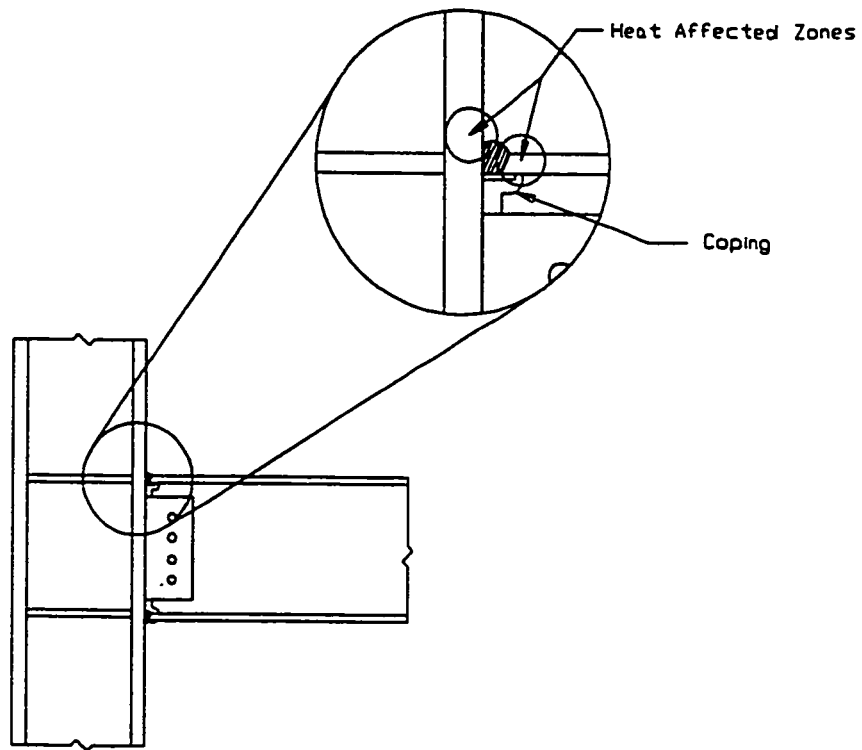
Figure 2.5 Crack locations of connections tested by Popov and Stephen (1970)
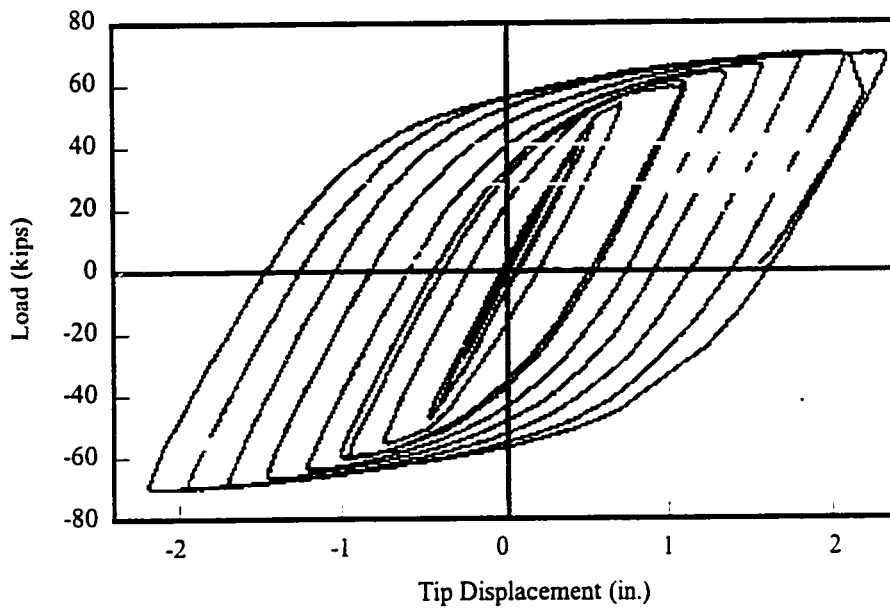
Figure 2.6   Load versus beam tip displacement curve for one BWWF connection without
column stiffeners from the Popov, Amin, Louie and Stephen (1986) test program
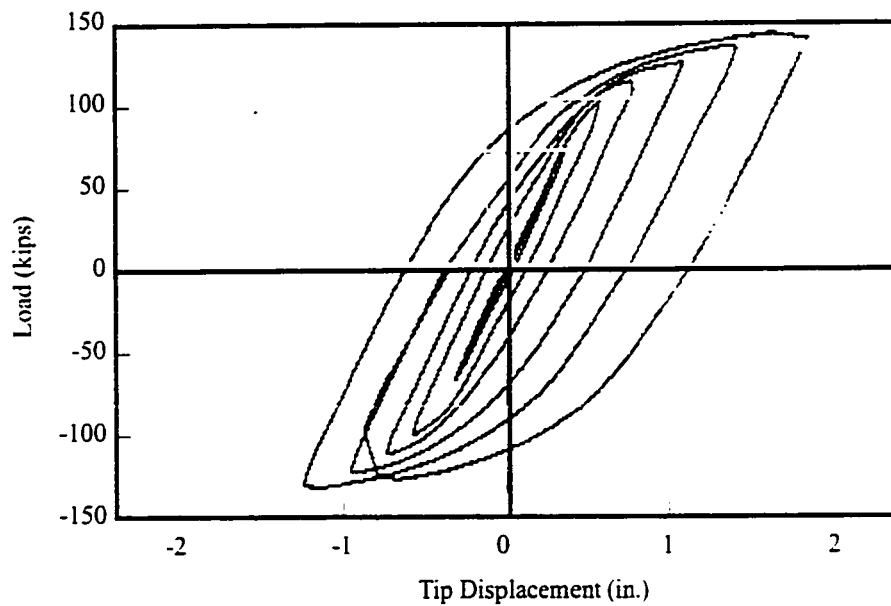
Figure 2.7   Load versus beam tip displacement curve for one BWWF connection with
column stiffeners from the Popov, Amin, Louie and Stephen (1986) test program
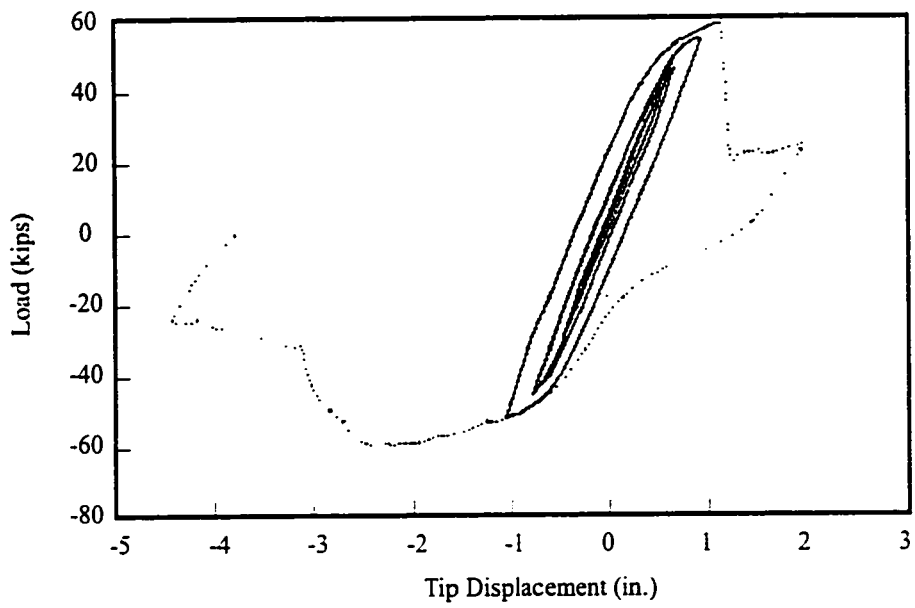
Figure 2.8 Load versus tip displacement curve of specimen #1 from the Engelhardt
and Husain (1992) test program
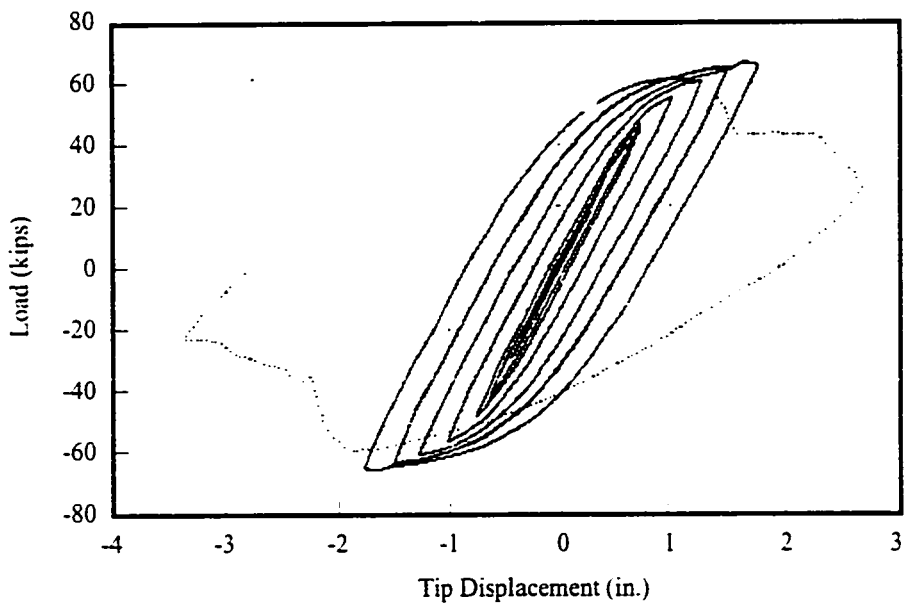
Figure 2.9 Load versus beam tip displacement curve of specimen #3 from the Engelhardt
and Hussain (1992) test program
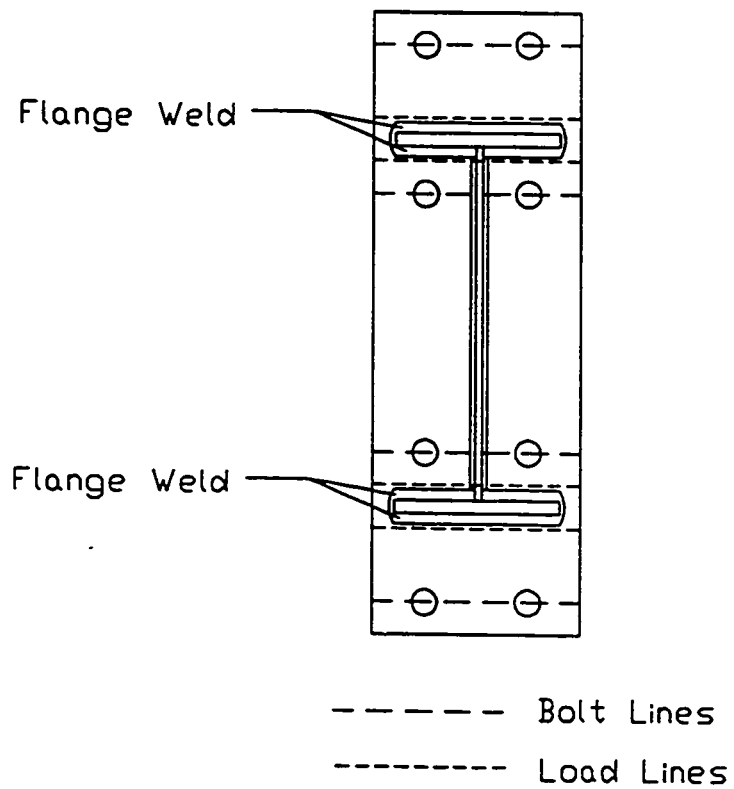
Figure 2.10 Bolt lines and load lines in an extended end plate
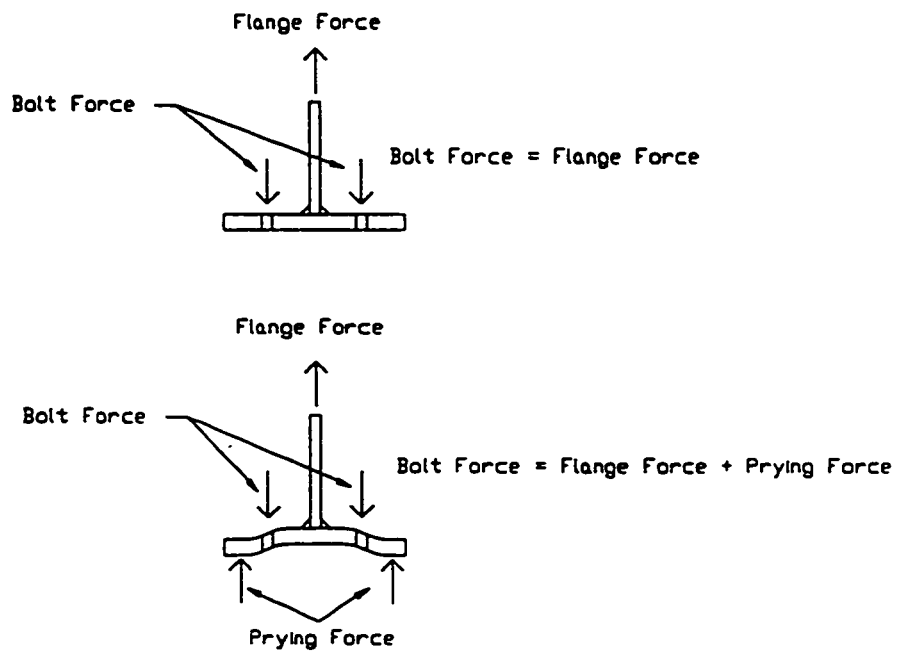
Figure 2.11 Bolt forces, with and without prying action
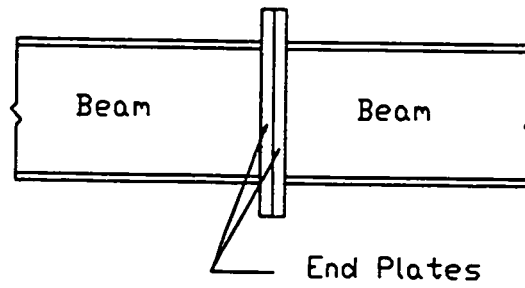
(a) Beam to beam connection
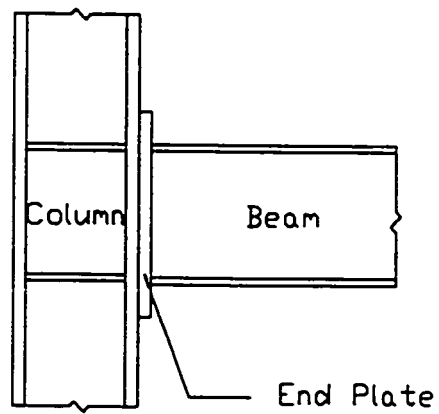
(b) Beam to column connection

Figure 2.12 End plate connections

47
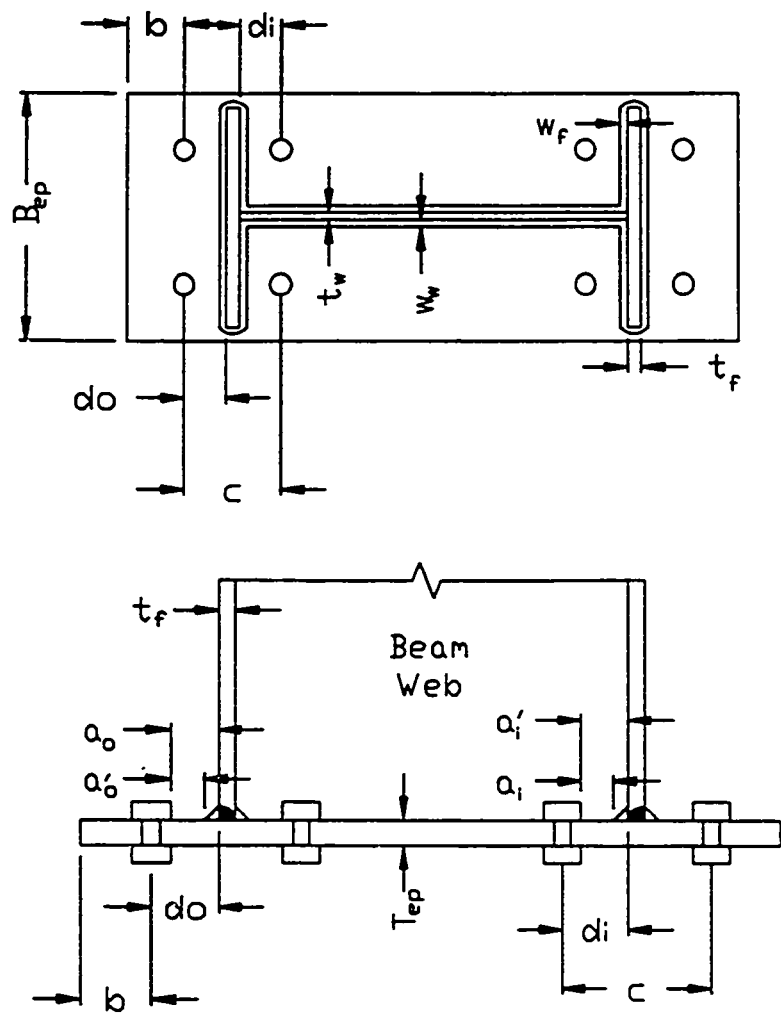
Figure 2.13 Common end plate geometric variables
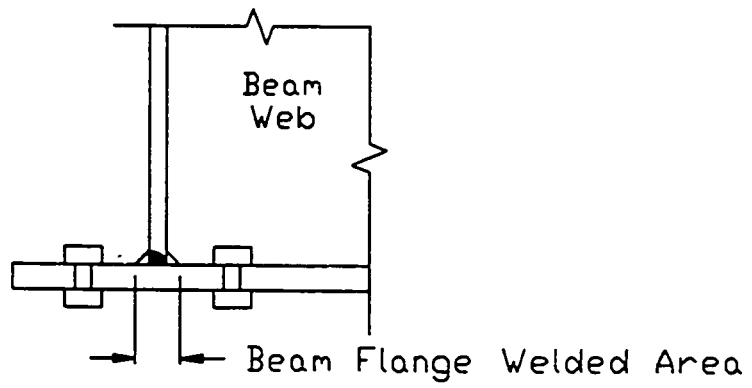
Figure 2.14 Beam flange welded area

hogging yield lines

sagging yield lines
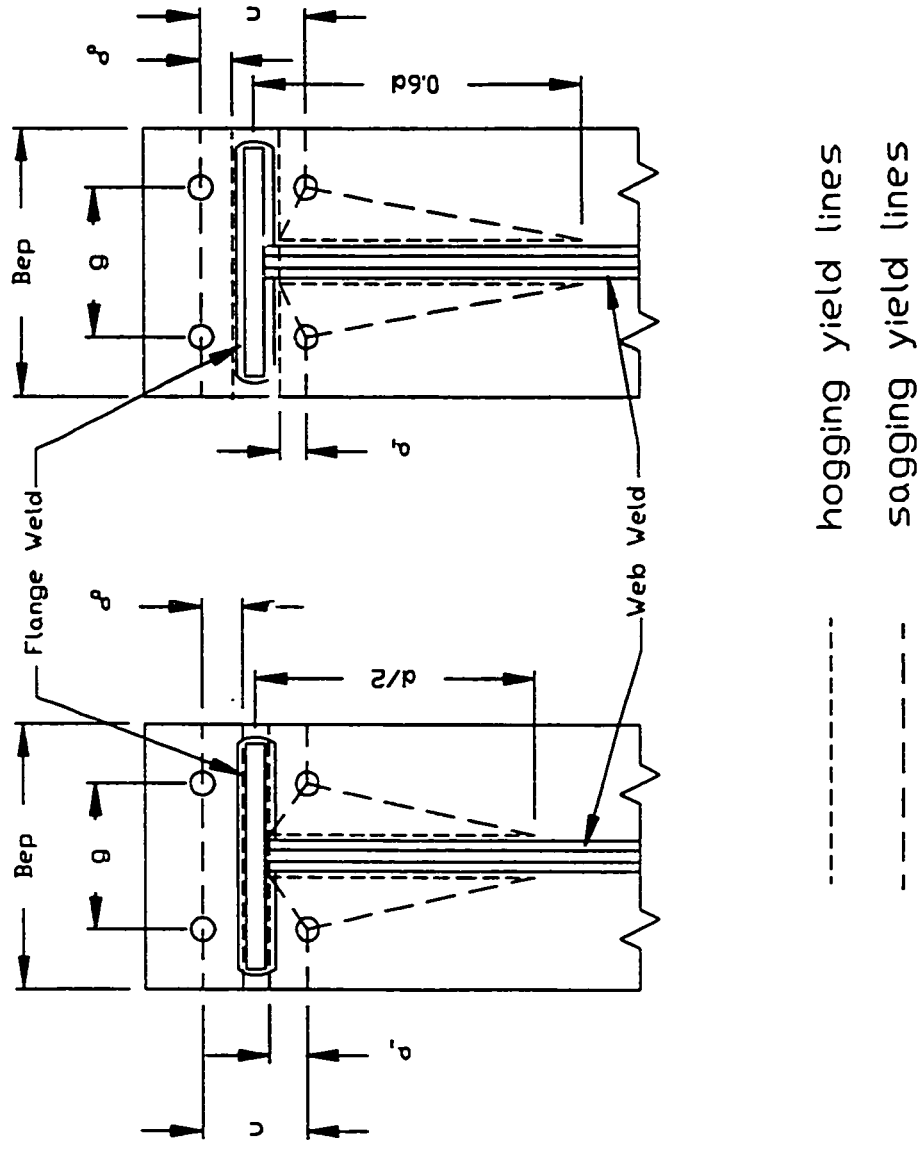
Figure 2.15 Yield line patterns used by Surtees and Mann (1970) and Whittaker and Walpole (1982)

50
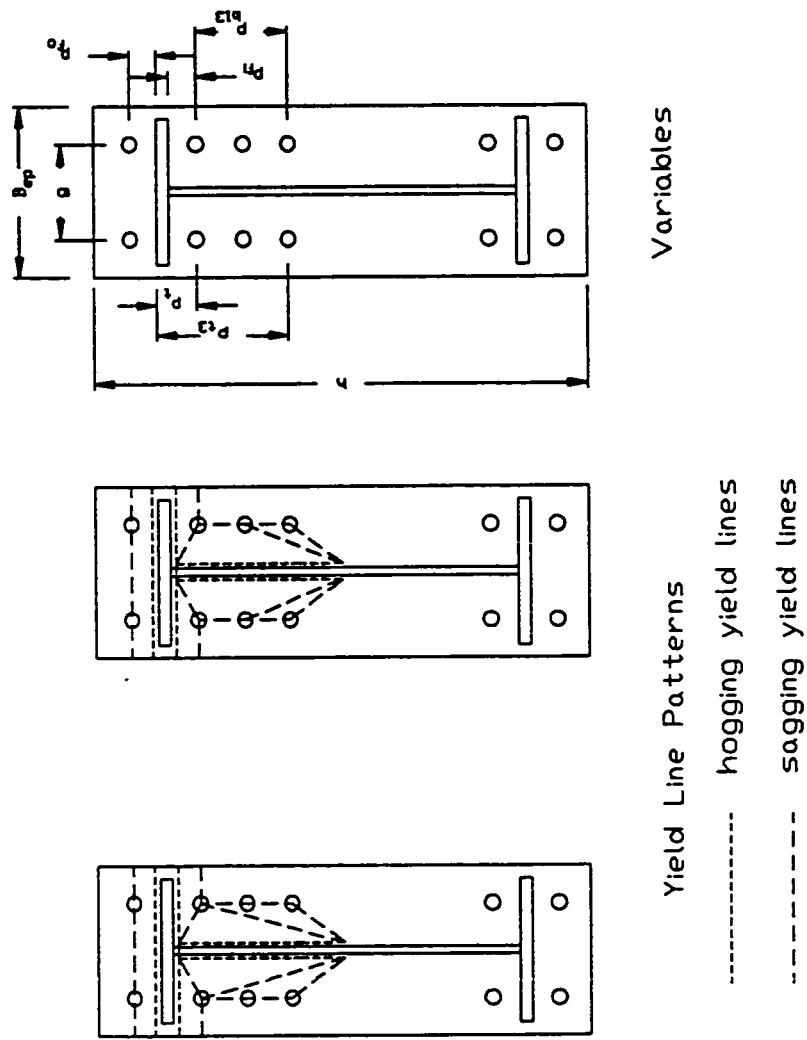
Figure 2.16 Yield Lines and Variables used by Murray and Borgsmiller (1995)

51
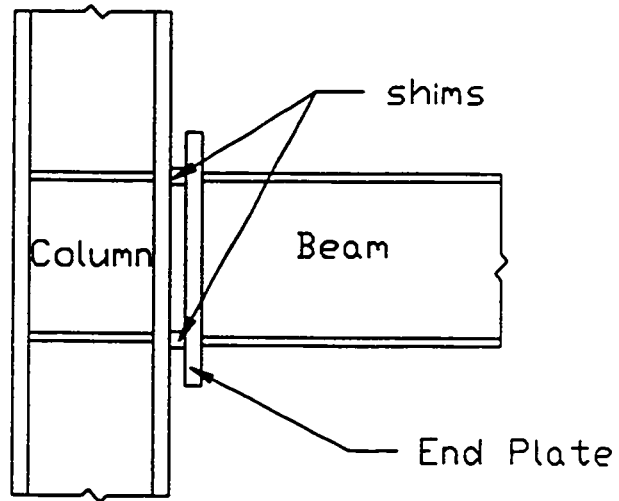
Figure 2.17 Shim placement in Murray and Meng's third test

3.   EXPERIMENTAL PROGRAM

3.1   Goals

The literature review revealed that little research has been performed on the behaviour of extended end plate moment connections under cyclic loading and that extended end plate moment connection performance could be better understood. Much of the previous work on extended end plate moment connections, including both monotonic and cyclic loading (Bose and Hughes, 1995; Korol et al., 1990; Ghobarah et al., 1990; Tsai and Popov, 1990, 1989) involved the failure of the entire connection, making it difficult to determine the factors contributing to the performance of the connection. The testing program described in the following was developed to investigate the effect of various parameters on the performance of the extended end plate.

The parameters investigated were:

- beam size
- bolt layout
- use of extension stiffeners
- end plate thickness, and
- welding techniques.

In addition, bolt behaviour was monitored on seven connections. The parameters were investigated by confining failure to the end plate and allowing both the beam and column to remain elastic. Twelve specimens were designed to fail the end plate, and three were designed to fail the beam and end plate. The test program consisted of 15 uniaxial cyclically loaded tests. All specimens were tested to failure. A summary of all connections tested is presented in Table 3.1.

3.2   Test Specimens

The experimental program included 15 tests grouped in three categories: small (S), medium (M) and large (B). The small size beams used were W360x51, the medium size beams used were W460x97, and the large size beams were W610x125.

The beams and end plates for all connections were of CAN/CSA-G40.21-92 Grade 300W steel. The end plates for all connections were fabricated at the University of Alberta

(U of A). All the end plates of same thickness were cut from the same stock. The end plates were flame cut and the holes were punched and then drilled to final size. Complete penetration welds were used along the flanges and the web for all connections, and fillet welds were used along the stiffeners. A description of the welding procedures adopted for the preparation of the test specimens is presented in Sections 3.3.2 and 3.3.3.

3.2.1 S Series

The S series tests consisted of three connections (Figure 3.1) which used one W360x51 (small) beam. The S series of tests were part of a pilot test program to investigate the effect of testing connections where a beam was connected to a column with a weak end plate. Connections S-1 and S-2 used a tight bolt configuration (the bolts were at two bolt diameters from the beam flanges and spaced equally on either side) but end plates of different thickness. The bolt spacing from the beam flanges, in terms of bolt diameters, is listed for all connections tested in Table 3.2. Connections S-2 and S-3 consisted of the same end plate thickness but different bolt configurations. S-3 used a relaxed bolt configuration (a connection where the bolts on the outside of the flange were placed at three bolt diameters from the flange and the bolts on the inside of the flange were placed at two bolt diameters.) All welding for the S series was done at the U of A following the procedure described in Section 3.3.3. A summary of bolt layout, number of bolts, types of bolts, end plate thickness and the use of extension stiffeners is given in Table 3.1.

3.2.2 M Series

The M series tests consisted of seven connections (Figures 3.2, 3.3). Connections M-1 to M-5 used one W460x97 (medium) beam and connections M-6 and M-7, fabricated by Waiward Steel Fabricators (WSF) used a W460x97 beam from a different heat. Connection M-1 had a tight eight bolt configuration and connection M-2 had a relaxed eight bolt configuration. Connections M-3 and M-4 had the same bolt configuration as M-2 but were designed for a greater moment capacity. The capacity of M-3 was increased by using a thicker end plate (19 mm) whereas the greater capacity of M-4 was achieved by

using extension stiffeners. Connection M-5 used a tight 16 bolt configuration and was designed to fail both the end plate and the beam. Connections M-6 and M-7 were similar to connections M-4 and M-5 but were welded by WSF using a different welding technique described in Section 3.3.3.

3.2.3 B Series

In order to investigate the effect of beam size, five connections (Figures 3.4 and 3.5) of characteristics similar to the five specimens of the M Series were tested using a W610x125 (large) beam. One beam was used for all the large connection tests. Connection B-1 had a tight eight bolt configuration with the bolts placed 1.75 bolt diameters away from the flanges and a 15.9 mm thick end plate. Connection B-2 had a relaxed eight bolt configuration with the bolts placed 5.3 bolt diameters away from the outside of the flanges. The end plate for connection B-2 was 15.9 mm thick. Connections B-3 and B-4 had the same bolt configuration as B-2 but were designed with a greater capacity. The capacity of B-3 was increased by using a thicker end plate (19 mm) whereas the greater capacity of B-4 was achieved by using extension stiffeners. Connection B-5 used a tight 16 bolt configuration as shown in Figure 3.5 and was designed to reach the plastic moment capacity of the beam.

3.3   Preparation of Test Specimens

3.3.1   Fabrication of End Plates

The end plates were all fabricated at the U of A. The end plates were flame cut from 13 mm, 13.3 mm, 15.9 mm and 19 mm plate of CAN/CSA-G40.21-92 Grade 300W steel. The holes were marked and punched to 19 mm diameter holes and drilled to the final diameter. The areas of the end plates to be welded were ground to remove the millscale.

3.3.2   Welding Preparation

Prior to welding the end plates to the beams, the ends of the beams were cut square and the flanges beveled at a 45 degree angle. The flame cut surface was ground to provide a smooth surface for welding. The web was ground to give a 45 degree double bevel and a

smooth surface for welding. The beam was then positioned on saw horses and the end plates were tack welded in place.

Test specimens M-6 and M-7, fabricated by WSF, were prepared in the same way as those by the U of A with the exception of 20 mm weld access holes. The weld access holes were made in the web near the flanges so that the back weld could be made continuous over the full width of the flanges. This was done to ensure full weld penetration over the entire width of the flanges.

3.3.3 Welding Processes

The welding of the specimens and preparation of the beams was performed at the U of A with the exception of specimens M-6 and M-7. Specimens M-6 and M-7 were welded by WSF. The root of the complete penetration flange weld performed at the U of A used a 3 mm E4101'ʊ electrode, current of 125 A, voltage of 21-23 V and a travel speed of 76-380 mm/min. The large variability in welding speed was due to the unevenness of the prepared surface. The fill flush weld was made with a 3 mm E48018 electrode, current of 150 A, voltage of 27-29 V and a speed of 76-380 mm/min. The reinforcing fillet weld was made with a 4 mm E48018 electrode, current of 180 A - 190 A, voltage of 21-23 V and a travel speed of 76-380 mm/min. The back side root weld was made with a 3 mm E41010 electrode, current of 150 A, voltage of 21-23 V and a travel speed of 76-380 mm/min. All welds were performed in the flat position.

WSF used semi automatic flux-cored arc welding. WSF welds were made with a 2 mm E4802-T-9-CH electrode, current of 350 A, voltage of 26 - 27 V and a speed of 280 - 305 mm/min. All welds were performed in the flat position.

3.3.4 Test Columns

A W310x118 test column was used for the small beam tests. Stiffeners were welded in the test column across from the flanges of the W360x51 beam, and end plates were welded on either end enabling the column to be securely fastened to the reaction frame.

A W310x143 test column was used for the medium and large beam tests. The panel zone was reinforced with both stiffeners and doubler plates, shown in Figure 3.6. In order

to use the column for the two different sizes of tests the column had to be rotated to use both flanges. By rotating the column the problem of overlapping holes, created by the different sizes of beam was avoided. After the first four tests (B-1 to B-4) the W310x143 test column was rotated so that the W460x97 beam could be bolted onto the other flange. A pair of horizontal stiffeners were added to accommodate the shallower beam. Part of the W610x125 stiffener had to be removed to accommodate the bolts for testing the medium size beam specimens M-5, and M-7. The pair of stiffeners aligned with the bottom flange of the W460x97 beams were removed for testing of specimen B-5, the final test specimen of the test program.

3.3.5   Connections

After the holes were drilled in the test column and the end plates were welded to the beam, the beam was bolted to the column. The bolts were tightened using the turn of the nut method. There was some difficulty in bringing the end plate into contact with the column flange at all holes due to the warping of the end plate induced by welding. In cases where the end plate could not entirely be brought into contact shims were used to fill the gap between the end plate and the column flange.

3.3.6   Ancillary Tests
3.3.6.1 Tension Coupons

Thirty one coupon tests were performed. Two coupons were taken from each of the three beam flanges, and two were taken from each of the beam webs, from the beams used in the medium and large beam tests. Three coupons were taken from the flanges and three from the webs of the beam used in the small test series. These coupons were taken from the center of the beams, to ensure that the material had not yielded. The coupons taken from the beam were taken parallel to the length of the beam. The strains in the center of the beams was monitored throughout testing. Two coupons were taken from the column flanges and two were taken from the column web for the W310x143 column and no coupons were taken from the W310x118 column. These coupons were taken half way between the column center and the reaction point to ensure no yielding had occurred in the

beam. Again the column strains were monitored through-out the test program. The coupons were taken parallel to the length of the beam. Three coupons were taken from excess end plate material using the 15.9 mm and 19 mm plates. These coupons were taken in the long direction of the end plates. The properties of the materials used in the S series of tests were taken from University of Alberta Structural Engineering Reports 194 and 208.

The tension coupons were machined in accordance with the requirements of ASTM A 370-94 (1994), with a gage length of 50 mm and a section width of 12.5 mm. An MTS 1000 universal testing machine was used to carry out the tests, which were conducted at a strain rate of approximately 10 $\mu\varepsilon$/s in the elastic range and 50 $\mu\varepsilon$/s in the inelastic range. Strain in the coupons was measured using a clip-on extensometer.

The 13.3 mm, 13.0 mm and the 19 mm thick end plates used in the small series of tests had static yield stresses of 295 MPa, 285 MPa and 356 MPa, and ultimate stresses of 501 MPa, 510 MPa and 504 MPa, respectively. The W360 x 51 beam flange had an average static yield stress of 335 MPa and an average ultimate stress of 542 MPa.

The 15.9 mm and 19 mm end plates used in the medium and large beam series of tests had average static yield stresses of 332 MPa and 337 MPa respectively. The average ultimate stresses were 510 MPa and 504 MPa, respectively. The three beams had average static yield stresses 357 MPa (W610x125), 349 MPa (W460x97 #1) and 329 MPa (W460x97 #2), and average ultimate stresses of 535 MPa (W610x125), 485 MPa (W460x97 #1) and 529 MPa (W460x97 #2). The beams denoted #1 were the beams used to make the connections welded at the University of Alberta. The beams denoted #2 were the beams used to make the connections welded at Waiward Steel.

The results of the individual tension tests are shown in Tables 3.3 and 3.4 a, b and the stress versus strain curves for each coupon are presented in Appendix A.

3.3.6.2 Bolts

Four bolts were tested in tension; two were 28.5 mm A325 bolts and two were 31.8 mm A490 bolts. There were no 25.4 mm A490 bolts tested, as the elongation of only 28.5 mm and 31.8 mm A490 bolts was measured during the connection tests. Due to the limited capacity of the testing apparatus the bolts were only loaded to 450 kN. The

28.5 mm A325 bolts yielded at approximately 350 kN and the 31.8 mm A490 bolts did not yield. The slope of the load versus elongation relationship for the 28.5 mm A325 bolts was 1728 kN/mm. The load versus elongation relationship for the 31.8 mm A490 bolts was 2635 kN/mm. The load versus elongation plots are shown in Appendix B.

3.4   Test Setup and Instrumentation

The small beam tests were conducted in load frame #1 shown in Figure 3.7 where the column and jack were positioned horizontally and the beam was in the vertical position. This load frame was inadequate for the medium and large beam tests. Load frame #2, shown in Figure 3.8 was used to test the medium and large beam test specimens.

3.4.1   Load Frame #1

The W310x118 test column had 25 mm end plates welded on both ends, and was bolted between to W310x118 columns 600 mm above the floor. The test column was then tied to the strong floor a distance of 600 mm on either side of the panel zone centerline and supported on 460 mm long pedestals.

An 890 kN hydraulic jack with a 400 mm stroke was used for all tests. For the S series tests the centerline of the jack was positioned 2 m from the end plate connection. Steel channels covered with Teflon pads provided lateral support at the free end of the beam of the test specimens. Runners were welded to the end of the beam to minimize friction between the test beam and the lateral supports. Strain gauges mounted to the beam were used to check statics to ensure that friction was negligible.

In all 3 tests the jack was attached to the beam using a combination of steel sections, plates and 12.7 mm dywidag bars.

3.4.2 Load Frame #2

The W310x143 test column was bolted to a WWF350x238 reaction column using four high strength rods at each reaction to transfer both shear and normal forces. The test column and the WWF350x238 reaction column were separated by 25 mm thick plates at both reaction points. There was no attempt to ensure a completely fixed or pinned reaction

for the test column as the panel zone rotation could easily be monitored. The WWF350x238 reaction column was braced above the test column.

The hydraulic jack was suspended vertically above the test specimen and positioned 2.5 m from the end plate connection. The jack attachment to the beam was identical to that for the S series tests but with eight, instead of four, dywidag bars to accommodate the higher loads.

The lateral support for the specimens was provided by Teflon pads attached to the beams that slid along channels as shown in Figure 3.9. The lateral support was positioned 2.0 m away from the connection.

3.4.3 Control and Data Acquisition

The load was controlled manually by controlling the oil pressure in the jack. Cable transducers were used to measure the column vertical displacement and the deformation of the beam at third points along the beam (Figure 3.10). The beam tip displacement and applied load were plotted with a pen plotter during each test, giving the visual feedback needed to control the test manually. The load in the jack was monitored by the pressure readings in the jack and a load cell. The horizontal and vertical movements of the test column reaction points were monitored using cable transducers.

To double check the load cell readings and ensure that the friction developed in the lateral support was negligible, 16 electrical strain gages were mounted on the beam 200 mm from the end plate and four electrical strain gages were mounted at beam midspan. To monitor the column behaviour and check panel zone rotation, four electrical strain gages were mounted 600 mm on either side of the center of the panel zone of the large beam; 100 mm past the reach of the longest end plate tested (Figure 3.11).

Rotation meters were placed at the center of the panel zone and at the beam midheigth adjacent to the end plate to determine the end plate rotation.

Four linear variable displacement transducers (LVDT's) were mounted from the column stiffeners and positioned to measure the end plate displacement; this corresponds to the amount the end plate lifted off the column face (Figure 3.10). The displacement was measured at the end of each beam flange - end plate interface.

tests, one measuring the elongation of a bolt adjacent the inside flange and one measuring the elongation of the bolt adjacent the outside flange. It was evident after the first four medium beam size tests that there were large prying forces in, and unequal load distributions between, the bolts inside the flanges and the bolts outside the flanges. In order to assess the prying action and the load distribution between the bolts, the elongation of two of the bolts were monitored during testing of specimens M-3 to M-7 and B-5.

All instrumentation was monitored and recorded electronically by a fluke 2401A data acquisition system.

3.5   Testing Procedure

The loading procedure adopted for the test program was developed using the Applied Technology Council Guidelines for Testing of Components of Steel Structures (ATC24, 1992). The first two load levels for each test specimen were 100 kN and either 175 kN or 200 kN. The 100 kN load level corresponds to a low elastic load level and the 175 kN and 200 kN load levels correspond to either a medium or high elastic load level for all tests to ensure that all instrumentation was working properly. Three cycles were performed at each load level. The third load level was taken as the yield load, the load level at which the beam tip displacement versus load curve ceased to be linear. The beam tip displacement was increased by 25 percent of the beam tip displacement at yield for each of the subsequent blocks of cycles. Three cycles were performed in each block.

Failure of a specimen was taken as the point at which a marked drop in load for identical beam tip displacements was observed. At this stage the end plate had usually cracked extensively. Test specimen B-5 was the only specimen not tested to failure. Specimen B-5 was loaded up to the capacity of the test frame. At that point the test was abandoned although the test specimen had not shown imminent sign of failure.

Table 3.1 Summary of Connection Details

Specimen	Bolt Layout	Number of Bolts	Size and Grade of Bolts	End Plate Thickness (mm)	Stiffeners
S-1	Tight	8	22 mm A490	19	No
S-2	Tight	8	25.4 mm A490	13	No
S-3	Relaxed	8	25.4 mm A490	13.3	No
M-1	Tight	8	28.5 mm A325	15.9	No
M-2	Relaxed	8	28.5 mm A325	15.9	No
M-3	Tight	8	31.8 mm A490	19	No
M-4	Relaxed	8	31.8 mm A490	15.9	Yes
M-5	Tight	16	28.5 mm A325	19	Yes
M-6	Relaxed	8	31.8 mm A490	15.9	Yes
M-7	Tight	16	28.5 mm A325	19	Yes
B-1	Tight	8	25.4 mm A490	15.9	No
B-2	Relaxed	8	25.4 mmA490/ 28.5 mm A325*	15.9	No
B-3	Relaxed	8	31.8 mm A490	19	No
B-4	Relaxed	8	31.8 mm A490	15.9	Yes
B-5	Tight	16	28.5 mm A325	19	Yes

* - Specimen B-2 - 25.4 mm A490 bolts ruptured and were replaced by 28.5 mm A325 bolts.

Table 3.2 Summary of Connection Bolt Layout

Specimen	Name	Number of Bolts	Bolt Diameter (mm)	Distance from Flange Inner Face (bolt dia.)	Distance from Flange Outer Face (bolt dia.)
S-1	tight	8	22.2	1.98	1.98
S-2	tight	8	22.2	1.98	1.98
S-3	relaxed	8	22.2	1.98	3.56
M-1	tight	8	25.4	1.77	1.77
M-2	relaxed	8	25.4	1.77	3.94
M-3	relaxed	8	31.8	1.42	3.15
M-4	relaxed, stiffened	8	31.8	1.42	3.15
M-5	tight, stiffened	16	28.5	1.57	1.57
M-6	relaxed, stiffened	8	31.8	1.57	3.15
M-7	tight, stiffened	16	28.5	1.42	1.57
B-1	tight	8	25.4	1.57	1.77
B-2	relaxed	8	25.4/28.5 *	1.77	4.28
B-3	relaxed	8	31.8	1.77	4.28
B-4	relaxed, stiffened	8	31.8	1.42	4.28
B-5	tight, stiffened	16	28.5	1.57	1.57

* - Specimen B-2 - 25.4 mm A490 bolts ruptured and were replaced by 28.5 mm A325 bolts.

Table 3.3 Material Properties for Small Tests

Coupon	Elastic Modulus (MPa)	Static Yield Stress (MPa)	Dynamic Yield Stress (MPa)	Static Ultimate Stress (MPa)	Failure Strain ($\mu\epsilon$)
EP13.3	207 600	295	n/a	501	n/a
EP13	200 000	285	n/a	510	n/a
EP19	same as 19 mm end plate in M and B tests				
F1	217 000	356	n/a	528	n/a
W1	214 000	376	n/a	544	n/a
F2	227 000	325	n/a	544	n/a
W2	205 000	367	n/a	557	n/a
F3	196 000	323	n/a	547	n/a
W3	202 000	369	n/a	557	n/a

Nomenclature:

EP13.3 - 13.3 mm thick end plate

EP13 - 13 mm thick end plate

EP19 - 19 mm thick end plate

F   - Flange of W360 x 51

W   - Web of W360 x 51

Data taken from the University of Alberta Structural Engineering Report No. 208 and the University of Alberta Structural Engineering Report No. 194.

Table 3.4 a Material Properties for Medium and Large Tests (Beams and Column)

Coupon	Elastic Modulus (MPa)	Static Yield Stress (MPa)	Dynamic Yield Stress (MPa)	Static Ultimate Stress(MPa)	Failure Strain (με)
CF #1	220 700	333	340	518	389 000
CF #2	220 000	315	329	512	383 000
CW #1	220 400	344	362	512	383 000
CW #2	218 700	343	360	521	370 000
Mean	*219 950*	*334*	*348*	*516*	*381 250*
std. dev.	*881*	*13.5*	*16.0*	*4.50*	*8015*
BF #1	196 200	324	340	511	377 000
BF #2	201 800	330	350	519	375 000
BW #1	211 600	386	404	553	334 000
BW #2	205 800	386	406	558	329 000
Mean	*203 850*	*357*	*375*	*535*	*353 750*
std. dev.	*6496*	*34.2*	*34.9*	*23.7*	*25 786*
MF #1	209 000	351	367	541	360 000
MF #2	206 100	353	360	537	364 000
MW #1	207 700	347	371	524	n/a
MW #2	207 600	345	369	515	382 000
Mean	*207 600*	*349*	*367*	*529*	*368 667*
std. dev.	*1186*	*3.65*	*4.79*	*12.0*	*11 719*
MOF #1	213 400	335	342	492	n/a
MOF #2	191 700	316	335	491	393 000
MOW #1	223 800	336	355	482	363 000
MOW #2	202 300	330	351	473	367 000
Mean	*207 800*	*329*	*346*	*485*	*374 333*
std. dev.	*13 866*	*9.22*	*9.00*	*8.89*	*16 289*

Nomenclature:

C   - W310 x 143 column
B   - W610 x 125 beam
M   - W460 x 97 beam used in five successive tests
MO - W460 x 97 beam used to investigate welding techniques
F   - Flange
W   - Web

65

Table 3.4 b Material Properties for Medium and Large Tests (End Plates)

Coupon	Elastic Modulus (MPa)	Static Yield Stress (MPa)	Dynamic Yield Stress (MPa)	Static Ultimate Stress (MPa)	Failure Strain (με)
EP15.9 #1	193 600	335	n/a	519	410 000
EP15.9 #2	200 100	330	337	507	411 000
EP15.9 #3	198 200	331	343	504	416 000
Mean	*197 300*	*332*	*340*	*510*	*412 333*
std. dev.	*3342*	*2.65*	*4.24*	*7.94*	*3214*
EP19 #1	204 400	337	356	509	375 000
EP19 #2	207 800	337	356	502	372 000
EP19 #3	n/a	337	356	500	381 000
Mean	*206 100*	*337*	*356*	*504*	*376 000*
std. dev.	*2404*	*0*	*0*	*4.73*	*4583*

Nomenclature:

EP15.9 - 15.9 mm thick end plate

EP19   - 19 mm thick end plate
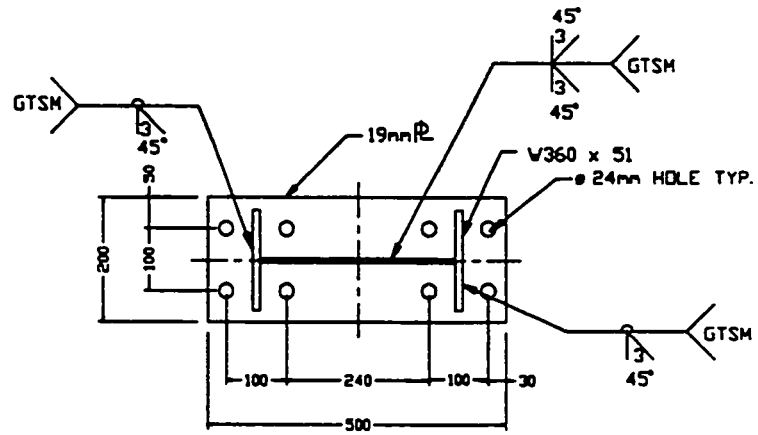
End Plate S-1
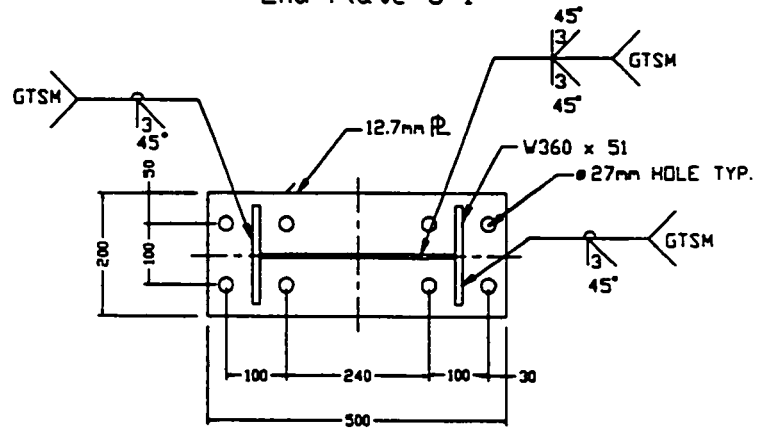
End Plate S-2
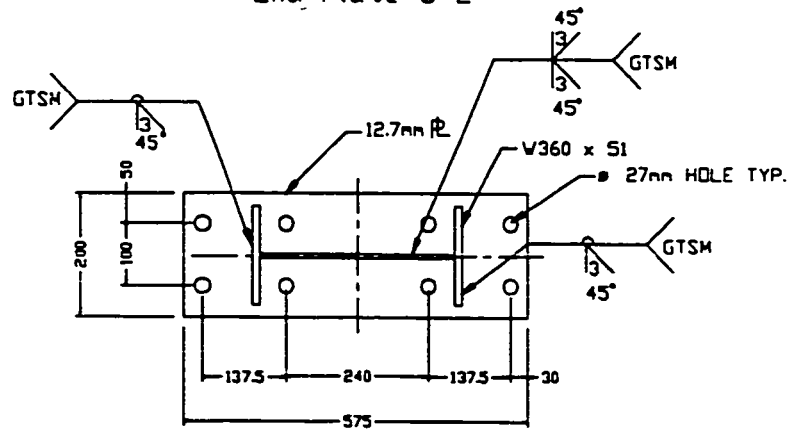
End Plate S-3

Figure 3.1 S Series End Plates

End Plate M-1

End Plate M-2
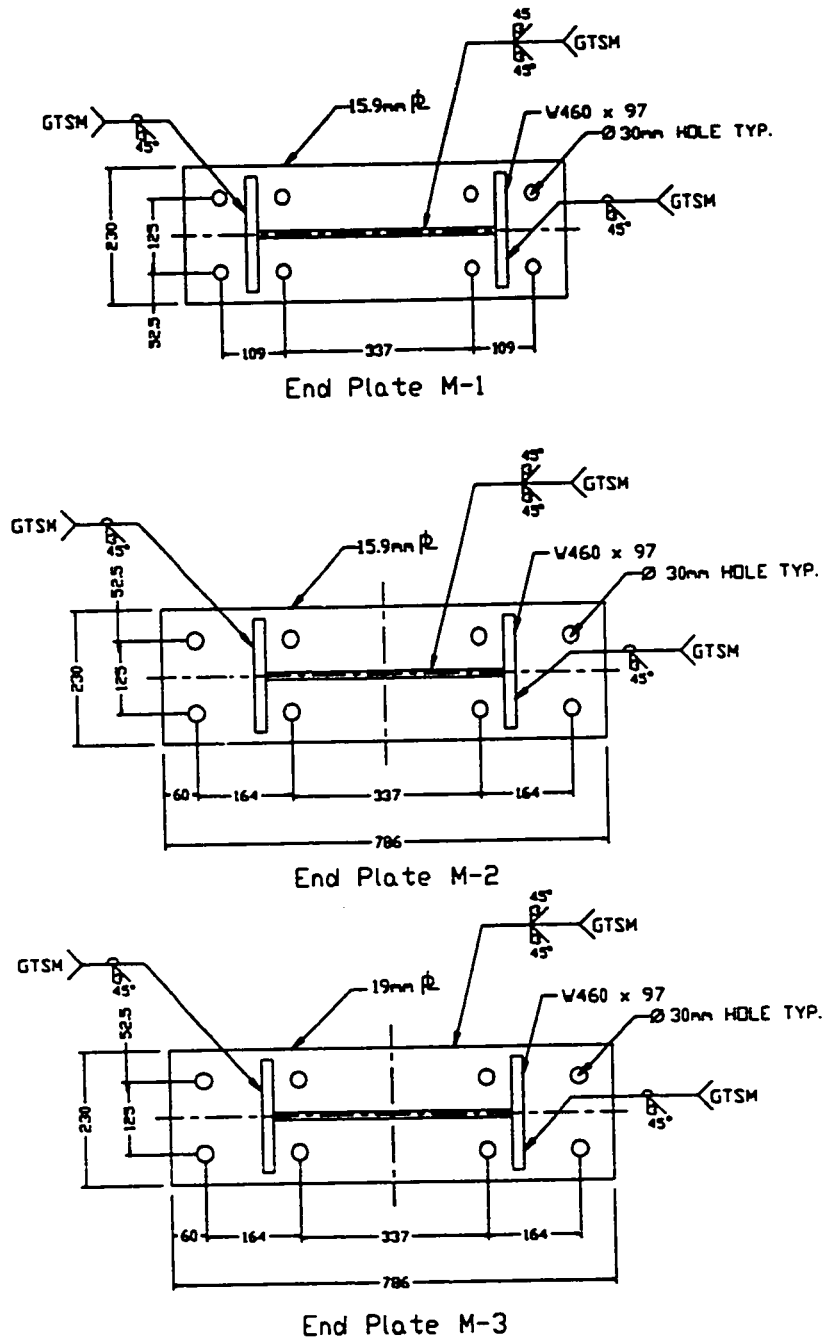
End Plate M-3

Figure 3.2 M Series End Plates (M-1, M-2, M-3)

End Plates M-4 and M-6

End Plates M-5 and M-7
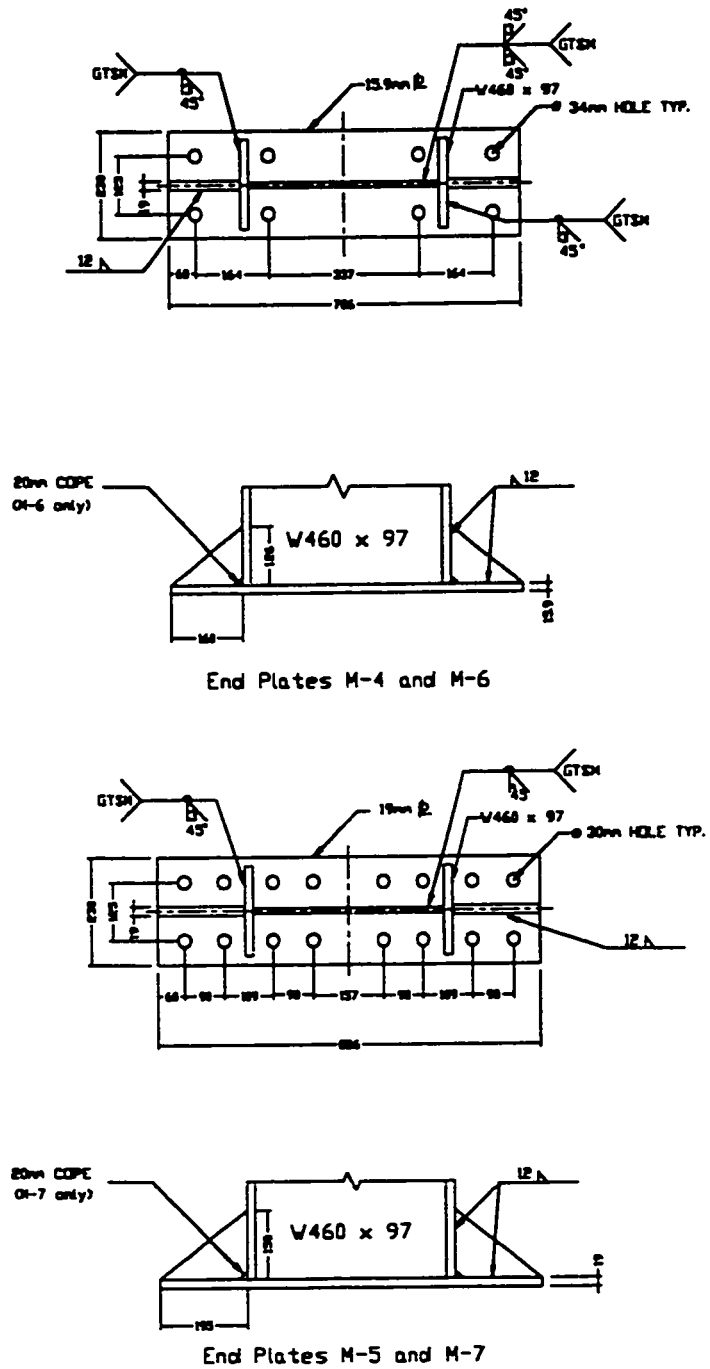
Figure 3.3 M Series End Plates (M-4, M-5, M-6, M-7)

69
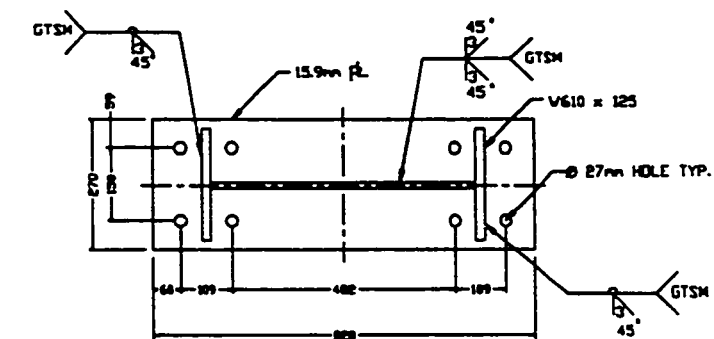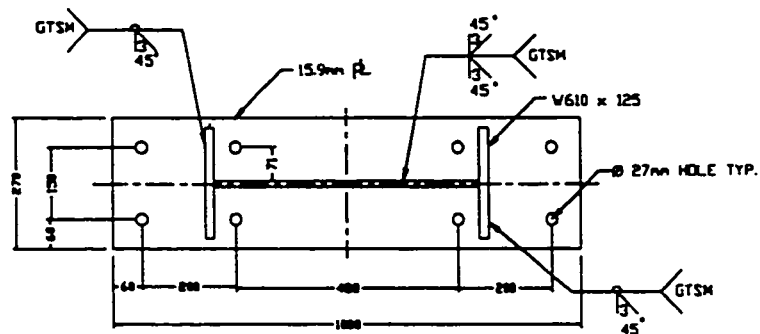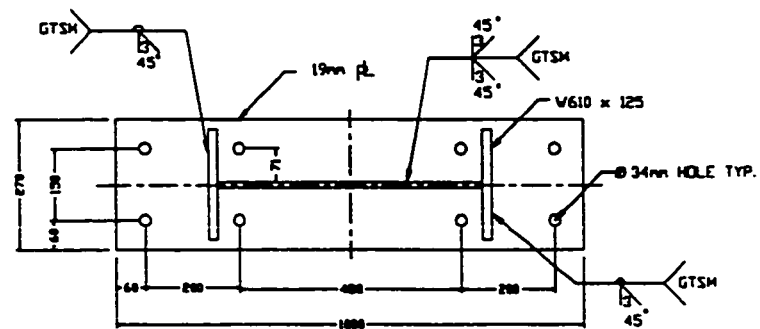
Figure 3.4 B Series End Plates (B-1, B-2, B-3)
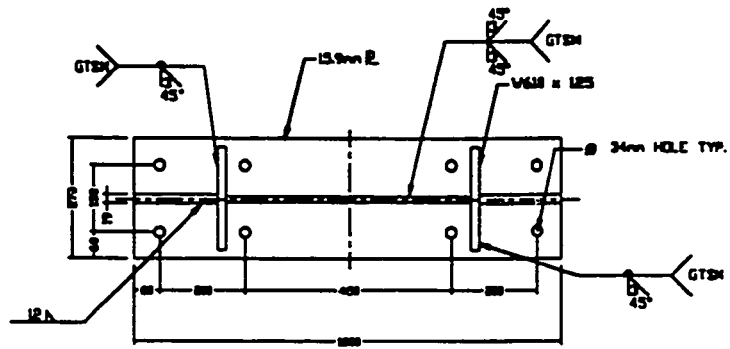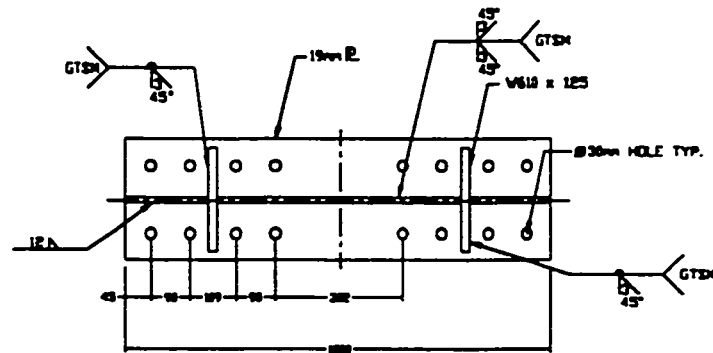
Figure 3.5 B Series End Plates (B-4, B-5)
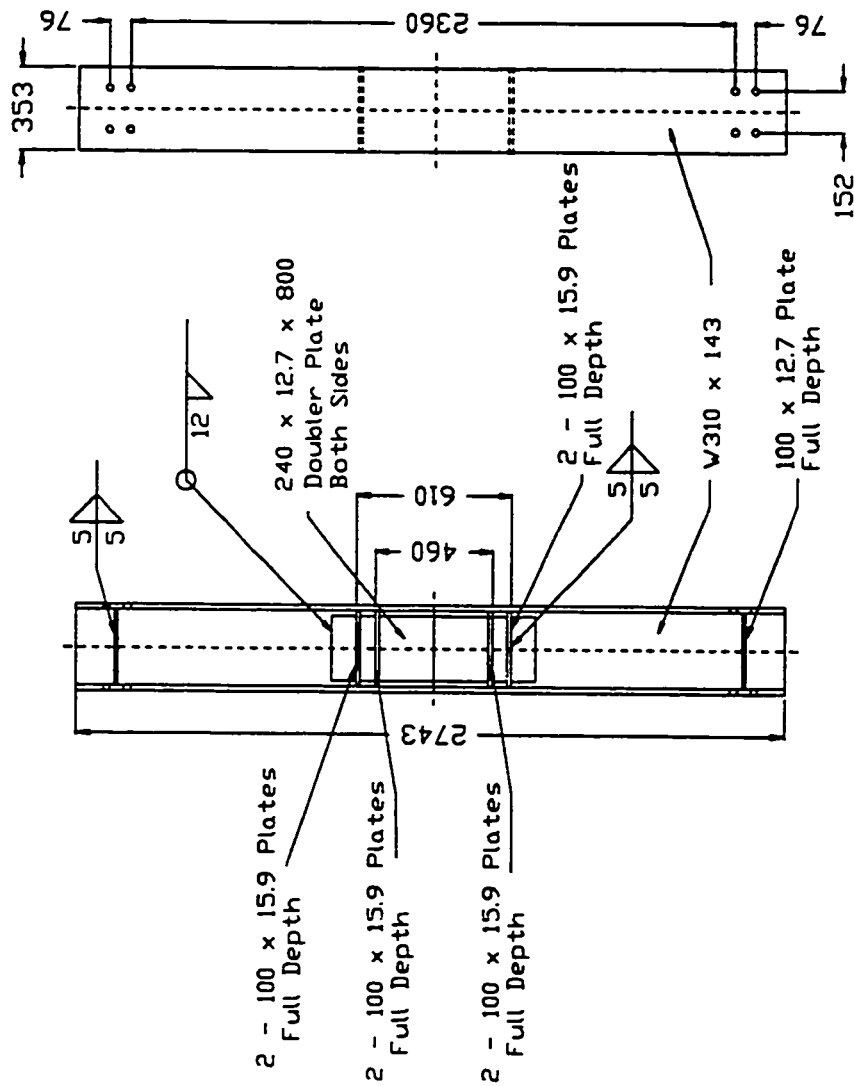
Figure 3.6 Test Column W310x143

72
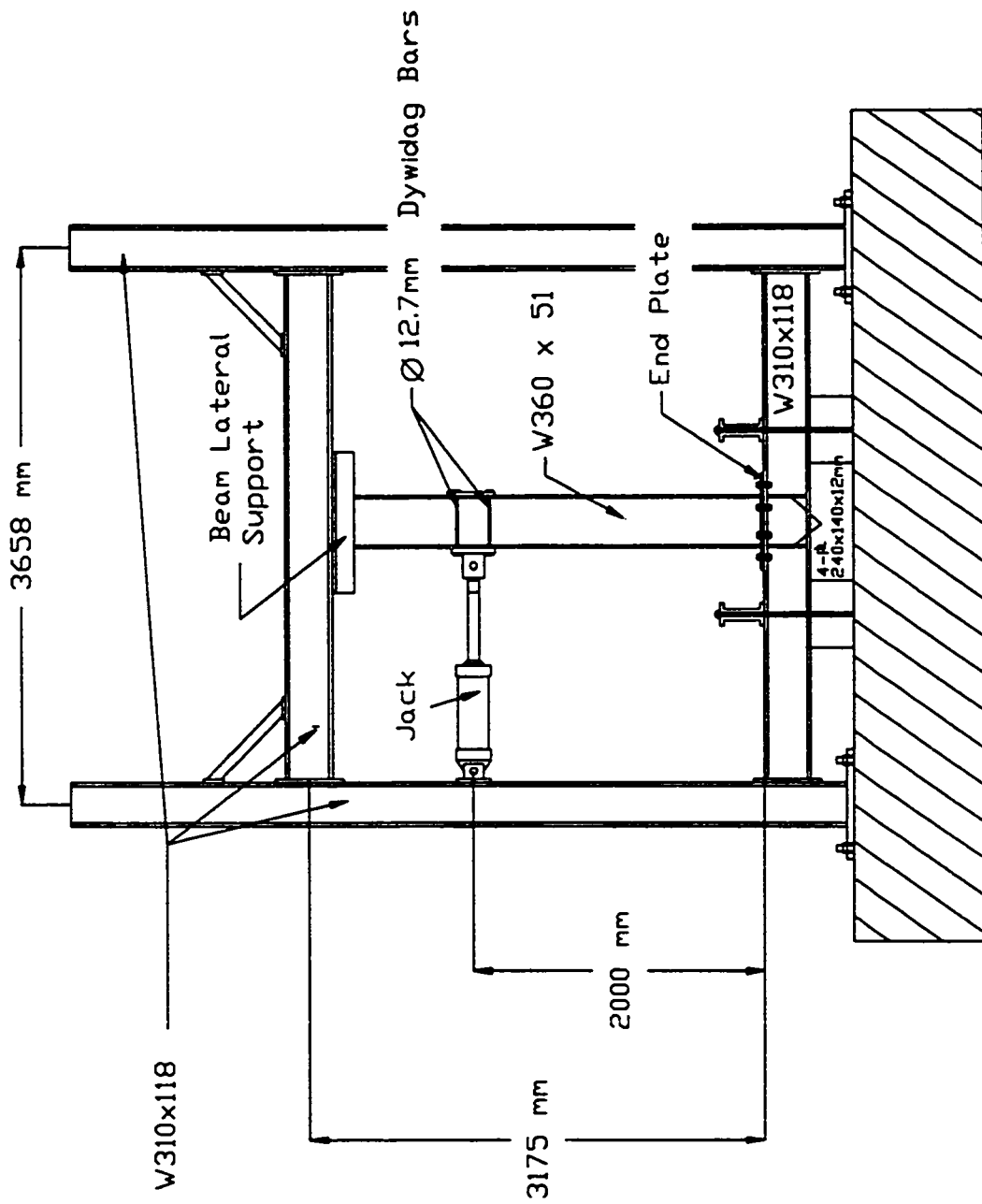
Figure 3.7 Load Frame #1

Figure 3.8 Load Frame #2

74
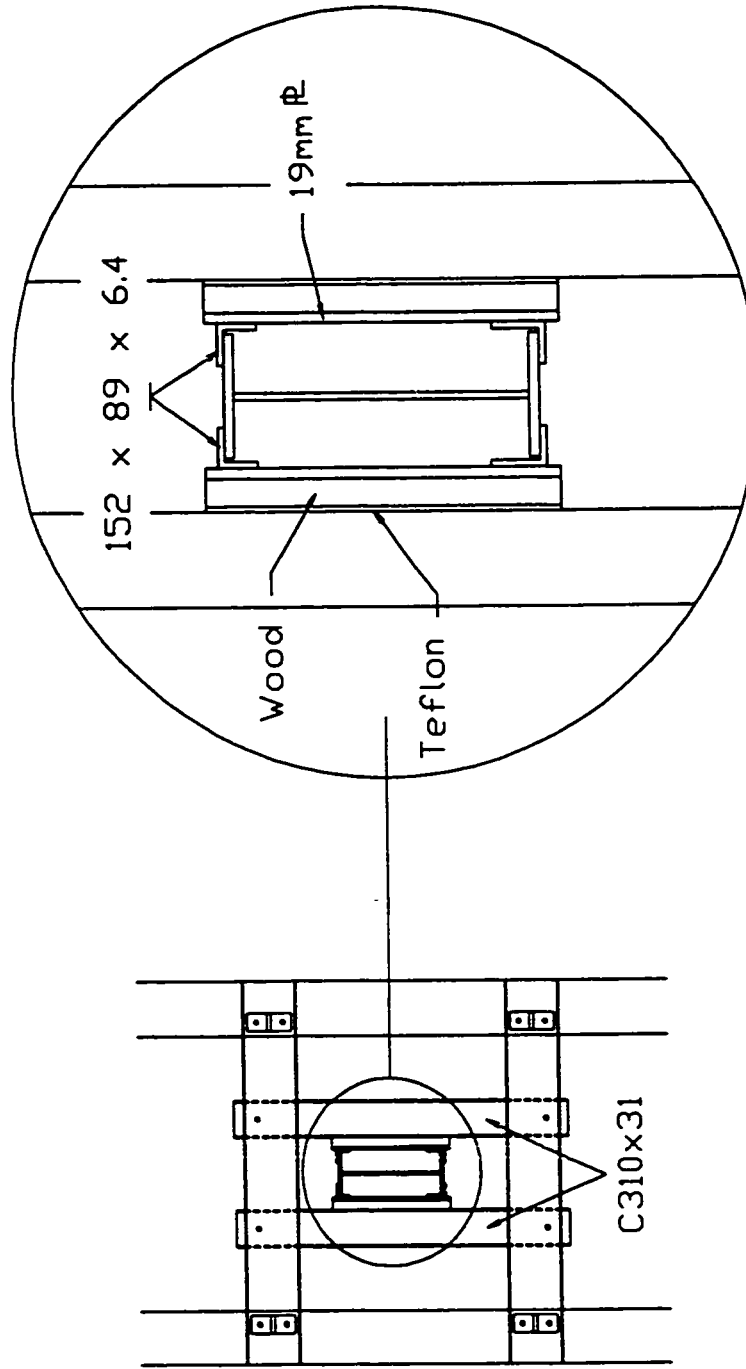
Figure 3.9 Lateral Support, Load Frame #2

75
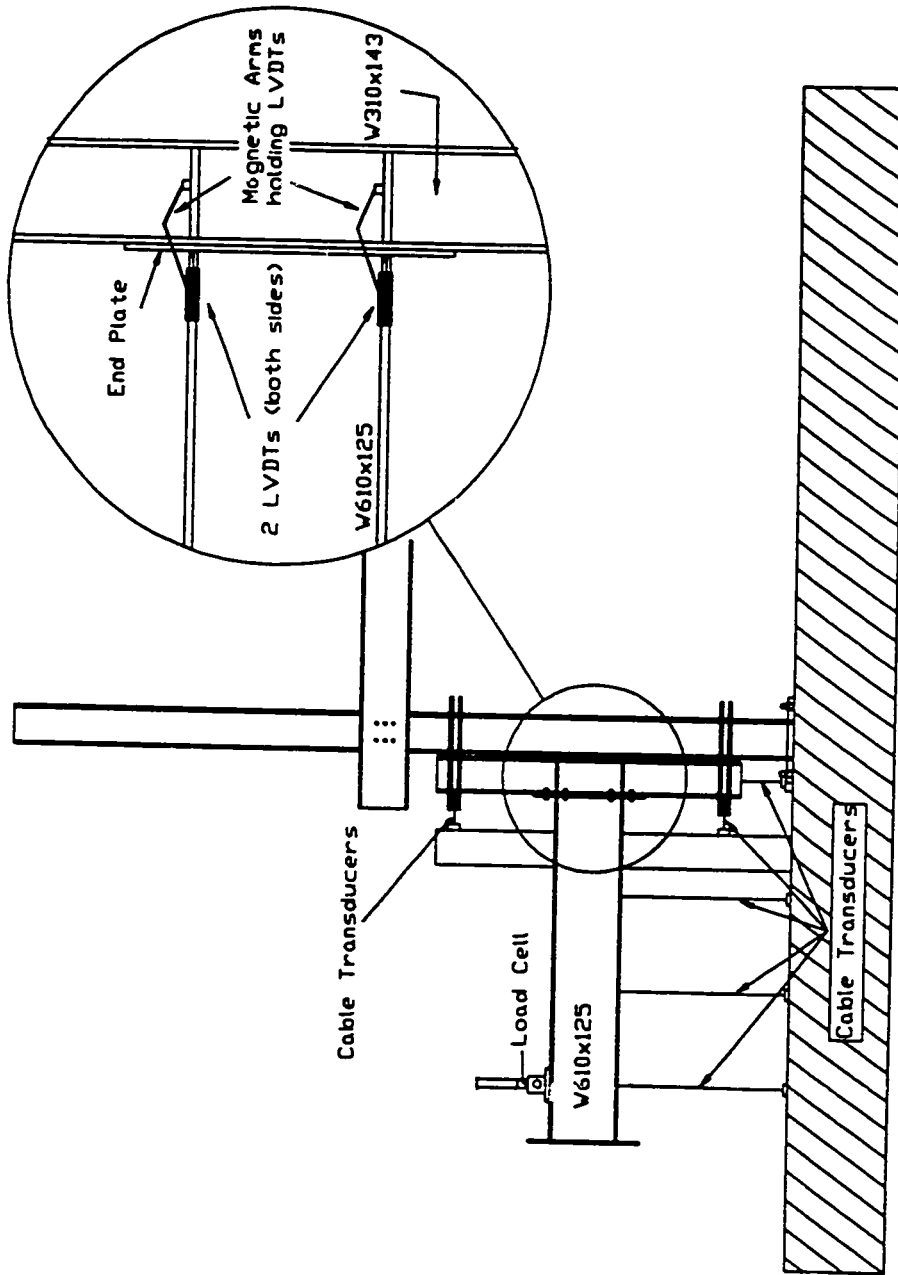
Figure 3.10 Instrumentation
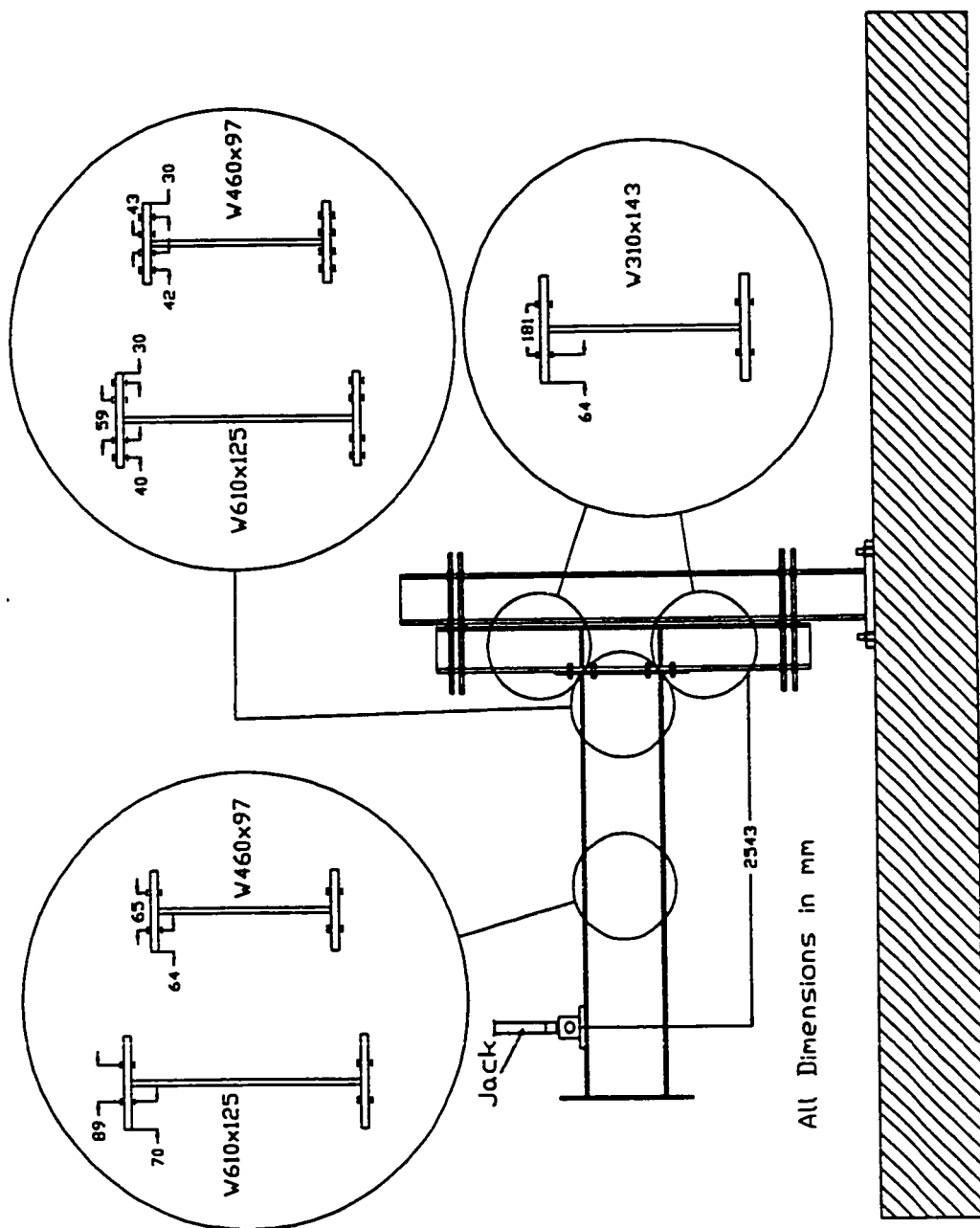
Figure 3.11 Strain Gage Locations
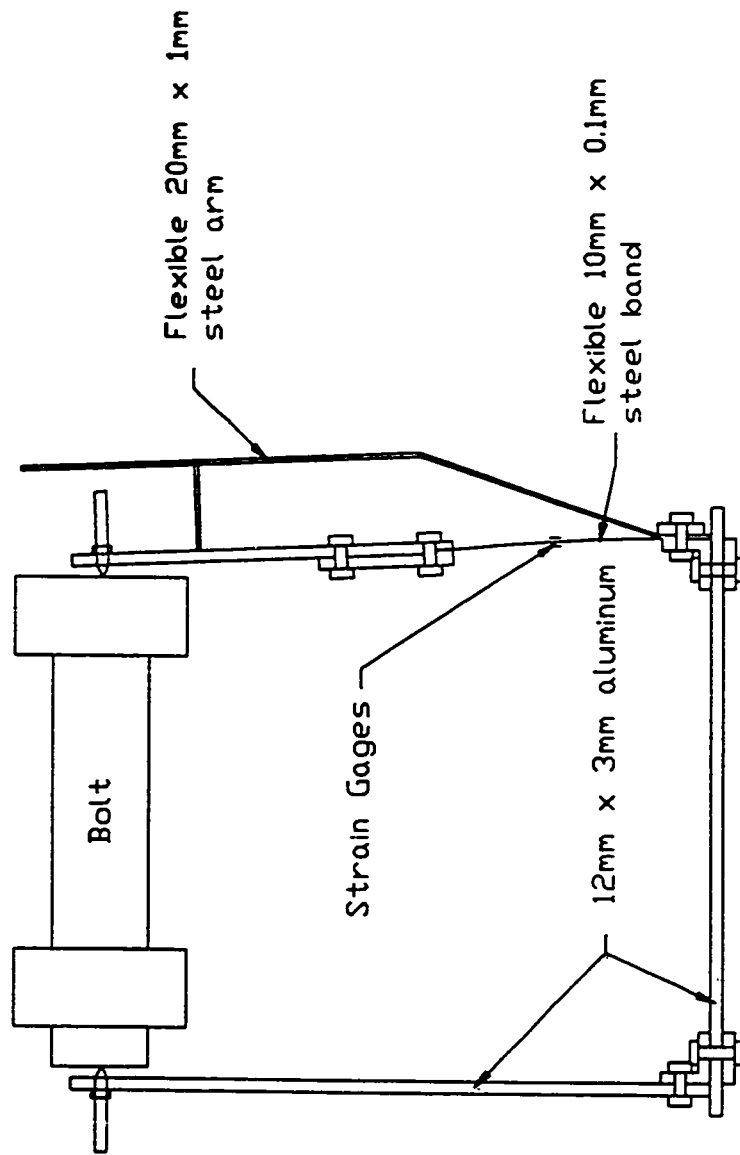
Figure 3.12 Bolt Extensometers

Fifteen full-scale extended end plate moment connections were tested under quasi-static cyclic loading. The parameters investigated in the experimental program were beam size, bolt layout, use of extension stiffeners, end plate thickness, welding procedure and bolt behaviour. Except for one test specimen, all connections were tested to failure. Eleven test specimens were designed to develop the full capacity of the end plate before yielding of the beam or column. The remaining specimens were designed to develop the plastic moment capacity of the beam before failure of the end plate. The specimens that failed in the end plate developed cracks at the toes of the connection full penetration welds and/or the toe of the stiffener fillet welds. The cracking at the toe of the flange full penetration welds frequently began adjacent to the bolts. Extended end plates with an eight bolt configuration, (four bolts around each flange) were used for twelve of the fifteen tests and extended end plates with a sixteen bolt configuration, (eight bolts around each flange) were used for the remaining specimens. The connections designed to fail the end plate and beam failed by a combination of the crack patterns mentioned above and plastification of the beam.

In order to evaluate the specified parameters three beam sizes were tested. Two bolt layouts and two end plate thicknesses were examined on each of the three beam sizes. The effect of extension stiffeners was investigated using the medium and large beam sizes. Four medium size beam connections and two large size beam connections were designed with extension stiffeners. Welding procedure was investigated using the medium size beam connections. Bolt behaviour was examined in seven test specimens.

In the following presentation of test results, the crack development is explained for each connection. Two stages of cracking are discussed, namely, the cracks observed at yield and the cracks observed at failure. Yield is defined as the stage at which the beam tip displacement versus load plot deviates from a straight line and failure is taken as the stage where the connection experienced a drop in maximum attainable load. Since the crack patterns for many of the connections are similar, a reference system has been developed to avoid repetition. In this reference system a total of twelve different crack types have been identified. A description of the different crack types is shown in Table

exterior flange weld toe. All cracks occurred at the weld toes.

The crack location designation does not specify which flange or which side of the flanges (left or right), cracks formed. Therefore it is possible for a connection that developed type A cracks on one flange to have either one or two type A cracks. Type A cracks may form adjacent to each of the bolts. As well, the crack location reference system does not specify near which flange the cracks occurred. It is however, noted in the text whether or not crack development was different on the two flanges. Information concerning which flange, or side of flange, near which cracks developed was considered extraneous. The extended end plate terminology used in the crack location reference system and in the following text is shown in Figure 4.1 (a). Typical extended end plate cracks are shown in Figure 4.1 (b). The crack patterns for all connection sizes tested, are shown in Figures 4.2 through 4.15. The crack patterns do not give the actual crack lengths but show the approximate locations of crack development. All cracks occurred in the heat affected zones at the weld toes, therefore the welds are excluded from the figures showing the crack locations.

4.1 Effect of Beam Size on Tight Bolt Configurations

Connections S-2, M-1 and B-1 were all designed to investigate the effect of beam size on connections with tight bolt configurations. The crack patterns of connections S-2, M-1 and B-1 are shown in Figures 4.3, 4.5 and 4.12, respectively. At yield, connection S-2 developed type A cracks. Connection M-1, at first yield, developed type A, B and D cracks simultaneously on one flange, but developed only type A and D cracks on the other flange. At yield, connection B-1 developed type A cracks on both flanges. By failure, type C and F cracks had formed on both flanges, of both the medium and large size beam connections but only type C cracks had formed on the small size beam connection. By failure, type G cracks had also formed on the medium size beam connection. Figures 4.16, 4.17 and 4.18 are examples of the crack development and end plate deformation at failure of connections M-1 and B-1. Table 4.2 presents a summary of crack patterns and maximum end plate lift off for all connections.

shown in Figures 4.40, 4.42 and 4.51, respectively. The medium size beam connection showed the best rotation ductility of the three tight bolt configurations. Rotation ductility is taken as the maximum rotation the connection was able to sustain through one full load cycle divided by the connection rotation at first yield. The amount of rotation required to yield the connection decreased with increasing beam size. The yield rotation was 0.35 degree for the small beam, 0.13 degree for the medium beam and 0.07 degree for the large beam. The maximum end plate rotation did not show the same trend. The maximum rotation was 1.16 degrees for the small, 1.30 degrees for the medium and 0.58 degree for the large size beam connection. The medium and large size beam connections were able to withstand an increase of 50 percent in load after first yield while the small size beam connection sustained only an eight percent increase. It is possible that the apparent poorer performance of the small connection may be partially attributed to the thinner end plate used. The small size beam connection used 13.3 mm plate whereas the medium and large size beam connections used 15.9 mm plate. Table 4.3 presents a summary of connection performance; moments, rotations and rotation ductilities.

The amount of energy dissipated during each test was evaluated by calculating the area under the hysteresis loops of the moment versus end plate rotation curves. Figures 4.58, 4.60 and 4.67 show the cumulative energy dissipated in relation to the number of inelastic excursions of connections S-2, M-1 and B-1, respectively. An inelastic excursion was denoted as half of one hysteresis loop. A comparison of the energy dissipation curves for specimens S-2, M-1 and B-1 indicate that specimen M-1 dissipated the most energy while S-2 dissipated the least amount of energy. This was directly related to the number of inelastic excursions sustained by each connection. Connection M-1 sustained 20 inelastic excursions, while B-1 and S-2 sustained 15 and 9 inelastic excursions respectively. Table 4.4 compares the amount of energy dissipated and the number of inelastic excursions for all the connections tested.

4.2 Effect of Bolt Configuration (same end plate thickness)

4.2.1 Small Size Beam Connections

Connections S-2 and S-3 were designed with the same end plate thickness but with different bolt configurations. Connection S-2 had a tight bolt configuration whereas S-3 had a relaxed bolt configuration.

Crack locations at yield and failure, for connection S-2 and at failure for connection S-3 are shown in Figures 4.3 and 4.4, respectively. Connection S-2 developed type A cracks at yield and type C cracks by failure. Connection S-3 developed both type C and F cracks by failure. The crack pattern at yield of connection S-3 was not recorded. Examples of type C, F and G cracks in connection S-3 at failure are shown in Figure 4.19.

The moment versus end plate rotation curves of connections S-2 and S-3 are shown in Figures 4.40 and 4.41, respectively. Connections S-2 and S-3 achieved similar moment capacities. Connection S-3, however, showed a significantly higher rotation ductility (15.8 versus 3.3) and a greater maximum end plate rotation. Connections S-2 and S-3 rotated 1.16 and 1.9 degrees, respectively, prior to failure.

Figures 4.58 and 4.59 show the cumulative energy dissipated in relation to the number of inelastic excursions for connections S-2 and S-3. Connection S-3, although sustaining fewer inelastic excursions than S-2 (7 versus 9), dissipated more energy. Connection S-3, however, was loaded to much greater rotations than connection S-2 in the first few inelastic load cycles, and only one load cycle was performed at each load level. This may explain why connection S-3 did not sustain more inelastic excursions or dissipate more energy.

4.2.2 Medium Size Beam Connections

Connections M-1 and M-2 were designed with the same end plate thickness but with different bolt configurations. Connection M-1 had a tight bolt configuration whereas M-2 had a relaxed bolt configuration. Crack locations for connections M-1 and M-2 are shown in Figures 4.5 and 4.6, respectively. The crack pattern observed in connection M-1 was described in Section 4.1. Connection M-2 developed type D and G cracks at

yield and type A cracks formed at the first load level beyond yield. By failure connection M-2 had developed type C, F and G cracks. At failure, the type C cracks had extended far enough into the end plate to release most of the load from the exterior bolts. The release of load from the exterior bolts shifted the force in the bolt group to the interior bolts and caused rupture of one of the interior bolts. Figure 4.20 shows cracks in the end plate after rupture of one of the bolts in connection M-2. Figure 4.21 shows the extent of end plate deformation at failure in connection M-2.

Figures 4.42 and 4.43 show the moment versus end plate rotation for connections M-1 and M-2, respectively. Connection M-2 had a much greater rotation ductility than connection M-1 (23.0 versus 10.0). The increase in ductility is because the yield rotation was decreased 38 percent and the maximum rotation was increased 42 percent. This additional ductility of connection M-2 was accompanied by a 45 percent reduction in the moment at yield and a 29 percent reduction in maximum moment.

The maximum end plate lift off, defined as the maximum separation between the column flange and the end plate measured at the beam flange level, of connection M-2 was 75 percent greater than for connection M-1. It was also noted that the largest end plate lift off occurred at the exterior weld toe level in connection M-2, and not at the beam flange level, where end plate lift off was measured (Figure 4.72). Maximum end plate lift off, measured at the beam flange level is shown in Table 4.2. The maximum end plate lift off listed in Table 4.2 is the maximum recorded in the last complete loading cycle. The actual end plate lift off reached a maximum just before the connection failed but generally before a load block could be completed and was therefore not reported.

Figures 4.60 and 4.61 show the cumulative energy dissipated as a function of the number of inelastic excursions for connections M-1 and M-2, respectively. Connection M-2 had a greater energy dissipation capacity and was able to sustain a greater number of inelastic excursions than connection M-1 (32 versus 20).

4.2.3 Large Size Beam Connections

Connections B-1 and B-2 were designed with the same end plate thickness but with different bolt configurations. Connection B-1 had a tight bolt configuration where as B-2

had a relaxed bolt configuration. Crack locations for connections B-1 and B-2 are shown in Figures 4.12 and 4.13. The crack patterns in specimen B-1 were described in Section 4.1. Connection B-2 developed type D cracks at first yield which became type F cracks by failure. Figure 4.22 shows a type F crack in connection B-2. Figure 4.23 shows the deformation of end plate B-2 at failure. Except for the crack pattern, the comparison between connections B-1 and B-2 is quite similar to the comparison between connections M-1 and M-2.

Figures 4.51 and 4.52 show the moment versus end plate rotation of connections B-1 and B-2, respectively. The relaxed bolt configuration (B-2) again offered enhanced rotation ductility but suffered a loss in strength of 33 percent. The relaxed bolt configuration resulted in an increased rotation prior to failure with no change in yield rotation. The maximum end plate lift off was 60 percent larger in connection B-2 than in B-1 and, again, the largest actual end plate lift off was located under the toe of the weld on the exterior flange face rather than under the beam flange.

Figures 4.67 and 4.68 show the cumulative energy dissipated as a function of the number of inelastic excursions for connections B-1 and B-2, respectively. The specimen with the relaxed bolt configuration (B-2) again was able to sustain a greater number of inelastic excursions and dissipate more energy than the specimen with the tight bolt configuration (B-1).

4.2.4 Conclusion

The use of a relaxed bolt configuration over a tight bolt configuration improves connection rotation capacity. This improvement however, appears to decrease with increasing beam size and is accompanied by a decrease in moment. In the connections tested, the improved rotation capacity of the medium and large size beam connections was accompanied by a decrease in maximum moment capacity. There was little change observed in the moment capacity of the small size beam connections.

The relaxed bolt configuration, as well as improving rotation capacity, enables connections to dissipate more energy than the tight bolt configuration. The medium and large size beam connections with a relaxed bolt configuration were able to sustain

tight bolt configuration counterparts. The small size beam connection with tight bolt configuration experienced close to the same number of inelastic excursions and dissipated only slightly more energy than the small size beam connection with a relaxed bolt configuration. This discrepancy from the medium and large size beam connections, however, may be attributed to the more aggressive loading sequence adopted for the testing of connection S-3. More aggressive loading may lead to decreased cumulative energy dissipation.

The main disadvantage of the relaxed bolt configuration is an uneven distribution of bolt forces. The interior of the relaxed bolt configuration connection is far more rigid than the exterior. This imbalance of connection rigidity causes most of the load in the bolt group to be carried by the interior bolts. Using the relaxed bolt configuration would lead to the use of exceptionally large interior bolts.

4.3 Effect of Bolt Configuration (similar connection capacity)

Tests comparing the tight and the relaxed bolt configurations designed for similar moment capacity were only performed on the medium and large size beam connections. The enhanced strength for the relaxed bolt configuration was achieved using two different methods: by increasing end plate thickness, and by adding end plate extension stiffeners, as shown in Figures 3.3 and 3.5. This section examines the effect of strengthening by increasing end plate thickness.

4.3.1 Medium Size Beam Connections

Connection M-3, although designed to have a moment capacity similar to that of M-1, reached a yield load of 70 percent that of connection M-1 and a maximum load of 84 percent that of connection M-1. Crack locations at yield and failure for connection M-1 and M-3 are shown in Figure 4.5 and 4.7, respectively. The crack patterns for connection M-1 are discussed in Section 4.1. At yield, connection M-3 developed type B, D and G cracks. By failure, connection M-3 developed type C, F, and G cracks.

Figure 4.24 shows type C, F and G cracks in connection M-3, at failure. Figure 4.25 shows type C and F cracks extending through end plate M-3, at failure.

Moment versus rotation curves for M-1 and M-3, are presented in Figures 4.42 and 4.44, respectively. There was no improvement in either the yield rotation, maximum end plate rotation or rotation ductility. The maximum end plate lift off for both connections was the same (Table 4.3).

Figures 4.60 and 4.62 show the cumulative energy dissipated as a function of the number of inelastic excursions for connections M-1 and M-3, respectively. The amount of energy dissipated in connection M-3 was similar to that in M-1 until the 14th inelastic excursion. Connection M-3 failed during the 15th inelastic excursion. Connection M-1 dissipated more energy and sustained a larger number of inelastic excursions than connection M-3.

4.3.2 Large Size Beam Connections

Specimen B-3 was designed to develop a slightly greater moment capacity than specimen B-1 because the plate thickness required to achieve a similar moment capacity was not readily available. One inch A490 bolts were initially used for connection B-3. The interior one inch A490 bolts broke prior to end plate failure and were replaced by 1-1/4 in. A490 bolts to complete the test (Figure 4.26). Because of this bolt failure, two yield load levels were found for connection B-3. The first yield load, attributed to the plastic deformation of the one inch A490 bolts, was 74 percent of the load level reached in test specimen B-1. The second yield load (with 1-1/4 inch A490 bolts), attributed to crack initiation in the end plate, was slightly less than for connection B-1. The maximum load for connection B-3 was similar to that of connection B-1.

Crack locations for connections B-1 and B-3 at yield and failure are shown in Figures 4.12 and 4.14, respectively. The crack patterns for connection B-1 were discussed in Section 4.1. Connection B-3 developed type A and D cracks at yield. By failure, connection B-3 had developed type C and F cracks on both flanges. Figure 4.27 shows the end plate deformation and the propagation of a type F crack through end plate B-3 at failure. Figure 4.28 shows a type C crack at failure of connection B-3.

and B-3, respectively. Connection B-3 reached a maximum rotation almost twice as large as connection B-1 and a rotation ductility almost five times as large (40 versus 8.3). The maximum end plate lift off of B-3 was almost double that of connection B-1.

Figures 4.67 and 4.69 show the cumulative energy dissipated as a function of the number of inelastic excursions for connections B-1 and B-3, respectively. As with the medium size beam connections the dissipated energy was approximately the same in both specimens until the 15th inelastic excursion, but in this case the tight bolt configuration (B-1) failed. Connection B-3, therefore, sustained a greater number of inelastic excursions (26 versus 15) and dissipated more energy than connection B-1.

4.3.3 Conclusions

When designed for the same moment capacity, by adjusting end plate thickness, the relaxed bolt configuration connection offers to clear improvement over the tight bolt configuration connection. The relaxed bolt configuration may however offer a larger rotation capacity and rotation ductility than the tight bolt configuration connection.

Although the crack patterns of the medium and large size beam connections were similar, their behaviour was not. Connections M-1 and M-3 had similar rotation ductilities and end plate rotations, but connection B-3 had a substantially larger maximum rotation and rotation ductility than connection B-1. In the large size beam connections, the connection with a relaxed bolt configuration dissipated more energy than the connection with a tight bolt configuration. This was not the case for the medium size beam connections where the tight bolt configuration connection dissipated more energy than the relaxed bolt configuration connection.

A distinct disadvantage of the relaxed bolt configuration is the uneven distribution of bolt forces.

4.4 Effect of End Plate Extension Stiffeners

The second method used to strengthen the end plates with a relaxed bolt configuration connection was the addition of end plate extension stiffeners. The

aligned with the web of the beam (Figure 3.5). The thickness was selected to prevent local buckling. The relaxed bolt configuration with stiffeners was compared with two other connection designs, the tight bolt configuration without extension stiffeners and the relaxed bolt configuration without extension stiffeners. All three connection designs used 15.9 mm thick end plates.

4.4.1 Medium Size Beam Connections

A comparison of connection M-2 (relaxed bolt configuration with no extension stiffeners) and M-4 (a relaxed bolt configuration with extension stiffeners) shows that the addition of extension stiffeners increases both the yield and ultimate loads. The yield load was increased by 104 percent and the maximum load was increased by 49 percent.

Crack locations at yield and failure for connections M-2 and M-4 are shown in Figures 4.6 and 4.8, respectively. Crack patterns for connection M-2 are discussed in Section 4.2.2. Connection M-4, at first yield, developed a type D crack at one flange, and a type E crack at the other flange. At a beam tip displacement 1.5 times the yield displacement, type A and H cracks were observed. By failure, type C, F, G, and L cracks formed. Figure 4.29 shows a type L crack in connection M-4 at failure. Figure 4.30 shows type F and G cracks in the same connection.

The moment versus end plate rotation curves for connections M-2 and M-4 are shown in Figures 4.43 and 4.45, respectively. Extension stiffeners increased the yield rotation by over 100 percent. The stiffeners resulted in a large reduction in maximum rotation and rotation ductility. The reduction in rotation ductility can be partly attributed to the increased rotation at yield. The end plate lift off in connection M-4 was drastically reduced.

Figures 4.61 and 4.63 show the cumulative energy dissipated as a function of the number of inelastic excursions for connections M-2 and M-4, respectively. The number of inelastic excursions decreased 40 percent with the addition of extension stiffeners (19 versus 32) while the amount of energy dissipated decreased only nine percent (197 kJ versus 217 kJ).

4.4.2 Large Size Beam Connections

Crack locations at failure for connections B-2 and B-4 are shown in Figures 4.13 and 4.15, respectively. The crack patterns for connection B-2 were discussed in Section 4.2.3. At yield, connection B-4 developed type D cracks on both flanges. At a beam tip displacement of 1.25 times the yield displacement, type G cracks formed. At a yield beam tip displacement 1.75 times the yield displacement, type J cracks formed. Once the type J cracks formed the maximum load began to drop. By failure type F, G and L cracks had developed, and the type L cracks extended through the end plate. Figure 4.31 shows type L cracks in connection B-4 at failure. Figure 4.32 shows the end plate deformation of connection B-4 at failure.

The moment versus end plate rotation curves for B-2 and B-4 are shown in Figures 4.52 and 4.54, respectively. Comparison of connections B-2 and B-4 shows that the addition of extension stiffeners to end plate connections with a relaxed bolt configuration increases both the yield and ultimate loads. This is consistent with the observations made earlier on the medium size beam connections. The yield load was increased by 51 percent and the maximum load was increased by 81 percent.

The end plate yield rotations and maximum rotations were approximately the same for both B-2 and B-4. The rotation ductility the same for both connections. Connection B-4 had a maximum end plate lift off 19 percent larger than the maximum end plate lift off for connection B-2.

Figures 4.68 and 4.70 show the cumulative energy dissipated as a function of the number of inelastic excursions for connections B-2 and B-4, respectively. The addition of extension stiffeners to the large beam connections decreased the energy dissipation capacity of the connection, the reverse effect that occurred in the medium beam connections. The number of inelastic excursions were approximately the same for both connections B-2 and B-4.

The addition of extension stiffeners to the relaxed bolt configuration improves the moment capacity of extended end plate connections but indicates no clear trend concerning the other performance criteria. The yield rotation was significantly improved for the medium size beam connection and remained unchanged for the large beam connection. The maximum rotation and the rotation ductility were reduced for the medium beam connection but remained the same for the large beam connection. The energy dissipation capacity was improved for the large beam connection but was reduced for the medium beam connection.

4.5   Effect of End Plate Extension Stiffener and Relaxed Bolt Configuration

The second comparison of extension stiffeners on extended end plate connections was made with connections of similar moment capacity. The two connections with similar moment capacity were the relaxed bolt configuration connection with extension stiffeners and the tight bolt configuration connection without extension stiffeners.

4.5.1 Medium Size Beam Connections

Crack patterns for connections M-1 and M-4 are shown in Figures 4.5 and 4.8 and were discussed in Sections 4.1 and 4.4.1, respectively.

Figures 4.42 and 4.45 show the moment versus end plate rotation of connections M-1 and M-4, respectively. Connection M-4 had a 13 percent higher yield load than connection M-1 and only a slightly higher maximum load. Connection M-4 was able to reach greater yield and maximum rotations than connection M-1. The rotation ductility of the connection dropped slightly due to the initial increase in yield rotation. The end plate lift off was smaller for connection M-4 than for M-1.

Figures 4.60 and 4.63 show the cumulative energy dissipated as a function of the number of inelastic excursions for connections M-1 and M-4, respectively. The use of extension stiffeners on the medium beam connection increased the amount of energy dissipated but with one less inelastic excursion.

Crack patterns for connections B-1 and B-4 are shown in Figures 4.11 and 4.14 and discussed in Sections 4.1 and 4.4.2, respectively.

Figures 4.51 and 4.54 show the moment versus end plate rotation curves for connections B-1 and B-4, respectively. Connections B-1 and B-4 had approximately the same yield load but connection B-4 had a 30% increase in maximum load. The connection rotation at yield was the same for both B-1 and B-4. Connection B-4 had increased maximum rotation and rotation ductility. Unlike the medium size beam connections, the end plate lift off was much greater for the connection with stiffeners.

Figures 4.67 and 4.70 show the cumulative energy dissipated as a function of the number of inelastic excursions for connections B-1 and B-4, respectively. The amount of energy dissipation in connections B-1 and B-4 was approximately the same until failure of connection B-1 during the 15th inelastic excursion. Connection B-4 was able to dissipate more energy and undergo more excursions into the inelastic range than B-1.

4.5.3 Conclusions

The use of a stiffened relaxed bolt configuration significantly increases the maximum rotation of extended end plate connections over the use of an unstiffened tight bolt configuration connection. The use of a stiffened relaxed bolt configuration also increases the energy dissipation capacity. The increase in energy dissipation capacity may be more pronounced on larger size beam connections.

Other performance criteria showed no clear trends for both tested connection sizes. The medium size beam connection with extension stiffeners showed an increase in yield load. This was not observed in the large size beam connection. The rotation ductility of the medium size beam connection was decreased slightly as a result of the stiffeners addition, but it was increased for the large size beam connection.

4.6 Effect of End Plate Thickness

The effect of end plate thickness was investigated on test specimens with a relaxed bolt configuration.

4.6.1 Medium Size Beam Connections

The only difference between connection M-2 and connection M-3 was end plate thickness. Connection M-2 had an end plate thickness of 15.9 mm and M-3 had an end plate thickness of 19 mm. Crack locations for connections M-2 and M-3 are shown in Figures 4.6 and 4.7 and were discussed in Sections 4.2.2 and 4.3.2, respectively.

Figures 4.43 and 4.44 show the moment versus rotation curves for connections M-2 and M-3, respectively. By increasing the end plate thickness the yield and maximum connection loads increased. The yield rotation, however, was the same for both tests. The maximum rotation, rotation ductility and maximum end plate lift off were reduced when the end plate thickness was increased.

Figures 4.61 and 4.62 show the cumulative energy dissipated as a function of the number of inelastic excursions in connections M-2 and M-3, respectively. Increasing the end plate thickness also reduced the number of inelastic excursions and energy dissipation.

4.6.2 Large Size Beam Connections

Connections B-2 and B-3 were identical except for end plate thickness. End plates for connections B-2 and B-3 were 15.9 mm and 19 mm thick, respectively. Crack locations for connections B-2 and B-3 are shown in Figures 4.13 and 4.14 and were discussed in Sections 4.2.3 and 4.3.3, respectively.

The moment versus rotation curves for connections B-2 and B-3 are shown in Figures 4.52 and 4.53, respectively. The yield and maximum loads were increased with the use of the thicker end plate. The yield rotation was approximately the same for connection B-2 and B-3. The maximum rotation and rotation ductility of B-3 was considerably higher than that of B-2, and the maximum end plate lift off was greater.

Figures 4.68 and 4.69 show the cumulative energy dissipated as a function of the number of inelastic excursions for connections B-2 and B-3, respectively. Connections B-2 and B-3 experienced approximately the same number of inelastic excursions but connection B-3 dissipated substantially less energy.

4.6.3 Conclusions

Increasing end plate thickness increases the yield and maximum loads but decreases the energy dissipation capacity of extended end plate connections. Other performance criteria showed no clear trends between connections sizes. The maximum rotation, rotation ductility and maximum end plate lift off were reduced for the medium size beam connection but increased for the large size beam connection.

4.7 Effect of Beam Size

Comparison of connections M-1 through M-4 with B-1 through B-4 respectively indicates that medium size beam connections are more ductile than large size beam connections. The medium size beam connections had higher yield and maximum rotations than their large size beam connections counterparts. The small size beam connections cannot be justly compared with the medium and large size beam connections because of the different end plate thickness.

4.8 Effect of Welding Procedure

The effect of welding process and joint preparation on the performance of extended end plate connections was investigated with medium size beam connections. Two tests were performed to compare the weld performance on connections designed to fail the end plate, and two tests were performed to compare the weld performance on connections designed to develop the full capacity of the beam before failure of the end plate. The connections designed to fail the end plate, M-4 and M-6, had a relaxed eight bolt configuration and end plate extension stiffeners. The connections designed to develop the full capacity of the beam prior to failure of the end plate, M-5 and M-7, had a tight sixteen bolt configuration and end plate extension stiffeners. The difference in welding procedure was discussed in Section 3.3.2. The welding processes used were SMA (shielded metal arc) welding and FCA (flux cored arc) welding. The FCA welded specimens were prepared with weld access holes.

4.8.1 End Plate Failure

Connection M-4 was SMA welded and connection M-6 was FCA welded. Crack locations at yield and failure for connection M-4 and M-6 are shown in Figures 4.8 and 4.10. The crack patterns of connection M-4 are discussed in Section 4.4.1. Connection M-6 developed type G and H cracks at yield. At a beam tip displacement of 1.25 times the yield displacement type D crack had formed at both flanges and type J cracks were detected. By failure, type F and L cracks had formed. Figures 4.33 and 4.34 show type F and L cracks in connection M-6 at failure.

Figures 4.45 and 4.48 show the moment versus end plate rotation curves for connections M-4 and M-6. The yield load for connection M-4 was 14 percent higher than that for M-6 but the maximum load was 5 percent lower. The yield and maximum rotations were slightly higher for connection M-4 and the rotation ductility was slightly higher for connection M-6.

Figures 4.63 and 4.65 show the cumulative energy dissipated as a function of the number of inelastic excursions for end plates M-4 and M-6, respectively. End plate M-6 was able to dissipate more substantially more energy than M-4 (259 kJ versus 197 kJ) and underwent more inelastic excursions (28 versus 19). Connection M-6 also dissipated energy through yielding of the beam, but most of the energy dissipation was done by the end plate. The amount of energy dissipated by the end plate was determined by calculating the area under the moment versus end plate rotation curve and the energy dissipated by the beam was determined by calculating the area under the moment versus beam plastic hinge rotation curve.

4.8.2 Beam and End Plate Failure

Crack locations for connections M-5 (SMA welded) and M-7 (FCA welded) are shown in Figures 4.9 and 4.11 respectively. Connection M-5 developed type A and D cracks at yield but they did not grow during the remainder of the test. Figure 4.35 shows type A and D cracks in connection M-5 at failure. Failure of connection M-5 occurred from out of plane deformation of the beam, as shown in Figure 4.36. No cracks were evident in connection M-7 at first yield. Connection M-7 developed type A and D cracks

however, occurred by failure of the end plate, rather than out-of-plane deformation of the beam. Type C, F and M cracks formed during the test. Figure 4.37 shows the stiffener tearing out of the beam in connection M-7 at failure.

Figures 4.46 and 4.49 show the moment versus end plate rotation curves for connections M-5 and M-7, respectively. Figures 4.47 and 4.50 show the moment versus connection rotation curves for connections M-5 and M-7, respectively. Both moment versus end plate rotation and connection rotation curves are shown because specimens M-5 and M-7 experienced permanent deformation in both the end plate and the beam. Two yield loads are reported for each connection, one for yielding of the end plate and one for yielding of the connection. It is possible to have two yield loads because the designation of yield is denoted as the deviation from a straight line of the moment versus rotation curve. Yielding of the end plate quickly causes deviation from a straight line of the moment versus end plate rotation curve, it has a lesser impact on the moment versus connection rotation curve. The gentler deviation from a straight line of the moment versus connection rotation curve increases the subjectivity of the determination of yield, meaning that more material is required to yield before the deviation from a straight line, of the moment versus connection rotation curve, is pronounced enough to denote yielding.

The end plate of connection M-7 yielded at a slightly higher load than connection M-5 (660 kN·m versus 600 kN·m) but at approximately the same rotation. The overall connection of M-7 also yielded at a slightly higher load than the overall connection M-5 (790 kN·m versus 775 kN·m) but at approximately the same rotation. At failure end plate M-5 achieved 0.5 degree rotation in the positive direction and 0.25 degree in the negative direction. At failure, connection M-7 achieved 0.6 degree of rotation in both directions. Overall connection M-5 reached a rotation of 3.0 degrees before failing, while M-7 reached a rotation of 2.85 degrees. The smaller maximum rotation for the overall connection of specimen M-7, could be due to the larger demand placed on the end plate.

Figures 4.64 and 4.66 show the cumulative energy dissipated in relation to the number of inelastic excursions of connections M-5 and M-7. Energy dissipation and

4.8.3 Conclusions

The FCA welding process appears to provide a slightly less flexible connection with somewhat better energy dissipation capacity. However, due to the large variability in the welding speeds for the SMA welded specimens it is difficult to draw conclusions. It is also possible that the differences in moments, rotations and energy dissipation capacities fall within reasonable experimental variation. No tests were duplicated to verify the level of experimental variation.

4.9 Bolt Behaviour

Bolt behaviour was not originally selected as one of the parameters to be investigated in this test program. This explains why the elongation of the interior and exterior bolts of all connections tested were not measured and why only limited observations were made. It was the interesting visual observations of bolt bending and loss of preload during the first portion of the test program that lead to the closer scrutiny of bolt behaviour in the second portion of the test program. The beginning of bolt monitoring is deemed the beginning of the second portion of the test program.

On a number of connections tested, extreme bending of bolts and loss of preload were observed. Bolt bending can clearly be observed in connections M-3, M-7 and B-4 in Figures 4.25, 4.37 and 4.32, respectively. The loss of preload was noticed because numerous bolts were only finger tight when testing was concluded. These observations lead to the monitoring of one interior and one exterior bolt for connections M-2, M-3, M-4, M-5, M-6, M-7 and B-5. Unfortunately the data for tests M-3 and M-4 was incomplete and could not be used.

A number of problems were identified with the data collected on bolt behaviour. One of the difficulties was that the initial bolt force was not known. Without the initial force it is difficult to determine the amount of load sharing between bolts. Another difficulty is that only the average elongation of the bolts was obtained. Since the bolts

than the other. This partial plastification makes it difficult to directly compare bolt elongation to bolt load. The connection moment versus bolt elongation curves are presented in Appendix B for comparison with future tests. Two curves are shown for each of the bolts tested; one is the elongation of the bolts in the elastic range and the other is the elongation of the bolts throughout the entire test. Aside from these difficulties, a couple of interesting observations were made.

The first observation was that the interior bolts in all the connections measured, experienced larger plastic deformations than the exterior bolts. These larger plastic deformations indicate that the interior bolts carry more load than the exterior bolts. This can be seen from the total bolt elongation shown on the connection moment versus bolt elongation plots in Appendix B for all connections, and if the zero connection moment is considered to be the zero bolt elongation in each cycle, the interior bolts show greater elongation in every tensile excursion. The exception here is connection M-6 where the interior bolts have approximately the same amount of bolt elongation. Connection M-6 is the only connection presented here that used 31.8 mm A490 bolts.

The second observation was that connection B-5 showed the interior bolts going into tension when the adjacent to flange was in compression. One possible explanation for the tensile load in the interior bolts is that the end plate bent slightly away from the column flange during the initial stages of loading on the interior of the connection. The bent plate pushed out on the interior bolts and forced them into tension. Once the bolts began to deform plastically this behaviour reverted to normal, i.e. the forces in the bolts were consistent with the force in the adjacent to flange.

4.10 Complete Connection Failure

Four of the test specimens, S-1, M-5, M-7, and B-5, were designed to develop the full capacity of the beam before failure of the end plate. Connection S-1 used a tight eight bolt configuration. Connections M-5, M-7 and B-5 used a tight 16 bolt configuration. Connection B-5 unfortunately was not tested to failure because the load frame itself was showing excessive deflections.

respectively. No cracking was observed in the end plate of connection B-5. Examples of cracking in end plates M-5, M-7 and S-1 at failure are shown in Figures 4.36 and 4.38. No photos of B-5 are shown because the connection was not tested to failure.

The moment versus end plate rotation curves for connections S-1, M-5, M-7 and B-5, are shown for these specimens in Figures 4.39, 4.46, 4.49 and 4.55. The moment versus connection rotation curves for specimens M-5, M-7 and B-5 are shown in Figures 4.47, 4.50 and 4.56. No moment versus connection rotation curve was determined for connection S-1. It can be seen from comparing the curves for each of the connections that an end plate connection designed to cause plastification of the beam can result in very stable and well developed hysteresis loops, even when there is some pinching occurring in the moment versus end plate rotation curve. The yield rotations of the end plates for connections S-1, M-5, M-7 and B-5 were 0.40, 0.03, 0.05, and 0.04 respectively. The yield rotations for connections M-5, M-7 and B-5 were 0.85, 0.85 and 1.25 respectively. The maximum end plate rotations obtained by connections S-1, M-5, M-7 and B-5 were 1.12, 0.4, 0.68 and 0.7 degrees, respectively. Again connection B-5 was not tested to failure. The maximum connection rotations obtained by M-5, M-7 and B-5 were 3.00, 2.78 and 1.61.

By involving the beam in the energy dissipation process the energy dissipation capacity for the connections was increased. The amount of energy dissipated by specimens M-5, M-7 and B-5 are presented in Figures 4.64, 4.66 and 4.71, respectively. The cumulative energy dissipated is divided into the amount of energy dissipated by the specimen (beam and connection) and the amount of energy dissipated by the end plate. Insufficient data was collected to separate the energy dissipated by the beam from the energy dissipated by the end plate in connection S-1. The cumulative energy dissipated by the end plate alone is shown in Figure 4.57.

The end plate in connection M-5 dissipated very little energy when compared to the beam, however because the end plate was not the cause of failure of the connection, the full energy dissipation capacity of the end plate was not realized. The end plate in connection M-7 dissipated 20 percent as much energy as the beam. In specimen M-7

failure of the connection was attributed to failure of the end plate so the full energy dissipation capacity of the connection was not realized. The end plate in connection B-5 dissipated 48 percent as much energy as the beam.. Neither the beam or the end plate of connection B-5 showed any signs of failure. By comparing the energy dissipation capacities of the beams and the end plates of connections M-5, M-7 and B-5 it can be seen that end plates can take an active role in energy dissipation when properly detailed.

Comparing the performance of the above connections, with the performance of connections designed to fail the end plate alone, it can be seen that the tight sixteen bolt configurations used, were able to dissipate comparable amounts of energy while developing the moment capacity of the beams. By looking at the energy dissipated by connection M-7, however, which failed due to cracking of the end plate, it appears that the stiffened sixteen bolt configuration was not able to dissipate as much energy as the stiffened eight bolt configuration. One explanation for this may be that the actual loading pattern of endplate M-7 wad different than M-4. Because the rotation of specimen M-7 was due to a combination of beam rotation and connection rotation the end plate was not loaded to the same extent as in connection M-4 (i.e. end plate M-7 had maximum rotation of only 0.68 degree compared to 1.34 degrees for connection M-4). The additional cycles of load required to force this rotation would have caused significant increases in the amount of energy dissipated.

Type	Crack Description
A	- Adjacent to a bolt at an exterior flange weld toe
B	- Adjacent to a flange tip at an exterior flange weld toe
C	- Along an entire exterior flange weld toe
D	- Adjacent to a bolt at an interior flange weld toe
E	- Adjacent to a flange tip at an interior flange weld toe
F	- Along an entire interior flange weld toe
G	- Adjacent to a bolt at a web weld toe
H	- Adjacent to a bolt at an extension stiffener weld toe
J	- At an extension stiffener toe, at an extension stiffener-end plate interface weld toe
K	- At an extension stiffener toe, at an extension stiffener-beam interface weld toe
L	- Along an entire extension stiffener -end plate interface weld toe
M	- Along an entire extension stiffener-beam interface weld toe

Note: - All cracks occurred at the toe of a flange full penetration weld.

- Example crack locations are shown in Figure 4.1(b).

Table 4.2 Summary of Connection Performance: Crack Patterns and Maximum End Plate Lift Off.

Specimen	Cracks Types at First Yield	Cracks Types at Failure	Maximum End Plate Lift Off (mm)
S-1	n/a	C	n/a
S-2	A	C	n/a
S-3	n/a	C, F	n/a
M-1	A, B, D	C, F, G	14.9
M-2	D, G	C, F, G	20.0
M-3	B, D, G	C, F, G	14.8
M-4	D, E, G	C, F, G, L	12.5
M-5	A, D, YB	A, D, OB*	6.5
M-6	G, H	F, G, L*	16.5
M-7	YB	C, F, M*, YB	6.8
B-1	A	C, F	7.8
B-2	D	F	12.6
B-3	A, D	C, F	15.0
B-4	D	F, G, L*	15.5
B-5	YB	n/a	n/a

Extended End Plate Crack Location Code given in Table 4.1

*	- main reason for the drop in load
YB	- yielding of beam
OB	- out of plane buckling of beam

Connection	Moment at First Yield (kN·m)	Yield Rotation (deg.)	Maximum Moment (kN·m)	Maximum Rotation (deg.)	Rotation Ductility (Maximum Rotation / Yield Rotation)
S-1	320	0.40	390	1.12	2.8
S-2	180	0.35	190	1.16	3.3
S-3	140	0.12	195	1.90	15.8
M-1	460	0.13	700	1.30	10
M-2	255	0.08	495	1.85	23
M-3	320	0.08	585	1.20	15
M-4	502	0.18	740	1.34	7.4
M-5	600	0.03	1025	0.4	13.3
M-5 (overall)	775	0.85	1025	3.00	3.5
M-6	440	0.13	775	1.78	9.8
M-7	650	0.05	1100	0.68	13.6
M-7 (overall)	790	0.85	1100	2.78	3.3
B-1	520	0.07	770	0.58	8.3
B-2	344	0.07	550	1.01	14.4
B-3	385	0.03	750	1.20	40
B-4	520	0.07	1000	1.41	13.9
B-5	890	0.04	1485*	0.70	n/a
B-5 (overall)	1380	1.25	1485*	1.61	n/a

Note:

- All above reported information is regarding end plate failure alone unless otherwise specified.

- If the maximum rotation varied depending on the direction of loading the smaller value of maximum rotation was selected for this table.

* - The maximum moment of this specimen was limited by the capacity of the test frame.

Table 4.4 Number of Inelastic Excursions Beyond Yield and Cumulative Connection Energy Dissipation

Connection	Number of Inelastic Excursions	Cumulative Energy Dissipation (kJ)
S-1	21	81
S-2	9	16
S-3	7	36
M-1	20	149
M-2	32	217
M-3	14	101
M-4	19	197
M-5 (end plate / overall)	33	38 / 710
M-6 (end plate / overall)	28	259 / 361
M-7 (end plate / overall)	39	131 / 782
B-1	15	63
B-2	25	92
B-3	26	141
B-4	27	229
B-5 (end plate / overall)	11	80 / 166

Note:
- All above reported information is regarding end plate failure alone unless otherwise specified.
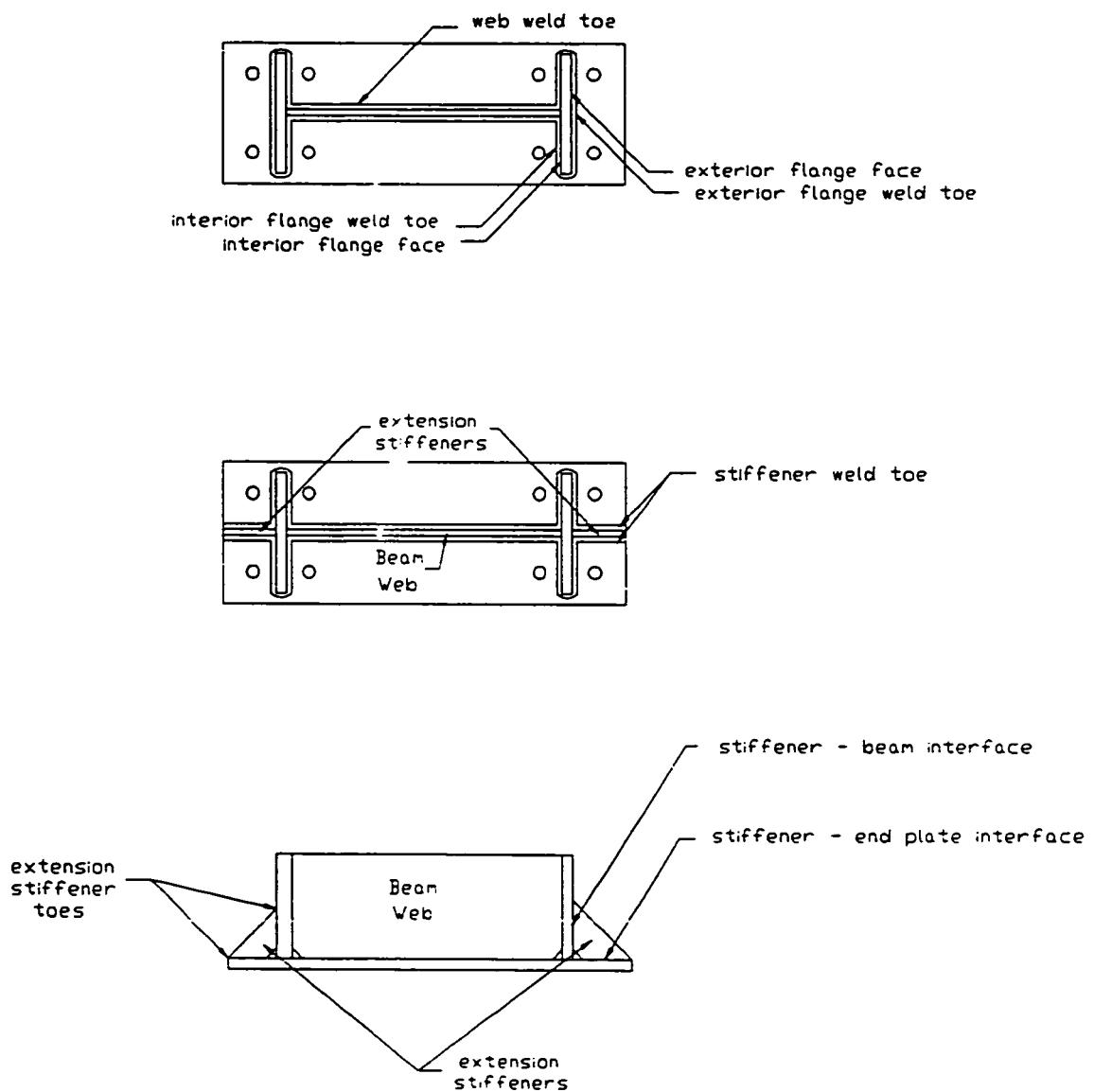
Figure 4.1 (a) End Plate Terminology used in Crack Location Reference System
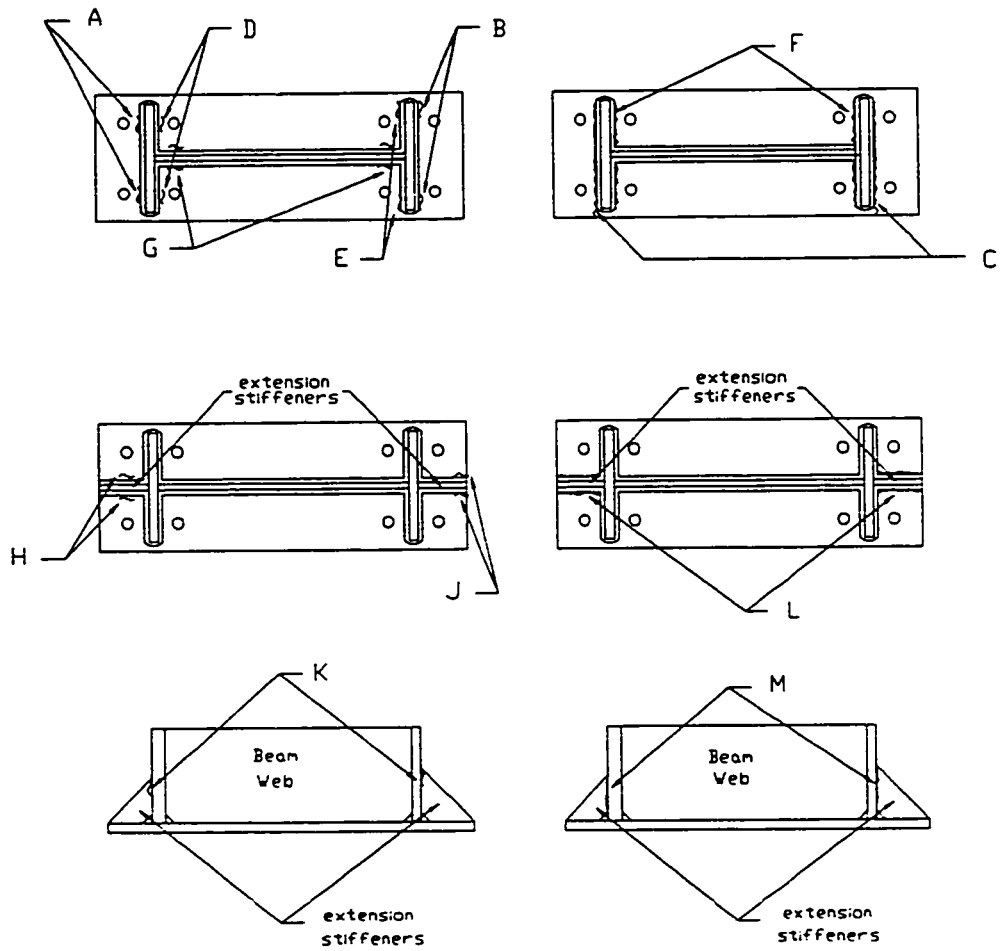
Figure 4.1(b) Typical Extended End Plate Crack Locations
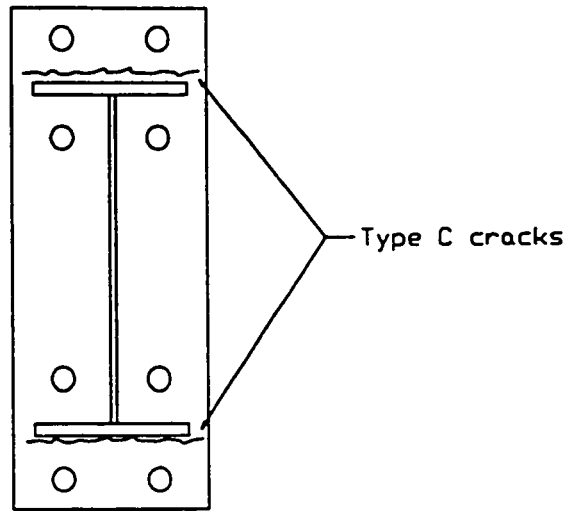
Failure

Figure 4.2 Crack Locations at Failure for Connection S-1
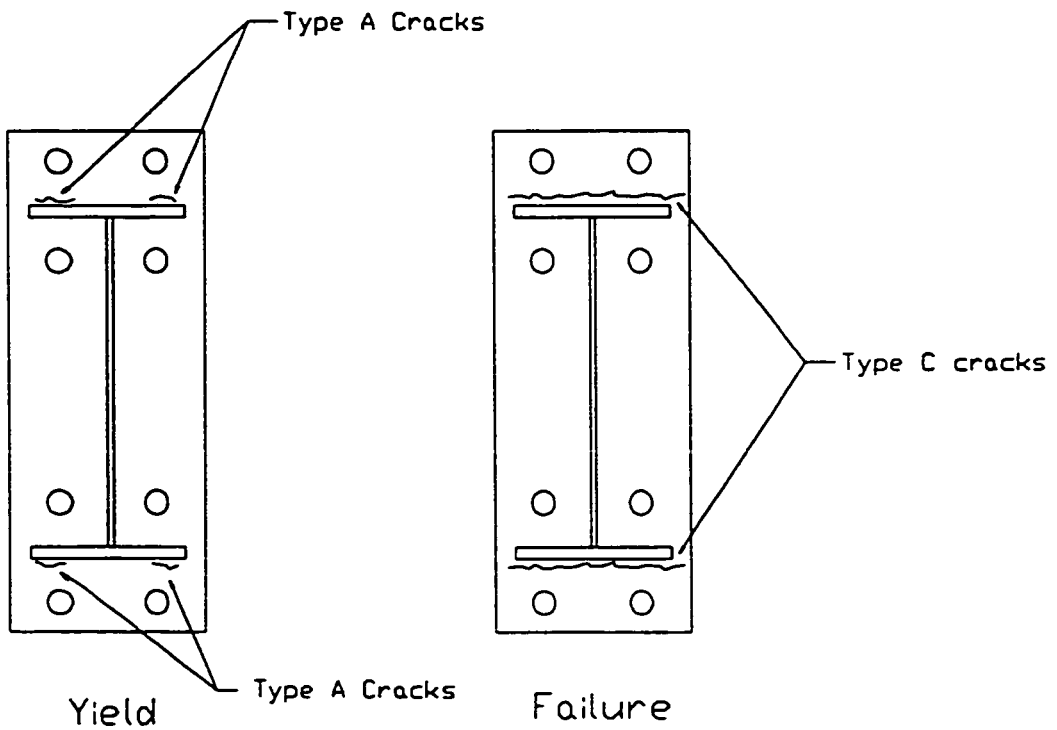
Figure 4.3 Crack Locations at Yield and Failure for Connection S-2
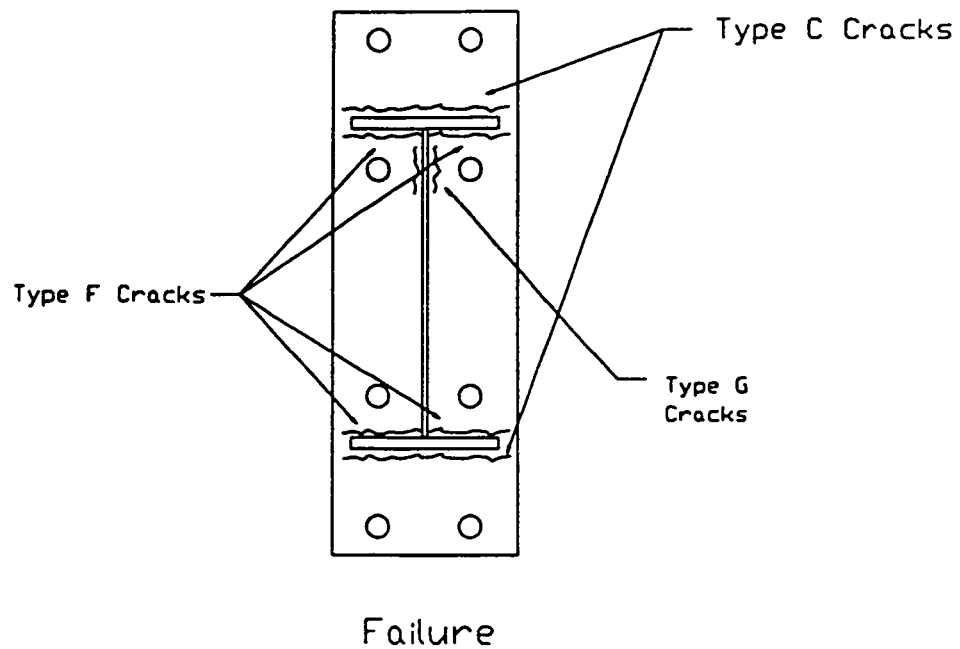
Figure 4.4 Crack Locations at Failure for Connection S-3
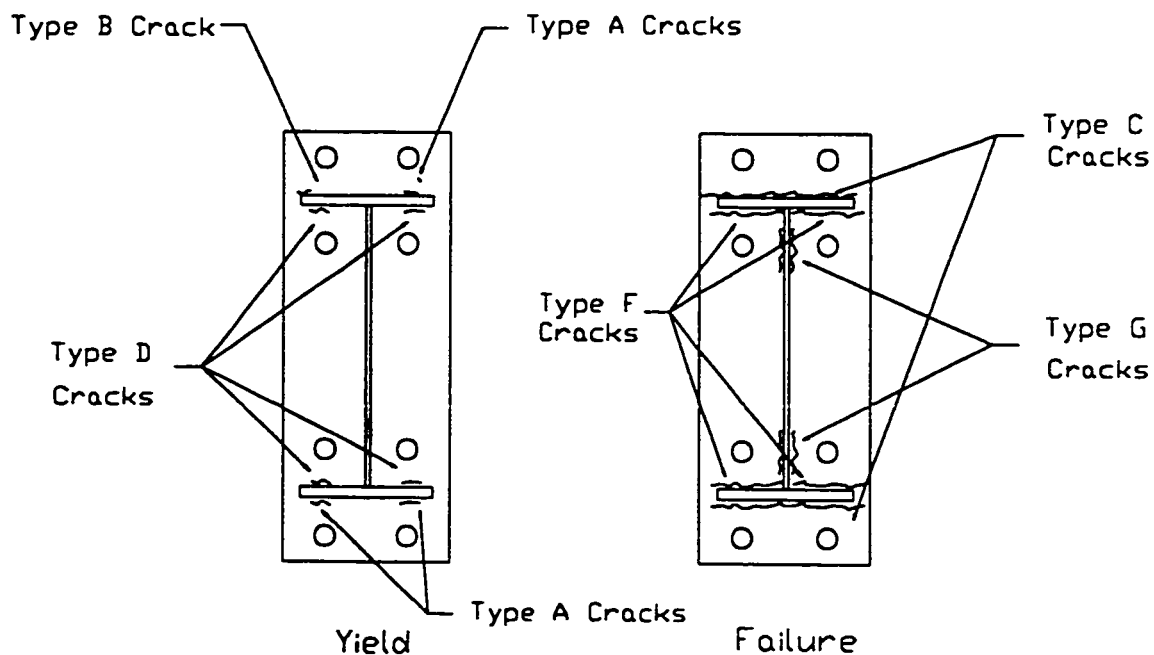
Figure 4.5 Crack Locations at Yield and Failure for Connection M-1
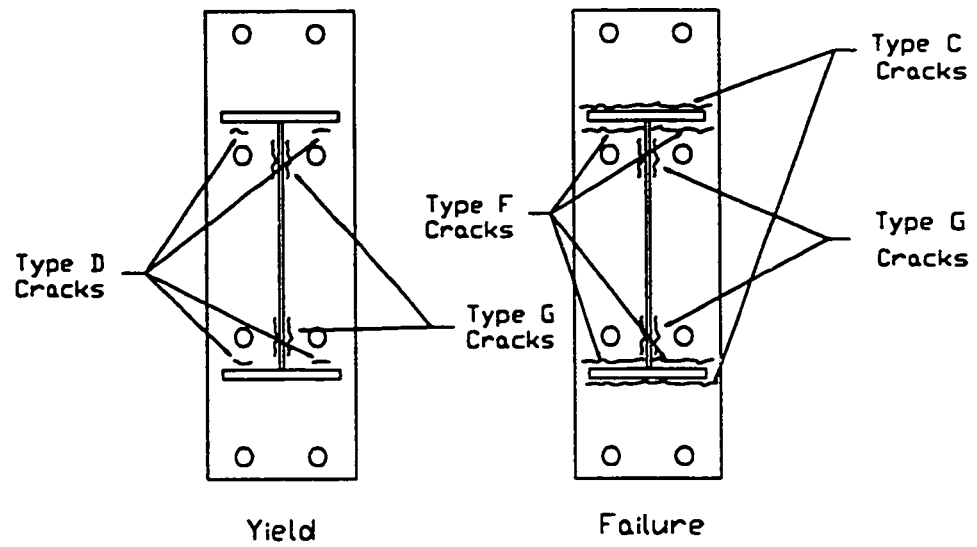
Figure 4.6 Crack Locations at Yield and Failure for Connection M-2
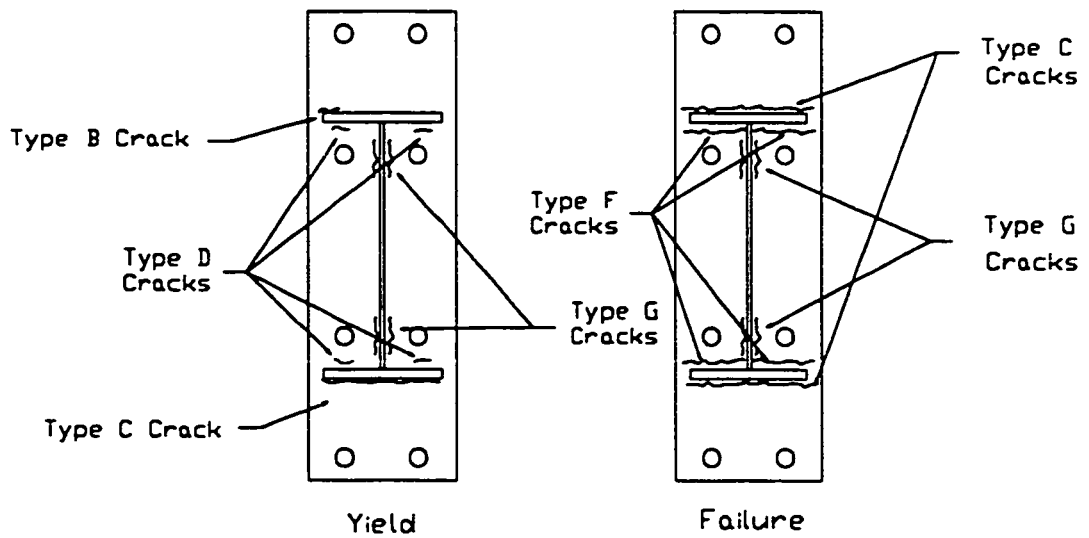
Figure 4.7 Crack Locations at Yield and Failure for Connection M-3

108
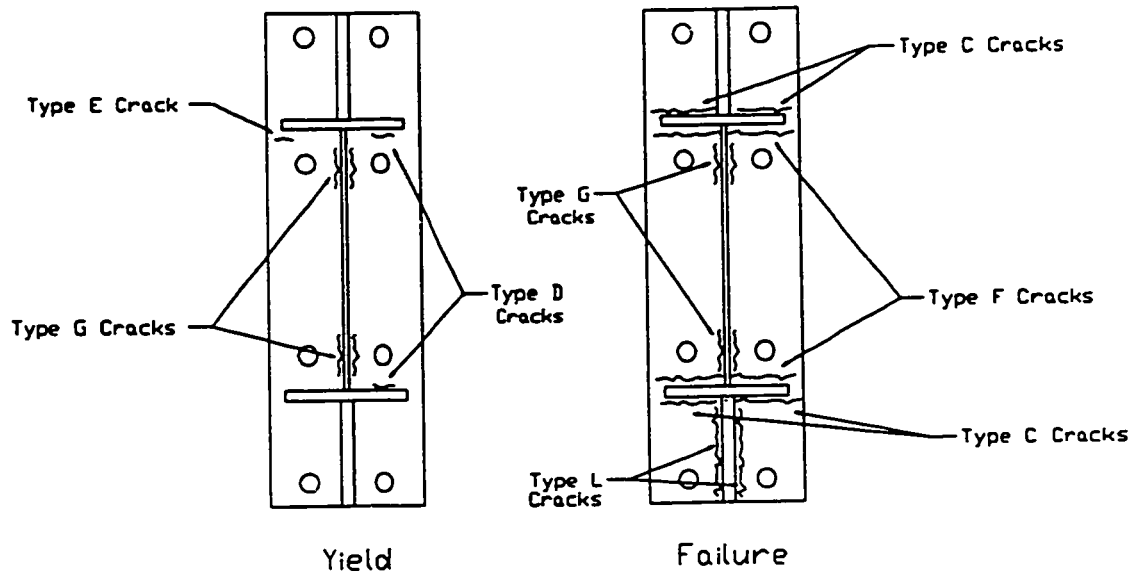
Figure 4.8 Crack Locations at Yield and Failure for Connection M-4
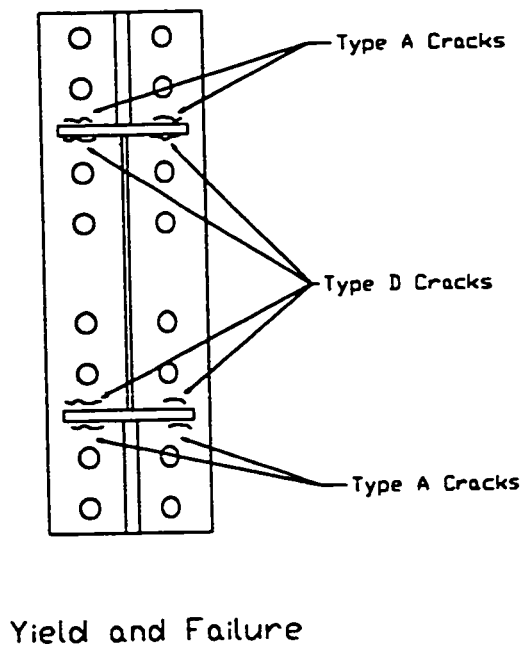
Figure 4.9 Crack Locations at Failure for Connection M-5
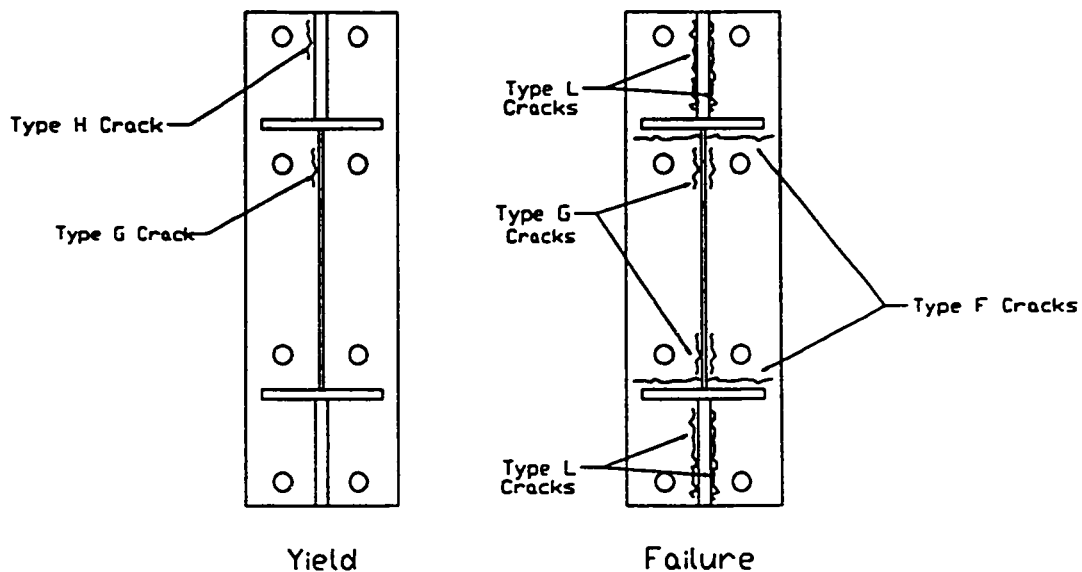
Figure 4.10 Crack Locations at Yield and Failure for Connection M-6
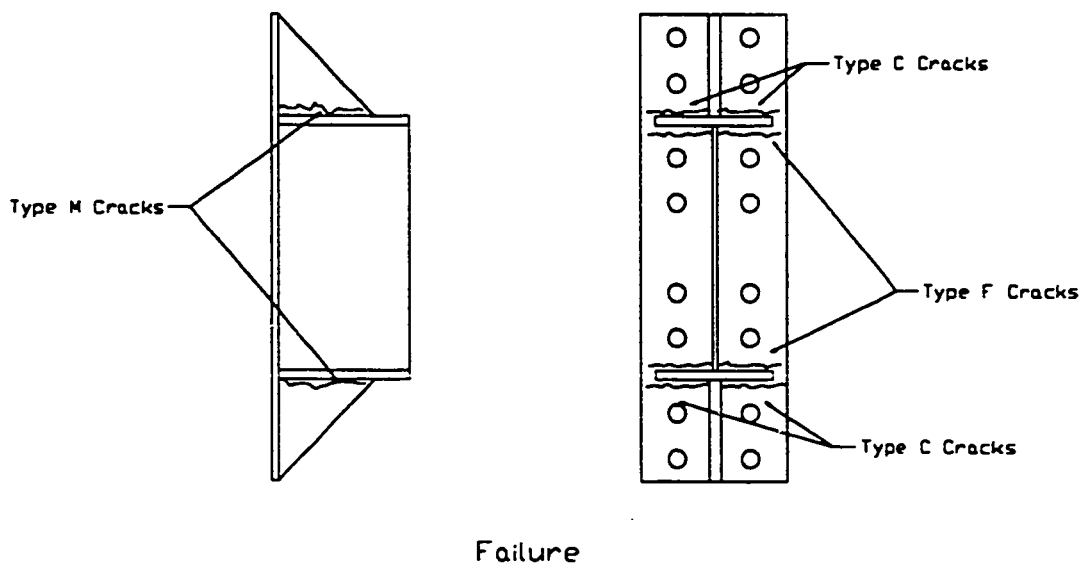
Figure 4.11 Crack Locations at Failure for Connection M-7
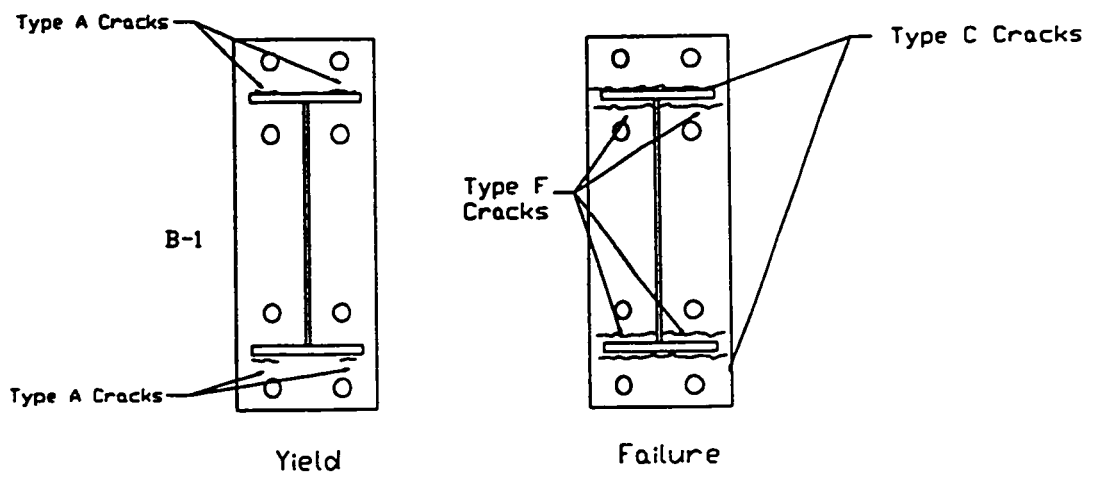
Figure 4.12 Crack Locations at Yield and Failure for Connection B-1
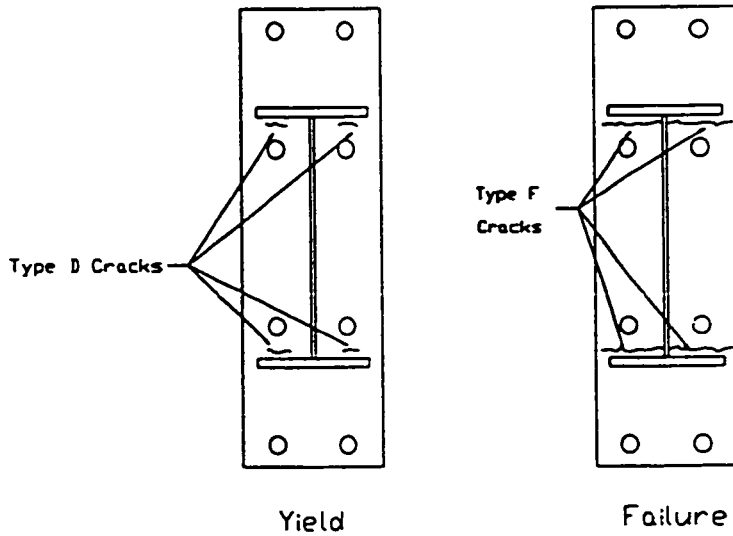
Figure 4.13 Crack Locations at Yield and Failure for Connection B-2

111
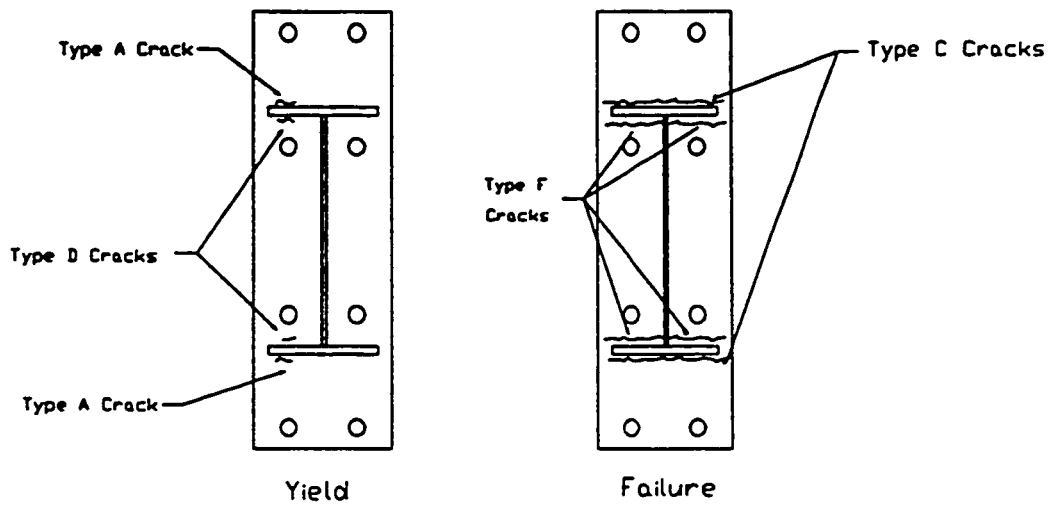
Figure 4.14 Crack Locations at Yield and Failure for Connection B-3
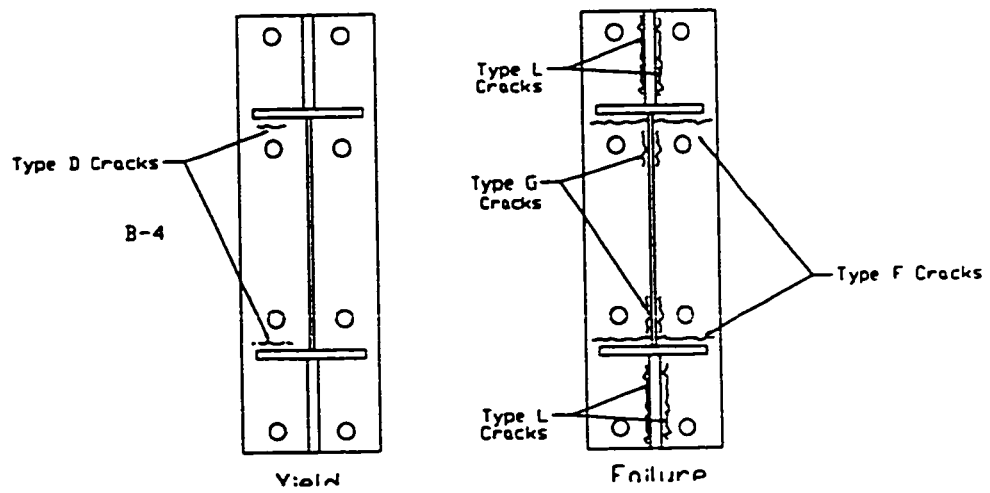
Figure 4.15 Crack Locations at Yield and Failure for Connection B-4

112

Figures 4.16 Type F and G cracks in connection M-1 (at failure)

Figures 4.17 A type C crack in connection B-1 (at failure)

113
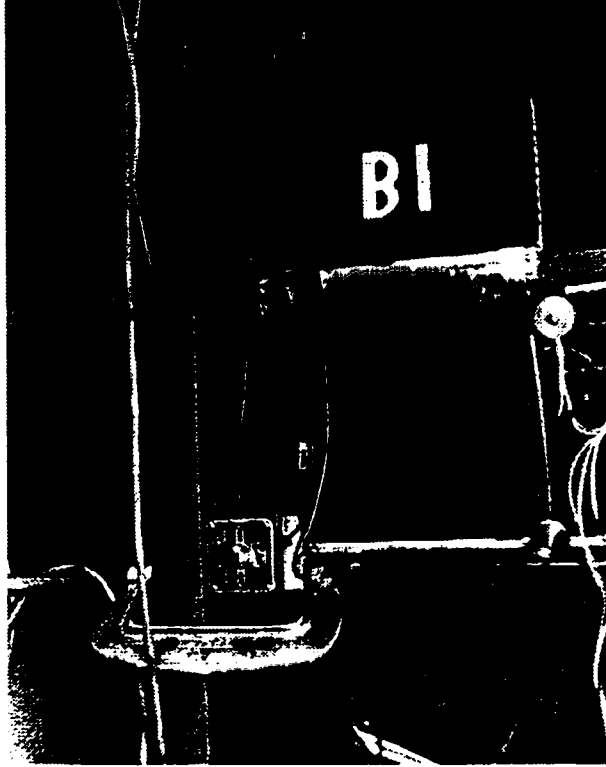
Figure 4.18 End plate deformation of connection B-1 (at failure)
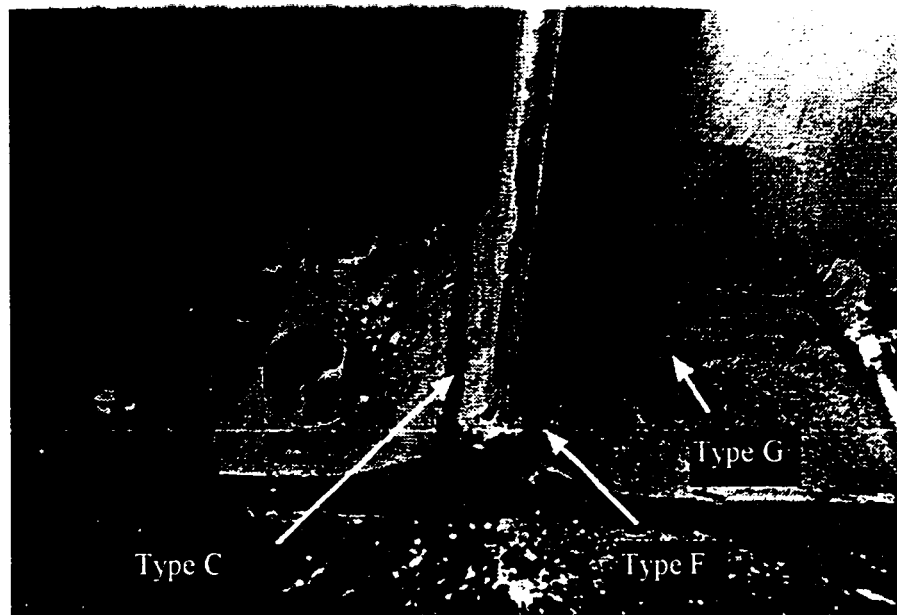
Figure 4.19 Cracks in end plate S-3 (at failure)

114

Figure 4.20 Cracks in end plate M-2 (at failure)

Figure 4.21 End plate deformation at failure in connection M-2

Figure 4.22 A type F crack in connection B-2 (at failure)
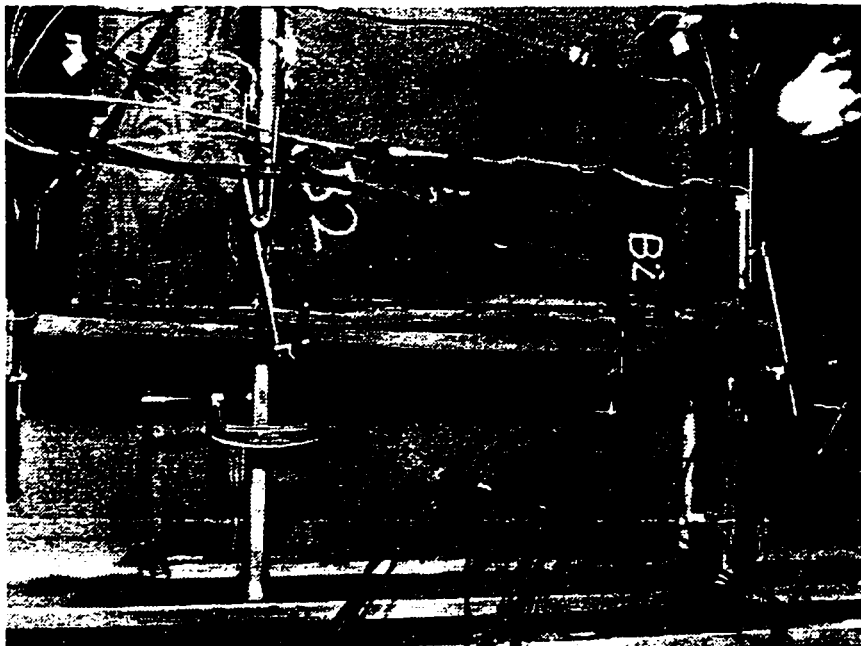
Figure 4.23 End plate deformation of connection B-2 (at failure)

Figure 4.24 Type C, F and G cracks in connection M-3 (at failure)
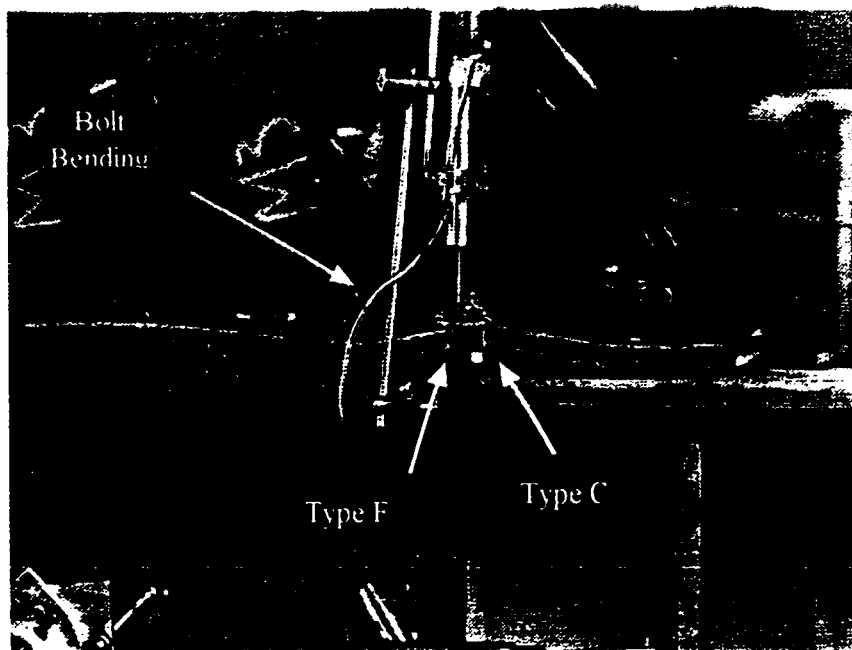
Figure 4.25 Type C and F cracks, extending through end plate M-3 (at failure)

Figure 4.26 End plate deformation of specimen B-3 after the rupture of an interior one inch A490 bolt
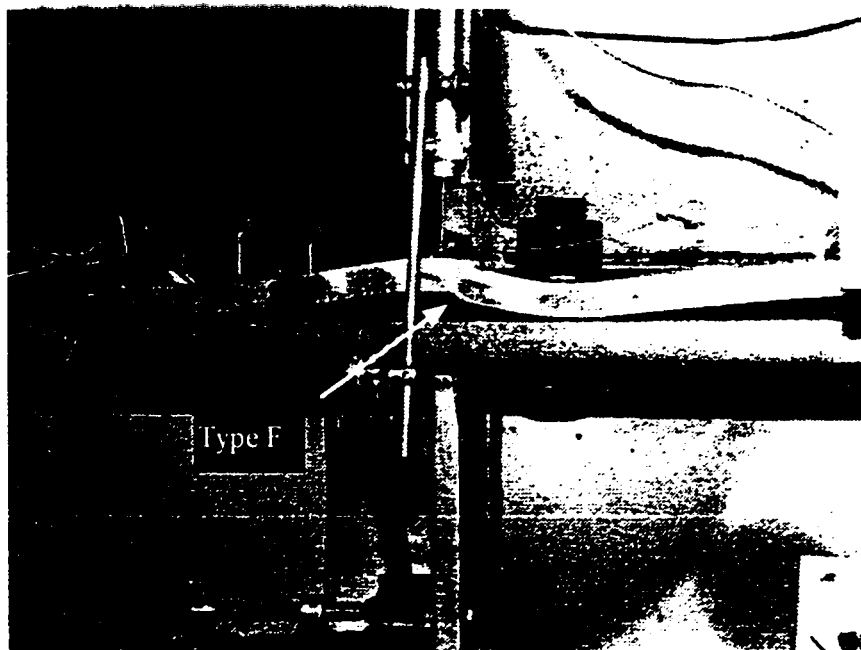
Figure 4.27 End plate deformation and propagation of a type F crack through the end plate in connection B-3 (at failure)

118

Figure 4.28 A type F crack in connection B-3 (at failure)
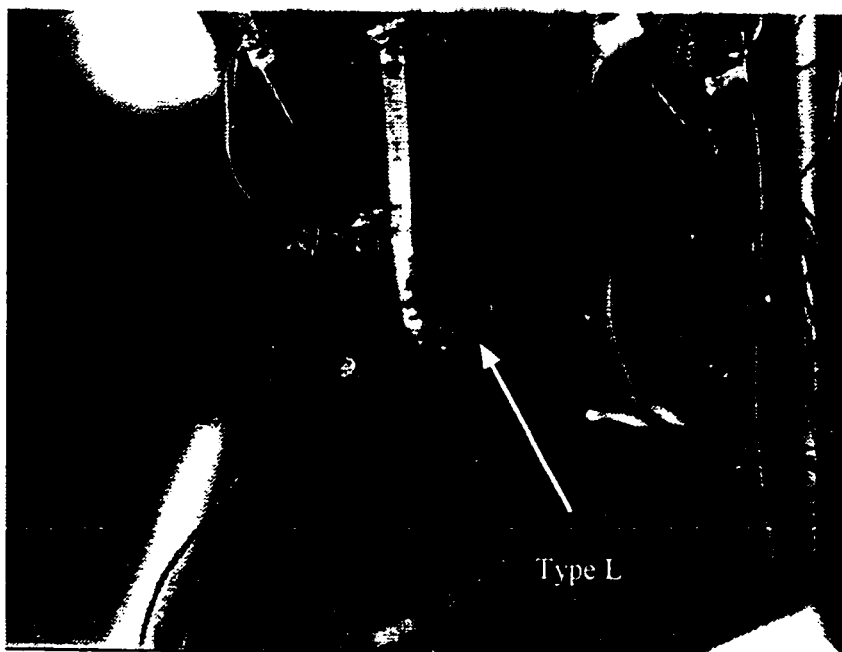
Figure 4.29 A type L crack in connection M-4 (at failure)

Figure 4.30 Type F and G cracks in connection M-4 (at failure)

Figure 4.31 A type L crack in connection B-4 (at failure)

120
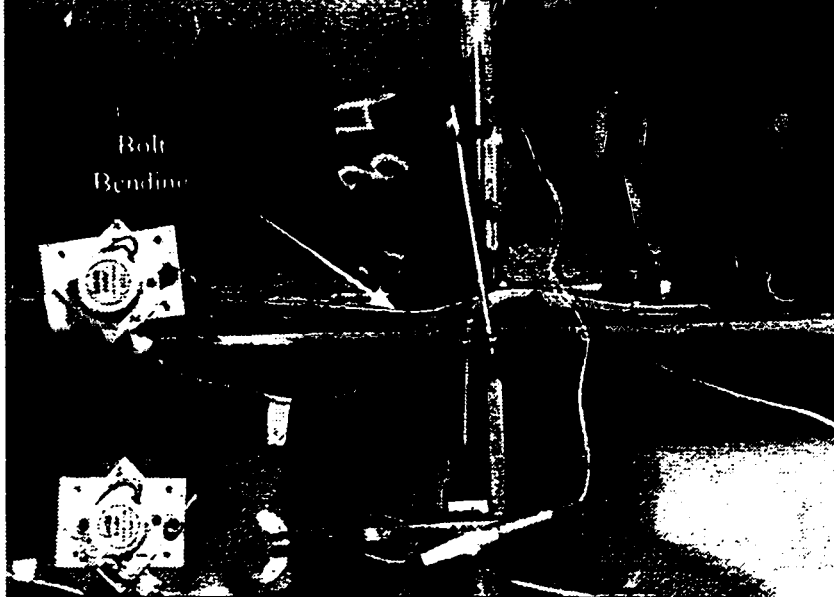
Figure 4.32 End plate deformation in specimen B-4 (at failure)
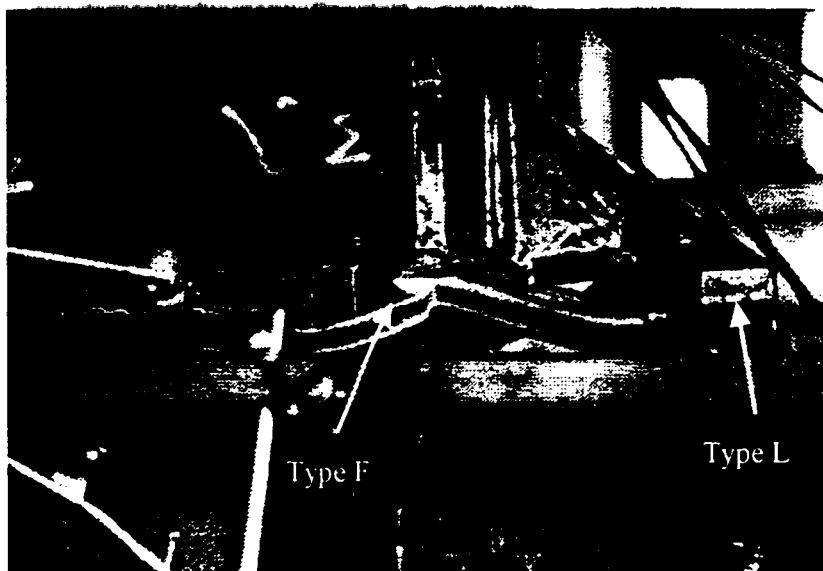
Figure 4.33 Large type F and L cracks in connection M-6 (at failure)

Figure 4.34 Type L cracks in connection M-6 (at failure)
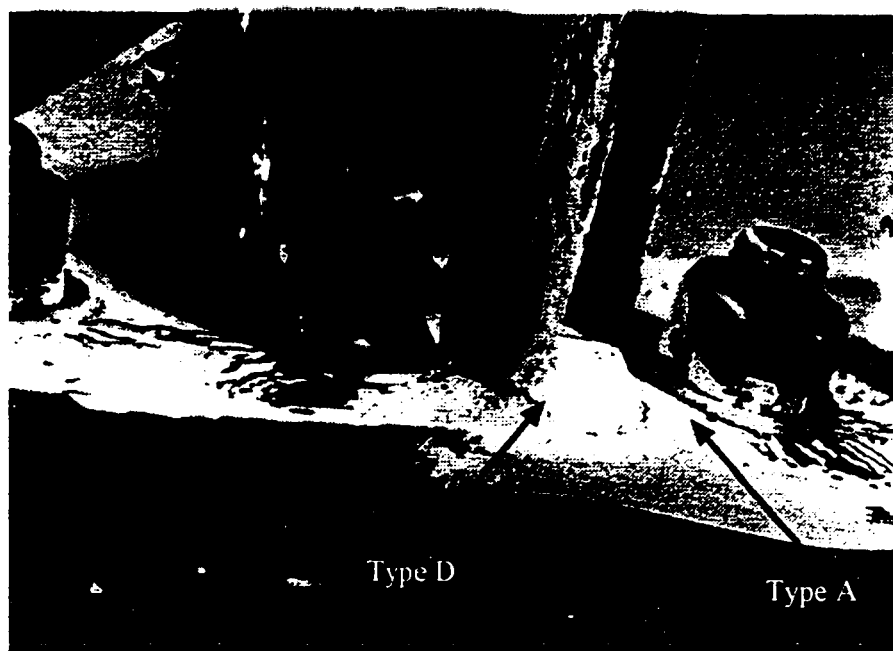
Figure 4.35 Type A and D cracks in connection M-5 (at failure)
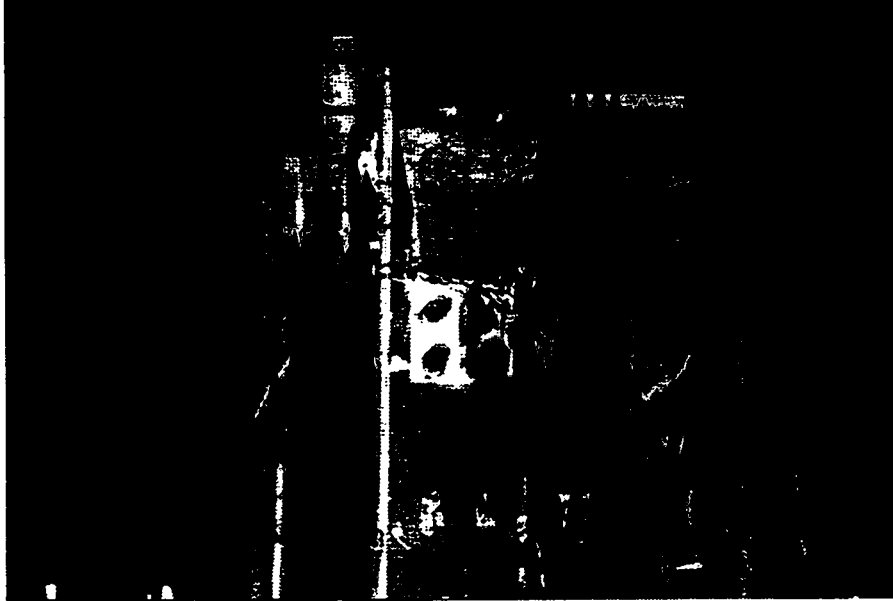
Figure 4.36 Out of plane buckling of the beam of specimen M-5
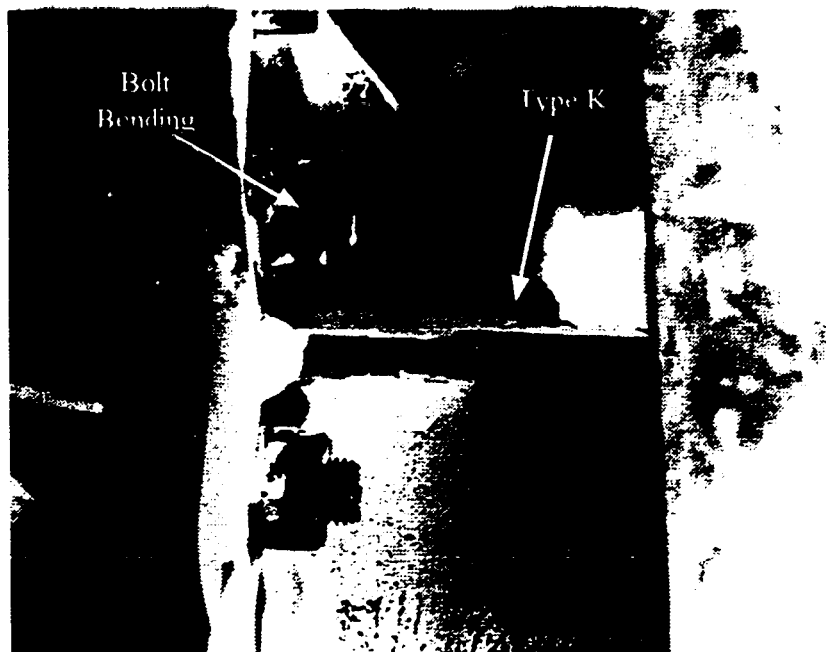
Figure 4.37 Type K cracks in connection M-7 (at failure)

Figure 4.38 A type C crack in connection S-1 (at failure)
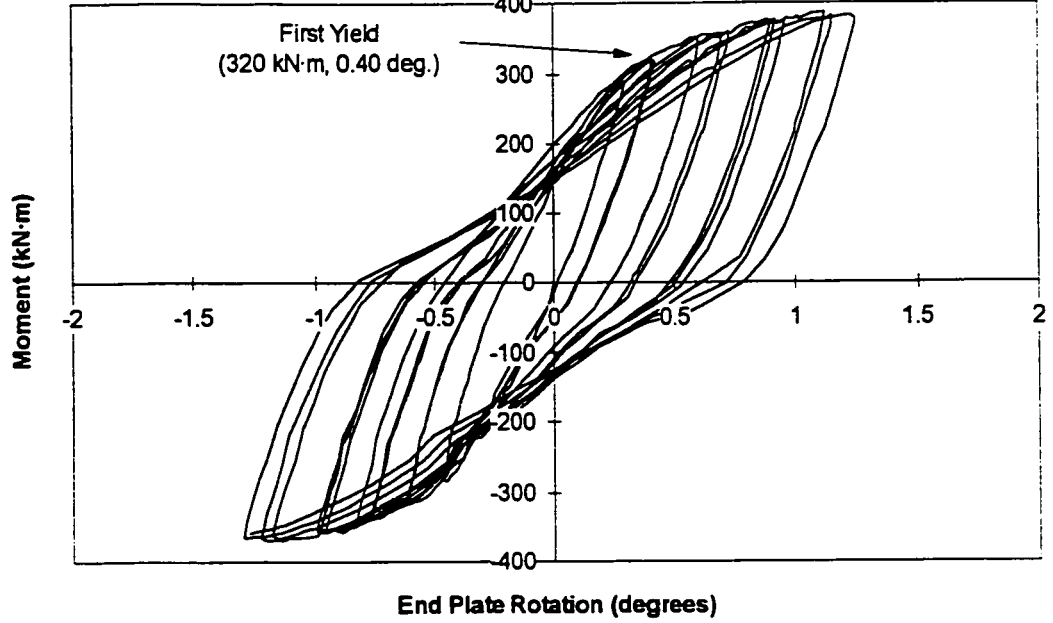
Figure 4.39 Moment versus End Plate Rotation for Connection S-1
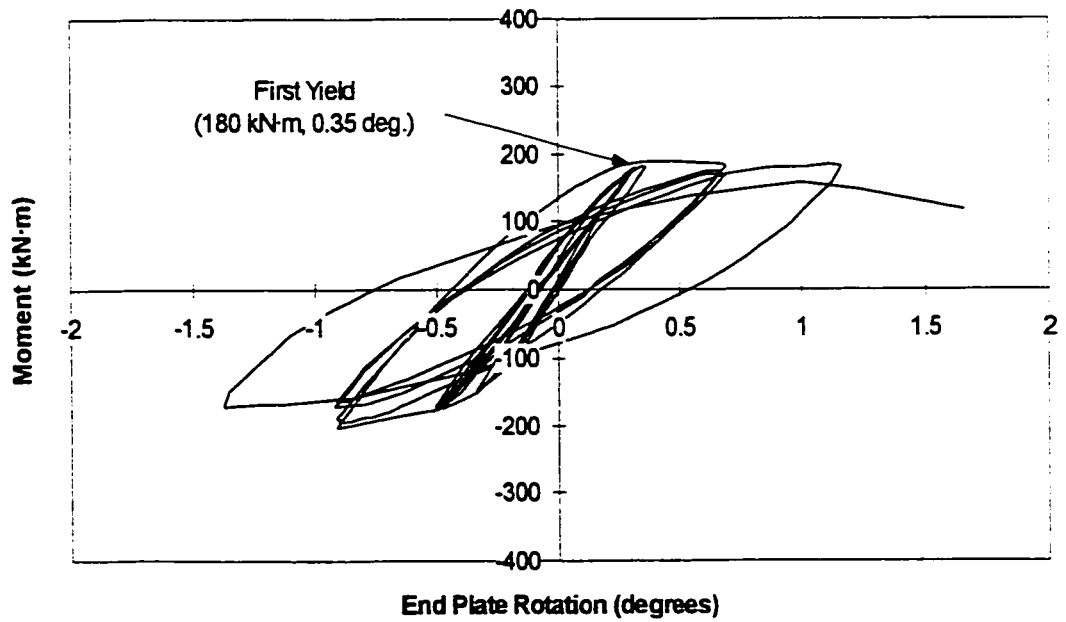
Figure 4.40 Moment versus End Plate Rotation for Connection S-2
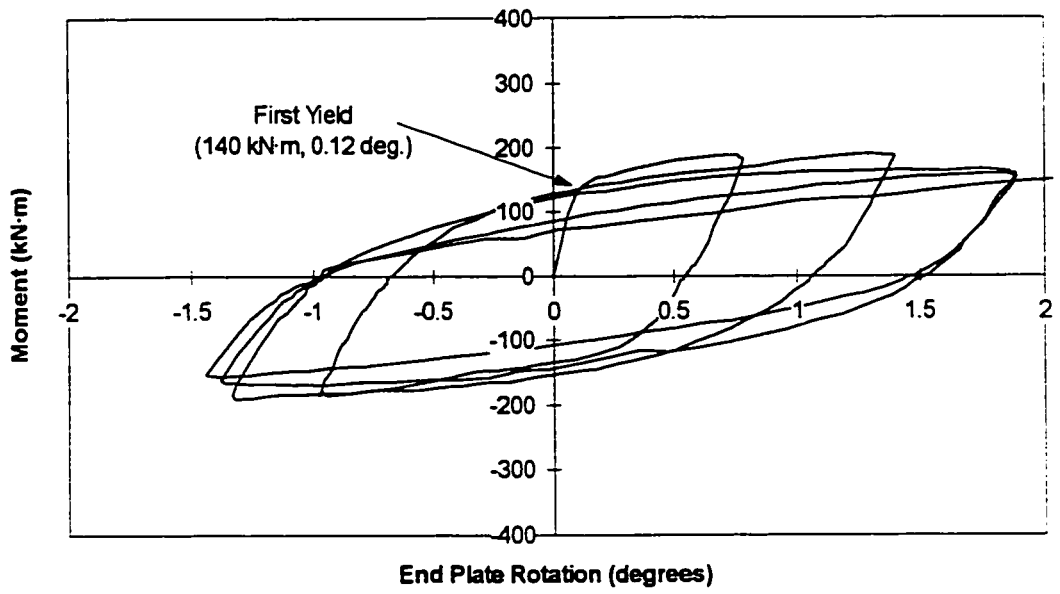
Figure 4.41 Moment versus End Plate Rotation for Connection S-3
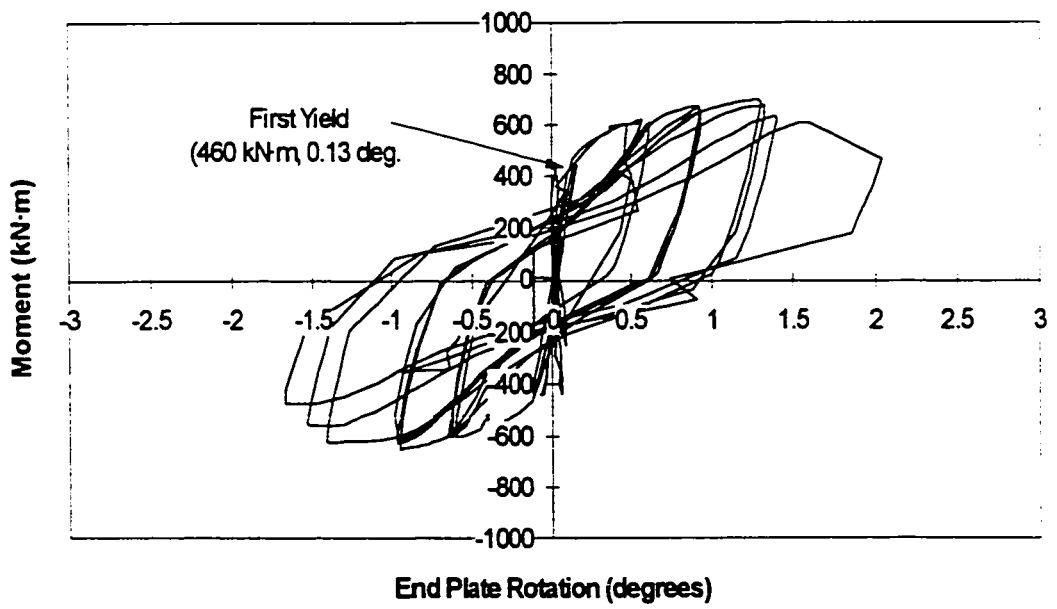
Figure 4.42 Moment versus End Plate Rotation for Connection M-1

126
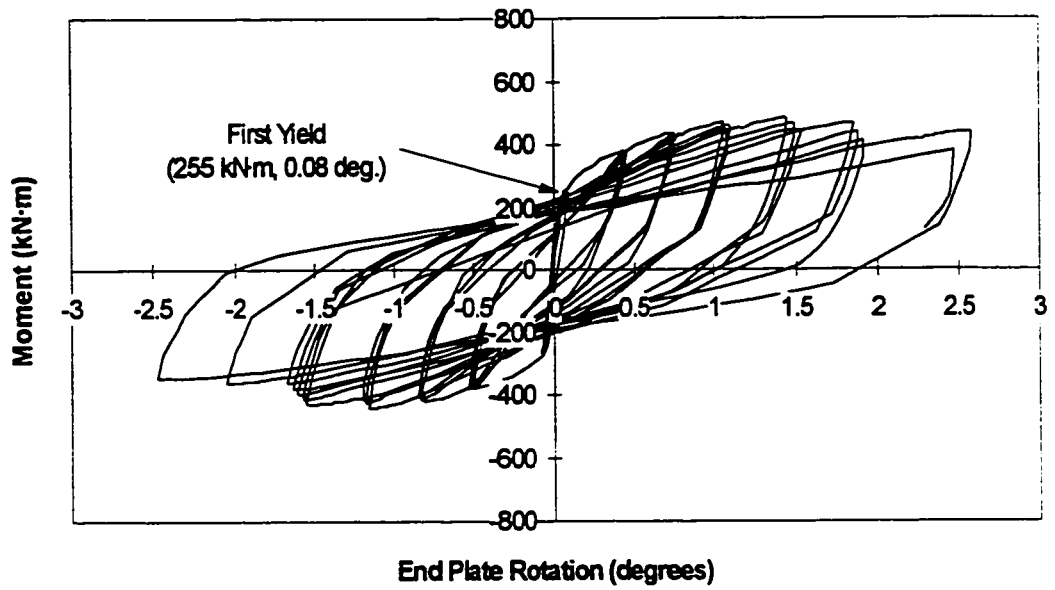
Figure 4.43 Moment versus End Plate Rotation for Connection M-2
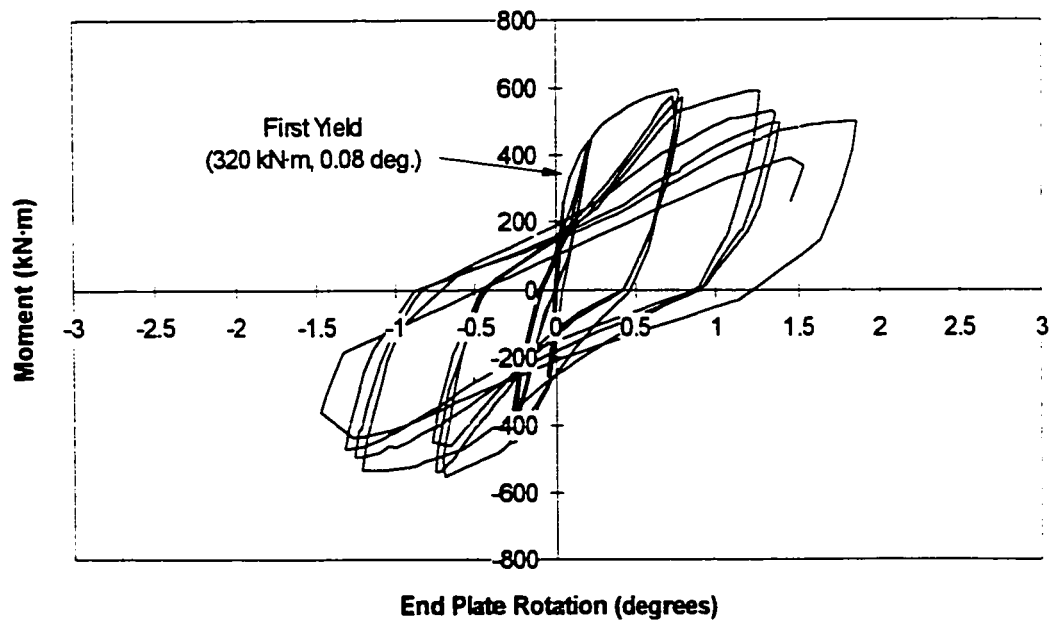
Figure 4.44 Moment versus End Plate Rotation for Connection M-3

127
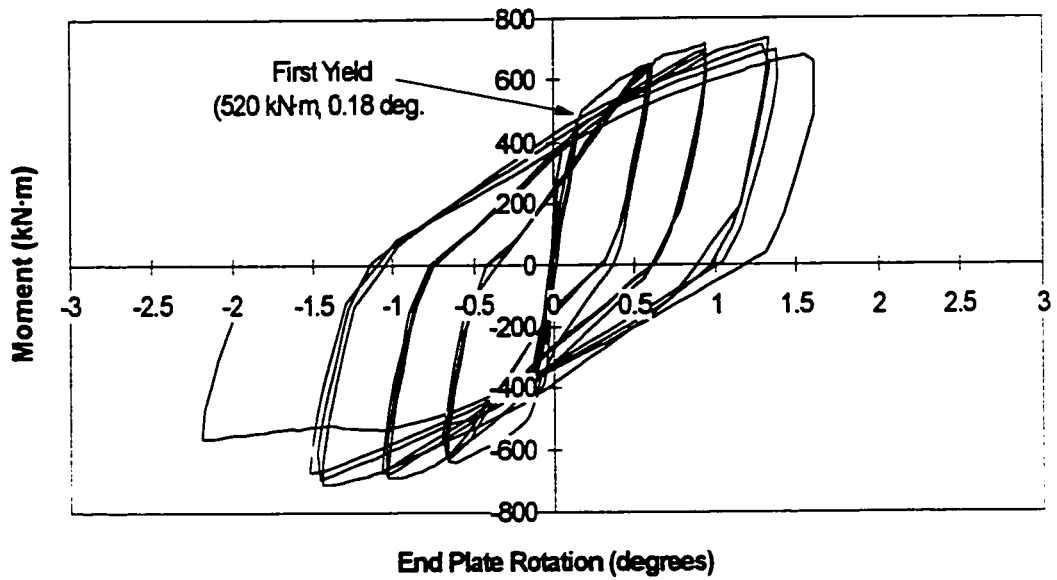
Figure 4.45 Moment versus End Plate Rotation for Connection M-4
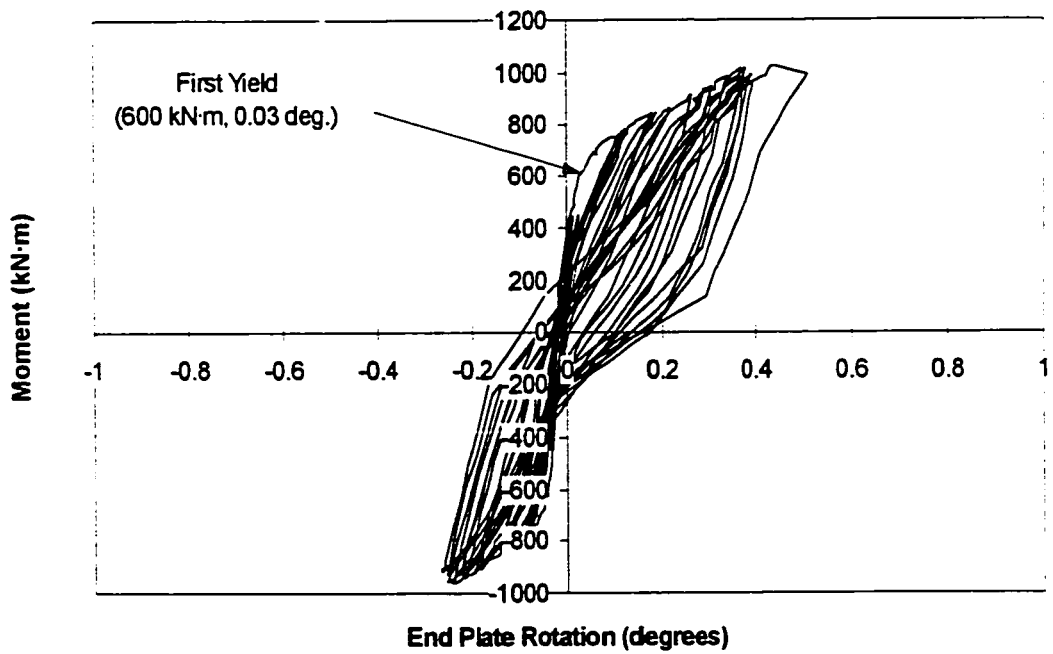
Figure 4.46 Moment versus End Plate Rotation for Connection M-5
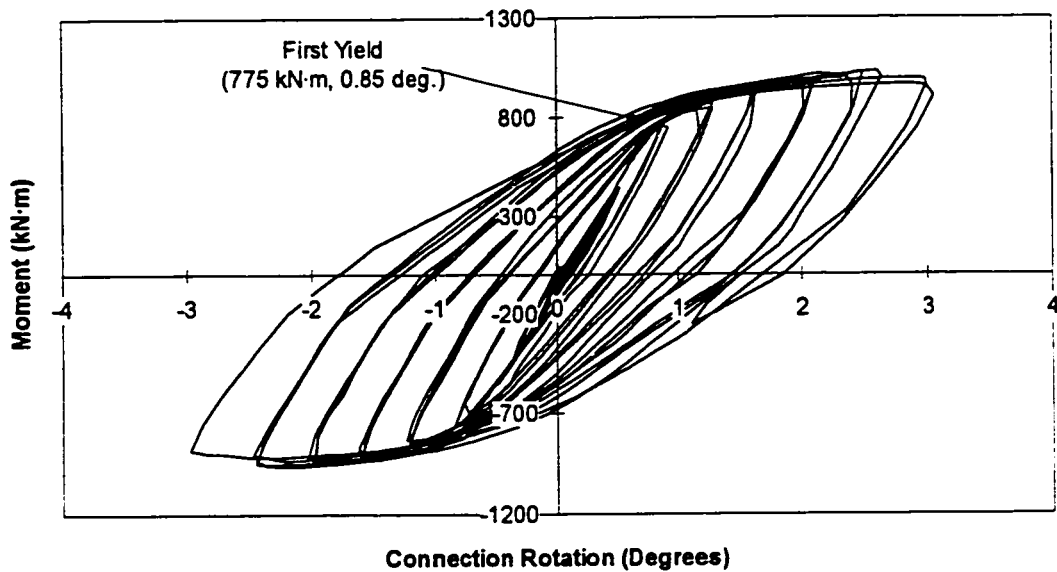
Figure 4.47 Moment versus Connection Rotation for Connection M-5
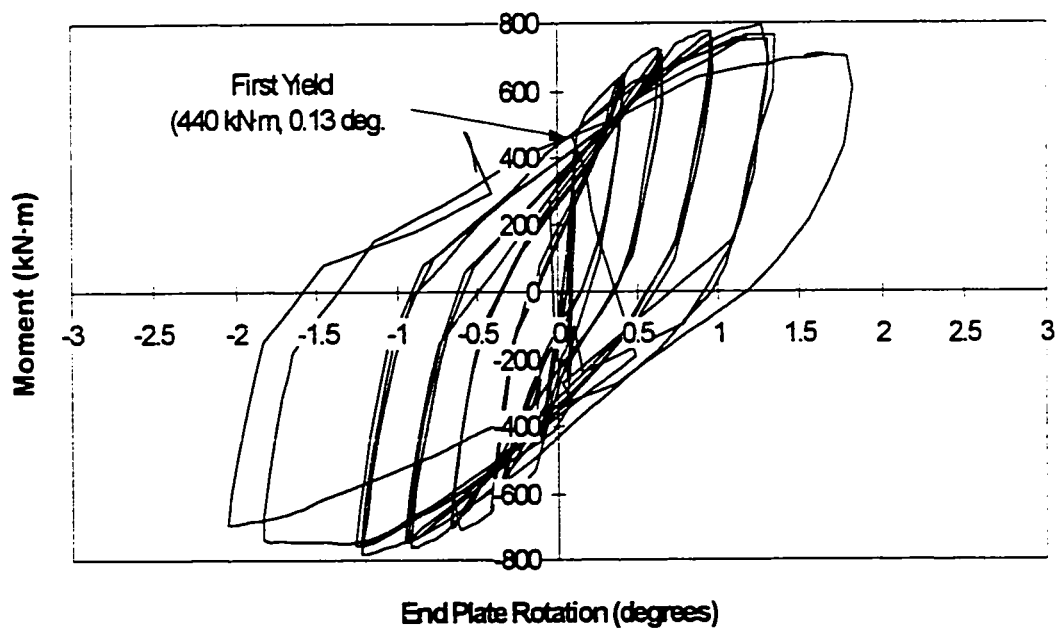
Figure 4.48 Moment versus End Plate Rotation for Connection M-6
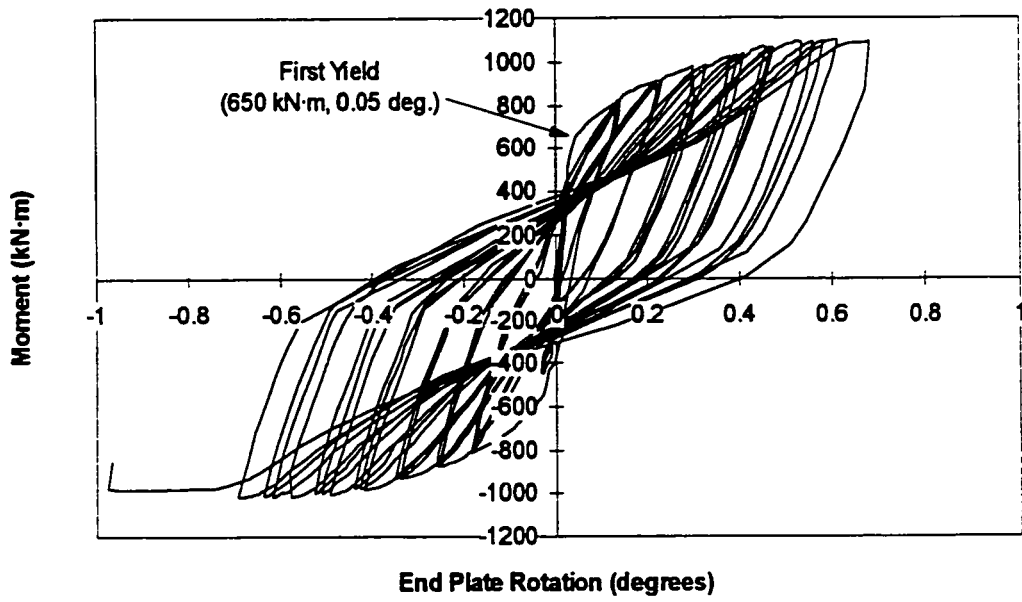
Figure 4.49 Moment versus End Plate Rotation for Connection M-7
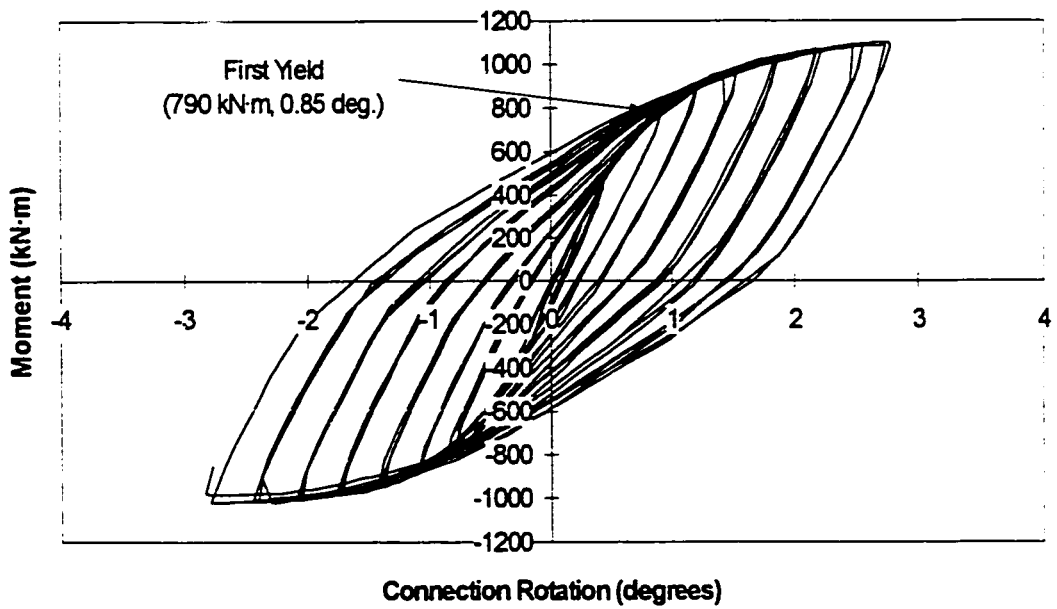
Figure 4.50 Moment versus Connection Rotation for Connection M-7
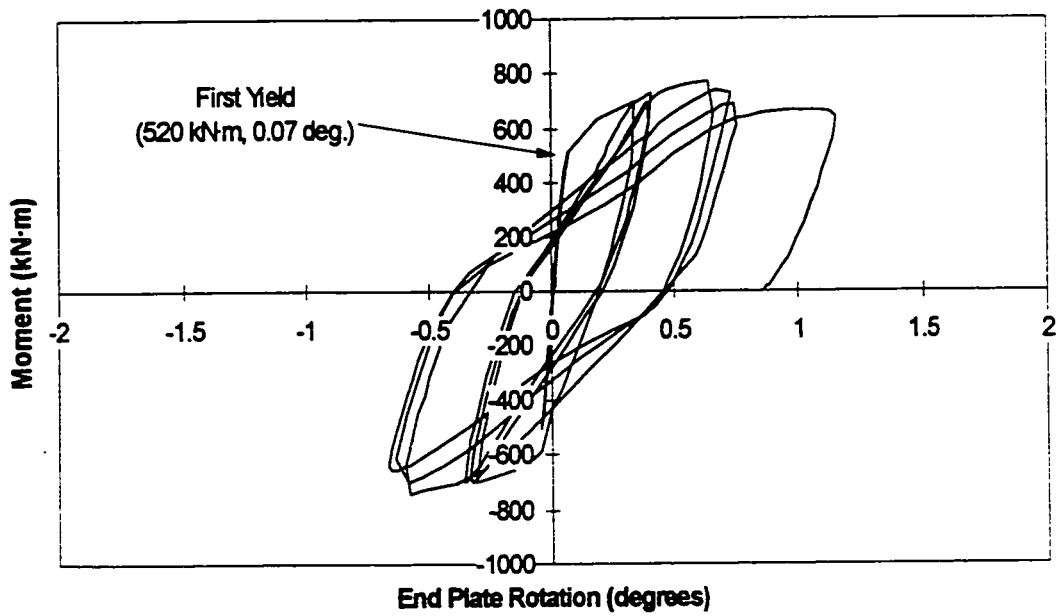
Figure 4.51 Moment versus End Plate Rotation for Connection B-1
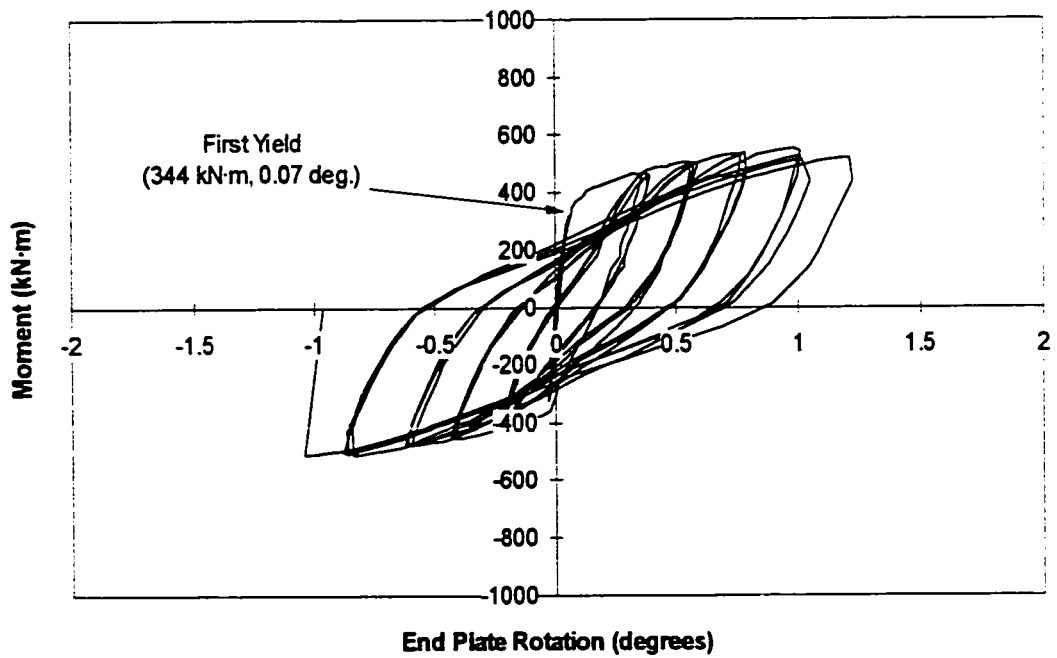
Figure 4.52 Moment versus End Plate Rotation for Connection B-2

First Yield
(385 kN·m, 0.03 deg.)
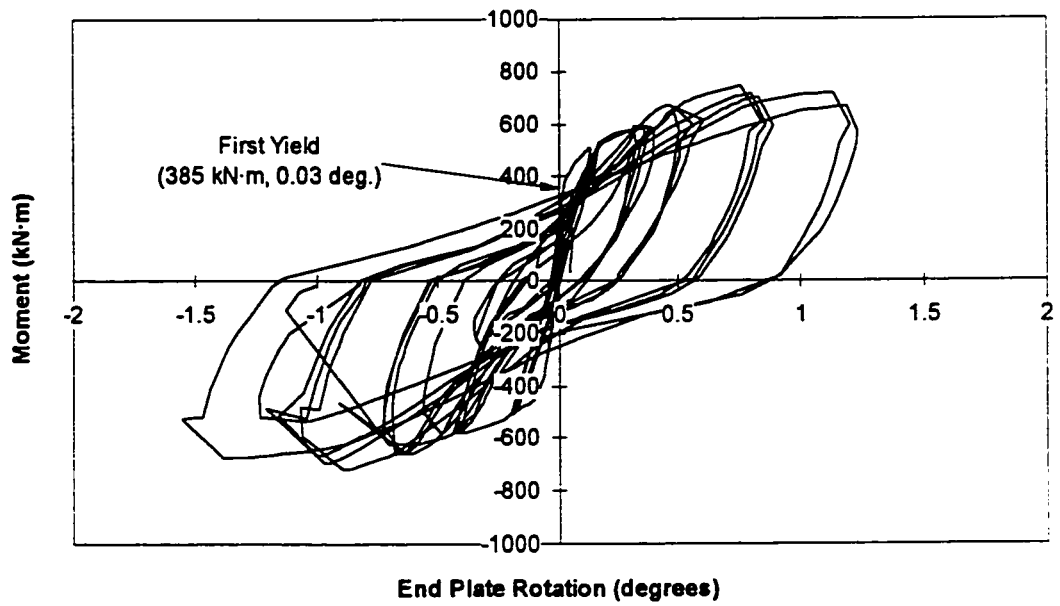
Figure 4.53 Moment versus End Plate Rotation for Connection B-3

First Yield
(520 kN·m, 0.07 deg.)
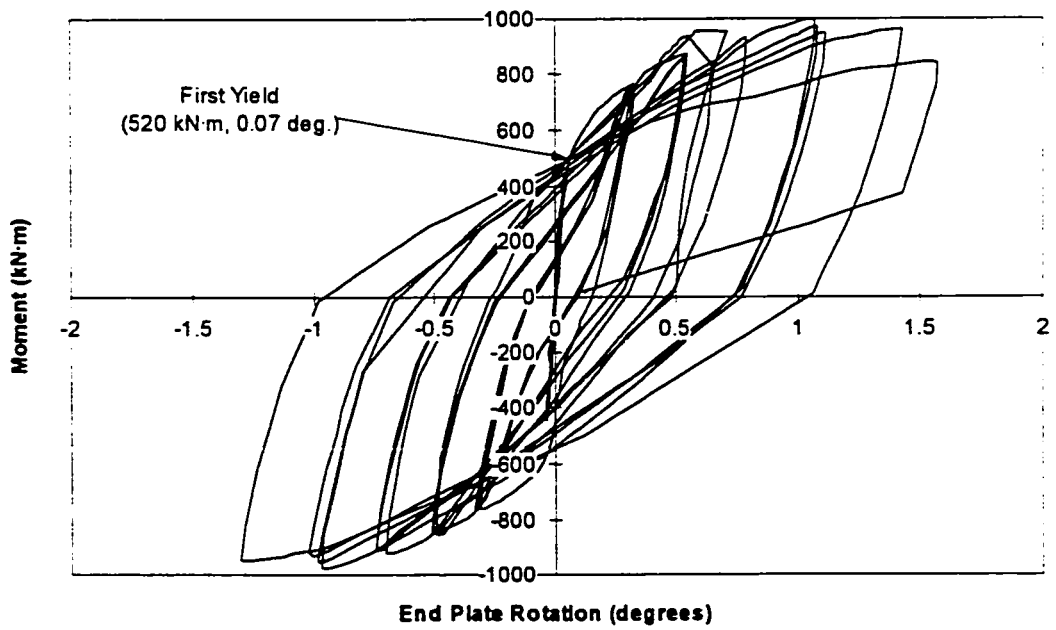
Figure 4.54 Moment versus End Plate Rotation for Connection B-4

132
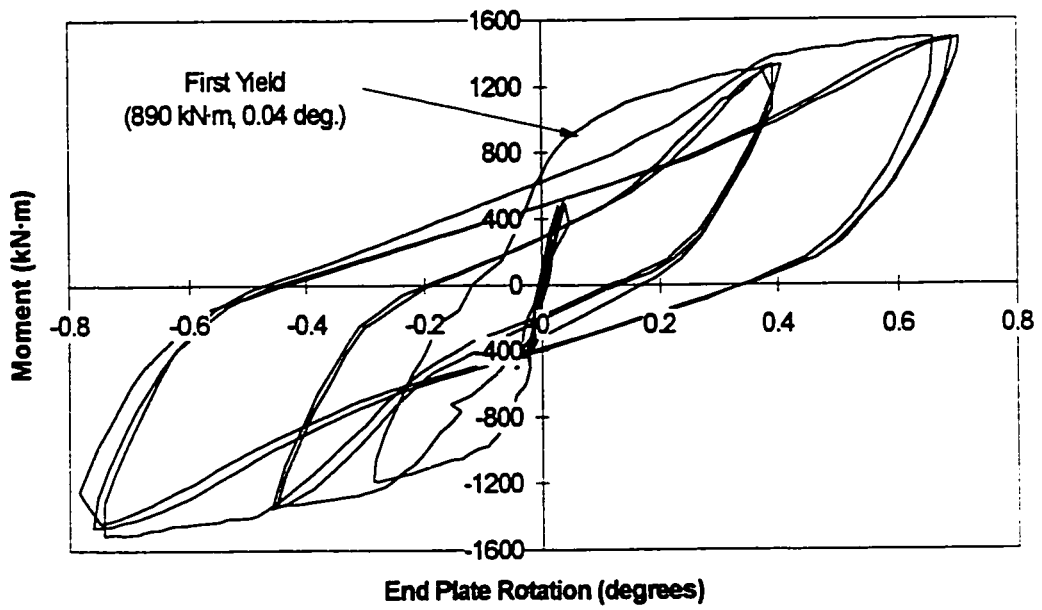
Figure 4.55 Moment versus End Plate Rotation for Connection B-5
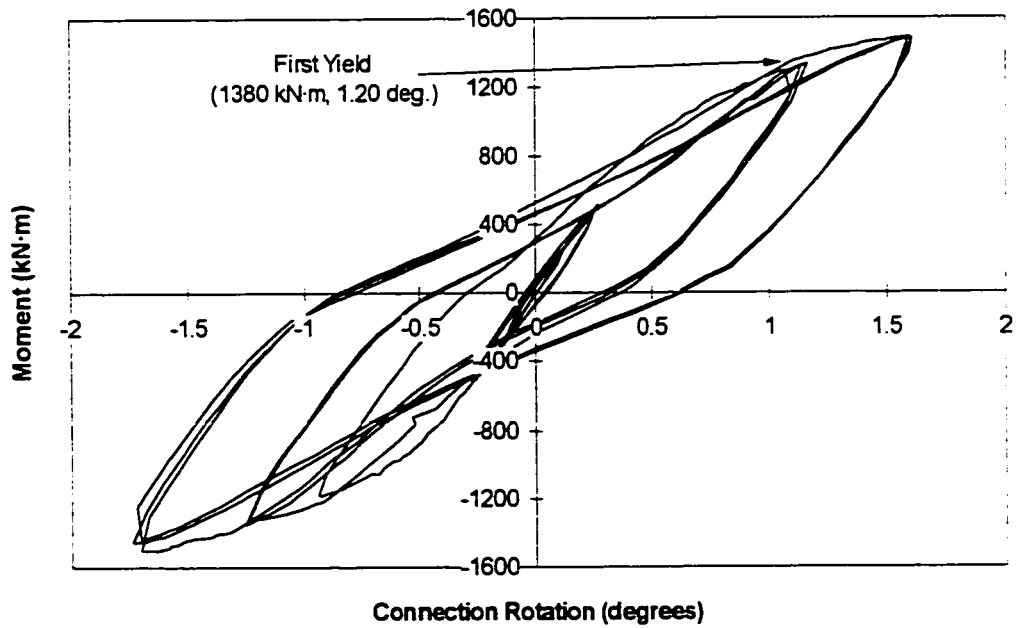
Figure 4.56 Moment versus Connection Rotation for Connection B-5

133
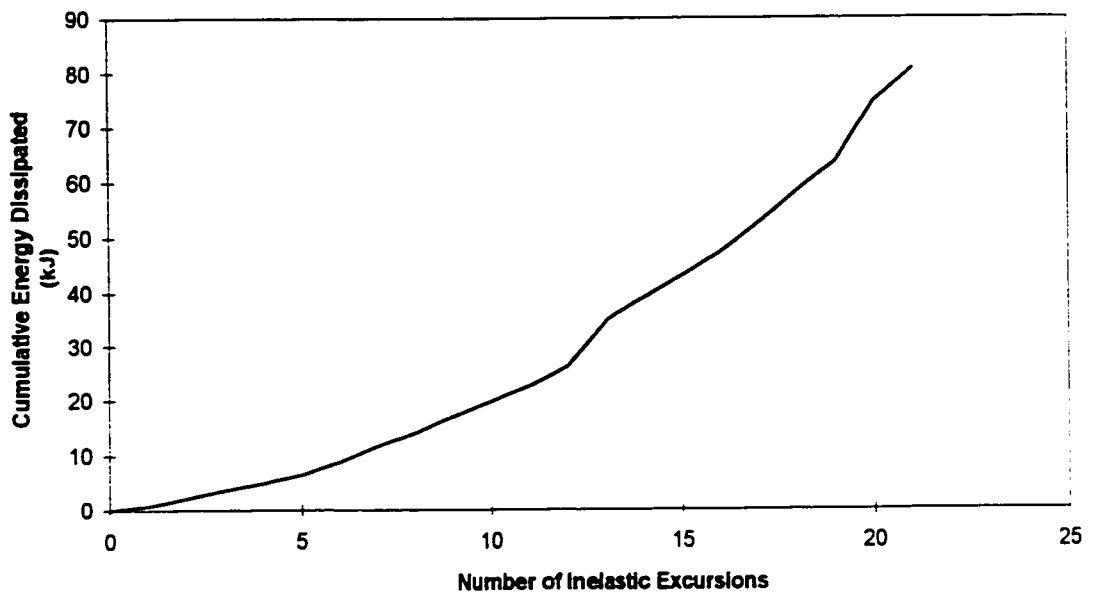
Figure 4.57 End Plate Energy Dissipation in Connection S-1
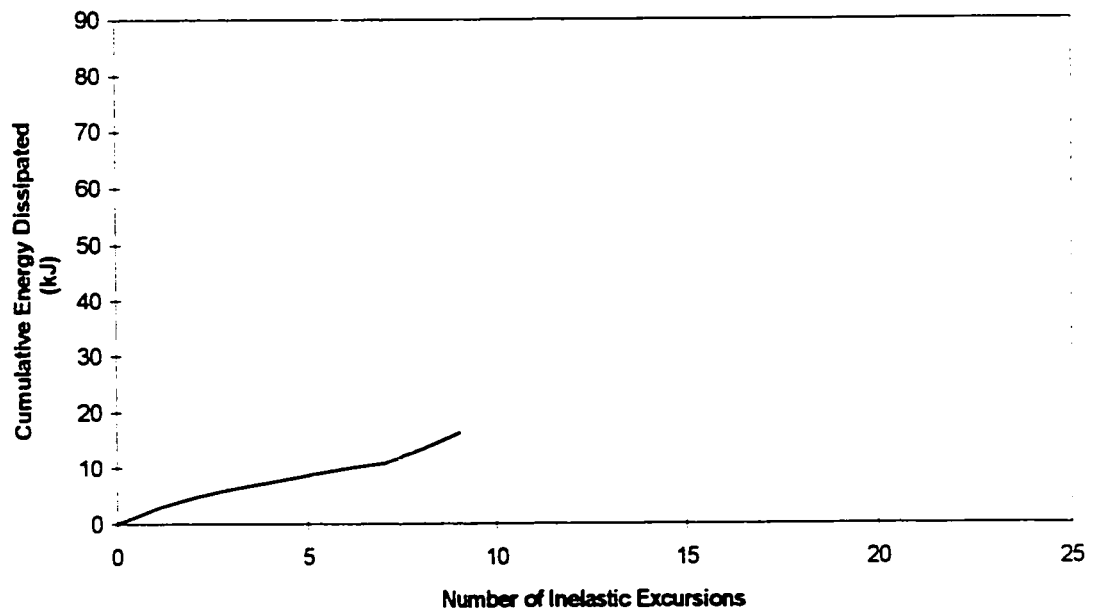
Figure 4.58 End Plate Energy Dissipation in Connection S-2

134
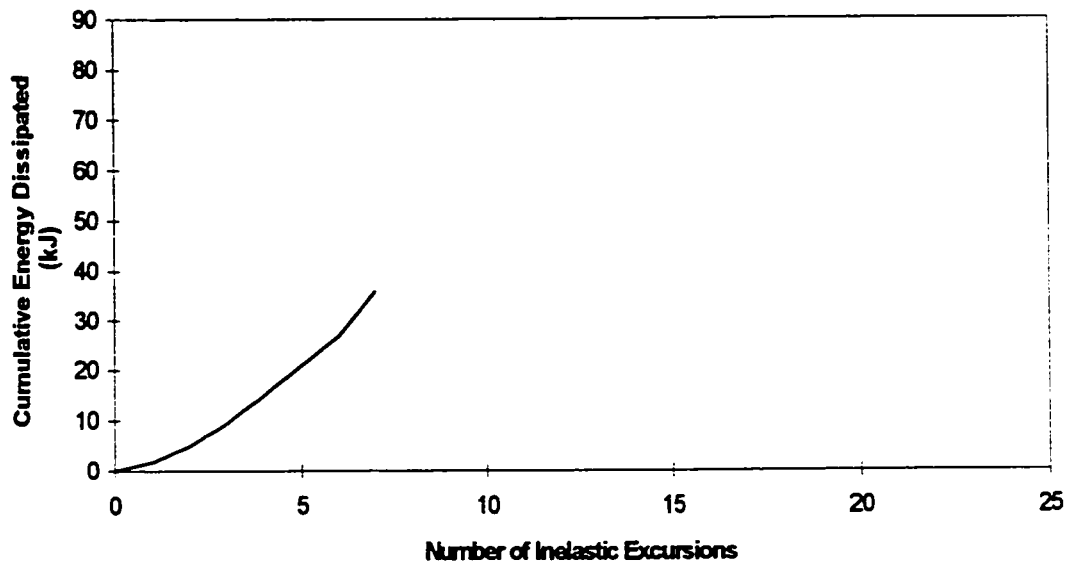
Figure 4.59 End Plate Energy Dissipation in Connection S-3
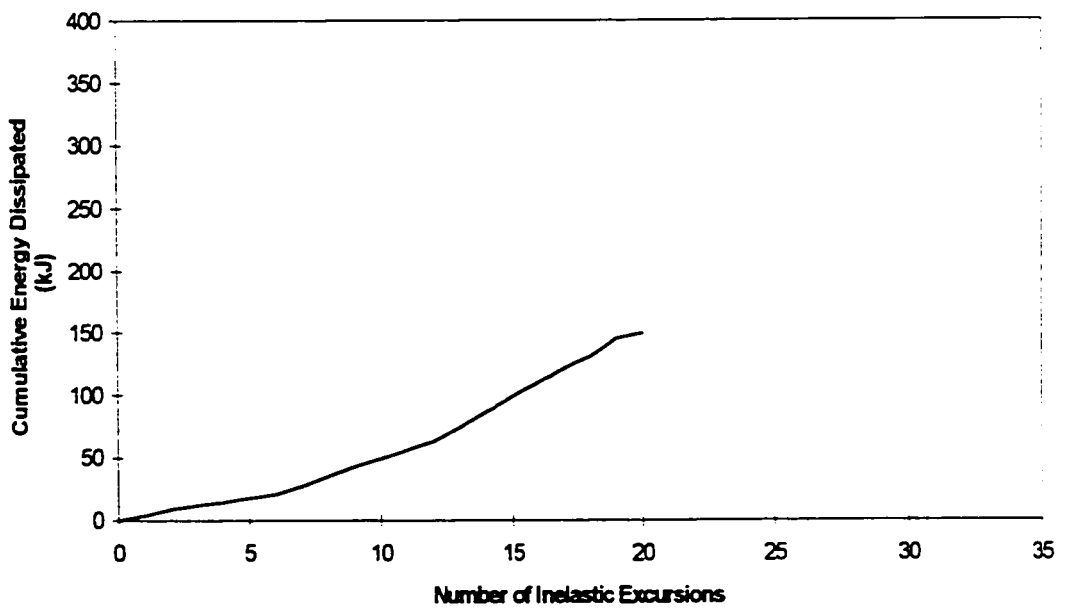
Figure 4.60 End Plate Energy Dissipation in Connection M-1

135
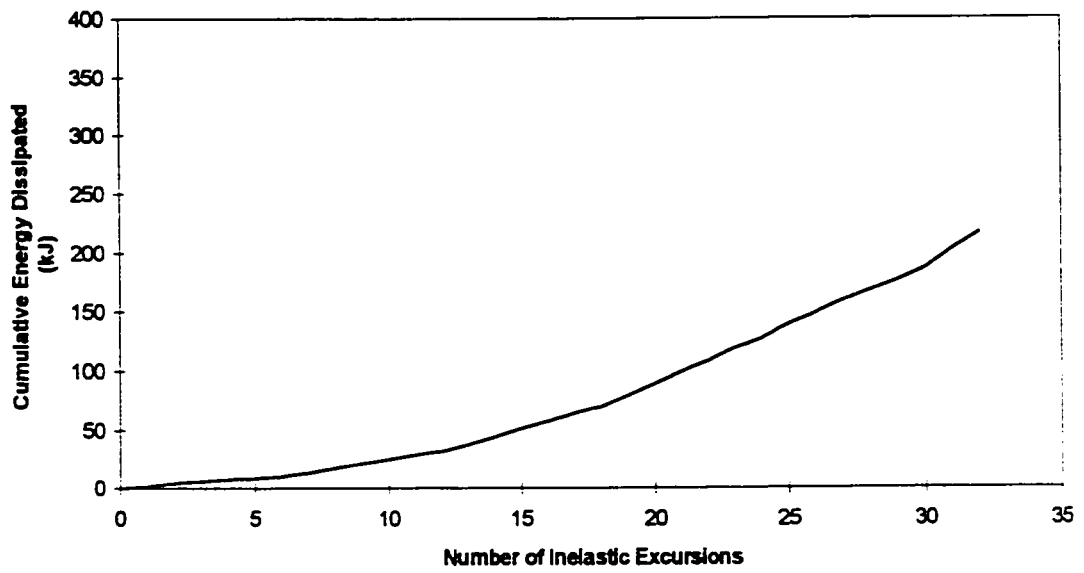
Figure 4.61 End Plate Energy Dissipation in Connection M-2
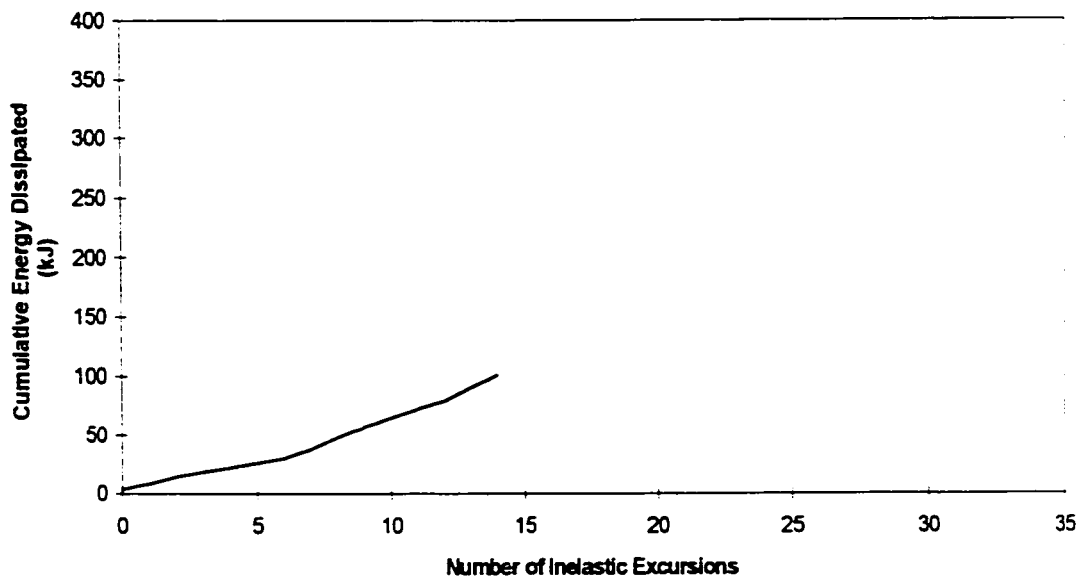
Figure 4.62 End Plate Energy Dissipation in Connection M-3
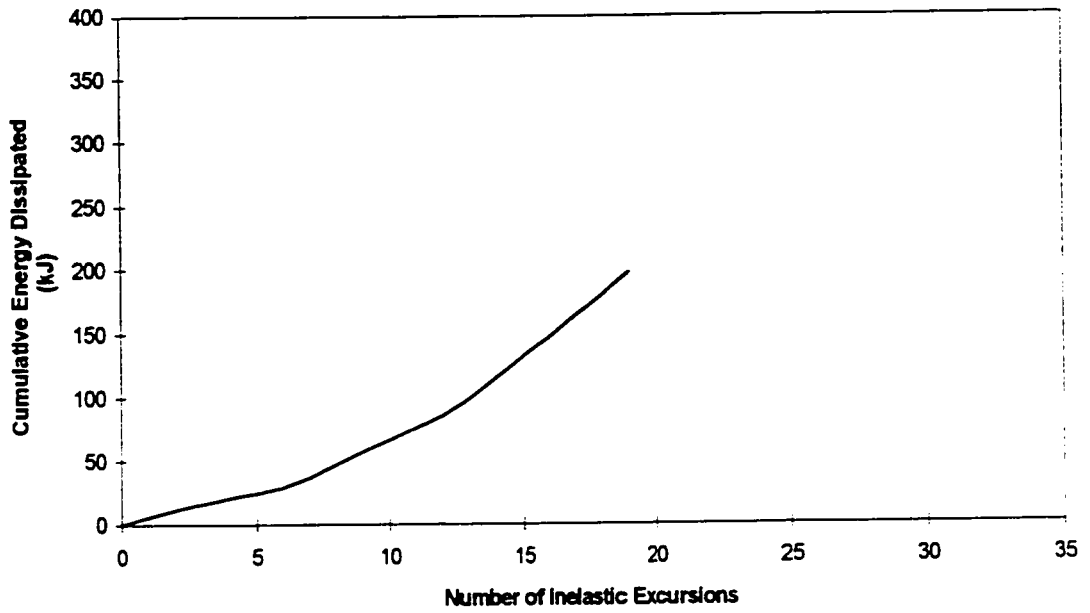
Figure 4.63 End Plate Energy Dissipation in Connection M-4
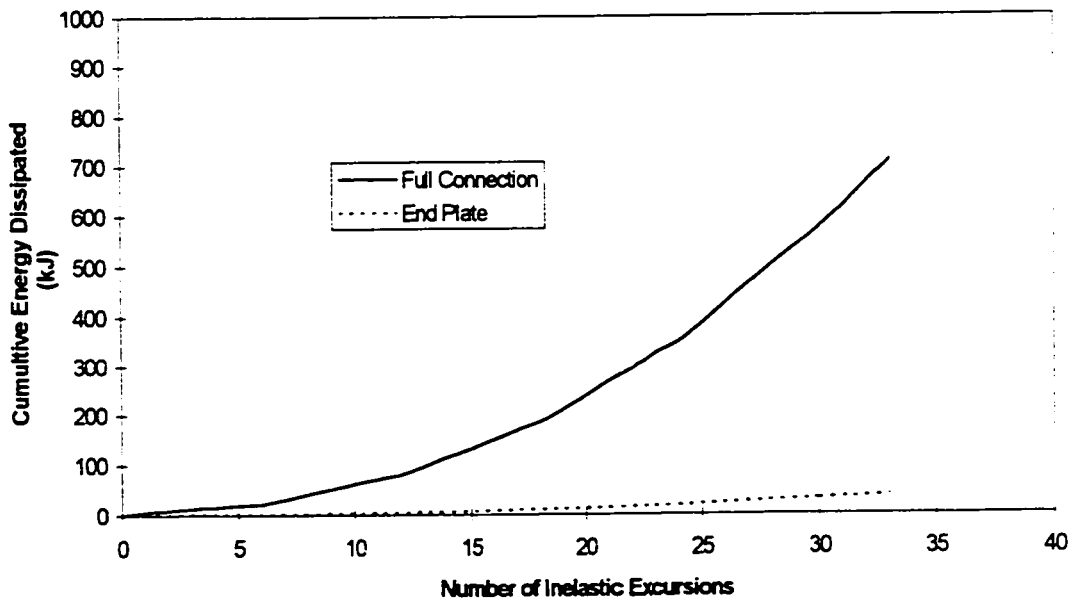
Figure 4.64 End Plate and Full Connection Energy Dissipation in Connection M-5
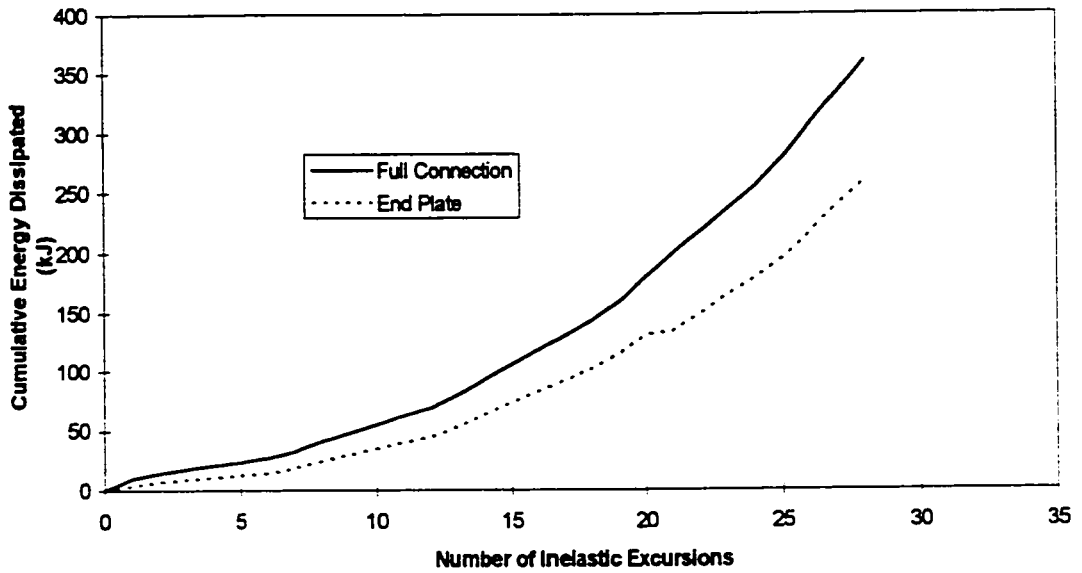
Figure 4.65 End Plate and Full Connection Energy Dissipation in Connection M-6
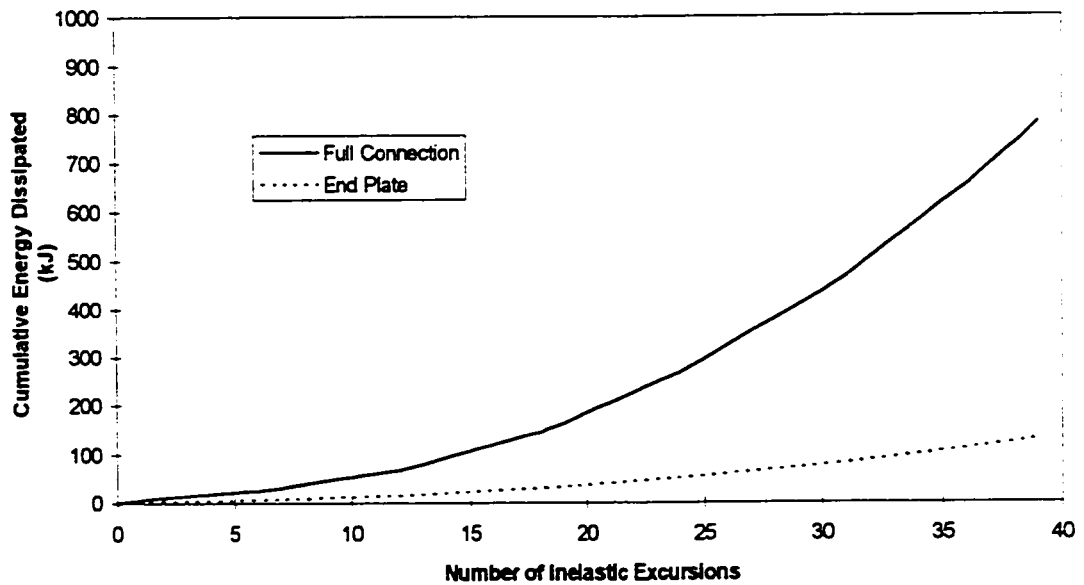
Figure 4.66 End Plate and Full Connection Energy Dissipation in Connection M-7
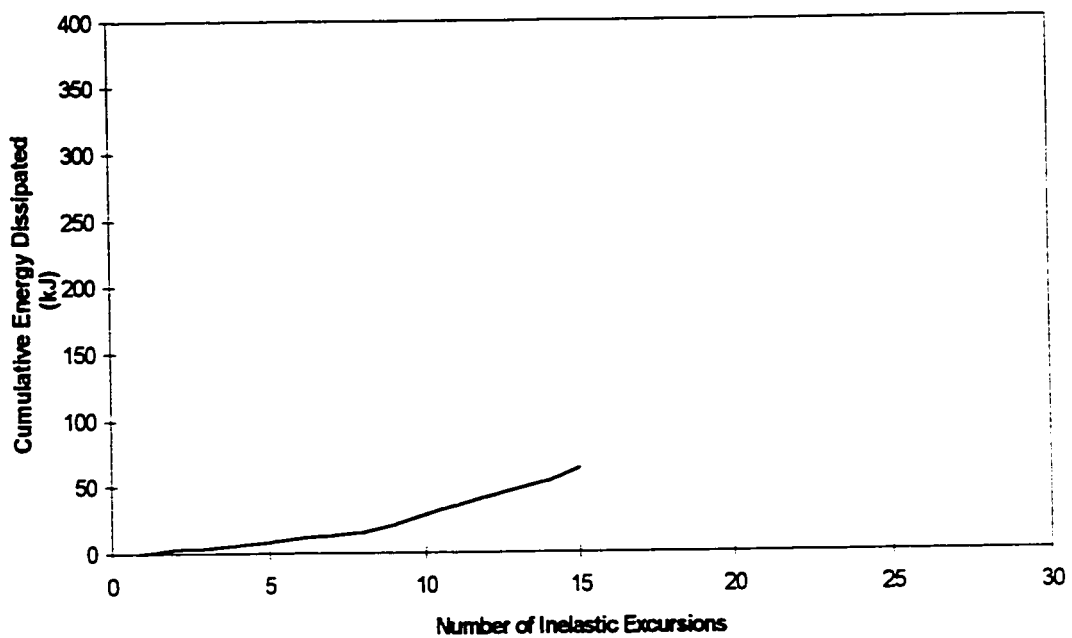
Figure 4.67 End Plate Energy Dissipation in Connection B-1
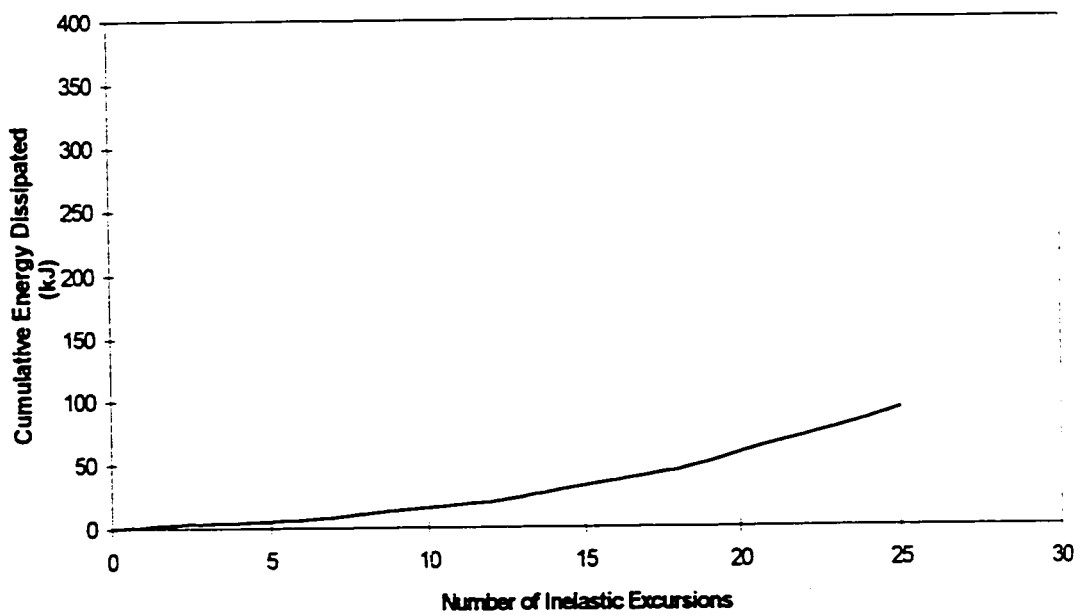
Figure 4.68 End Plate Energy Dissipation in Connection B-2

139
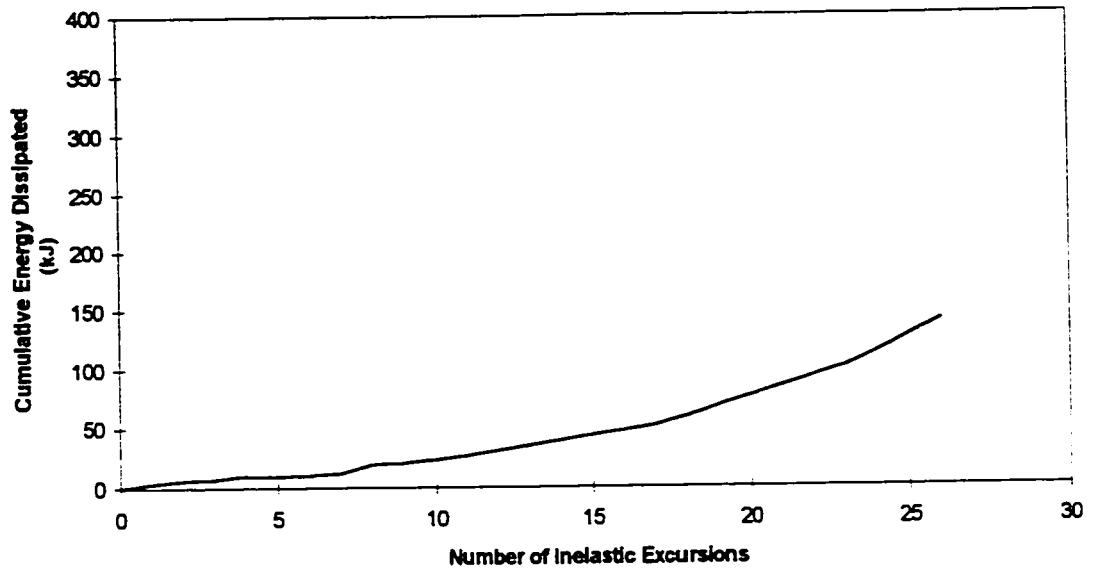
Figure 4.69 End Plate Dissipation Energy Dissipation in Connection B-3
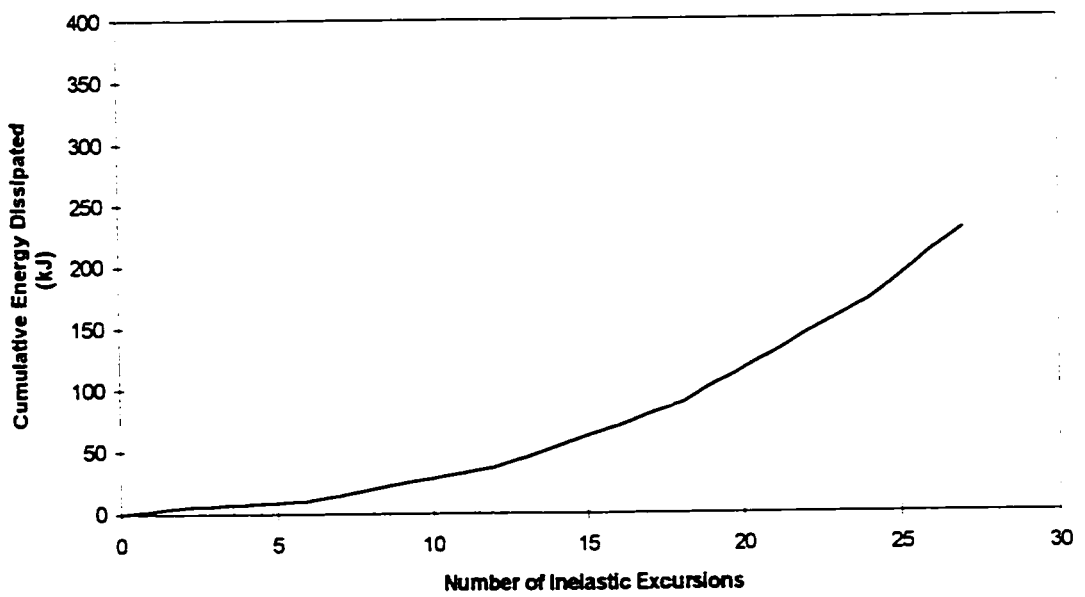
Figure 4.70 End Plate Energy Dissipation in Connection B-4
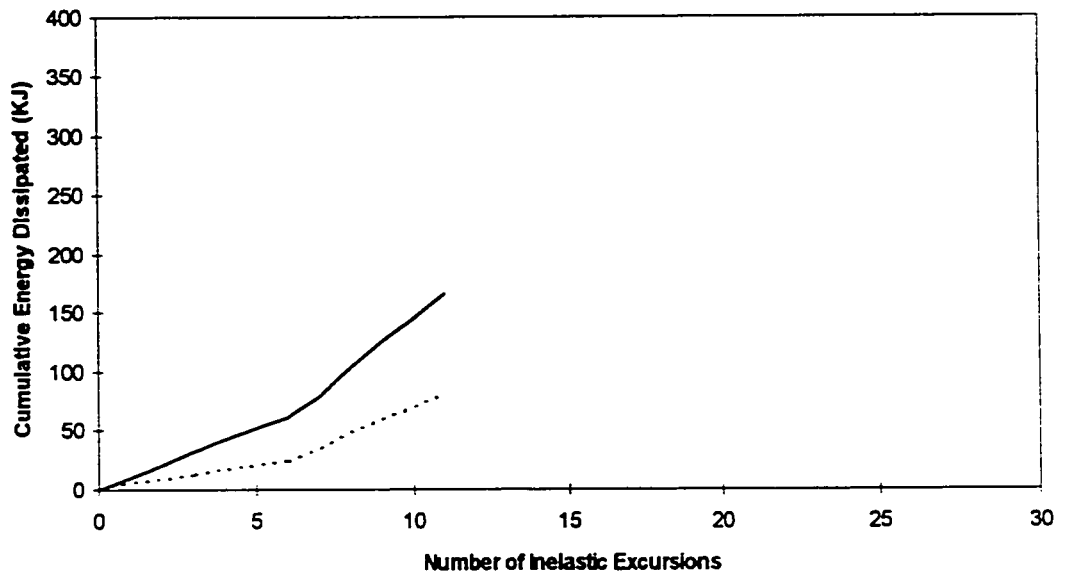
Figure 4.71 Full Connection Energy Dissipation in Connection B-5
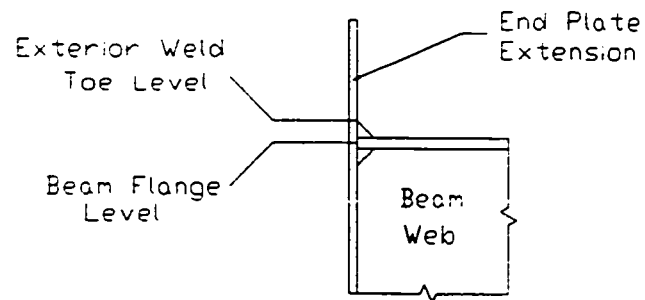
Figure 4.72 Locations of Maximum End Plate Lift Off from Column Flange

5. Comparison of Test Results

This chapter presents a comparison of the U of A test results with other test results and with predictions from a number of analytical models.

5.1 Comparison with Other Test Programs

The concentration of this research program on end plate failure, as opposed to overall connection failure, makes it difficult to compare the results of this test program with those of others. Three aspects of the test results will be used as a basis of comparison with other test programs, namely, moment versus rotation, cumulative energy dissipation and general observations.

5.1.1 Moment versus Rotation

The moment versus rotation curve characterizes the behaviour of moment connections and can therefore be used as a basis of comparison. However, because of the focus of the U of A test program on the behaviour of the end plate alone, as opposed to the behaviour of the entire connection, a comparison is not straightforward. Many earlier test programs on extended end plate moment connections investigated the behaviour of the entire connection or, at the very least, the behaviour of connections where plastic deformation occurred in more than one component of the connection. Obviously this affects the moment versus rotation behaviour of the connection.

Another problem with test result comparison with earlier programs, is that monotonic loading rather than cyclic loading was used in many of the earlier test programs. Connections under monotonic loading are able to undergo more rotation than connections under cyclic loading. As well, in earlier test programs load versus beam tip displacement curves were frequently reported rather than moment versus rotation curves. Beam tip displacement curves reflect both the elastic and inelastic deformations in the beam, column, connection and test frame. Unless duly accounted for this may lead to wide variation in the recorded test results.

geometry between test programs, such as beam flange thickness, beam depth and end plate thickness, leads to variation in the number of parameters to which differing performance may be attributed. The more parameters are varied the harder it is to compare test results.

Different inelastic loading patterns between test programs are another problem. The inelastic loading pattern is the number of cycles performed in each load block, and the increase in displacement or rotation between each load block. The larger the number of cycles in each load block the larger the cracks become before progressing to the next load block. Further crack growth may reduce the maximum obtainable moment and/or decrease the moment-rotation ratio. Therefore, it is difficult to compare test results obtained with different loading histories.

Other problems with test result comparison are the variation of yield strengths between specimens and the variation of yield designation between test programs. With different yield strengths, geometrically identical connections could have different performances. Because of different yield designations in test programs, two connections that performed identically could be reported differently. Different yield designations between test programs also affect the loading pattern of the connections, as load blocks beyond yield are increased based on some percentage of the yield beam tip displacement.

For these reasons, a comparison of the moment versus rotation curves of the U of A test program is made only with the test results obtained by Ghobarah et al. (1992). The research of Ghobarah et al. (1992) was chosen because of the similarity in connection size, plate thickness and presentation of test results, to the U of A test program. However, even with the noted similarities, comparison of the test results between the two test programs is not straightforward. Ghobarah et al. performed four tests to investigate the performance of the column panel zone in extended end plate moment connections under cyclic loading.

Two specimens from the U of A test program were chosen for direct comparison with test results from the McMaster University test program (Ghobarah et al., 1992). Specimens M-1 and M-4 were chosen because of their similarity with specimens CC-1 and CC-3 from the Ghobarah et al. test program. Connections CC-1 and M-1 were both designed with a tight bolt configuration without extension stiffeners. Connections CC-3 and M-4, although with different bolt configurations (tight and relaxed) were both designed with extension stiffeners and thinner end plates than connections CC-1 and M-1, respectively. Table 5.1 summarizes some of the characteristics of the four connections. Table 5.2 lists the observed moments and connection rotations of specimens CC-1, CC-3, M-1 and M-4. The reported rotations are attributed to the deformation of the connection of the specimen (end plate, bolts, extension stiffeners, panel zone and column flange). The yield and maximum moments observed in specimen M-1 were larger than the corresponding values observed for specimen CC-1 (460 kN·m and 700 kN·m for M-1 versus 385 kN·m and 535 kN·m for CC-1). The yield rotations, maximum rotations and rotation ductilities of CC-1 and M-1 cannot be compared because a moment versus connection rotation curve was not presented for specimen CC-1. The yield and maximum moments observed in specimen M-4 were larger than in specimen CC-3 (510 kN·m and 740 kN·m for connection M-4 versus 370 kN·m and 550 kN·m for connection CC-3). These higher values may be attributed to the heavier beam used in the U of A test program. The yield and maximum connection rotations observed in specimen M-4 were larger than the corresponding values in specimen CC-3 (0.2 and 1.35 degrees versus 0.09 and 0.5 degree). Both test programs showed that extension stiffeners enable the use of thinner end plates and perform well under cyclic loading.

There are many reasons that may explain the discrepancies in moments and connection rotations between the two test programs. The main problem was connection design. Despite some similarities the connection details were different. The beam size, column size, end plate dimensions, bolt size, bolt layout and stiffener size were different. The connections used in the Ghobarah et al. (1992) test program

were designed using a different philosophy than the specimens used in the U of A test program. Connections CC-1 and CC-3 were designed to fail both the column panel zone and the beam whereas connections M-1 and M-4 were designed to fail the end plate alone. The lower connection rotations observed in specimen CC-3 may be attributed to this yielding of different components. Because failure of the connection in specimen CC-3 was due to beam buckling, and the failure of connection M-4 was due to end plate failure, it is obvious that more demand was placed on the connection of specimen M-4 than the connection of CC-3. With this larger demand, even if the overall specimen rotation (connection rotation plus rotation due to hinging of the beam) was the same for both specimens, connection M-4 (end plate, bolts and extension stiffener) would have to undergo more rotation than connection CC-3.

The loading sequence adopted for the U of A test program was different from the loading sequence used by Ghobarah et al. (1992). As outlined in Section 3.5, testing at U of A involved three cycles in each load block and the beam tip displacement between subsequent load blocks was increased by 25 percent of the yield beam tip displacement. The loading sequence used by Ghobarah et al. involved two cycles in each load block and the beam tip displacement between subsequent load blocks was increased by 50 percent of the yield displacement. Since each inelastic cycle of loading causes an accumulation of damage in the connection, the greater the number of cycles per load block the lower the possible maximum moments and rotations attainable before failure. For the same reason, the smaller the increase in beam tip displacement between load blocks, the lower the moments and rotations attainable by the connection. It should also be noted that yield was determined theoretically by Ghobarah et al. while in the U of A test program yield was denoted as the deviation from a straight line of the load versus displacement curve.

It is evident from a comparison that, despite some similarities, there are differences between the two test programs. Numerical comparison between test programs serves only to verify the findings of a single test program. For example both test programs showed that extension stiffeners increase connection moment capacity.

of others in Section 5.1.4.

5.1.3 Energy Dissipation

Energy dissipation is an important characteristic of structural members and connections in seismic design. Connection energy dissipation is measured by calculating the area under the moment versus rotation curve or the load versus beam tip displacement curve. There has been little mention in earlier research regarding the energy dissipation of moment connections.

To the author's knowledge, only one other research program (Ghobarah et al., 1992) investigated the energy dissipation capacity of extended end plate moment connections. Ghobarah et al. (1992) calculated the cumulative energy dissipated in relation to the number of inelastic excursions of four extended end plate moment connections. The total energy dissipation was separated into three components, namely, panel zone, beam, and connection (end plate, bolts and column flange) components. The cumulative energy dissipated by these components in two of the four connections tested by Ghobarah et al. and two of the connections tested at the U of A is summarized in Table 5.3.

There were two concerns with comparing the energy dissipation of the two test programs: the differences in the inelastic loading patterns and the method of calculating energy dissipation. The concerns regarding the inelastic loading pattern were discussed in Section 5.1.2. The concerns regarding the calculation of energy dissipation were alleviated with a simple analysis. A comparison was made between the area under the load versus beam tip displacement curves (excluding the contribution of the test frame and elastic beam bending) and the area under the moment versus rotation curves for connections M-1 and M-2 from the U of A test program. The calculations showed that the areas under the moment versus rotation curve and the load versus beam tip displacement curve are similar. The cumulative energy dissipated by connection M-1 and M-2, using the area under the load versus beam tip displacement curves was 167 kJ and 221 kJ, respectively. The corresponding

values obtained from the moment versus end plate rotation curves were 149 kJ and 217 kJ, respectively. This demonstrated that a comparison of the cumulative energy dissipation capacities between the U of A tests and the Ghobarah et al. (1992) tests could be made.

A comparison of the cumulative energy dissipated in the medium size beam connections from the U of A test program with Ghobarah et al.'s test program (Table 5.3), shows that the end plates alone have the potential to dissipate comparable amounts of energy to the combined beam and connection. For example, the beam and connection from specimen CC-3 (thin end plate and stiffeners) dissipated 135 kJ while the end plate of connection M-4 dissipated 197 kJ. This comparison appears to indicate that there is little advantage in terms of the number of sustainable inelastic excursions and cumulative energy dissipation between having plastic deformation in the end plate alone or in the combined beam and connection. There are however two reasons to explain this behaviour. The first is that the connections which experienced plastic deformation of both the beam and the connection achieved the majority of the specimen rotation from the inelastic beam bending. The end plate did not contribute fully to the rotation of the specimen. The larger the rotations of a connection the more energy it can dissipate. Another reason is that connections in the U of A test program used heavier beam sizes and a less aggressive loading sequence (more load cycles were performed in each load block and smaller increases in beam tip displacement between load blocks was used) than used in the Ghobarah et al. (1992) test program. These two differences enable connections to dissipate more energy.

5.1.4 General Comparisons

General comparisons between the U of A test program and various previous research corroborate earlier findings. Conclusions drawn from the U of A research, which are similar to previous research, are listed hereafter with references.

The U of A test results indicate that medium size beams give a more ductile response than large size beams for extended end plate connections. Although many different sizes of beams have been tested with end plate connections there has been

connections. This idea has only been mentioned recently by Bose and Hughes (1995). As mentioned in Chapter 2, Bose and Hughes found that end plate connections with beams smaller than 686 UB were ductile and beams deeper than 762 UB were not ductile. Roeder and Foutch (1996) made a similar observation, although with BWWF moment connections. Roeder and Foutch, looking at the results of 91 tests, concluded that the best ductility for BWWF moment connections was obtainable with small and medium size beams. The ductile response of the medium size connections can be seen best by comparing the maximum rotations and rotation ductilities presented in Table 4.3.

The end plate failure modes observed in the U of A test program were similar to those observed in earlier test programs. The end plates predominantly cracked in the heat affected zone at the toe of the flange full penetration welds. Chasten et al. (1992) and Bose and Hughes (1995) reported that end plate cracking in the heat affected zones adjacent the flanges, was the predominant failure mode of end plate connections.

Extension stiffeners were found to increase the capacity of the extended end plate moment connection. This can be seen by comparing the performance of connections M-3 with M-4, and B-3 with B-4 (Figures 4.44, 4.45, 4.53 and 4.54). Similar observations were made by Tsai and Popov (1989) and Ghobarah et al. (1992).

Small increases in end plate thickness were shown to have a large impact on the performance of the connection. This was observed by comparing the performance of connection M-2 with M-3, and B-2 with B-3 (Figures 4.43, 4.44, 4.52 and 4.53). A similar observation was made by Tsai and Popov (1989).

The test results showed that the interior bolts attract more load than the exterior bolts. This is in agreement with observations made by Agerskov (1976), Krishnamurthy (1978), Grundy et al. (1980), and Fleishman et al. (1991).

Bolt bending was identified as a possible problem with extended end plate moment connections under cyclic loading, especially with thin end plates. The bending of bolts causes one side of the bolt to plastically deform earlier than the other. This earlier plastic deformation may result in earlier bolt fracture than in a connection

design where bolt bending did not occur. Fleishman et al. (1991) and Bose and Hughes (1995) also reported bolt bending in extended end plate moment connections.

The U of A test program, as most previous research, showed that extended end plate connections have excellent ductility, are good energy dissipaters and could perform well in seismic zones.

5.2 Prediction Equations

Two prediction equations were used to design the extended end plate connections in this test program. The connections in the S series were designed using Eq. 2.11 proposed by Mann and Morris (1977). The connections in the M and B series were designed using a modified version of Eq. 2.14 proposed by Whittaker and Walpole (1982).

Once the connections from the S series were designed and tested, the prediction equations given in the literature review were evaluated. The evaluated prediction equations were Eqs. 2.8 to 2.11, Eq. 2.14, Eq. 2.15, and Eq. 2.19 to Eq. 2.22. These equations predict the end plate thickness required to develop a desired connection moment based on specimen geometry and material properties. Evaluation of the prediction equations was done by comparing the predicted plate thicknesses with the actual plate thicknesses used in the tests. The maximum experimental moments were used as the design moments in the prediction equations. The actual thicknesses, predicted thicknesses and predicted to actual thickness ratios for the S series of tests are presented in the first two rows of Table 5.5. The values of the parameters used in the evaluated prediction equations are shown in Appendix C.

The prediction equation in best agreement with the S series test results (Eq. 2.14, from Whittaker and Walpole (1982)) was modified to improve the agreement. This modified version of Whittaker and Walpole's equation was then used to design the M and B series connections. Upon completion of the test program, the above mentioned prediction equations, including the modified version of the Whittaker and Walpole (1982) design equation, were evaluated using all 15 tests. The actual end plate thicknesses, the predicted end plate thicknesses and the predicted to actual end

plate failure.

5.2.1 Whittaker and Walpole (1982) and Modified Whittaker and Walpole (1997) Prediction Equations

Whittaker and Walpole's prediction equation was modified to obtain better agreement with the S series test results and to include the presence of extension stiffeners in the formulation. The modified version of Whittaker and Walpole's equation resulted in better agreement with the test results for all but two of the 15 connections tested. The modified prediction equation accurately predicted the required end plate thicknesses in this test program. The biggest advantages of the modified version of the Whittaker and Walpole equation are that it accommodates both end plate connections with and without extension stiffeners, and end plate connections with unequal bolt spacing.

The yield line pattern proposed by Whittaker and Walpole (1982) is shown in Figures 2.11 and 5.1. Figure 2.11 shows the general yield line pattern. Figure 5.1 shows both the yield line pattern and yield line notation. Yield line notation has been added to facilitate the explanation of the change in yield line patterns between the original Whittaker and Walpole (1982) equation and the modified Whittaker and Walpole equation (1997).

The yield lines proposed by Whittaker and Walpole (1982) have been labeled as follows. Hogging yield lines A and B are located at the exterior and interior flange weld toes and extend over the entire width of the end plate. Hogging yield lines C extend along the web weld toes, on either side of the web, from the interior flange weld toe to a location 0.6 times the beam depth away from the flange centerline. Sagging yield line D, passing through the centerline of the exterior bolts, extends over the width of the end plate and sagging yield lines E extend perpendicularly inward from the edges of the end plate to the center of the interior bolts. Sagging yield lines F extend from the centers of the interior bolts to the toe of the weld along the web to a distance 0.6 times the beam depth from flange centerline. Sagging yield lines G extend

from the center of the interior bolts to the junction of the interior flange weld to the web weld toe.

The yield line pattern proposed by Whittaker and Walpole (1982) was modified in the present study to reflect the discrepancies between the Whittaker and Walpole yield lines and the yield lines observed in the S series test specimens. Modifications were also made to encompass extended end plate connections with extension stiffeners. The modifications made to Whittaker and Walpole's proposed yield line pattern and equation can be seen by comparing Figures 5.1 and 5.2 and are shown in Table 5.4. The yield line pattern used to develop the modified Whittaker and Walpole equation is shown in Figure 5.2. The modifications to the yield line pattern used to arrive at the new equation are listed and explained in the following.

General modifications for extended end plate connections are:

1. Hogging yield line B along the interior flange of the connection was shortened to reflect the fact that the yield line does not extend under the web. The length of the yield line is taken as the width of the end plate minus the thickness of the web and the weld reinforcement.

2. Hogging yield lines C, extending from the interior flange weld toe, along the web weld toe, to 0.6 times the beam depth, were shortened to 0.35 times the beam depth. It was obvious from the tests in the S series that these yield lines extended along the web weld toe over a distance much smaller than 0.6 times the beam depth. A value of 0.35 was estimated from observation of the S series test specimens.

3. Sagging yield line D, extending through the exterior bolts over the width of the end plate, was moved from the bolt center to the edge of the bolt shaft nearest the beam flange. Yield line theory assumes a linear relationship between yield lines in order to calculate hinge rotation. Since the bolt head restricts this linearity near the bolt, it was considered appropriate to move yield line D closer to the beam flange. Moving the yield line to the edge of the bolt shaft allows a better approximation of the rotation occurring at yield line D.

4. Sagging yield lines E, extending from the interior bolts perpendicularly to the edge of the end plate, were moved from the bolt center to the edge of the bolt shaft

151

nearest the beam flange. Sagging yield lines E were moved for the same reason yield lines D were moved.

5. Sagging yield lines F and G were adjusted to accommodate movement of the sagging yield lines E.

Additional modifications made to accommodate extension stiffeners are:

1. Hogging yield lines H were added along the toes of the extension stiffener fillet welds.

2. Hogging yield line A, extending along the exterior flange weld toe, was shortened. Instead of the entire width of the end plate, the width of the end plate minus the width of the stiffener and the stiffener welds was used. This yield line does not extend under the stiffener.

3. Sagging yield line D, passing through the exterior bolts was replaced with a yield line configuration similar to that on the interior of the connection. New sagging yield lines I extend from adjacent the exterior bolt shafts, next to the beam flange to the toe of the stiffener welds at the edge of the end plate. Sagging yield lines J and K extend from adjacent the exterior bolt shaft, next to the beam flange, to the toe of the flange weld at the flange to stiffener junction, and perpendicularly to the edge of the end plate, respectively.

The proposed modified Whittaker and Walpole (1997) prediction equations for end plate connections both with and without extension stiffeners are shown in Table 5.4.

5.2.2 Evaluation of the Prediction Equations

Including the modified version of Whittaker and Walpole's prediction equation, ten equations were evaluated using the U of A test results. The modified version of Whittaker and Walpole's equation was also evaluated using the test results obtained by Ghobarah et al. (1992).

Two important assumptions were made in the evaluation of the prediction models. The maximum experimental connection moments were used as the design

moments to calculate the required plate thickness. This may lead to significant discrepancies between predicted and actual plate thicknesses because the evaluated models were not necessarily intended to predict the ultimate capacity of the connection. The second assumption concerns the bolt distances from the flanges. The modified Whittaker and Walpole equation is the only equation that accounts for unequal bolt distances from the flanges. Because the other prediction equations were not designed to accommodate unequal bolt spacing from the interior and exterior flanges, the average distance was used.

The modified Whittaker and Walpole prediction equation was the most accurate of the ten equations evaluated and was able to predict the end plate thickness of all connections tested. The ratios of predicted to actual thickness ranged from 0.87 to 1.10. When considering end plates less than 16 mm thick, the ratios of predicted to actual end plate thickness, using the modified Whittaker and Walpole equation were 0.97 to 1.10. Predicted plate thicknesses are given for connections experiencing end plate failure alone.

Excluding the modified Whittaker and Walpole equation, Whittaker and Walpole's prediction equation gave the most accurate results. The ratios of predicted to actual thickness ranged from 1.03 to 1.22. The Whittaker and Walpole equation, however, could not accommodate stiffened end plate connections.

Excluding both the modified version of Whittaker and Walpole's equation, and the Whittaker and Walpole equation, the prediction models greatly underestimate the moment capacity of extended end plate connections. The ratios of predicted to actual thickness using these prediction models are shown in Table 5.5. Detailed prediction equations are shown in Appendix C.

As previously mentioned the modified Whittaker and Walpole prediction equation was also evaluated using the test results presented by Ghobarah et al. (1992). Table 5.6 shows the actual end plate thicknesses used in Ghobarah et al.'s connections, the predicted end plate thicknesses using the modified Whittaker and Walpole equation and the predicted to actual thickness ratios. Since the yield strength of the end plates was not reported in the referenced paper it was assumed to be 300 MPa with an

overstrength factor of 15 percent. All predictions showed that a thinner end plate was capable of reaching the experimental moment. This is in agreement with Ghobarah's test results as no specimen experienced end plate failure. It is however, difficult to accurately evaluate the prediction equations using Ghobarah et al.'s test results since the end plates did not fail in the tests. The values of the parameters used in the prediction of the required plate thicknesses of Ghobarah et al's connections are presented in Appendix C.

The last column in Table 5.5 presents plate thickness predicted using the AISC (1994) recommended design equation. The extended end plate design equation suggested by AISC 1994 (Eq. 2.22) is conservative, even though the connections tested in this program violated a restriction AISC puts on extended end plate connections, namely that all connections were cyclically loaded.

Table 5.1 Comparison between Ghobarah et al. (1992) and the U of A (1997)

Connection Specifications

Connection	Ghobarah et al. (1992)		U of A (1997)	
	CC-1	CC-3	M-1	M-4
Beam	W410x60	W410x60	W460x97	W460x97
Column	W310x129	W310x129	W310x143	W310x143
End Plate	647x221x28	647x221x22	820x270x15.9	1000x270x15.9
Doubler Plate	No	No	800x240x12.7	800x240x12.7
Bolt Size	25.4 mm	25.4 mm	25.4 mm	31.8 mm
Bolt Grade	A490	A490	A490	A490
End Plate Stiffener	No	120x120x9	No	195x160x19

155

Table 5.2 Comparison Between Ghobarah et al. (1992) and ... (....)

Connection	Yield Moment (kN·m)	Maximum Moment (kN·m)	Yield Rotation (degrees)	Maximum Rotation (degrees)
CC-1	385	535	n/a	n/a
CC-3	370	550	0.09	0.5
M-1	460	700	0.13	1.3
M-4	510	740	0.2	1.35

Notes:

- Moments of connection CC-1 were determined using the load versus beam tip displacement curves from Ghobarah et al. (1992).
- All moments are at the column face.
- Rotations for CC-1 and CC-3 are those attributed to deformation of the connection (end plate, bolts, extension stiffeners, column flange and panel zone)
- Rotations for M-1 and M-4 are those attributed to deformation of the connection (end plate, bolts and extension stiffeners)

Table 5.3 Connection Energy Dissipation Summary

Connection	Inelastic Excursions	Cumulative Energy Dissipated (kJ)		
		Panel Zone	Connection (End Plate, Bolts and Column Flange)	Beam and Connection
CC-1	24	60	n/a	240
CC-3	19	60	30	135
M-1	20	n/a	149	149
M-4	19	n/a	197	197

Table 5.4 Differences Between the Whittaker and Walpole (1982) and the Modified Whittaker and Walpole Prediction Equations.

Whittaker and Walpole Equation	Modified Whittaker and Walpole Equation without extension stiffeners	Modified Whittaker and Walpole Equation with extension stiffeners
$T_{ep} = (\frac{M_b}{K})^{\frac{1}{2}}$	$T_{ep} = (\frac{M_b}{K})^{\frac{1}{2}}$	$T_{ep} = (\frac{M_b}{K})^{\frac{1}{2}}$
$K = F_{yep} d_f (J + S)$	$K = F_{yep} d_f (J + Q + S)$	$K = F_{yep} d_f (H + I + Q + S)$
		$H = \dfrac{B_{ep} - t_s}{2(do - w_f - \dfrac{d_b}{2})}$
		$I = \dfrac{2X}{g - t_s - 2w'_s - d_b}$
$J = \dfrac{2B_{ep}}{c - t_f - 2w_f}$	$J = \dfrac{B_{ep}}{2(do - \dfrac{d_b}{2} - w_f)}$	
	$Q = \dfrac{B_{ep} - t_f - 2w_w}{2(di - w_f - \dfrac{d_b}{2})}$	$Q = \dfrac{B_{ep} - t_f - 2w_w}{2(di - w_f - \dfrac{d_b}{2})}$
$S = \dfrac{2p}{g - t_b - 2w_w}$	$S = \dfrac{2p}{g - t_b - 2w_w - d_b}$	$S = \dfrac{2p}{g - t_b - 2w_w - d_b}$

157

Table 5.5 Actual Thickness, Predicted Thickness and Predicted to Actual Thickness Ratios

Connections	Actual End Plate Thickness	Prediction Models										
		Modified Whittaker and Walpole (1997)	Grundy et al. (1978)	Witteveen et al. (1982)	Krishnamurthy (1978)	Surtees and Mann, (1970)	Packer and Morris, (1977)	Mann and Morris, (1979)	Whittaker and Walpole, (1982)	Kukreti #1, (1990)	Kukreti #2, (1990)	AISC (1994)
S-2	13.3	12.94 (0.97)	31.31 (2.35)	30.01 (2.26)	18.92 (1.42)	17.16 (1.29)	22.7 (1.71)	22.14 (1.66)	14.56 (1.09)	n/a n/a	n/a n/a	17.83 (1.34)
S-3	13	13.79 (1.06)	35.28 (2.71)	28.04 (2.16)	24.53 (1.89)	17.62 (1.36)	26.61 (2.05)	24.95 (1.92)	15.38 (1.18)	n/a n/a	n/a n/a	23.12 (1.78)
M-1	15.9	17.38 (1.09)	42.33 (2.67)	47.3 (2.98)	26.2 (1.65)	24.24 (1.53)	29 (1.83)	29.93 (1.89)	19.33 (1.22)	n/a n/a	n/a n/a	24.7 (1.56)
M-2	15.9	16.81 (1.06)	44.53 (2.80)	39.2 (2.47)	33.35 (2.10)	22.2 (1.40)	34.13 (2.15)	31.49 (1.98)	19.41 (1.22)	n/a n/a	n/a n/a	31.45 (1.98)
M-3	19	17.74 (0.93)	48.39 (2.55)	43.59 (2.29)	35.21 (1.85)	24.13 (1.27)	37.79 (1.99)	34.22 (1.80)	21.1 (1.11)	n/a n/a	n/a n/a	33.20 (1.75)
M-4	15.9	16.7 (1.05)	n/a n/a	n/a n/a	n/a n/a	n/a n/a	n/a n/a	n/a n/a	n/a n/a	37.12 (2.34)	28.11 (1.77)	n/a n/a
M-6	15.9	17.14 (1.08)	n/a n/a	n/a n/a	n/a n/a	n/a n/a	n/a n/a	n/a n/a	n/a n/a	38.92 (2.45)	29.63 (1.87)	n/a n/a
B-1	15.9	17.48 (1.10)	35.65 (2.25)	18.21 (1.15)	22.56 (1.42)	20.73 (1.31)	24.9 (1.57)	25.21 (1.59)	16.39 (1.03)	n/a n/a	n/a n/a	21.27 (1.34)
B-2	15.9	15.29 (0.96)	43.39 (2.73)	32.48 (2.05)	35.76 (2.25)	20.08 (1.26)	32.55 (2.05)	30.68 (1.93)	17.71 (1.12)	n/a n/a	n/a n/a	33.72 (2.12)
B-3	19	16.5 (0.87)	50.27 (2.65)	44.38 (2.34)	39.52 (2.08)	23.26 (1.22)	38.89 (2.05)	35.55 (1.87)	20.52 (1.08)	n/a n/a	n/a n/a	37.26 (1.96)
B-4	15.9	16.57 (1.04)	n/a n/a	n/a n/a	n/a n/a	n/a n/a	n/a n/a	n/a n/a	n/a n/a	48.95 (3.08)	30.35 (1.91)	n/a n/a

Notes:
- All dimensions are in mm.
- Predicted to actual thickness ratios are in brackets

Table 5.6 Actual Thickness, Predicted Thickness and Predicted to Actual Thickness
Ratios using the Modified Whittaker and Walpole Equation and Ghobarah et al.
(1992) Test Results

Connections	Actual End Plate Thickness	Modified Whittaker and Walpole (1997) Prediction Equation	
		Predicted End Plate Thickness	Predicted / Actual
CB-1	28	20.79	0.74
CC-1	28	20.00	0.71
CC-2	28	22.56	0.81
CC-3	22	20.47	0.93

Notes:

- All dimensions are in mm.

- No above connection experienced end plate failure
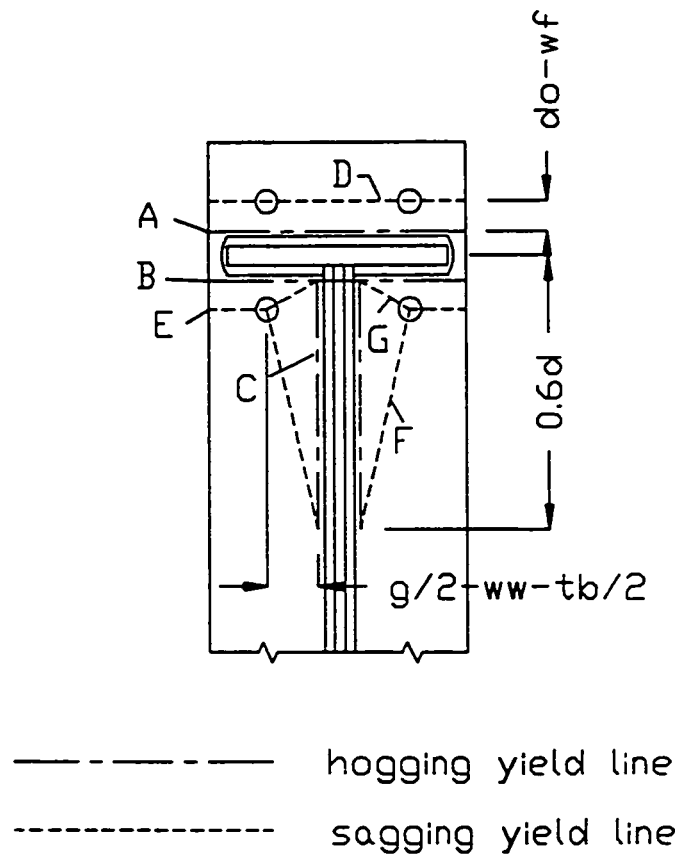
Figure 5.1 Whittaker and Walpole (1982) Yield Line Patterns
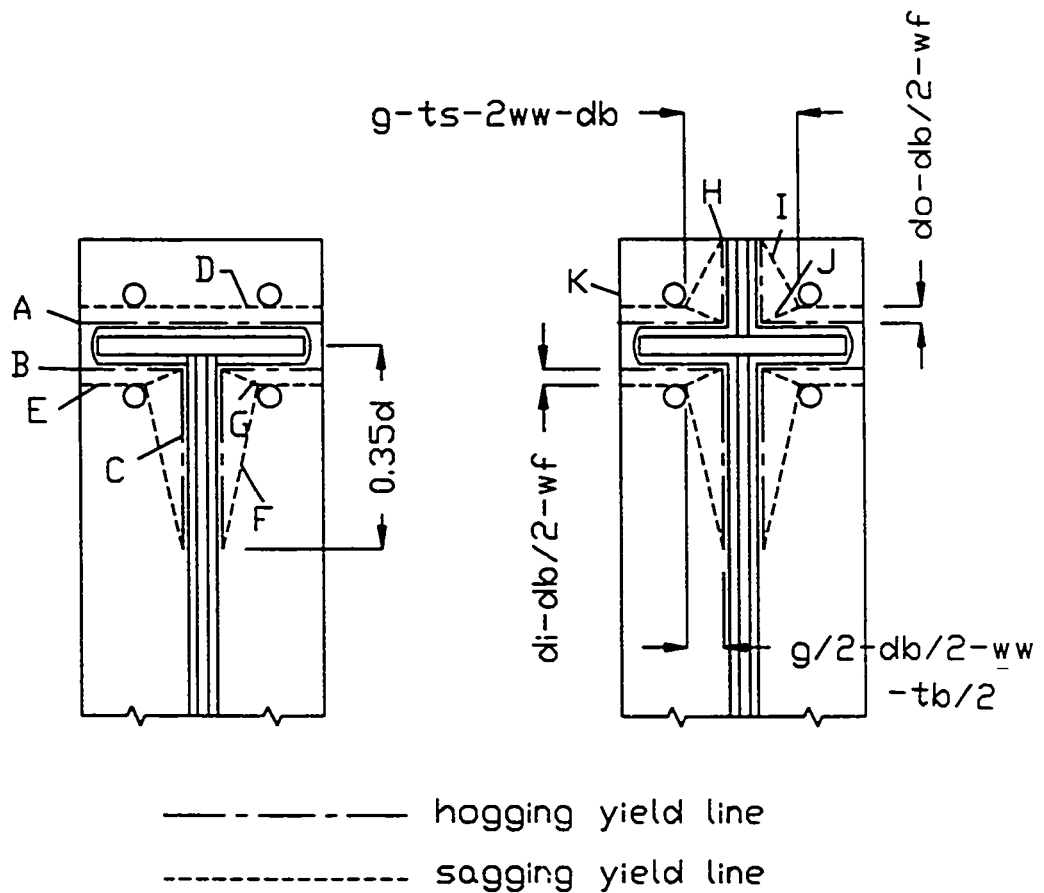
Figure 5.2 Modified Whittaker and Walpole Yield Line Patterns

6.1 Summary

Fifteen extended end plate moment connections were fabricated and tested under quasi-static cyclic loading. In twelve of the fifteen connections the failure was confined to the end plate while the beam and column remained elastic. These twelve connections were designed to examine various end plate parameters and their effect on connection behaviour. The parameters investigated were beam size, bolt configuration, end plate extension stiffeners, end plate thickness, and welding procedure. Three test specimens were designed to develop the plastic moment capacity of the beam. Bolt behaviour was monitored in some of the test specimens.

Three beam sizes were used in the test program, namely, W360x51 (small), W460x97 (medium) and W610x125 (large). The test program comprised three specimens with a small size beam, seven specimens with a medium size beam, and five specimens with a large size beam. The effect of welding procedure was investigated only in the medium size beam connection specimens.

Two bolt patterns were investigated, a tight bolt configuration with bolts between 1.4 and 2 bolt diameters from the beam flanges, and a relaxed bolt configuration with the exterior bolts moved to between 3.1 and 4.2 bolt diameters from the beam flanges. These bolt configurations were examined on all three beam sizes.

The effect of end plate thickness was examined using connections with relaxed bolt configurations. Two different plate thicknesses were investigated with each beam size.

The use of end plate extension stiffeners, in conjunction with a relaxed bolt configuration, was investigated on medium and large size beam connections designed to fail the end plate. Stiffeners were also used in conjunction with a 16-bolt configuration in order to develop the plastic moment capacity of the beam.

Two welding procedures were investigated. Test specimens prepared using shielded metal-arc welding with E41018 electrode for full penetration welds with no weld access holes were compared with flux-cored arc welding on test specimens prepared with weld access holes. These welding procedures were investigated using medium size beam

two specimens designed to yield the beam before yielding the end plate.

In addition to the experimental program, a literature survey was conducted and ten models, developed to predict the capacity of extended end plate moment connections, were evaluated. The evaluation was based on the test results obtained in the test program. Nine of the prediction equations were obtained from the literature review and one was derived based on the test results of the U of A preliminary test program.

6.2 Conclusions

The following conclusions are based on the results obtained from this research.

1. Extended end plate connection behaviour is affected by beam size. Medium size beam connections appear to be more ductile than large size beam connections.

2. Connections with relaxed bolt configurations are more flexible and can dissipate more energy than connections with tight bolt configurations, when the connections are designed with the same end plate thickness. Connections with relaxed bolt configurations however have a lower moment capacity and much of the bolt force in the bolt group is carried by the interior bolts.

3. Connections with relaxed bolt configurations and a plate thickness selected to give the same moment capacity as connections with tight bolt configurations offer little, if any, improvement in performance.

4. The addition of extension stiffeners increase connection moment capacity and yield rotation.

5. Extended end plate connections with a relaxed bolt configuration and extension stiffeners are able to dissipate more energy than connections with the same end plate thickness, a tight bolt configuration and no extension stiffeners.

6. Increases in end plate thickness result in stronger connections.

7. Bolt bending and loss of preload are common in extended end plate connections with thin end plates under cyclic loading.

8. Interior bolts, even on tight bolt configuration connections, carry more load than the exterior bolts.

163

9. The shielded metal-arc welding, without weld access holes, and the flux-cored arc welding with weld access holes tested, showed little if any difference in behaviour and capacity. Due to the large variability in the speeds at which the shielded metal-arc welding was performed, it is difficult to draw any conclusions between the welding techniques.

10. Extended end plate connections can be designed to remain elastic while forcing plastic hinging in the beam under cyclic loading.

11. The modified Whittaker and Walpole (1997) prediction equation gives the most accurate predictions of the ten equations evaluated and can accommodate end plate connections with or without extension stiffeners and with or without equal bolt spacing from the beam flanges.

6.3 Recommendations

This test program indicated that the effect of beam size, end plate thickness, bolt layout and the use of extension stiffeners on the behaviour of extended end plate moment connections are significant. The test program also showed that properly designed extended end plate connections have the potential to perform well in seismic zones. However, further investigation is needed to confirm their performance under seismic loads. It is therefore recommended that further research be carried out to:

1. Investigate the behaviour of extended end plate connections under quasi-dynamic cyclic loading;

2. Establish an optimum range of beam size for use with extended end plate connections, comparing cost effectiveness and energy dissipation capacity with other types of moment connections. Extended end plate connections have indicated, in this research and the work of others, that their behaviour is related to beam size. It may be that the enhanced performance of extended end plate connections over other types of connections makes them economically viable for medium size beams but not for large beams. Special attention should be directed to connections with extension stiffeners.

3. Investigate the performance of connections with various end plate configurations designed to develop the capacity of the beam and column. The purpose of the

moment connection performance. The parameters that have been identified as being the most beneficial to end plate moment connection behaviour, such as the stiffened relaxed bolt configuration, should now be investigated under conditions closer to that in which it will actually be used, i.e. entire connection failure.

4. Study the effect of different bolt spacing of equally spaced bolts from the beam flanges. This would increase the flexibility of the connection but ease the problem of unequal load sharing between interior and exterior bolts.

5. Investigate the effect of prying action. There is need for an elaborate investigation into the effect of prying action on the many different types of end plate connections.

6. Investigate the experimental variability of extended end plate connection performance. Extended end plate connections are very sensitive to connection details. An investigation such as this would enable evaluation of the significance of the various parameters. Duplicate tests were not performed as part of this research program.

7. Evaluate the bolt grade which should be used in extended end plate connections.

References

AISC (1994). Manual of Steel Construction - Load and Resistance Factor Design Second Edition. American Institute of Steel Construction, Chicago, Illinois.

AISC Special Task Committee on the Northridge Earthquake (1994). *Assessing Steel Damage in the Northridge Earthquake*. Modern Steel Construction, Vol. 34, No. 5, pp. 14-18.

Agerskov, H. (1976). *High - Strength Bolted Connections Subject to Prying*. Journal of the Structural Division, ASCE, Vol. 102. No. ST1, pp. 161 - 175.

Anon. (1994a). *Localized Steel Damage*. Modern Steel Construction, Vol. 34, No. 4, pp. 22-23.

Anon. (1994b). *Steel Damage in LA: What Went Wrong*. Modern Steel Construction, Vol. 34, No. 6, pp. 18-24.

Astaneh-Asl, Abolhassan (1995). *Seismic Design of Bolted Steel Moment - Resisting Frames*. Steel Tips, Structural Steel Education Foundation, 82 pp.

Bose, B. and A.F. Hughes (1995). *Verifying the Performance of Standard Ductile Connections for Semi-Continuous Steel Frames*. Proceedings of the Institution of Civil Engineers - Structures and Buildings, Vol. 110, pp. 441-457.

Canadian Standards Association (1995*)*. Limit States Design of Steel Structures, CAN/CSA-S16.1 -94. December.

Canadian Institute of Steel Construction (1995). Handbook of Steel Construction Sixth Edition. December.

Chaston, C. P., L.-W. Lu, and G. C. Driscoll (1992). *Prying and Shear in End-Plate Connection Design*. Journal of Structural Engineering, ASCE, Vol. 118, No. 5, pp. 1295-1311.

Chen, Sheung-Jin, C.H. Yeh, and J.M. Chu (1996). *Ductile Steel Beam to Column Connections for Seismic Resistance*. Journal of Structural Engineering, ASCE, Vol. 122, No. 11, pp. 1292 - 1299.

Choi, C. K. and G. T. Chung (1996). *Refined Three Dimensional Finite Element Model for End-Plate Connections*. Journal of Structural Engineering, Vol. 122, No. 11, pp. 1307 - 1316.

Engelhardt, M. D. and A. S. Husain (1992). *Cyclic Tests on Large Scale Steel Moment Connections*. Report PMFSEL 92-2, Phil M. Ferguson Structural Engineering Laboratory, The Univ. of Texas at Austin, 121 pp.

Connection: Part 2. Modern Steel Construction. August 1996, pp. 46 - 55.

Fleischman, R.B., C.P. Chaston, L.-W. Lu, and G. C. Driscoll (1991). *Top-and -Seat-Angle Connections and End Plate Connections: Snug vs. Fully Pretensioned Bolts.* Engineering Journal, AISC, First Quarter, pp. 18 - 28.

Ghobarah, A., R. M. Korol, and A. Osman (1992). *Cyclic Behavior of Extended End-Plate Joints.* Journal of Structural Engineering, ASCE, Vol. 118, No. 5, pp. 1333-1353.

Ghobarah, A., A. Osman, and R. M. Korol (1990). *Behaviour of Extended End-Plate Connections Under Cyclic Loading.* Engineering Structures, Vol. 12, No. 1, pp. 15-27.

Grundy, P., I. R. Thomas, and I. D. Bennetts (1980). *Beam-to-Column Moment Connections.* Journal of Structural Engineering, ASCE, Vol. 106, No. ST1, pp. 313-330.

Iwankiw, N.R. and C.J. Carter (1996). *The Dogbone Connection: A New Idea to Chew On.* Modern Steel Construction, April 1996, pp. 18 - 23.

Hjelmstead, K.D. and E.P. Popov (1983). *Cyclic Behavior and Design of Link Beams.* Journal of Structural Engineering, Vol. 119, No. 10, pp. 2387 - 2403.

Kasai, K. and E.P. Popov (1986). *General Behaviour of WF Steel Shear Link Beams.* Journal of Structural Engineering, Vol. 112, No. 2, pp. 362 - 381.

Kaufman, E.J., M. Xue, L.-W. Lu and J.W. Fisher (1996). *Achieving Ductile Behavior of Moment Connections.* Modern Steel Construction, Jan. 1996, pp. 30 - 39.

Kaufman, E.J., M. Xue, L.-W. Lu, and J.W. Fisher (1996). *Achieving Ductile Behavior of Moment Connections.* Modern Steel Construction, June 1996, pp. 38 - 42.

Kennedy, N.A., S. Vinnakota and A.N. Sherbourne (1981). *The Split-Tee Analogy in Bolted Splices and Beam - Column Connections.* Proceedings of the International Conference on Joints in Structural Steelwork. pp. 2.138 - 2.157.

Korol, R. M., A. Ghobarah, and A. Osman (1990). *Extended End-Plate Connections Under Cyclic Loading: Behaviour and Design.* Journal of Constructional Steel Research, Vol. 16, No. 4, pp. 253 - 280.

Krawinkler, H. and E. P. Popov (1982). *Seismic Behavior of Moment Connections and Joints.* Journal of the Structural Division, ASCE, Vol. 108, No. ST2, pp. 373 - 391.

International Community of Structural Engineers, ASCE, pp. 1115 - 1122.

Krishnamurthy, N. (1978). *A Fresh Look at Bolted End-Plate Behavior and Design.* Engineering Journal / American Institute of Steel Construction, Vol. 15, No. 2, pp. 39 - 49.

Kukreti, A. R., M. Ghassemieh, and T. M. Murray (1990). *Behavior and Design of Large-Capacity Moment End Plates.* Journal of Structural Engineering, ASCE, Vol. 116, No. 3, pp. 809-828.

Malley, J.O. (1995). *Performance of Moment Resisting Steel Frames in the January 17, 1994 Northridge Earthquake.* Proceedings of the Third International Workshop on Connections in Steel Structures, pp. 28 - 31.

Mann, A. P. and L.J. Morris (1979). *Limit Design of Extended End-Plate Connections.* Journal of Structural Engineering, ASCE, Vol. 5, No ST3, pp. 511-526.

Murray, T.M. and J.T. Borgsmiller (1995). *Strength of Moment End-Plate Connections with Multiple Bolt Rows at the Beam Tension Flange.* "Connections in Steel Structures 3, Behavior Strength and Design", Proceedings of the Third International Workshop. pp. 169 - 178.

Murray, T.M. and R.L. Meng (1995). *Seismic Loading of Moment End-Plate Connections: Some Preliminary Results.* Proceedings of the Thrid International Workshop on Connections in Steel Structures.

Nelson, R.F. (1996). *Proprietary Solution.* Modern Steel Construction. Jan. 1996, pp. 40 - 44.

Packer, J.A. and L.J. Morris (1977). *A Limit States Design Method for the Tension Region of Bolted Beam Column Connections.* The Structural Engineer, Vol. 55, No. 10, pp. 446 - 458.

Popov, E.P. (1995). *What Went Wrong With Steel Connections at Northridge.* Proceedings of the Fourth International Symposium on Steel Structures and First International Symposium on Steel Structures Educators. pp. 199 - 218.

Popov, E.P. and R.M. Stephen (1970). *Cyclic Loading of Full Size Steel Connections.* EERC Report 70-3, Engineering Research Center, University of California, Berkeley, Bulletin No. 21.

Popov, E.P., N.R. Amin, J.J.C. Louie, and R.M. Stephen (1986). *Cyclic Behaviour of Large Beam - column Assemblies.* AISC Engineering Journal, First Quarter, Vol. 23. pp. 9 - 23.

Redwood, R.G. (1992). *Code Provisions for seismic design for concentrically braced frames*. Canadian Journal of Civil Engineering. Vol. 19, pp. 1025 - 1031.

Redwood R.G. and A.K. Jain (1992). *Code provisions for seismic design for concentrically braced steel frames*. Canadian Journal of Civil Engineering, Vol. 19, pp. 1025 - 1031.

Redwood, R.G. and V.S. Channagiri (1991). *Earthquake resistant design of concentrically braced steel frames*. Canadian Journal of Civil Engineering, Vol. 18, pp. 839 - 850.

Roeder, C.W. and E.P. Popov (1978). Eccentrically Braced Steel Frames For Earthquakes. Journal of the Structural Division, ASCE, Vol. 104, No. ST3, pp. 391 - 412.

Roeder, C.W. and D.A. Foutch (1996). *Experimental Results For Seismic Resistant Steel Moment Frame Connections*. Journal of Structural Engineering, Vol. 122, No. 6, pp. 581 - 588.

Rosenbaum, D.B. (1995). *Seismic Design Muddle Persists*. Engineering News Record, July 17, pp. 6 - 7.

Rosta, P. (1994). *L.A. Officials Eye New Joint*. Engineering News Record, Feb. 20, pp. 21.

Sabol, T. (1994). *Steel Damage In L.A.: What Went Wrong*. Modern Steel Construction, Vol. 34, pp. 18 - 24.

Shi, Y.J., S.L. Chan, and Y.L. Wong (1996). *Modeling for Moment - Rotation Characteristics for End - Plate Connections*, Journal of Structural Engineering, Vol. 122, No. 11, pp. 1300 - 1306.

Surtees, J.O. and A.P. Mann (1970). *End - Plate Connections in Plastically Designed Structures*. Conference on Joints in Structures, Vol. 1, Paper 5.

Tremblay, R., P. Timler, M. Bruneau, and A. Filliatrault (1995). Performance of Steel Structures During the 1994 Northridge Earthquake. Canadian Journal of Civil Engineering, Vol. 22, pp. 338 - 360.

Tsai, K.-C. and E. P. Popov (1990). *Cyclic Behavior of End-Plate Moment Connections*. Journal of Structural Engineering, ASCE, Vol. 116, No. 11, pp. 2917 - 2930.

Tsai, K.-C. and E.P. Popov (1989). *End Plate Moment Connections for Cyclic Loads* Proceedings of the Sessions Related to Steel Structures, ASCE Structures Congress '89, San Francisco, CA, May 1-5, pp. 569 - 578.

Beam - Column Moment Joints. Journal of Structural Engineering. Vol. 121, No. 6, pp. 925 - 931.

Walpole, W.R. (1985). *Beam-Column Joints*, Bulletin of the New Zealand National Society for Earthquake Engineering, Vol. 118, No. 4, pp. 369 - 380.

Whittaker, D. and W.R. Walpole (1982). *Bolted End Plate Connections for Seismically-Designed Steel Frames*. Research Report No. 82-11, Department of Civil Engineering, University of Cantebury, pp. 88 - 92.

Witteveen, J., J.W.B. Stark, F.S.K. Bijlaard and P. Zoetemeijer (1982). *Welded and Bolted Beam - to - Column Connections*. Journal of the Structural Division, ASCE, Vol. 108, No. ST2, pp. 433 - 455.

Appendix A

Results of Tension Coupon Tests

Material testing was performed in accordance with ASTM A 370-94. All tension coupons were machined with a 50 mm gauge length and a reduced section width of 12.5 mm.

An MTS 1000 universal testing machine was used to carry out the tests. The tests were conducted at approximately $10\mu\varepsilon$/s in the elastic range and $50\mu\varepsilon$/s in the plastic range. The strain in each coupon was measured using a clip-on extensometer until just prior the ultimate stress (engineering) was reached. Rupture strains were determined by piecing together and measuring the failed specimen. Data was recorded both electronically and with an analogue plotter throughout the tests. Four static stress values, three in the initial yield stress plateau and one near the ultimate stress, were obtained for each coupon when the strain rate was reduced to zero for an interval of two minutes.

Figures A.1 and A.2 present the engineering stress versus strain curves obtained from tension coupons from the flanges and from the web of the W310x143 column section, respectively.

Figures A.3 and A.4 present the engineering stress versus strain curves obtained from tension coupon tests from the flanges and from the web of the W610x125 beam section, respectively.

Figures A.5 and A.6 present the engineering stress versus strain curves obtained from tension coupon tests from the flanges and from the web of the W460x97 beam section used in the fabrication of all medium beam size connections except connections M-6 and M-7, respectively.

Figures A.7 and A.8 present the engineering stress versus strain curves obtained from tension coupon tests from the flanges and from the web of the W460x97 beam section used in the fabrication of connections M-6 and M-7, respectively.

Figures A.9 and A.10 present the engineering stress versus strain curves obtained from tension coupon tests from the flanges and from the web of the 15.9 mm and the 19 mm plate used in the fabrication of the test specimens.
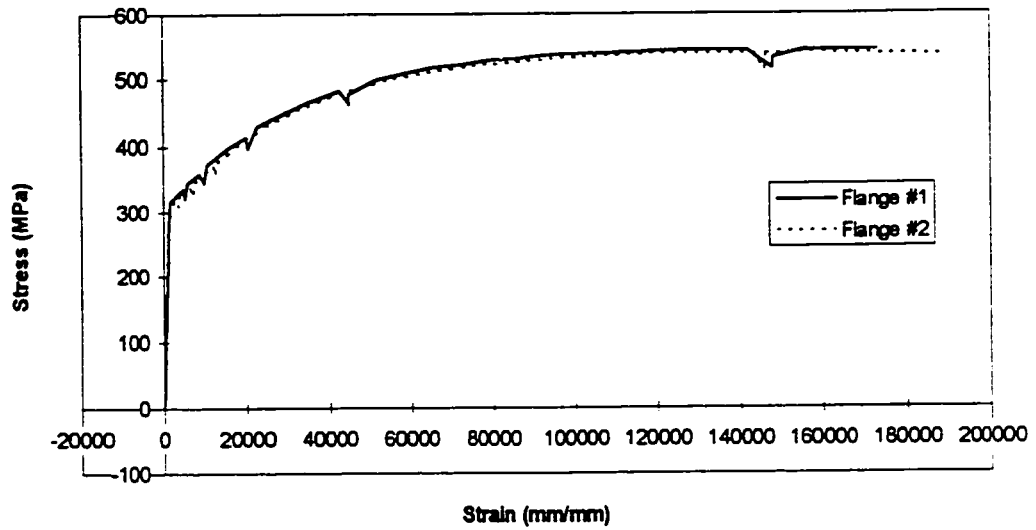
Figure A.1 Stress - strain curve for W310 x 143 column flange coupons
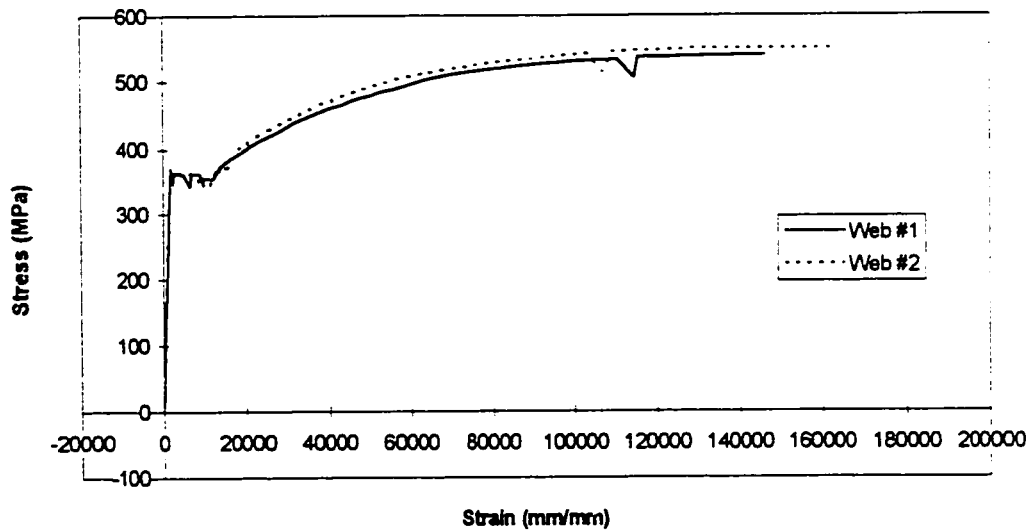
Figure A.2 Stress - strain curve for W310 x 143 column web coupons

173
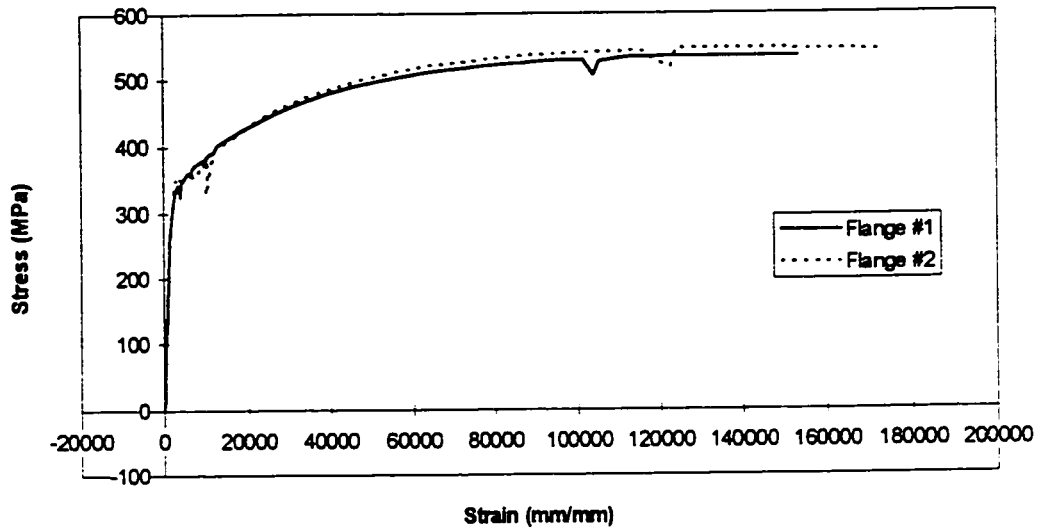
Figure A.3 Stress - strain curve for W610 x 125 beam flange coupons
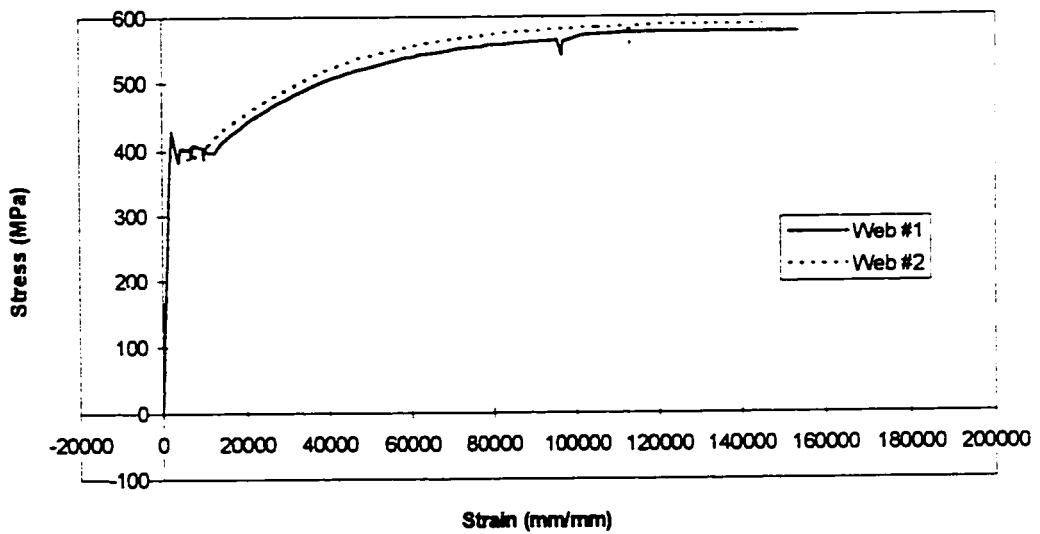
Figure A.4 Stress - strain curve for W610 x 125 beam web coupons

174
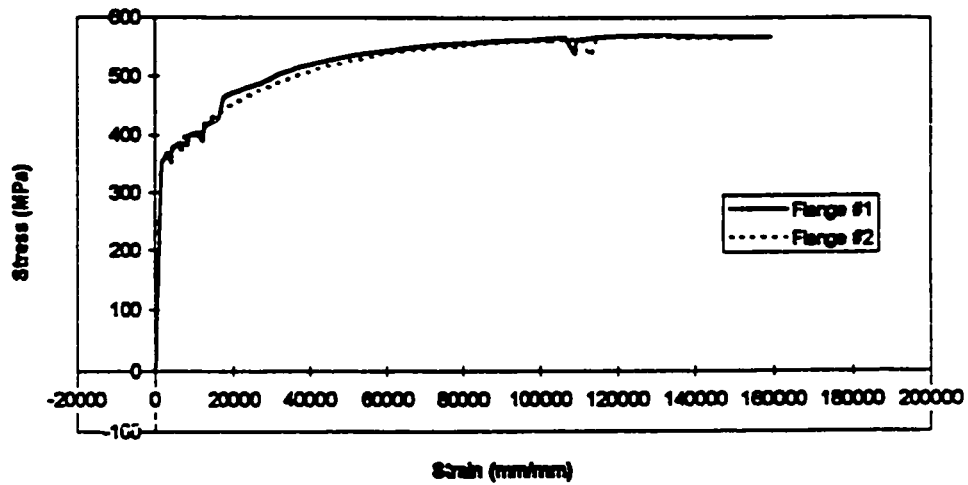
Figure A.5 Stress - strain curve for W460 x 97 #1 beam flange coupons
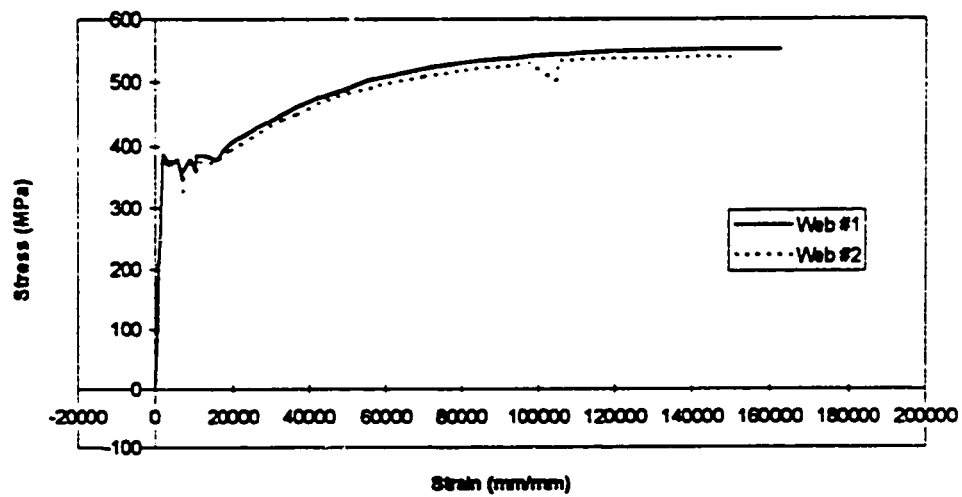
Figure A.6 Stress - strain curve for W460 x 97 #1 beam web coupons
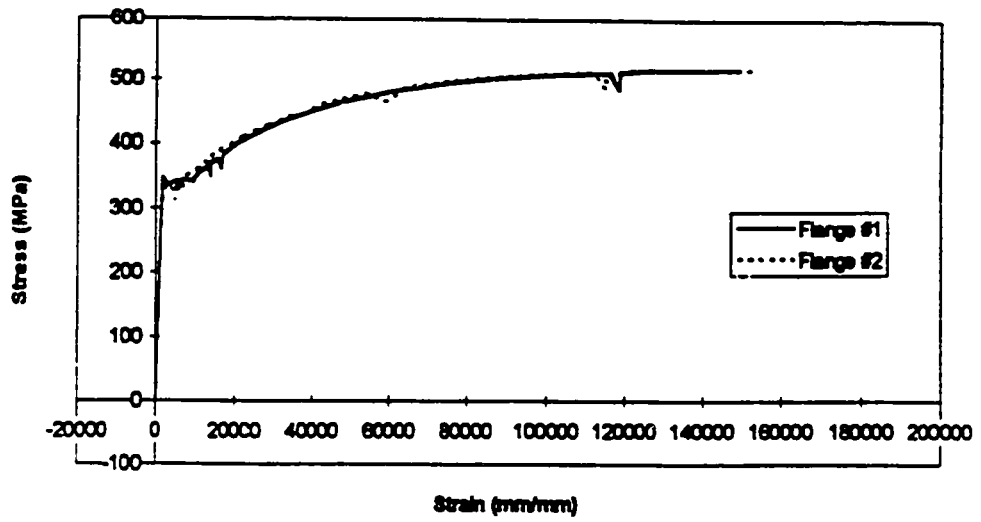
Figure A.7 Stress - strain curve for W460 x 97 #2 beam flange coupons
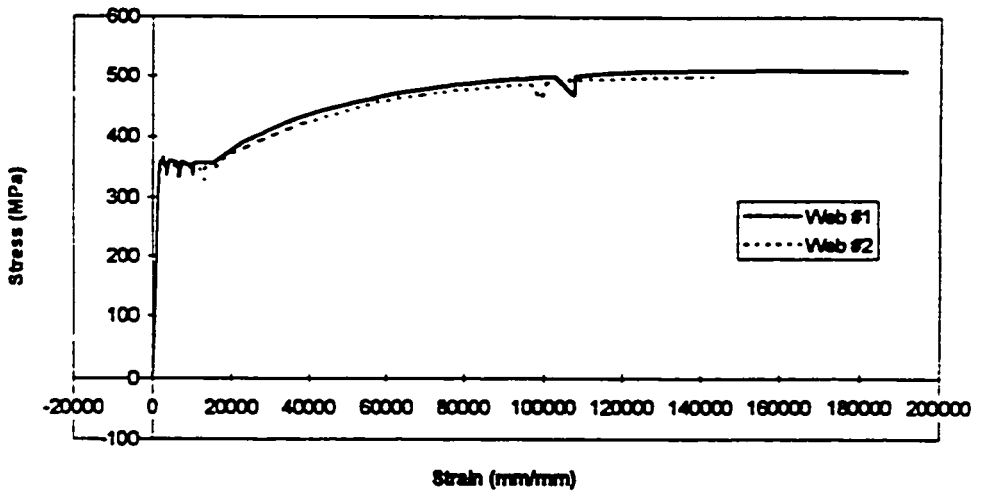
Figure A.8 Stress - strain curve for W460 x 97 #2 beam web coupons
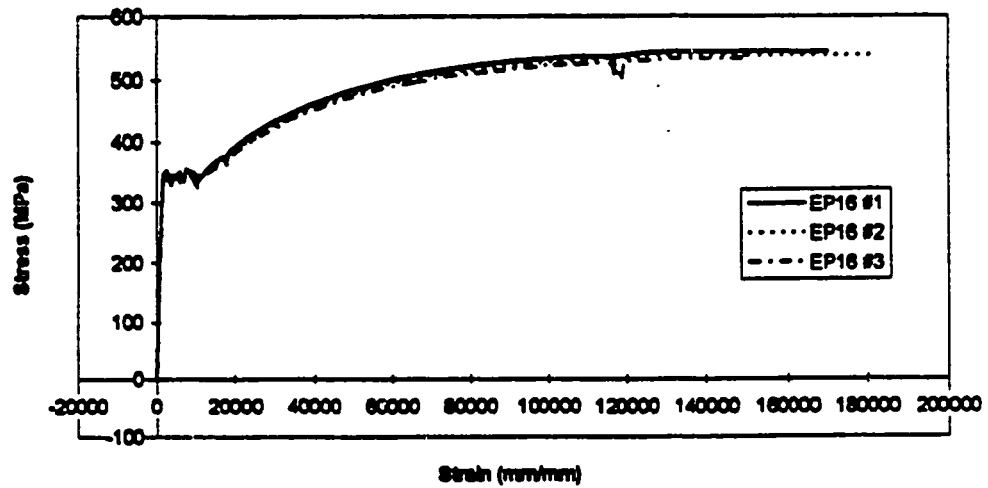
Figure A.9 Stress - strain curve for 15.9 mm thick end plate coupons
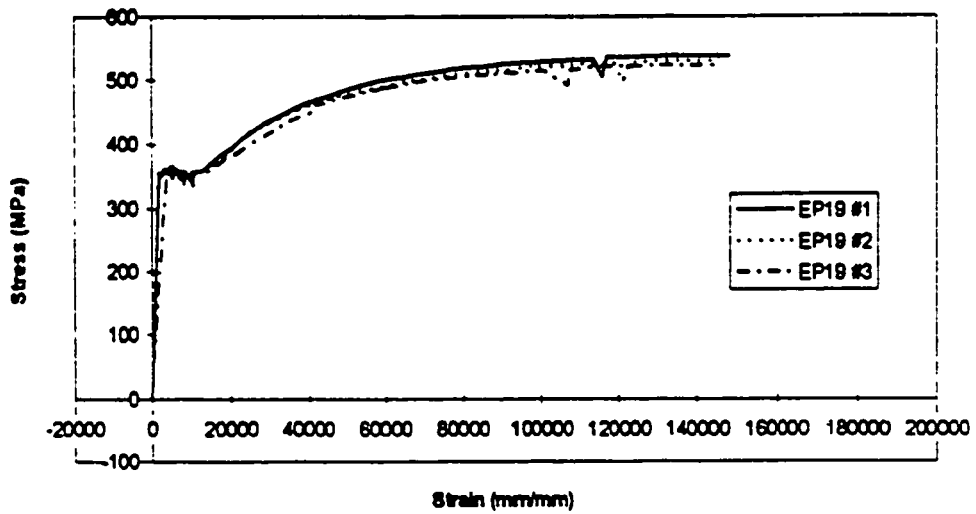
Figure A.10 Stress - strain curve for 19 mm thick end plate coupons

177

Appendix B

Results of Bolt Monitoring

.

The elongation of one interior one and one exterior bolt were monitored during the testing of connections B-5, M-2, M-5, M-6, and M-7. In the 16 - bolt connections the bolts that were nearest to the flange were monitored. The connection moment versus bolt elongation curves for each of the monitored bolts is presented twice, once showing bolt behaviour throughout the whole test, and once showing bolt behaviour while the connection was performing elastically.

To determine the load - elongation relationship of the bolts two 1-1/8 in. A325 bolts and two 1-1/4 in. A490 bolts were tested. The 1-1/8 in. A325 bolts were tested into the plastic range. The 1-1/4 in. A490 bolts were tested only in the elastic range.

Figures B.1 to B.5 show the connection moment versus bolt elongation data in the connection elastic and plastic range for connections B-5, M-2, M-5, M-6 and M-7, respectively.

Figures B.6 to B.10 show the connection moment versus bolt elongation data in the connections elastic range for connections B-5, M-2, M-5, M-6 and M-7, respectively.

Figures B.11 and B.12 show the load versus displacement curves from the ancillary tests of two 1-1/8" A325 and two 1-1/4" A490 bolts, respectively.

The elongation of one interior one and one exterior bolt were monitored during the testing of connections B-5, M-2, M-5, M-6, and M-7. In the 16 - bolt connections the bolts that were nearest to the flange were monitored. The connection moment versus bolt elongation curves for each of the monitored bolts is presented twice, once showing bolt behaviour throughout the whole test, and once showing bolt behaviour while the connection was performing elastically.

To determine the load - elongation relationship of the bolts two 1-1/8 in. A325 bolts and two 1-1/4 in. A490 bolts were tested. The 1-1/8 in. A325 bolts were tested into the plastic range. The 1-1/4 in. A490 bolts were tested only in the elastic range.

Figures B.1 to B.5 show the connection moment versus bolt elongation data in the connection elastic and plastic range for connections B-5, M-2, M-5, M-6 and M-7, respectively.

Figures B.6 to B.10 show the connection moment versus bolt elongation data in the connections elastic range for connections B-5, M-2, M-5, M-6 and M-7, respectively.

Figures B.11 and B.12 show the load versus displacement curves from the ancillary tests of two 1-1/8" A325 and two 1-1/4" A490 bolts, respectively.

Figure B.1 B-5 Bolt Elongation versus Connection Moment (Elastic and Plastic)
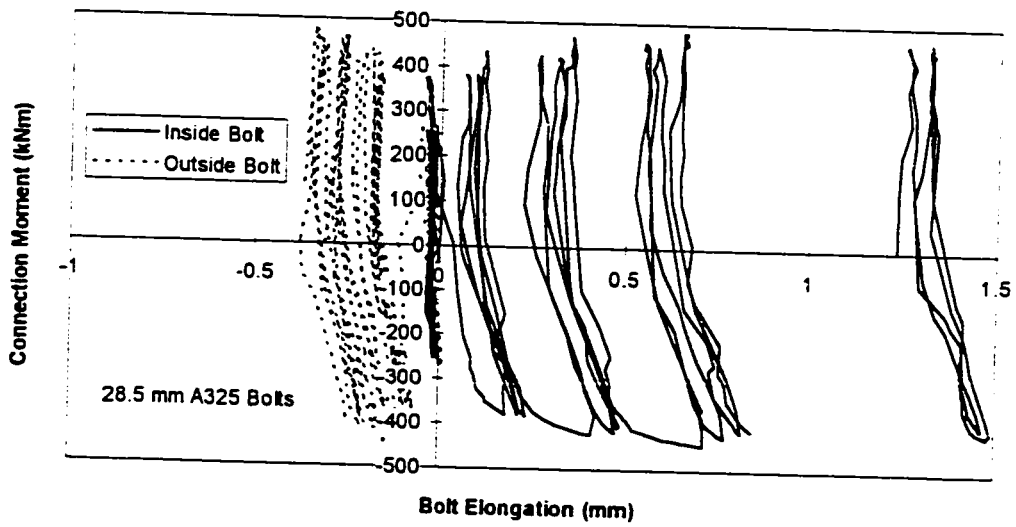
Figure B.2 M-2 Bolt Elongation versus Connection Moment (Elastic and Plastic)

181
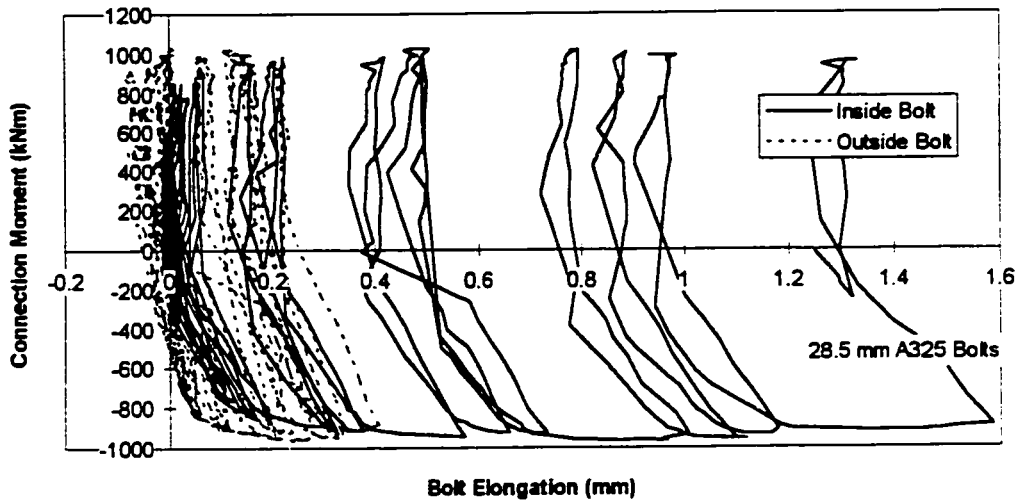
Figure B.3 M-5 Bolt Elongation versus Connection Moment (Elastic and Plastic)
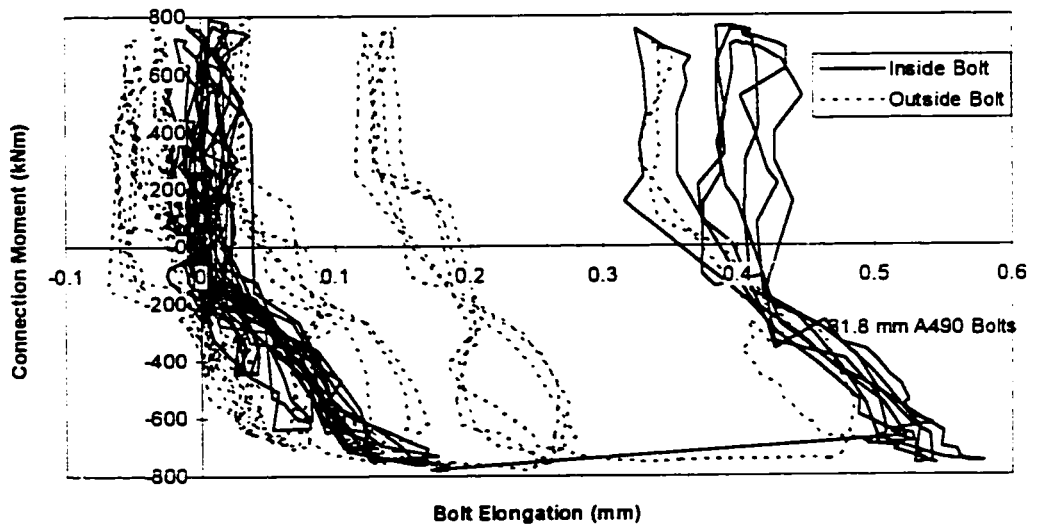
Figure B.4 M-6 Bolt Elongation versus Connection Moment (Elastic and Plastic)

182
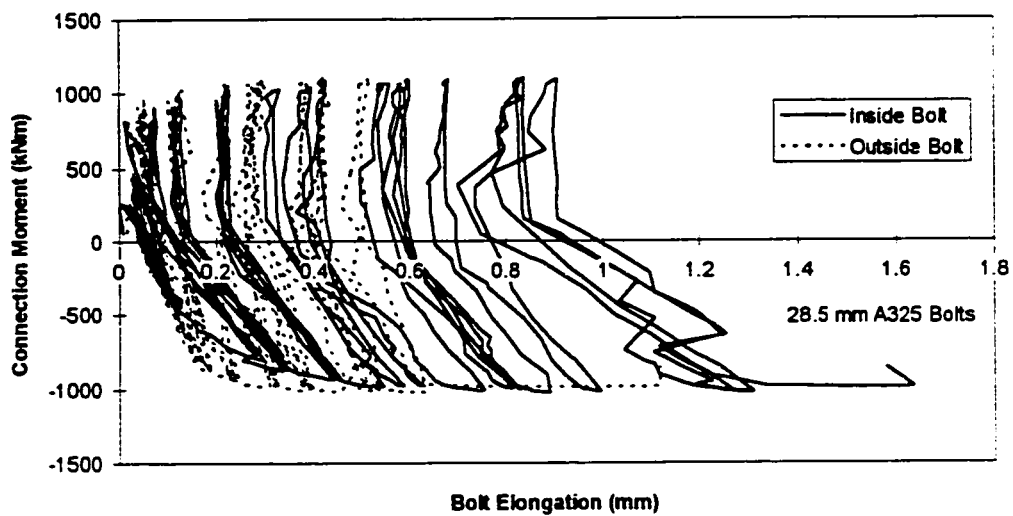
Figure B.5 M-7 Bolt Elongation versus Connection Moment (Elastic and Plastic)
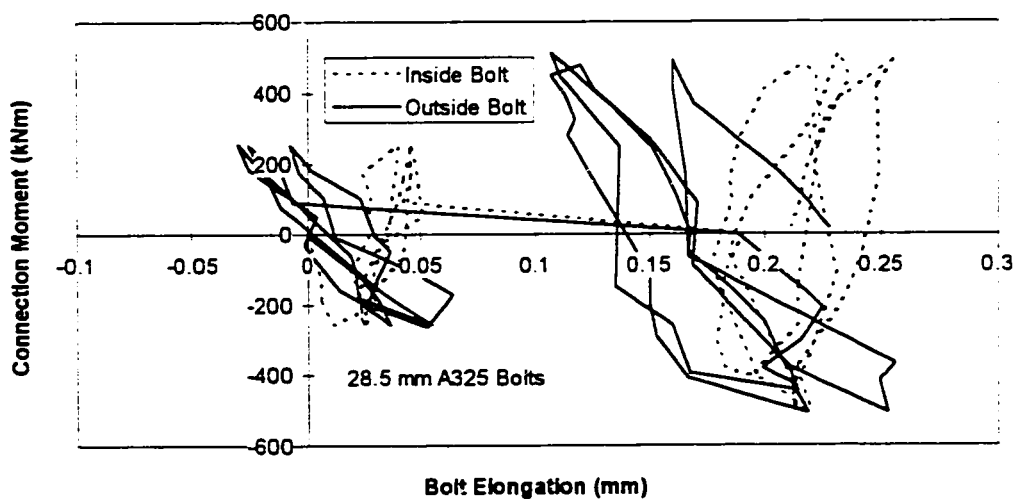
Figure B.6 B-5 Bolt Elongation versus Connection Moment (Elastic)

183
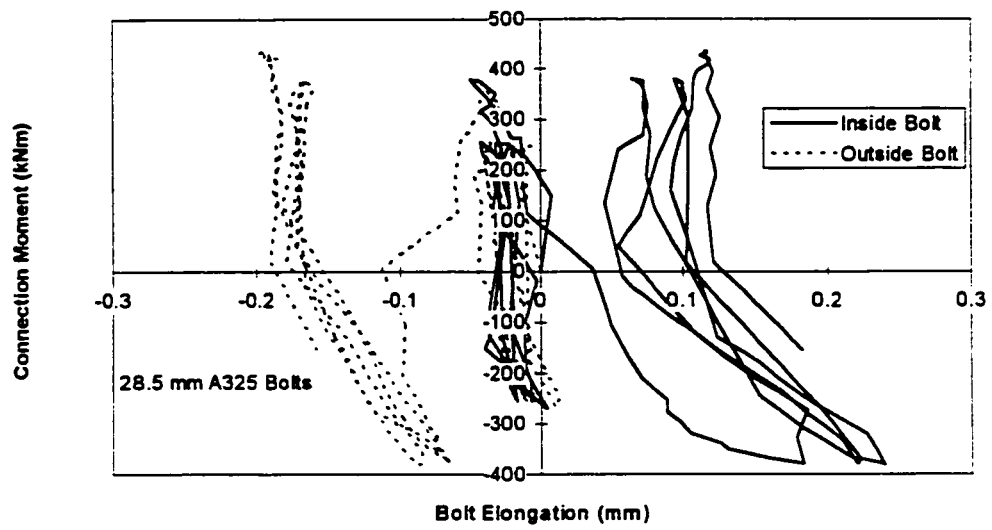
Figure B.7 M-2 Bolt Elongation versus Connection Moment (Elastic)
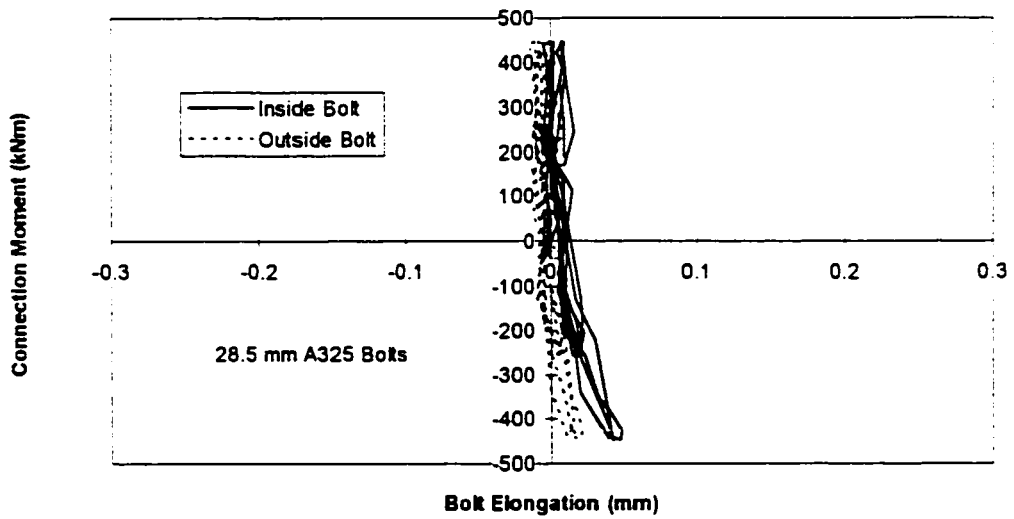
Figure B.8 M-5 Bolt Elongation versus Connection Moment (Elastic)
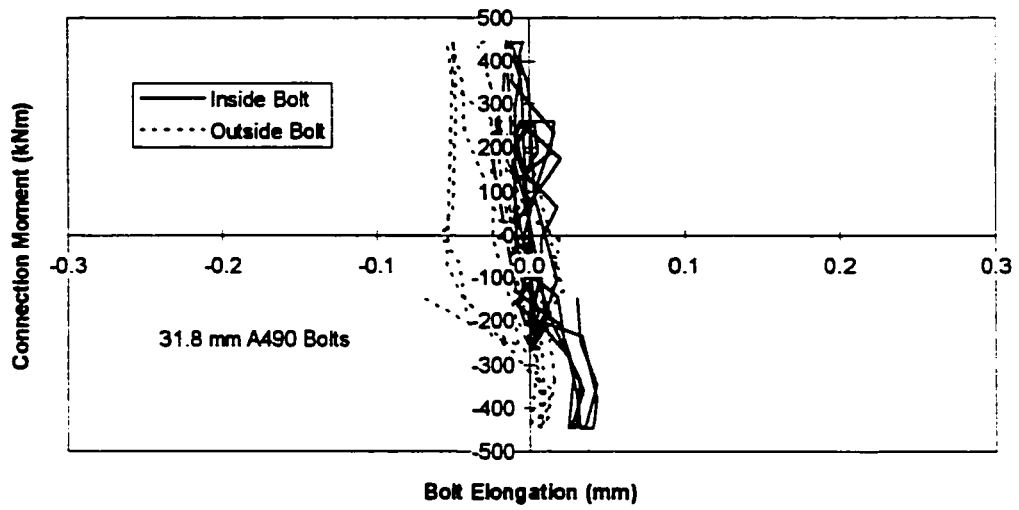
Figure B.9 M-6 Bolt Elongation versus Connection Moment (Elastic)
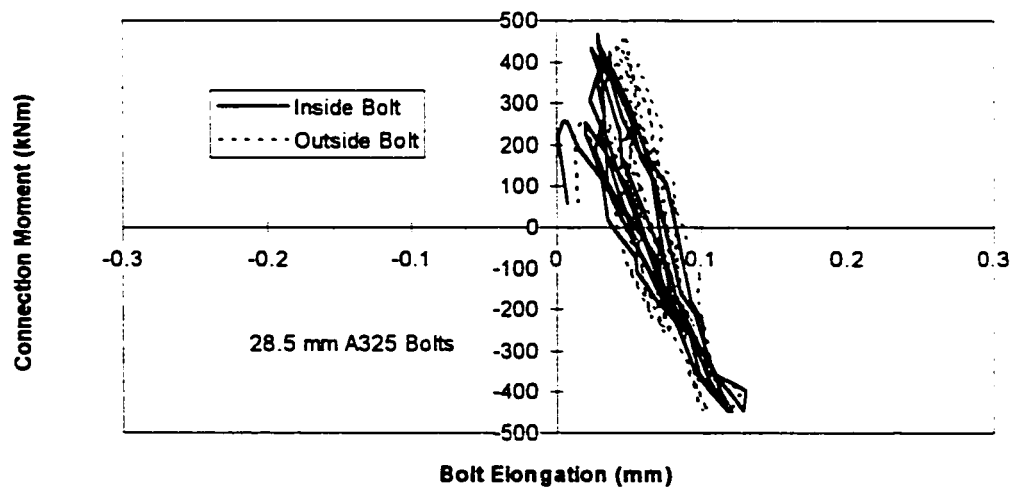
Figure B.10 M-7 Bolt Elongation versus Connection Moment (Elastic)

185
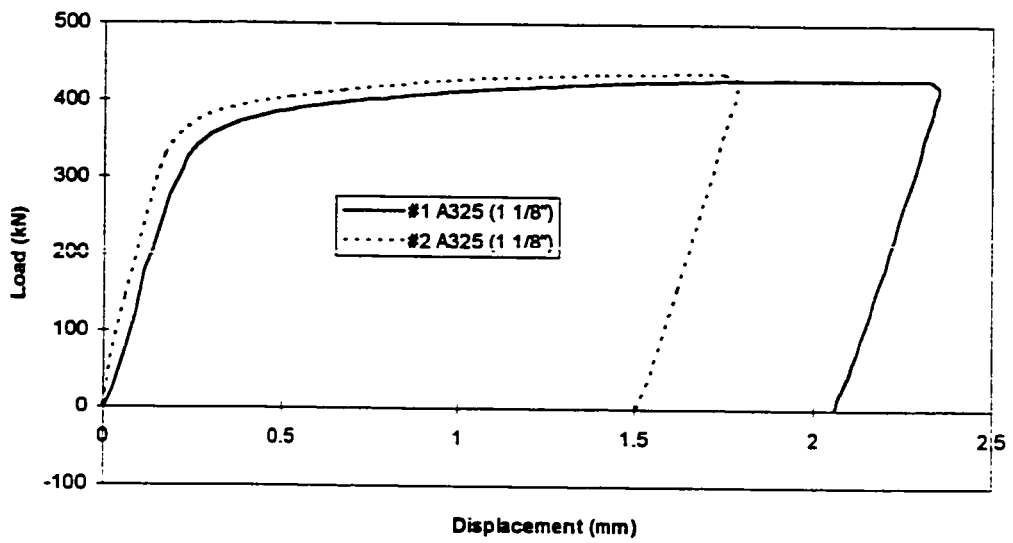
Figure B.11   A325 (1-1/8") Load - Displacement Curves
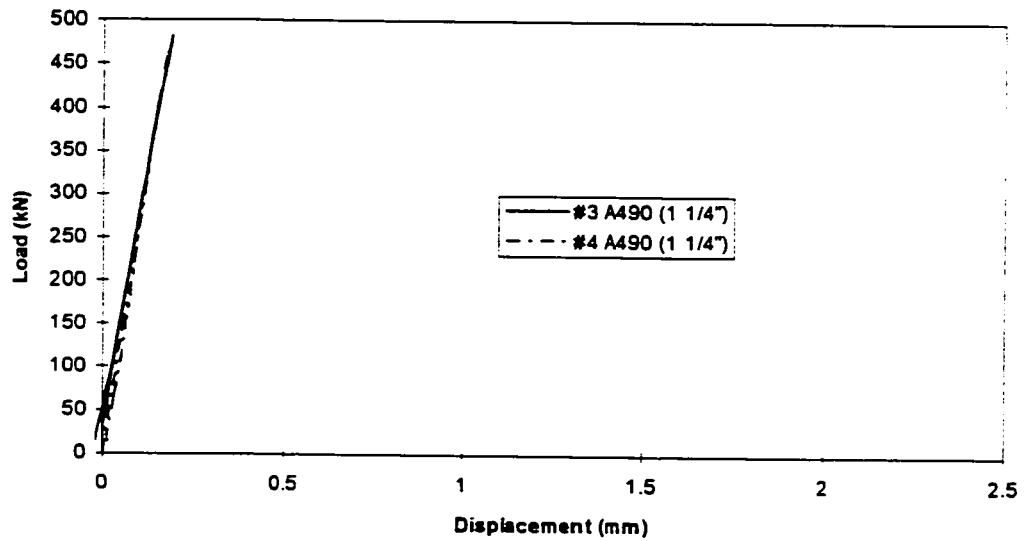
Figure B.12   A490 (1-1/4") Load - Displacement Curves

Appendix C

Values of the Parameters Used in the Prediction Equations

Ten end plate moment capacity prediction equations were evaluated. The values of the parameters used in these prediction equations are presented in tables C.1 to C.11, along with the predicted end plate thicknesses, the actual end plate thicknesses and the predicted to actual end plate thickness ratios. The maximum moment obtained experimentally was used as the design moment in the prediction equations.

Table C.12 shows the values of the parameters used in the prediction of the plate thickness of the extended end plate connections used in the Ghobarah et al (1992) test program. The modified Whittaker and Walpole equation was the prediction model used.

Table C.1 Detailed Predictions, S and M Series (Modified Whittaker and Walpole, 1997)

Definitions	S2 8 bolt	S3 8 bolt	M1 8 bolt	M2 8 bolt	M3 8 bolt	M4 8 bolt stiffener	M6 8 bolt stiffener
				Tests			
Beam = beam used in experiment	W360x51	W360x51	W460x97	W460x97	W460x97	W460x97	W460x97
Mb = failure moment (kN·m)	220	192	696	478	591	732	771
Fyep = end plate yield stress (MPa)	295	285	340	340	356	340	340
d = depth of beam (mm)	355	355	466	466	466	466	466
tf = flange thickness (mm)	11.6	11.6	19	19	19	19	19
df = d - tf = depth of the beam - flange thickness (mm)	343.4	343.4	447	447	447	447	447
Bep = end plate width (mm)	200	200	230	230	230	230	230
do = distance from outside bolt center to flange face (mm)	45	81.5	45	100	100	100	100
di = distance from inside bolt center to flange face (mm)	45	45	45	45	45	45	45
wf = width of flange weld (mm)	10	10	10	10	10	10	10
ww = width of web weld (mm)	10	10	10	10	10	10	10
db = bolt diameter (mm)	24	24	28.6	28.6	31.75	31.75	31.75
tw = web thickness (mm)	7.2	7.2	11.4	11.4	11.4	11.4	11.4
p = .35 x df = length of C yield line (mm)	120.19	120.19	156.45	156.45	156.45	156.45	156.45
g = bolt pitch (mm)	100	100	125	125	125	125	125
ts = stiffener thickness (mm)	n/a	n/a	n/a	n/a	n/a	15.875	15.875
ws = width of stiffener weld (mm)	n/a	n/a	n/a	n/a	n/a	10	10
X = distance from end of end plate to flange face	n/a	n/a	n/a	n/a	n/a	160	160
K = Fyep x df x (H + I + J + Q + S)	1319995.1	1014217.8	2305005	1691553	1878172	2625129.8	2625129.8
H= (Bep - ts)/(2 x (do - wf -db/2))	n/a	n/a	n/a	n/a	n/a	1.44	1.44
I = (2 x X)/(g - ts - 2 x ws - db)	n/a	n/a	n/a	n/a	n/a	5.58	5.58
J = Bep/(2 x (do - wf - db/2))	4.35	1.68	5.56	1.52	1.55	1.55	1.55
Q = (Bep - tf- 2 x ww)/(2 x (di - wf -db/2))	3.76	3.76	4.80	4.80	5.19	5.19	5.19
S = (2 x p)/(g - tb - 2 x ww - db)	4.93	4.93	4.81	4.81	5.06	5.06	5.06
Tep = (Mb/K)^0.5 = predicted end plate thickness (mm)	12.91	13.76	17.38	16.81	17.74	16.70	17.14
Ta = actual end plate thickness (mm)	13.30	13.00	15.88	15.88	19.00	15.88	15.88
Ratio of predicted to actual thickness	0.97	1.06	1.09	1.06	0.93	1.05	1.08

189

Table C.2 Detailed Predictions, B Series (Modified Whittaker and Walpole, 1997)

Definitions	Symbols	Tests			
		B1 8 bolt	B2 8 bolt	B3 8 bolt	B4 8 bolt stiffener
Beam = beam used in experiment	Beam	W610x125	W610x125	W610x125	W610x125
Mb = failure moment (kN·m)	Mb =	768	525	738	994
Fyep = end plate yield stress (MPa)	Fyep =	340	340	356	340
d = depth of beam (mm)	d =	612	612	612	612
tf = flange thickness (mm)	tf =	19.6	19.6	19.6	19.6
df = d - tf = depth of the beam - flange thickness (mm)	df =	592.4	592.4	592.4	592.4
Bep = end plate width (mm)	Bep =	270	270	270	270
do = distance from outside bolt center to flange face (mm)	do =	45	150	150	150
di = distance from inside bolt center to flange face (mm)	di =	45	45	45	45
wf = width of flange weld (mm)	wf =	12	12	12	12
ww = width of web weld (mm)	ww =	10	10	10	10
db = bolt diameter (mm)	db =	24	24	31.75	31.75
tw = web thickness (mm)	tw =	11.9	11.9	11.9	11.9
p = .35 x df = length of C yield line (mm)	p =	207.34	207.34	207.34	207.34
g = bolt pitch (mm)	g =	150	150	150	150
ts = stiffener thickness (mm)	ts =	n/a	n/a	n/a	19
ws = width of stiffener weld (mm)	ws =	n/a	n/a	n/a	12
X = distance from end of end plate to flange face	X =	n/a	n/a	n/a	195
K = Fyep x df x (H + I + J + Q + S)	K =	3324254	2245240	2712010	3618338
H= (Bep - ts)/(2 x (do - wf -db/2))	H =	n/a	n/a	n/a	1.03
I = (2 x X)/(g - ts - 2 x ws - db)	I =	n/a	n/a	n/a	5.18
J = Bep/(2 x (do - wf - db/2))	J =	6.43	1.07	1.11	1.11
Q = (Bep - tf- 2 x ww)/(2 x (di - wf-db/2))	Q =	5.67	5.67	6.95	6.95
S = (2 x p)/(g - tb - 2 x ww - db)	S =	4.41	4.41	4.80	4.80
Tep = (Mb/K)^0.5 = predicted end plate thickness (mm)	Tep =	17.48	15.29	16.50	16.57
Ta = actual end plate thickness (mm)	Ta =	15.88	15.88	19.00	15.88
Ratio of predicted to actual thickness	Ratio =	1.10	0.96	0.87	1.04

Table C.3 Detailed Predictions (Grundy et al., 1978)

Definitions	Symbols	Tests							
		S2 8 bolt	S3 8 bolt	M1 8 bolt	M2 8 bolt	M3 8 bolt	B1 8 bolt	B2 8 bolt	B3 8 bolt
Beam = beam used in experiment	Beam	W360x51	W360x51	W460x97	W460x97	W460x97	W610x125	W610x125	W610x1
Mb = failure moment (kN·m)	Mb =	220	192	696	478	591	768	525	
d = depth of beam (mm)	d =	355	355	466	466	466	612	612	6
tf = flange thickness (mm)	tf =	11.6	11.6	19	19	19	19.6	19.6	1
df = d - tf (mm)	df =	343.4	343.4	447	447	447	592.4	592.4	59
Pc = Largest compressive force in connection (N)	Fc=	6.41E+05	5.59E+05	1.56E+06	1.07E+06	1.32E+06	1.30E+06	8.86E+05	1.25E+
Pt = Largest tensile force in connection (N)	Ft=	6.41E+05	5.59E+05	1.56E+06	1.07E+06	1.32E+06	1.30E+06	8.86E+05	1.25E+
Fyep = end plate yield stress (MPa)	Fyep =	295	285	340	340	356	340	340	3
Fx = axial compressive force in connection (N)	Fx =	0	0	0	0	0	0	0	
Bep = end plate width (mm)	Bep =	200	200	230	230	230	270	270	2
di = from inside bolt center to flange face (mm)	di =	45	45	45	45	45	45	45	
do = from outside bolt center to flange face (mm)	do =	45	81.5	45	100	100	45	150	1
Tep = predicted end plate thickness (mm)	Tep =	31.26	35.23	42.33	44.53	48.39	35.65	43.39	50.
Ta = actual end plate thickness (mm)	Ta =	13.30	13.00	15.88	15.88	19.00	15.88	15.88	19.
Ratio of Predicted to Actual Thickness	Ratio =	2.35	2.71	2.67	2.80	2.55	2.25	2.73	2.

191

Table C.4 Detailed Predictions (Witteveen et al., 1982)

Definitions	Symbols	Tests							
		S2 8 bolt	S3 8 bolt	M1 8 bolt	M2 8 bolt	M3 8 bolt	B1 8 bolt	B2 8 bolt	B3 8 bolt
Beam = beam used in experiment	Beam	W360x51	W360x51	W460x97	W460x97	W460x97	W610x125	W610x125	W610x12
Mb = failure moment (kNm)	Mb =	220	192	696	478	591	768	525	73
d = depth of beam (mm)	d =	355	355	466	466	466	612	612	61
tf = flange thickness (mm)	tf =	11.6	11.6	19	19	19	19.6	19.6	19.
df = d - tf (mm)	df =	343.4	343.4	447	447	447	592.4	592.4	592.
F = flange force (obtained from experiment) (N)	F =	6.20E+05	5.41E+05	1.49E+06	1.03E+06	1.27E+06	1.25E+06	8.58E+05	1.21E+0
Fyep = end plate yield stress (MPa)	Fyep =	295	285	340	340	356	340	340	35
di = from inside bolt center to flange face (mm)	di =	45	45	45	45	45	45	45	4
do = from outside bolt center to flange face (mm)	do =	45	81.5	45	100	100	45	150	150
Bep = end plate width (mm)	Bep =	200	200	230	230	230	270	270	270
wb = bolt head width (mm)	wb =	36.5	36.5	46	46	51	41.25	41.25	50
ao = do - wf - 0.5 wb (mm)	ao =	16.75	16.75	8.00	12.00	9.60	14.38	14.38	9.6
ai = di - wf - 0.5 wb (mm)	ai =	16.75	53.25	8.00	67.00	64.60	14.38	119.38	114.6
g = bolt pitch (mm)	g =	100	100	125	125	125	150	150	150
b = from outside bolt to edge of end plate (mm)	b =	60	60	60	60	60	60	60	60
b<1.25xa'	b =	20.94	20.94	10.00	15.00	12.00	17.97	17.97	12.00
wf = width of flange weld (mm)	wf =	10	10	14	10	10	10	10	10
ww = width of web weld (mm)	ww =	10	10	10	10	10	10	10	10
4a' + 1.25b		142	142	107	123	113.4	132.5	132.5	113.
l = effective length if g <4a' + 1.25b	l =	193.17	193.17	169.50	191.75	178.40	229.96	229.96	203.40
if g > 4a' + 1.25b	l =	186.34	186.34	89.00	133.50	106.80	159.92	159.92	106.80
but l < Bep									
Tep = predicted end plate thickness (mm)	Tep =	29.93	27.96	47.30	39.20	43.59	18.21	32.48	44.38
Ta = actual end plate thickness (mm)	Ta =	13.30	13.00	15.88	15.88	19.00	15.88	15.88	19.00
Ratio of predicted to actual thickness	Ratio =	2.25	2.15	2.98	2.47	2.29	1.15	2.05	2.34

Table C.5 Detailed Predictions (Krishnamurthy, 1978)

Definitions	Symbols	Tests							
		S2	S3	M1	M2	M3	B1	B2	B3
		8 bolt	8 bolt	8 bolt	8 bolt	8 bolt	8 bolt	8 bolt	8 bolt
Beam = beam used in experiment	Beam	W360x51	W360x51	W460x97	W460x97	W460x97	W610x125	W610x125	W610x125
Fyb = yield stress of beam (MPa)	Fyb =	350	350	346	346	346	375	375	375
Mb = failure moment (kN•m)	Mb =	220	192	696	478	591	768	525	738
d = depth of beam (mm)	d =	355	355	466	466	466	612	612	612
tf = flange thickness (mm)	tf =	11.6	11.6	19	19	19	19.6	19.6	19.6
df = d - tf (mm)	df =	343.4	343.4	447	447	447	592.4	592.4	592.4
F = flange force (obtained from experiment) (N)	F =	6.41E+05	5.59E+05	1.56E+06	1.07E+06	1.32E+06	1.30E+06	8.86E+05	1.25E+06
Mt =0.25*F*pe (kNm)	Mt =	4.64E+06	6.60E+06	1.08E+07	1.48E+07	1.80E+07	9.29E+06	1.80E+07	2.48E+07
di = from inside bolt center to flange face (mm)	di =	45	45	45	45	45	45	45	45
do = from outside bolt center to flange face (mm)	do =	45	81.5	45	100	100	45	45	45
wf =width of flange weld (mm)	wf =	10	10	10	10	10	10	10	10
ww = width of web weld (mm)	ww =	10	10	10	10	10	10	10	10
peo = do - wf -1/4db (mm)	peo =	29.00	65.50	27.85	82.85	82.06	28.65	133.65	132.06
pei = di - wf - 1/4 db (mm)	pei =	29.00	29.00	27.85	27.85	27.06	28.65	28.65	27.06
pe = (pei+peo)/2	pe =	29.00	47.25	27.85	55.35	54.56	28.65	81.15	79.56
db = bolt diameter (mm)	db =	24	24	28.6	28.6	31.75	25.4	25.4	31.75
Ab = bolt Area (mm^2)	Ab =	452.38	452.38	642.41	642.41	791.71	506.69	506.69	791.71
By = bolt yield stress (MPa)	Fybolt =	490	490	490	490	490	490	490	490
Bu = bolt ultimate stress (MPa)	Fubolt =	1040	1040	1040	1040	1040	1040	1040	1040
Fyep = end plate yield stress (MPa)	Fyep =	295	285	340	340	356	340	340	356
Bep = end plate width (mm)	Bep =	200	200	230	230	230	270	270	270
fb = flange width (mm)	fb =	128	128	193	193	193	229	229	229
Af = flange area (mm^2)	Af =	1484.8	1484.8	3667	3667	3667	4488.4	4488.4	4488.4
tw = web thickness (mm)	tw =	7.2	7.2	11.4	11.4	11.4	11.9	11.9	11.9
Aw = beam web area (mm^2)	Aw =	2388.96	2388.96	4879.2	4879.2	4879.2	6816.32	6816.32	6816.32
M (as calculated with F obtained from exp.) (kN•m)	Md =	3.48E+06	5.66E+06	8.95E+06	1.45E+07	1.69E+07	7.79E+06	1.96E+07	2.50E+07
Tcp = predicted end plate thickness (mm)	Tcp =	18.82	24.40	26.20	33.35	35.21	22.56	35.76	39.52
Ta = actual end plate thickness (mm)	Ta =	13.30	13.00	15.88	15.88	19.00	15.88	15.88	19.00
Ratio of Predicted to Actual Thickness	Ratio =	1.41	1.88	1.65	2.10	1.85	1.42	2.25	2.08

Table C.6 Detailed Predictions (Surtees and Mann, 1970)

Definitions	Symbols	Tests							
		S2 8 bolt	S3 8 bolt	M1 8 bolt	M2 8 bolt	M3 8 bolt	B1 8 bolt	B2 8 bolt	B3 8 bolt
Beam = beam used in experiment	Beam	W360x51	W360x51	W460x97	W460x97	W460x97	W610x125	W610x125	W610x125
Mb = failure moment (kN·m)	Mb =	220	192	696	478	591	768	525	738
d = depth of beam (mm)	d =	355	355	466	466	466	612	612	612
tf = flange thickness (mm)	tbf =	11.6	11.6	19	19	19	19.6	19.6	19.6
df = d - tf (mm)	df =	343.4	343.4	447	447	447	592.4	592.4	592.4
Fyep = end plate yield stress (MPa)	Fyep =	295	285	340	340	356	340	340	356
tw = web thickness (mm)	tw =	6.5	6.5	11.4	11.4	11.4	11.9	11.9	11.9
Bep = end plate width (mm)	Bep =	200	200	230	230	230	270	270	270
di = from inside bolt center to flange face (mm)	di =	45	45	45	45	45	45	45	45
do = from outside bolt center to flange face (mm)	do =	45	81.5	45	100	100	45	45	45
c= di +do + tf (mm)	c =	101.6	138.1	109	164	164	109.6	214.6	214.6
g = bolt pitch (mm)	g =	100	100	125	125	125	150	150	150
Tep = predicted end plate thickness (mm)	Tep =	17.16	17.60	24.24	22.20	24.13	20.73	20.08	23.26
Ta = actual end plate thickness (mm)	Ta =	13.30	13.00	15.88	15.88	19.00	15.88	15.88	19.00
Ratio of Predicted to Actual Thickness	Ratio =	1.29	1.35	1.53	1.40	1.27	1.31	1.26	1.22

194

Table C.7 Detailed Predictions (Packer and Morris, 1977)

Definitions	Symbols	Tests							
		S2 8 bolt	S3 8 bolt	M1 8 bolt	M2 8 bolt	M3 8 bolt	B1 8 bolt	B2 8 bolt	B3 8 bolt
Beam = beam used in experiment	Beam	W360x51	W360x51	W460x97	W460x97	W460x97	W610x125	W610x125	W610x125
Mb = failure moment (kN·m)	Mb =	220	192	696	478	591	768	525	738
d = depth of beam (mm)	d =	355	355	466	466	466	612	612	612
tf = flange thickness (mm)	tf =	11.6	11.6	19	19	19	19.6	19.6	19.6
df = d - tf (mm)	df =	343.4	343.4	447	447	447	592.4	592.4	592.4
db = bolt diameter (mm)	db =	24	24	28.6	28.6	31.75	25.4	25.4	31.75
dh = bolt hole diamter (mm)	dh =	26	26	30.6	30.6	33.75	27.4	27.4	33.75
Fyep = end plate yield stress (MPa)	Fyep =	295	285	340	340	356	340	340	356
tw = web thickness (mm)	tw =	7.2	7.2	11.4	11.4	11.4	11.9	11.9	11.9
Bep = end plate width (mm)	Bep =	200	200	230	230	230	270	270	270
di = from inside bolt center to flange face (mm)	di =	45	45	45	45	45	45	45	45
do = from outside bolt center to flange face (mm)	do =	45	81.5	45	100	100	45	150	150
wf = flange weld thickness (mm)	wf =	10	10	14	10	10	10	10	10
Tep = predicted end plate thickness (mm)	Tep =	22.66	26.57	29.00	34.13	37.79	24.90	32.55	38.89
Ta = actual end plate thickness (mm)	Ta =	13.30	13.00	15.88	15.88	19.00	15.88	15.88	19.00
Ratio of Predicted to Actual Thickness	Ratio =	1.70	2.04	1.83	2.15	1.99	1.57	2.05	2.05

Table C.8 Detailed Predictions (Mann and Morris, 1979)

Definitions	Symbols	Tests							
		S2 8 bolt	S3 8 bolt	M1 8 bolt	M2 8 bolt	M3 8 bolt	B1 8 bolt	B2 8 bolt	B3 8 bolt
Beam = beam used in experiment	Beam	W360x51	W360x51	W460x97	W460x97	W460x97	W610x125	W610x125	W610x125
Mb = failure moment (kN•m)	Mb =	220	192	696	478	591	768	525	738
d = depth of beam (mm)	d =	355	355	466	466	466	612	612	612
tf = flange thickness (mm)	tbf =	11.6	11.6	19	19	19	19.6	19.6	19.6
df = d - tf (mm)	df =	343.4	343.4	447	447	447	592.4	592.4	592.4
Fyep = end plate yield stress (MPa)	Fyep =	295	285	340	340	356	340	340	356
tw =web thickness (mm)	tw =	7.2	7.2	11.4	11.4	11.4	11.9	11.9	11.9
Bep = end plate width (mm)	Bep =	200	200	230	230	230	270	270	270
di = from inside bolt center to flange face (mm)	di =	45	45	45	45	45	45	45	45
do = from outside bolt center to flange face (mm)	do =	45	81.5	45	100	100	45	150	150
Tep = predicted end plate thickness (mm)	Tep =	22.11	24.91	29.93	31.49	34.22	25.21	30.68	35.55
Ta = actual end plate thickness (mm)	Ta =	13.30	13.00	15.88	15.88	19.00	15.88	15.88	19.00
Ratio of Predicted to Actual Thickness	Ratio =	1.66	1.92	1.89	1.98	1.80	1.59	1.93	1.87

Table C.9 Detailed Predictions (Whittaker and Walpole, 1982)

Definitions	Symbols	Tests							
		S2	S3	M1	M2	M3	B1	B2	B3
		8 bolt	8 bolt	8 bolt	8 bolt	8 bolt	8 bolt	8 bolt	8 bolt
Beam = beam used in experiment	Beam	W360x51	W360x51	W460x97	W460x97	W460x97	W610x125	W610x125	W610x125
Mb = failure moment (kN•m)	Mb =	220	192	696	478	591	768	525	738
Fyep = end plate yield stress (MPa)	Fyep =	295	285	340	340	356	340	340	356
d = depth of beam (mm)	d =	355	355	466	466	466	612	612	612
tf = flange thickness (mm)	tf =	11.6	11.6	19	19	19	19.6	19.6	19.6
tw = web thickness (mm)	tw =	7.2	7.2	11.4	11.4	11.4	11.9	11.9	11.9
df = d - tf (mm)	df =	343.4	343.4	447	447	447	592.4	592.4	592.4
Bep = end plate width (mm)	Bep =	200	200	230	230	230	270	270	270
do = from outside bolt center to flange face (mm)	do =	45	81.5	45	100	100	45	150	150
di = from inside bolt center to flange face (mm)	di =	45	45	45	45	45	45	45	45
wf = width of flange weld (mm)	wf =	10	10	14	10	10	12	12	12
ww = width of web weld (mm)	ww =	10	10	10	10	10	10	10	10
p = .6 x df = length of C yield lines (mm)	p =	206.04	206.04	268.2	268.2	268.2	355.44	355.44	355.44
g = bolt pitch (mm)	g =	100	100	125	125	125	150	150	150
K = Fyep x df x (J + S)	K =	1042707	815693	1862027	1268174	1327853	2860334	1673606	1752364
J = 2*Bep/((c - tf - 2*wf)	J =	5.71	3.76	7.42	3.68	3.68	8.18	3.16	3.16
S = (2 x p)/(g - tb - 2 x ww)	S =	4.58	4.58	4.83	4.66	4.66	6.02	5.15	5.15
Tep = (Mb/ K)^.5 = end plate thickness (mm)	Tep =	14.53	15.34	19.33	19.41	21.10	16.39	17.71	20.52
Ta = actual end plate thickness (mm)	Ta =	13.30	13.00	15.88	15.88	19.00	15.88	15.88	19.00
Ratio of Predicted to Actual Thickness	Ratio =	1.09	1.18	1.22	1.22	1.11	1.03	1.12	1.08

Table C.10 Detailed Predictions (Kukreti et al., 1990)

Definitions	Symbols	Tests		
		M4 8 bolt stiffener	M6 8 bolt stiffener	B4 8 bolt stiffener
Beam = beam used in experiment	Beam	W460x97	W460x97	W610x125
Mb = failure moment (kN•m)	Mb =	732	771	994
Fyep = end plate yield stress (MPa)	Fyep =	340	340	340
d = depth of beam (mm)	d =	466	466	612
tf = flange thickness (mm)	tf =	19	19	19.6
df = d - tf (mm)	df =	447	447	592.4
F = flange force (N)	F =	1.64E+06	1.72E+06	1.68E+06
Bep = end plate width (mm)	Bep =	230	230	270
do = from outside bolt center to flange face (mm)	do =	100	100	150
di = from inside bolt center to flange face (mm)	di =	45	45	45
g = bolt pitch (mm)	g =	125	125	150
db = bolt diameter (mm)	db =	31.75	31.75	31.75
ts = stiffener thickness (mm)	ts =	19	19	19
Tep1 = End plate thickness required to limit plate speration (mm)	Tep1 =	37.12	38.92	48.95
Tep2 = End plate thickness required to limit end plate strain (mm)	Tep2 =	28.11	29.63	30.35
Ta = actual end plate thickness (mm)	Ta =	15.88	15.88	15.88
Ratio of Predicted to Actual Thickness (Tep1)	Ratio 1 =	2.34	2.45	3.08
Ratio of Predicted to Actual Thickness (Tep2)	Ratio 2 =	1.77	1.87	1.91

Table C.11 Detailed Predictions AISC (1994)

Definitions	Symbols	Tests							
		S2	S3	M1	M2	M3	B1	B2	B3
		8 bolt	8 bolt	8 bolt	8 bolt	8 bolt	8 bolt	8 bolt	8 bolt
Beam = beam used in experiment	Beam	W360x51	W360x51	W460x97	W460x97	W460x97	W610x125	W610x125	W610x125
Fyb = yield stress of beam (MPa)	Fyb =	350	350	346	346	346	375	375	375
Mb = failure moment (kN•m)	Mb =	220	192	696	478	591	768	525	738
d = depth of beam (mm)	d =	355	355	466	466	466	612	612	612
tf = flange thickness (mm)	tf =	11.6	11.6	19	19	19	19.6	19.6	19.6
df = d - tf (mm)	df =	343.4	343.4	447	447	447	592.4	592.4	592.4
F = flange force (obtained from experiment) (N)	F =	6.41E+05	5.59E+05	1.56E+06	1.07E+06	1.32E+06	1.30E+06	8.86E+05	1.25E+06
Mt =0.25*F*pe (kNm)	Mt =	4.64E+06	6.60E+06	1.08E+07	1.48E+07	1.80E+07	9.29E+06	1.80E+07	2.48E+07
di = from inside bolt center to flange face (mm)	di =	45	45	45	45	45	45	45	45
do = from outside bolt center to flange face (mm)	do =	45	81.5	45	100	100	45	150	150
wf = width of flange weld (mm)	wf =	10	10	10	10	10	10	10	10
ww = width of web weld (mm)	ww =	10	10	10	10	10	10	10	10
peo = do - wf - 1/4 db (mm)	peo =	29.00	65.50	27.85	82.85	82.06	28.65	133.65	132.06
pei = di - wf - 1/4 db (mm)	pei =	29.00	29.00	27.85	27.85	27.06	28.65	28.65	27.06
pe = (pei+peo)/2 (mm)	pe =	29.00	47.25	27.85	55.35	54.56	28.65	81.15	79.56
db = bolt diameter (mm)	db =	24	24	28.6	28.6	31.75	25.4	25.4	31.75
Ab = bolt area (mm^2) =	Ab =	452.38	452.38	642.41	642.41	791.71	506.69	506.69	791.71
By = bolt yield stress (MPa)	By =	490	490	490	490	490	490	490	490
Bu = bolt ultimate stress (MPa)	Bu =	1040	1040	1040	1040	1040	1040	1040	1040
Fyep = end plate yield stress (MPa)	Fyep =	295	285	340	340	356	340	340	356
Bep = end plate width (mm)	Bep =	200	200	230	230	230	270	270	270
fb = flange width (mm)	fb =	128	128	193	193	193	229	229	229
Af = beam flange area (mm^2)	Af =	1484.8	1484.8	3667	3667	3667	4488.4	4488.4	4488.4
tw = web thickness (mm)	tw =	7.2	7.2	11.4	11.4	11.4	11.9	11.9	11.9
Aw = beam web area (mm^2)	Aw =	2388.96	2388.96	4879.2	4879.2	4879.2	6816.32	6816.32	6816.32
M (as calculated with F obtained from exp.) (kN•m)	Md =	1.39E+07	2.26E+07	3.58E+07	5.80E+07	6.77E+07	3.12E+07	7.83E+07	1.00E+08
Tep = predicted end plate thickness (mm)	Tep =	17.74	23.01	24.70	31.45	33.20	21.27	33.72	37.26
Ta = actual end plate thickness (mm)	Ta =	13.30	13.00	15.88	15.88	19.00	15.88	15.88	19.00
Ratio of Predicted to Actual Thickness	Ratio =	1.33	1.77	1.56	1.98	1.75	1.34	2.12	1.96

199

Table C.12 Predicted Plate Thickness for the connections of Ghobarah et al. (1992)

Definitions	Symbols	Tests				Comments
		CB-1 8 bolt	CC-1 8 bolt	CC-2 8 bolt	CC-3 8 bolt	
Beam = beam used in experiment	Bcam	W360x57	W410x60	W410x60	W410x60	
Mb = failure moment (kN·m)	Mb =	535	550	700	740	from Ghobarah et al.'s charts
Fyep = yield strength of the end plate (MPa)	Fyep =	345	345	345	345	*
d = depth of beam (mm)	d =	358	407	407	407	
tf = flange thickness (mm)	tf =	13.1	12.8	12.8	12.8	
df = d - tf (mm)	df =	344.9	394.2	394.2	394.2	
Bep = end plate width (mm)	Bep =	203	221	221	221	
do = from outside bolt center to flange face (mm)	do =	53.45	53.6	53.6	53.6	
di = from inside bolt center to flange face (mm)	di =	53.45	53.6	53.6	53.6	
wf = width of flange weld (mm)	wf =	10	10	10	10	assumed
ww = width of web weld (mm)	ww =	10	10	10	10	assumed
db = bolt diameter (mm)	db =	25.4	25.4	25.4	25.4	
tw = web thickness (mm)	tw =	7.9	7.7	7.7	7.7	
p = .35 x df = length of C yield lines (mm)	p =	120.715	137.97	137.97	137.97	
g = bolt pitch (mm)	g =	110	134	134	134	
ts = stiffener thickness (mm)	ts =	n/a	n/a	n/a	9.00	
ws = width of stiffener weld (mm)	ws =	n/a	n/a	n/a	10.00	assumed
X = distance from end of end plate to flange face	X =	n/a	n/a	n/a	120.00	
K = Fyep x df x (I1+I+J+Q+S)	K =	1238214.2	1375597.4	1375597	1765839	
J = Bep/(2 x (do - wf - db/2))	J =	3.30	3.58	3.58	n/a	
Q = (Bep - tf- 2 x ww)/(2 x (di - wf-db/2))	Q =	2.85	3.13	3.13	3.13	
S = (2 x p)/(g - tb - 2 x ww - db)	S =	4.26	3.41	3.41	3.41	
I1= (Bep - ts)/(2 x (do - wf -db/2))	I1=	n/a	n/a	n/a	3.43	
I = (2 x X)/(g - ts - 2 x ws - db)	I =	n/a	n/a	n/a	3.02	
Tep = (Mb/K)^0.5 = predicted end plate thickness (mm)	Tep =	20.79	20.00	22.56	20.47	
Ta = actual end plate thickness (mm)	Ta =	28.00	28.00	28.00	22.00	
Ratio = Ratio of predicted to actual thickness	Ratio =	0.74	0.71	0.81	0.93	

Note:
* 300 MPa steel, overstrength factor = 15 % assumed